The properties of concrete sandwich beams with polystyrene concrete cores

Shendy El Barbary, Mohamed E.

THE PROPERTIES OF CONCRETE SANDWICH BEAMS WITH POLYSTYRENE CONCRETE CORES

by

MOHAMED E. SHENDY EL BARBARY

B.Sc., M. Sc., Civil Engineering

A thesis submitted for the degree of

Doctor of Philosophy

The Department of Engineering

University of Durham

July 1981

SYNOPSIS

The difficulties of producing and handling ultra-light weight concrete mixes having the desirable properties of the cores of sandwich beams have delayed the appearance of sandwich construction in concrete.

This research has been planned to construct, and to study the behaviour of sandwich beams in which the faces are constructed of fine concrete of high stiffness and the cores are of concrete of much lower stiffness.

The cores were made to have low density and stiffness by using expanded polystyrene beads as aggregates. A satisfactory technique for handling the bead-concrete has been developed, where sawdust as filler material is added. The influence of each one of the mix ingredients has been demonstrated for specified sizes of polystyrene beads making possible design for such bead-concrete of required density and/or strength for core use.

Thin faces of 10 mm. thickness and reinforced by steel meshes of different cross-sectional area were made and examined. Their properties were determined also by laboratory procedure for use in beam analysis.

The experimental work on several sets of beams was carried out so as to demonstrate the influence on beam deformation and ultimate strength of such factors as reinforcement content and differences of face and core moduli and strengths. Beams of repeatable characteristics were constructed successfully by following a special manufacturing technique developed in the laboratory.

In the context of the test data and analysis with the sandwich beam theory, the necessary conditions for the beam to have agreement between values of the experimental and theoretical deformations has been demonstrated, formulating especially the ratio between the bending and shear stiffness, and the modulus of the tension face.

A method of beam analysis by finite element was carried out also and the results reported in the last part of the thesis. These results were found to be closely compatible with experimental results.

ACKNOWLEDGEMENTS

The research described in this dissertation has been carried out at the Engineering department of Durham University. It was financed by the Faculty of Engineering of Al-Azhar University, Cairo, Egypt. It has been the outcome of the help of many people who extended their help, support, encouragement and friendship.

I would like to start with my deepest thanks and gratitude to my supervisor Dr. Girvan M. Parton for his invaluable guidance and great help; without his constructive advice generously given throughout this work this thesis would, of course, not have been realized.

The encouragement and friendship of the staff of the department is acknowledged with gratitude, and special thanks to Professor G.R. Higginson, the Head of the Department, for extended use of departmental facilities.

My thanks also to the technical staff, and especially Mr. Brian Scurr and Mr. J. Watkins of the structural and concrete laboratory, Frank Emery of the wood workshop and the chief technician, Mr. C. Campbell. To Mrs. Inger Mitchell and Miss Marion Morris, inter library loans staff, Durham University.

I would also like to thank Mrs. Margaret Bell very much for her care and skill in the preparation of the typescript. Generally, I would express my gratitude and thanks to the English people as a whole, and the people of Durham University and the North East in particular for making me and my family welcome with comfortable accommodation and living facilities throughout the years of this work, giving me a great chance to achieve this research.

The financial support of the Egyptian government for this research is gratefully acknowledged, and my thanks for the people who encourage such grants for post-graduate work and who helped me to get this grant; in particular, Professors M.H. Khorshed and A.A. Mokhtar of Al-Azhar University and Professor M.El Adwy Nassef of Cairo University, Faculties of Engineering.

Lastly, but not the least, I am grateful to my family, Mother, wife Amal, daughter Riham and son Haitham, for their love and continuous encouragement.

CONTENTS

NOTATIONS

The following notations are those generally used in this thesis. If others are used they will be mentioned following their appearance.

A	The effective cross-sectional area of sandwich beam = b x (c + f)
A_c	Cross-sectional area of core
A_s	Cross-sectional area of reinforcement in one face normal to its length
A_F	Cross-sectional area of face
a	Distance from support to the load (shear span)
b	Width of sandwich beam
c	Depth of core of sandwich beam
C_c	Cement content in kg per cubic metre of aggregates
$D_F = (EI)_F$	Bending stiffness of face about its N.A.
D	The 2nd moment of the faces about N.A. of beam $= \sum A_F.E_F.d^2$, i.e. due to the virtual area of faces
D_b	Bending stiffness of sandwich beam due to faces $= D + 2\ D_F$
D_c	Bending stiffness of sandwich beam due to the compression zone of the core
D_s	Shear stiffness of sandwich beam
d	The effective depth of sandwich beam, equal to the distance between the centre lines of the upper and lower faces = c + f
$E = E_c$	Modulus of elasticity of concrete in compression
E_s	" " " steel reinforcement
E_F	" " " face
E_{Fc} & E_{Ft}	The face modulus in compression and tension respectively
F_c	Cylinder compressive strength

f	Thickness of face
G	The shear modulus of polystyrene concrete mix = shear modulus of core of sandwich beam
I_p	The polar second moment of area about an axis through the centre of cross-section of circular shaft
L	Distance between two circles on shaft where the angle of twisting is measured at each circle
M	Bending moment on sandwich beam at midspan
M_{Fu}	Bending moment of the upper face at midspan
M_{Fl}	" " " lower " "
M_c	" " resisted by core
N	Normal force in the face
N_c	Normal force resisted by core
P	Total load on sandwich beam
P_F	Beam's ultimate load due to maximum strength of faces
P_Q	" " " " " shear stress of core
Q	Shear force
r	Radius on solid circular shaft where shear stress is calculated
S	Face designation
T	The torque on each end of circular shaft
U	Strain energy
u	Cubic compressive strength
W	Load on each of the two ends of face sample tested for determining its flexural stiffness
W_i	Weight of water used to give the required workability in initial mix
W_T	The total weight of water to give the required workability in the designed mix

$\overline{\sigma_N}$ Normal stress in face due to the normal force N

$\overline{\sigma_{M_F}}$ " " " " " " the local bending moment in the face

$\overline{\sigma_T}$ = $\overline{\sigma_N}$ + $\overline{\sigma_{M_F}}$

τ Shear stress of the polystyrene concrete mix

τ_{cf} Failure shear stress of the core mix

ρ Concrete density

ρ_s Saturated density of polystyrene concrete

ρ_d Dry density " " "

Δ Total deflection

Δ_b Deflection due to bending moment

Δ_s Deflection due to shear

ξ_N Face strain due to normal force N

ξ_{M_F} " " " local bending moment in the face

In the upper face it is $\xi_{M_{Fu}}$ and in lower face it is $\xi_{M_{Fl}}$

ξ_T = ξ_N + ξ_{M_F}

η The percentage of the ratio of the cross-sectional area of reinforcement in one face to the area of core of sandwich beam

μ Expression of the ratio between the bending stiffness of sandwich beam to its shear stiffness including the modulus of elasticity of the tension face

= $(D_b/D_s)\ E_{Ft}$

CHAPTER ONE

INTRODUCTION AND HISTORICAL BACKGROUND

The sandwich beam (or panel) is a particular type of laminated structure. It consists of two thin sheets which are called faces separated by an intermediate, thick layer which is called the core of the sandwich. The faces are required to be thin, stiff and strong and the core layer is supposed to be of low-density material which is less stiff and strong. This arrangement combines a relatively high stiffness with lightness, because the stiff faces are situated at the top and the bottom of the beam similar to the flanges of an I-beam.

The principles of sandwich construction perhaps were used first by the Egyptians many centuries before Christ. They spliced two types of wood together, where the strong wood was put on the exterior of inferior wood to obtain strong members. There is also evidence that the Germans used laminated steel in their armour as early as the fifteenth century (33). The earliest example of using the principle of sandwich panels in Britain is the Britannia Tubular Bridge, which was built in 1864 in North Wales, to carry the railway across the Menai Strait. Compression panels were made of malleable iron sheets on wooden cores (18).

During the second world war there was one of the most spectacular applications of modern structural sandwich construction in the design of the Mosquito bomber by de Haviland, employing birch plywood facings with a light-weight balsa

wood core. The wooden cores and faces for aeroplanes were no longer used after the war.

Owing to the rapid growth in size of both civil and military planes, and because of the increase in aeroplane speeds a reduction in the airframe and wing weights was required. For similar reasons the surfaces of both fuselages and wings were required, also, to be smoother. The subject was interesting to many investigators in different countries at that time. During the war years and after the war, in the forties, much research was published dealing with the theoretical and experimental investigations establishing sandwich construction theory for beams, plates and columns.

Several useful research projects were carried out also determining the methods for testing sandwich elements and materials (2). The Forest Products Laboratory in the United States (in the late forties) presented a series of reports in the field showing the properties of some low-density materials for sandwich cores and the properties of honeycomb and corrugate cores of different materials (24, 36, 41). There are many references in the works of Allen (1), Plantema (31) and Parton (30). However, the Forest Products Laboratory may be considered as the main centre of the research works which have been done in this field.

Plastic sandwich constructions have been found advantageous in radar industry. The stiff dome-like shields were made from non-metalic faces or cellular rubber honeycombs and foamed plastics (26). One of the well-known examples of the plastic sandwich structure is the dome of the Ballistic

Missile Early Warning System in the United States, which was 140 feet in diameter. The sandwich panels of this dome were made to have a basic skin of 0.042 in. thickness and 6 in. thickness of honeycomb craft paper core. For more examples of employing plastic in sandwich constructions see Elliott's references (15).

Extensive research in this field has developed successful methods of sticking together cores and faces of different materials, and several sandwich panels are produced now commercially in many countries. The faces usually are made of metal (aluminium), hard plastic, reinforced plastic, plywood and hardboard. The core may be in the form of honeycomb, corrugated sheets or expanded plastic foam. The materials for the faces and cores are determined according to the purpose of the panels employment. From some of these panels (hardboard or plywood faces and polyurethane and PVC foam core). Several pyramids, polyhedral domes and polyhedral shells were constructed and their behaviour was studied by Parton (30) and others (11).

The applications of sandwich construction in building generally have lagged behind the aircraft and motor vehicle industry, i.e. the great growth in this structural form has been more of interest to aero-space and the motor industry rather than building. The reason may be attributed to the importance of lightness of the structure in aircraft more than in buildings where economy and durability is more important. However this structural form can be of great benefit for the purposes of insulation from heat loss, weather and

sound in the interior and external walls and the roofs of houses and other buildings.

"Cemesto Board" is the proprietory name of the first commercial sandwich board to be used in a house which was built in 1933 using sandwich panels of fibreboard faces and cement asbestos core in America. Many houses of that type were built during world war II due to the demands for cheap, rapidly built houses.

In 1947 a test house was built using sandwich panel in the grounds of the U.S Forest Products Laboratory at Madison Wis. to investigate the long term behaviour of sandwich panels. The exposure test results over 15 years indicated that the wall panels made of resin-impregnated paper cores and plywood facings have demonstrated excellent performance, based on retention of stiffness and strength. In this case, the losses in stiffness and strength due to the passage of time are insignificant (43).

The development of fabricating techniques and the availability of a great variety of facing and core materials gave to sandwich construction a great chance to appear recently in building construction. In the late fifties many houses were built in different countries with different materials.

In building, in 1956, the Monsanto "House of the future" was built with a prefabricated shell made from laminated sandwich panels. The panels consisted of a honeycomb core of 4 in. thickness and faces of fibre reinforced polyester plastic. The house was constructed in the form of four curved wings

which were cantilevered from a central core with a basic unit of 8 ft. x 16 ft. The panels were bonded with material having good fire and water resistance characteristics. The test on-site indicated that the structural performance of this house was successful from the architectural and structural points of view. Unfortunately, the cost at that time could not compete with the traditional techniques of building (15).

One of the early excellent examples of plastic sandwich construction is the experimental French all-plastic house which was built in a prefabricated panelised system. The house was built for the Salon des Arts Manger de Paris in 1956. The house has 6000 cubic feet of useful volume and weighed only 1800 lb (26).

Sandwich units of aluminium facings with plastic foam core were used also for building a house for the Stuttgart plastics Exhibition in Germany in 1958 (26). In different countries (America, Italy, Russia, Belgium and Holland) there are many examples of such sandwich houses which were built at that time (26). These early houses were built either for testing as research projects or as exhibition buildings.

Concrete is still the most important material used for building construction due to the advantages such as cheapness, fire resistance, resistance to rodents, and easy casting in different forms. Because of the disadvantages of high density and bad insulation, over the last fifty years extensive researches have been carried out to demonstrate the methods for producing concrete of low density and good insulation characteristics. Lightweight concrete usually is made in one

of the following three types:

(1) Aerated concrete, which is made by producing gas causing voids in the cement matrix. Sometimes it is called cellular, foamed or gas concrete.

(2) Lightweight aggregate concrete which is made by using lightweight aggregate in the mix instead of the ordinary aggregate.

(3) No fines concrete, which is made by omitting the fine aggregate from the mix.

The use of lightweight concrete in roof construction is to be recommended because it gives, in addition to the benefit of insulation, the advantage to the designer of reducing the size of the other elements, such as the sections of the columns and the foundations. Since sandwich construction has so many advantages it must be sensible to combine these with the benefits of cement concrete, and try to develop sandwich construction in concrete.

Little attention has been paid in the past to the use of concrete in sandwich construction. The reason may be attributed to the difficulty of producing a lightweight concrete which can satisfy the recommended conditions of the core. In a concrete sandwich the concrete for the core is required to have the following properties:-

(1) It must be of low density to satisfy the requirement of lightness noting that the efficiency of the sandwich is realized when the weight of the core is approximately of value equal to the weight of the faces.

(2) It is required to be elastically compressible and flexible to accept and to follow the face and the beam deformations.

(3) It must be stiff enough to keep the faces acting together with the right distance between them and to resist the shear stresses.

(4) It must have a good bond characteristic with the faces to prevent the faces' sliding and buckling.

(5) It is supposed to have a good insulation characteristic with respect to sound and heating.

The use of concrete in sandwich construction aims to produce buildings having both sandwich and cement advantages with good insulation characteristics. Because lightweight concrete is used for the same purpose it would be most advantageous if the concrete sandwich provides the building with concrete elements of density lower than the density of the lightweight concrete presently used in loaded structures. In other words, the concrete sandwich will be more useful and successful in building (especially for the roofs of the houses) when its density is less than 1.3 t/m^3.

In order to achieve this very low density and still retain adequate strength and stiffness, two alternatives are available. The core concrete may be made either from aerated concrete, or by using a very lightweight aggregate.

In 1971 Thom (39) studied the possibility of using aerated concrete in sandwich beams and glass fibre reinforced concrete for faces. Thom's work indicated that in addition to

the core of the aerated concrete being brittle, the properties of the core were changeable through its depth. The upper part was found to be weaker than the bottom, i.e.there was no control to produce a homogeneous core of the same properties throughout its depth. However, due to these results and with reference to the result of some research which was published showing the properties and the practical aspects of aerated concrete in building use (16), it may be concluded that this type of lightweight concrete is not a suitable material to constitute the core of a sandwich beam or plate, especially when it is to be used in the roofs of buildings. Aerated concrete could be useful for the unloaded elements, like partition walls and for insulation purposes.

In 1976, research was carried out by Saglam at Durham University studying the properties of the fibre reinforced concrete facings of sandwich beams and slabs (33). Expanded polystyrene beads were used as lightweight aggregates to constitute the concrete of the core of the sandwiches made in that research. Due to the great lightness in the density of the expanded polystyrene beads and the consequent difficulty in manufacturing, a special technique has been used. The core was cast in layers by putting the beads of each layer in the mould first and pouring or spreading the cement paste over the beads. The sample after that was vibrated for a short period to allow the cement paste to go through the gaps between the beads. In this method there was no guarantee of producing a core of a homogeneous section or reasonable rigidity, so the cores made were found weak and unreliable.

In 1977, another attempt was made by Wright under the same supervision of Dr. Parton, also using expanded polystyrene beads for making the core and expanded steel mesh was used to reinforce the faces (45). At that time the expanded polystyrene beads were mixed with cement and water together in the concrete mixer (using a water/cement ratio of a value suitable for workability) and, after mixing, the concrete was poured into the moulds. When the samples were vibrated, most of the cement paste went down to the bottom layer of the core leaving the upper layer too lean. Accordingly, the bond between the upper face and the core was very weak. The core also was found to be brittle, and when the samples were tested in bending the upper faces bent and separated from most of the samples.

All the natural and the artificial lightweight aggregates which are used commonly for making lightweight concrete for loaded structures are not suitable for giving the core of the density and flexibility required, as mentioned before (5, 19, 34, 40). Using 'no-fines' lightweight aggregate is not suitable also, because the upper surface of the core will not be flat enough and, in consequence, the thickness of the upper face will not be exactly as designed.

Other work has been done at Durham under the same supervision to investigate the properties of core materials formed from similar mix components as the ones used in this project but using different cementing techniques (29).

The use of expanded polystyrene beads as an 'aggregate' in lightweight concrete is a development which requires much

further study. In principle, the objective is to use the aggregate to produce what is, in effect, a "controlled void"; in practice, the handling of the bead concrete requires some novel techniques and a new attitude to design. If the problems can be understood and overcome the rewards might be considerable; it may be possible to produce concrete of the required degree of flexibility, resilience and fire resistance as well as lightness.

From the work of Saglam (33) and Wright (45), it can be seen that the faces reinforced by expanded steel mesh have better performance in sandwich beams than fibre reinforced faces. This point needs more work also to obtain more evidence of the properties of the faces in both tension and compression and their applications to sandwich construction.

CHAPTER TWO

POLYSTYRENE CONCRETE FOR CORE USE, MANUFACTURE AND PROPERTIES

2.1 Introduction

The core of a concrete sandwich beam as mentioned before is required to be of density as low as possible in order to realize the advantage of structural sandwich beams, that of lightness and high strength to weight ratio.

The concrete of expanded polystyrene beads and cement paste filling the gaps between them is desirable to give a honeycomb section. Because of the wide disparity in the density of the mix ingredients - cement paste and beads - mixing and casting is difficult, especially for producing a homogeneous section. Such mixes have been used for insulation purposes, i.e. unloaded constructions (5 , 28). Previous attempts (33, 45) to produce expanded polystyrene bead concrete to be used in a core of sandwich beams were not successful enough to be used in structural elements, since the structural properties of the mixes were unknown. However, fully satisfactory placement techniques may be used in conjunction with the data provided by this research.

The experimental work done and explained in this chapter was planned to achieve a new technique for producing (mixing and casting) polystyrene - bead concrete with good workability to be used in loaded constructions, especially the cores of sandwich beams. Sawdust was added to the expanded polystyrene beads and cement paste. For three types

of expanded polystyrene beads varying in size or in bulk density, the effect of total water/cement ratio and cement content on concrete crushing strength, density and workability was found with variations in sawdust and polystyrene beads proportions.

2.2 Materials

2.2.1 Expanded polystyrene beads

It is known in ordinary and lightweight aggregate concrete, that the aggregates constitute about three-quarters of the volume of concrete and their properties affect the characteristics of the concrete. Because the expanded polystyrene beads occupy most of the volume of this concrete, they will be considered as a coarse lightweight aggregate for mixing purposes, but without consistent and reliable strength. The main purpose of the expanded polystyrene beads to be used in the mix - as mentioned before - is to organize the distribution of spongy voids throughout the cement matrix forming lightweight concrete of honeycomb section, good thermal insulation and flexibility. For simplicity the expanded polystyrene beads will be called, in this research, from now on by the commercial name, beads. They are produced in varying diameters as a result of the processing, which obtains the beads from the expandable polystyrene beads.

In brief, the beads are produced by heating the liquid styrene in water with addition of an expanding agent "pentane", which dissolve into the styrene to form small globules, which when solidified are called expandable polystyrene beads. When

the expandable polystyrene beads are heated in steam, the beads then expand and the expanding agent escapes leaving thousands of tiny cells with located air inside each, causing spongy beads of good thermal insulation. The beads are formed in varying diameters and density according to processing time and steam temperature (46). It is the lightest material to be used as lightweight aggregate. Some are produced with bulk density of about 12 kg/m^3. It is very cheap, but unfortunately, this material has no fire resisting capability and softens at 70°C. It has also a high resilient quality.

The beads used in this research were supplied by Shell Ltd. and were delivered in bags each of about 3.0 kg. weight. Three types of spherical shape were used in the experimental work carried out and described in this chapter. The classification depends on bead size and/or bulk density as shown in (table 2.1). As can be seen from table 2.1, beads may be of the same size with varying bulk density (type (1) and type (2)), and may have the same density with differences in the size (type (2) and type (3)). However, these three types were used to discover the effect of bead size or density on the mix and concrete characteristics.

The bulk density of the three types was measured with reference to B.S. 3681 part 2 1973. A wooden box of 300 x 300 x 150 mm. dimensions was used and beads were scooped inside the box without any tamping or shaking until the box was full. The top surface was floated with a steel ruler. The bulk density was calculated by dividing the weight of material filling the box on the box's size.

Table (2.1) : Types and properties of the polystyrene beads used in this research

Polystyrene beads designation	Gradation size dia.in mm.	Bulk density kg/m^3	Bulk specific gravity kg/m^3	Volume of voids between the beads (per cent)
type (1)	1.6 - 3.3	19.6	31.4	37.7
type (2)	1.7 - 3.3	16.4	26.2	38.0
type (3)	1.7 - 7.8	16.3	25.5	37.3

The bulk specific gravity and the size of the voids - or the gaps - between the beads were determined using the 'kerosene' method (34). To prevent the beads from floating up when kerosene or water was added, a conical flask was used with a cover, or filter. This was made from fine mesh and was fitted about 5 mm. down from the top of the flask. The volume of the flask was equal to the volume of water filling the flask up to the mesh cover. A dry sample of beads was put into the flask up to, and touching the mesh cover, the cover was fitted and the flask weighed to determine the total weight of beads used. Paraffin (or kerosene) was added to the beads in the flask until it reached to the filter. It was allowed to remain for about 2-3 minutes to wet all the surfaces of the beads. Then the paraffin or kerosene was poured out by turning the flask upside down - with some shaking - for about 3-4 minutes, leaving all beads surrounded by a film of paraffin. The volume of fluid required to bring the level to the mesh filter - or cover - was equal to the volume of the voids - or gaps - between beads. The bulk specific gravity was calculated using the next equation :

$$\text{Bulk specific gravity (dry)} = \frac{A}{W - V}$$

where :

A = weight of dry beads filling the flask till filter.

W = volume of flask (vol. of water filling flask)

V = volume of fluid filling flask with beads inside.

Typical results and calculation appear in Appendix (I.a)

Beads absorption was measured using the method mentioned later in 2.2.2 and the recorded results are considered negligible, since after one hour no absorption was recorded and it was 2 gm. only after 24 h.

2.2.2 Sawdust

Sawdust may be used as lightweight aggregate for producing some lightweight concrete, especially when nailing in concrete is required as with some types of precast units for roof construction of houses. Sawdust concrete may consist of portland cement and sawdust, with roughly equal parts in volume. Using sawdust of size between 6.3 mm. and 1.18 mm. (¼ in. and No. 14 B.S. test sieve) leads to the best results (28). With these dimensions sawdust takes the role of coarse aggregate.

In this research sawdust was used with another purpose in view. There is a great difference between the densities of beads and cement paste. The density of cement paste is more than 100 times the beads' density. This causes segregation during mixing and vibration and causes difficulty of manufacture. Sawdust is used as fine aggregate, increasing the surface area and retaining the cement matrix between the beads for a longer period without segregation during mixing and vibration.

All sawdust used in this research was natural, pure and collected as the result of woodworking in the workshop of the engineering department at Durham University. It was a mixture of different types of mahogany and white wood.

The sawdust used was sieved and passed through sieve No.14 B.S. (0.047 in.). The three grades of sawdust used in the experimental work and tests carried out in this chapter were kept, after sieving, in three covered tins each containing about 15 kg. mass, inside the control room. Table 2.2 shows typical sieve analyses using B.S. test sieves for three samples from the three tins and Figure (2.0) shows the grading.

An excess of fine particles in the sawdust was avoided by rejecting samples containing more than 16% passing No.100 sieve, and more than 6% passing No. 170 sieve.

The moisture content of the sawdust was measured at three different times using Speedy Moisture Tester type D.1. The results obtained were between 6.3 and 6.6 per cent. Bulk density with that moisture was 17.7 kg/m^3. and 16.6 kg/m^3. was recorded for dry oven samples.

Absorption measurements were also made on a companion 100 gm. sample. The sample was put in the conical flask which was used for beads density measurement and described before in Section 2.2, and water was added to cover the quantity of sawdust; the sample was stirred and agitated for about 3 minutes to remove any entrapped air. The flask was then filled with water to the filter and covered to avoid any loss of water by evaporation. The volume of water required to bring the water level to the reference mark - (mesh filter) - is equal to the volume of water absorbed by the sawdust. The results obtained from three air-dry samples, and another three oven-dry samples indicated; there was no absorption to be recorded after one hour, and the absorption after 24 h. was

Table (2.2) Typical sieve analysis of sawdust of three samples from three different batches.

Mesh No.	% Passing by weight			
	Sample (1)	Sample (2)	Sample (3)	Average
14	100.0	100.0	100.0	100.00
18	96.0	97.0	96.0	96.33
25	81.0	84.5	80.0	81.80
40	63.7	68.0	62.0	64.56
52	46.0	49.0	43.0	46.00
72	28.5	28.5	25.0	27.33
100	16.0	16.0	12.0	14.67
170	5.7	5.0	3.0	4.56
200	2.0	2.0	1.0	1.67

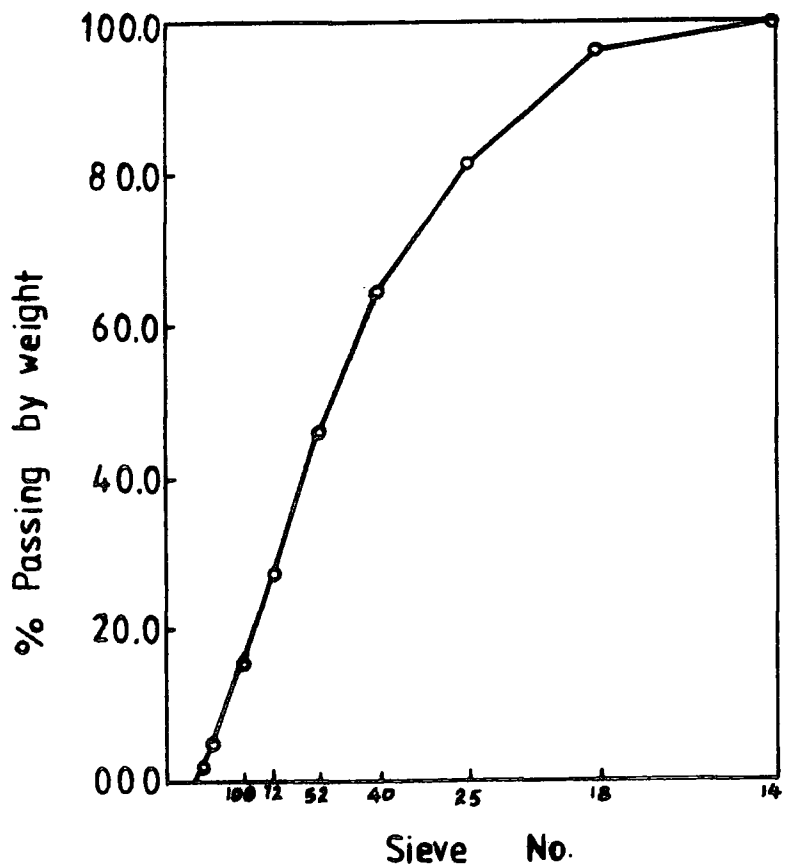

Figure (2.0) Grading curve of sawdust.

found between 6 and 7 gm. for the sample of 100 gm. weight of air or oven-dry sawdust. This test was very interesting, because it is known that sawdust has a high rate of absorption and the test results showed that most absorption happened during the first three minutes after the water was added. This indicates that the three minutes of concrete mixing time will be a suitable time for the sawdust to be saturated.

2.2.3 Cement

The rapid hardening portland cement was used for all experimental work carried out in this research. It was delivered to the laboratory a few bags at a time as required to avoid the effect of storage on its properties. The cement was kept in the control room well covered.

2.3 Concrete manufacture procedures

The experimental procedures described in this section were attempts to demonstrate the best method to be used for casting - or pouring - lightweight concrete so that the process can be fully controlled. The moulds of the dimensions stated later were chosen to be used in studying the effect of water/cement ratio on mix workability, castability, vibration and compaction. The same moulds were used for showing the influence of water/cement ratio on concrete density and strength according to the quantity of sawdust used and the cement content.

2.3.1 Moulds and mixing

Several wooden moulds, each of two similar sides and a bottom plate were constructed, each giving three separate cylinders of 2 in. diameter and 3 in. length (Appendix IV.a.1). The three specimens obtained in the assembled mould have the same conditions of pouring, vibrating, compacting and curing. The internal sides of the mould were greased or oiled five minutes before casting to prevent the cement paste adhesing to their sides, and to ease the specimens' removal.

The beads and sawdust, the latter in air-dry condition with the natural moisture determined beforehand, and dry cement were weighed - according to the mix proportion required in the method of design mentioned later - and placed in the concrete mixer in the order stated. (Using dry aggregates, this is the most reasonable method of operation for the laboratory tests in the case of lightweight aggregate concrete)(34). The quantity of water required was weighed and about a third was added to the mix before mixing commenced to avoid beads segregation. The remainder of the water was gently added during the first thirty seconds of mixing. Three minutes mixing were quite enough for all the particles of aggregates to be saturated and surrounded by cement paste, producing a mix of homogeneous constitution. A HOBART MODEL AE-200 MIXER was used.

2.3.2 Casting processing

It is known that compaction is one of the factors affecting the lightweight concrete properties. In the case of polystyrene concrete full compaction is not required. It

is necessary to develop a method of handling which will provide a constant standard of compaction when dealing with samples of different water/cement ratio and cement content. Three techniques have been tried and are described as follows:

1. In the first technique the mixture was poured into the moulds in two layers, each of about half the cylinders' height. The mould was vibrated after each layer for about 15 seconds, and a cement foam with floating beads was observed during vibration, especially in non-dry mixes and subsequently voids were formed and clearly appeared on the finished surface of the samples. In dry mixtures the construction of the cylinders was not homogeneous; some gaps were formed due to not enough compaction.

2. In the second try, using a wooden hand bar for tamping was not suitable, because the beads' spherical shape was destroyed. The compressibility of a dry mixture was higher than that of the wet mixture, and this caused unequal occurrence of the voids in the two mixes.

Comparative tests using this process are of doubtful value, and the main purpose of using the beads is thwarted, since the beads are partially crushed.

3. In the third attempt, three wooden solid cylinders of about 47 mm. diameter and 75 mm. length were made to sit on the concrete during the vibration. After pouring the first half into the mould, the solid wooden cylinders were put on the top of the concrete - before the vibration started, as shown in Appendix I.2. The cylinders were wrapped by a thin polythene sheet to prevent the concrete sticking to

their sides and to ease their movement. The moulds were vibrated for about 15-20 seconds, being held firmly on the vibration table during all the period of vibration. The total weight of the solid cylinders was designed to give a compacting weight of about 6.0 gm/cm^2, which was enough to prevent floatation segregation without any destruction to the spherical shape of the beads. The second halves of the cylinders were poured with the concrete a little higher than the top of the moulds, and plywood was held on the top of the mould, while the latter was held firmly on the vibration table during the second period of vibration. An electric vibration table type Allam No. 1336 was used. This procedure was found quite suitable to give all the mixes the same chance of compaction obtaining samples of good finished surface.

2.3.3 Curing

The moulds were covered with wet cloths after casting and were kept inside the control room in a temperature of about 22°C. The temperature variation did not exceed $\pm$ 1°C. Twenty four hours later the specimens were removed from the mould and were placed in a curing tank, where the temperature was kept at 20°C $\pm$ 1°C. Because most of the samples would float, and to avoid the use of weights for keeping them under the water, special wooden frames were made for the purpose, each one holding three samples. The samples were kept just under the top surface of the water. All the specimens were cured in the water tank for 6 days.

2.4 Density measurements and capping

Fully dry density measurements are difficult and not of much practical value where the samples need time to become fully dry, because oven temperature must be less than 70°C to avoid softening the beads. However, some mixes were dried for showing the moisture content and this will be discussed later.

The saturated density measurements seem more convenient and practical in general use. For the samples of the dimensions previously stated, saturated density was measured in the following manner : after the samples had been in the curing tank for six days, they were fully saturated and cured (rapid hardening cement being used). The samples were moved from the tank and paper hand towels were used to remove the surface water. All the three cylinders of the same mix were weighed and their volume was found by water displacement, and thus the saturated density was calculated.

The top surface of the samples obtained from the casting process was not quite flat and exactly parallel to the base surface, and to avoid eccentric loading, the cylinders were capped by plaster of Paris, which is a suitable material for capping such lightweight concrete (42). A special rig of two parallel plates, one of which was movable, was made to make the cap's top surface flat and exactly parallel to the base surface. A polythene sheet was used to prevent the plaster from sticking to the plate. The cylinders were tested 4 h. after the caps were placed.

2.5 Influence of the sawdust content on the mix and concrete properties

The main purpose of the sawdust, as mentioned before, is to improve the polystyrene concrete mix workability and to reduce the concrete brittleness. To achieve the effects of sawdust content on the properties of the mix and the concrete, and to determine the quantity of sawdust to be used in fulfilling its purpose successfully, several experimental laboratory procedures have been carried out and many mixes were made and tested. The results obtained were a guidance in determining suitable quantities of sawdust to be used in such lightweight concrete mixes.

2.5.1 Laboratory procedure

Two experimental programmes were carried out in this procedure. In the first one, four mixes were made and tested, where beads type (1) were used. The four mixes were mainly varying in the quantity of sawdust used in each. The volumes of sawdust in the mixes were designed to be 0.10, 0.20, 0.30 and 0.40 of the volume of the beads (Bulk Volumes). The mixes were designated respectively I,II, III and IV according to the quantities of the sawdust being used, (Table 2.3). Because the strength of concrete is influenced by the ratio of cement to aggregates, (cement content), the four mixes were designed to have the same cement content - 410 kg. cement per cubic meter of aggregates. The quantities of total water used for each mix were determined so as to keep all the mixes of the same consistency, i.e. the required workability, where three primary trial mixes were made first for each mix.

Initially, three cylinders of 2 in. diameter and 3 in. length were cast and tested, but for more reliable results three cylinders of 102 mm. diameter and 204 mm. length were made and tested from each mix.

The second programme was carried out to confirm the results obtained from the first one by using beads type (2). Two mixes, II and IV, were made, increasing the cement content to 620 kg. per cubic meter of aggregates, and two cylinders of 150 mm. diameter and 300 mm. length were cast and tested from each mix. Three cylinders of 2 x 3 in. dimension also were made for oven-drying and testing.

The moulds for the cylinders of 102 x 204 mm. dimensions were made from hard plastic rainwater pipe, cut along their length to ease stripping. A wooden base with 10 mm. upstanding plug was made.

The slit in the plastic mould was held together by a set of three jubilee clips and the longitudinal slit was sealed with mastic (plasticine) to prevent the escape of cement paste. Standard steel moulds were used for making the cylinders of 150 x 300 mm. dimensions.

All the concrete made in this procedure was mixed, cast and cured using the methods described in 2.3.

The crushing compression tests were carried out for all the cylinders at 7 days in Demison testing machine model T42 B4, 500 KN capacity, using the scale disk of 50 K.N. capacity for testing the cylinders of 102 x 204 mm. dimensions, and of 100 K.N.for the cylinders of 150 x 300 mm. dimension. All the samples were tested on the same rate of loading which was

adjusted to be 2 MN/m^2/minute. The cylinders were adjusted at testing to be centralized with the axis of the hemispherical seating of the machine, and two steel plates of 155 x 155 x 14.6 mm. were used to spread the load equally on the cylinder.

2.5.2 Results and discussions

The saturated density measurements and compression test results (average of the three samples) of cylinders of 102 x 204 mm. dimensions were recorded in table 2.3 according to the quantity of the sawdust used. It can be seen that the concrete density and strength increased with using more sawdust in the mix, but the increase in both is not proportional. The results indicate that increasing the volume of sawdust in the mix from 0.10 to 0.20 of the volume of the beads - Mix II - caused 3.8 per cent increment in concrete density and 7.8 per cent in the compression strength. Triplicating the sawdust in the mix - Mix III - led to increase of 10 per cent for both density and strength. When the quantity of sawdust increased four times, the density increased 23 per cent, while the compression strength is only 12 per cent higher. Calculating the compression strength per unit density showed that mix II has the highest efficiency and mix IV is of the lowest efficiency, where the compression strength per unit density of mix II is 16 per cent higher than that of mix IV. Mix I and mix III seem to have a similar efficiency figure (2.1). The results obtained from the cylinders of 2 x 3 in. dimensions were approximately similar.

The results of the cylinders of 150 x 300 mm. dimensions

Table (2.3) : Influence of sawdust ratio on the concrete density and compressive strength

Type of beads used	Dim. of test cylinders mm.	Mix Symbol	Sawdust/ beads by vol.	Cem.cont. in kg.per cub.met. of agg.	Conc.sat. density kg/m.^{3}	Comp. strength MN/m.^{2}	Comp.st. per unit density MN/m.^{2}
(1)	102x204	I	0.10	410.0	650.0	2.170	3.340
		II	0.20	410.0	675.0	2.340	3.740
		III	0.30	410.0	715.0	2.400	3.360
		IV	0.40	410.0	800.0	2.430	3.000
(2)	150x300	II	0.20	620.0	910.0	5.590	6.140
		IV	0.40	620.0	950.0	4.590	4.830

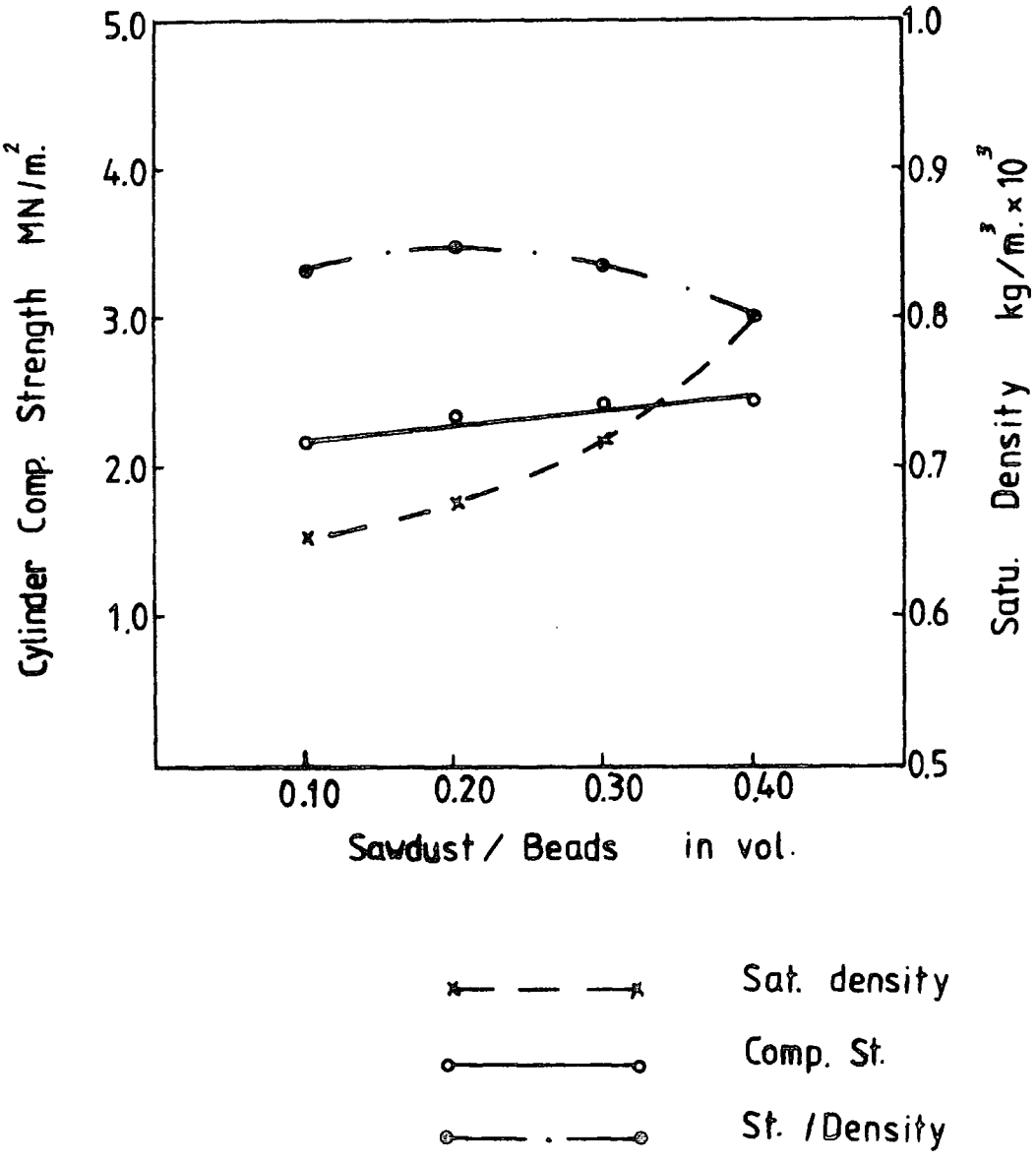

Figure (2.1) Concrete saturated density and compressive strength versus sawdust content.

* All mixes of same cement content; 410 kg. cement per cubic metre of aggregates.

** Test results of cylinders 102 x 204 mm. dimensions at 7 days.

which were carried out to compare mix II and mix IV with higher cement content (620 kg/m^3.) and other beads - beads type (2) - were recorded in table (2.3), and confirm the results obtained before. It can be seen that with this cement content and these dimensions of the samples, the mix IV, which only had 4.4 per cent increment in the density, has had a reduction in its strength of 18 per cent.

The saturated density of the cylinders 2 x 3 in. dimensions were found to be 1.0 and 0.925 gm/cm^3. for the concrete of the mixes IV and II respectively. When these cylinders were put in a drying oven of temperature 55^{o}C. for 3 weeks till the losses in weight nearly ceased, the reductions in the weights were found to be 23 and 17 per cent respectively, i.e. the concrete containing more sawdust - as expected - has the higher moisture content. In the oven-dry state samples of the two mixes have approximately the same density. When compression tests were carried out on the cylinder, the average results obtained from the three cylinders of each mix were found to be 5.5 N/mm^2. for the samples of mix IV and 6.27 for the samples of mix II.

The test results which were recorded during the concrete manufacture can be summarized in two main points. The first one is related to the concrete workability. It was observed that the mix of the lowest sawdust content - Mix I - is of the least efficiency in workability. It needs much careful vibration to obtain homogeneous samples. The volume of sawdust of 0.20 of the volume of beads was found to be enough to qualify the mixture for good workability. The second note is the initial shrinkage of the concrete after 24 hours from pouring. It was

found that the concrete of the highest volume of sawdust - Mix IV - had the highest value of the initial shrinkage. To formulate this note numerically, the top surface of the cylinders which were cast in the steel moulds were floated exactly horizontally with the top of the mould directly after the casting; 24 hours later the total length of the samples was measured after mould-stripping using a micrometer of accuracy 0.02 mm. with plywood plates. The results obtained showed that the reduction in the total length was about 2 and 2.7 per cent for the concrete of mix IV at cement content 620 and 410 respectively, while reductions of 0.7 and 1.0 per cent were found in the concrete of mix II at the same cement content.

It can be seen from the results obtained, that the mix containing sawdust of 0.4 times the volume of the beads is not to be recommended for both workability and strength. The quantity of sawdust of 0.20 times the volume of the beads is enough, and for more workability, sawdust of 0.30 can be used. However, the sawdust is necessary since it maintains the polystyrene concrete in a condition of good workability which makes vibration acceptable, giving a homogeneous sample with cement paste well distributed along all the length of the sample.

The strength of the sawdust as aggregate is very low since it causes fine voids to occur within the cement matrix, leading to concrete of lower strength. Because of this, it is important to add only the minimum amount of sawdust required to improve the workability. The effect of sawdust on the sample construction can be seen in figure (2.2), where two cylinders are shown using the polystyrene beads of large size

Figure (2.2) : Influence of sawdust on the cylinder construction and cement paste distribution after vibration.

(beads Type (3)), the cylinder on the right being made with sawdust of volume = 0.20 times the beads volume, and the other one made without sawdust. The quantity of water for each was determined as that required to give acceptable workability.

2.6 Effect of water content on the mix and concrete properties

The value of water/cement ratio is one of the most important factors affecting concrete properties. In lightweight concrete the total water used depends on the type of aggregate used. The quantities of water are required both to form the cement paste and to saturate the aggregate. Determining the value of water absorbed by the aggregate - especially in this research by the sawdust - is difficult, because it is changeable according to the moisture content of the aggregate and the rate of absorption. However, many mixes and much experimental work have been done in this section of the work and the results were obtained aiming to demonstrate the following points:-

(1) To show the effects of total water used on concrete strength, density and the mix workability.

(2) For showing the value of total water/cement ratio required for good workability.

(3) The results obtained were used for calculating and determining the net water/cement ratio required to form the cement paste to be used in such polystyrene concrete in practice.

2.6.1 Schedule of mixes and laboratory procedures

Taking into account the results which were obtained and recorded in (2.5), the mix of sawdust of volume 0.4 times the volume of the beads (Mix IV) was omitted. The mixes which were studied in this procedure were recorded in table (2.4) and were grouped according to the type of the polystyrene beads used (table 2.1).

In this research the cement content is formulated by the weight of the cement used in kg. per cubic meter of bulk volume of aggregates.

In the researches where the weight proportions are recommended for accuracy and because several mixes were required in this procedure, the weights of the cement were related to the weight of the beads used in the mix. To ease the laboratory work, avoiding the probability of mistakes in the weights, the weights of the polystyrene beads used were fixed in all mixes, accordingly using more sawdust or more beads of low density (which means increasing the volume of aggregates) causing decreases in the cement content for the same quantity of cement used, because of the way the cement content was defined. Table (2.4) shows the cement content versus the quantities of the cement and sawdust used for the three types of the polystyrene beads used. The values of the cement content were recorded to the nearest 5 kg.

The quantities of the mix ingredients which were required for making the three cylinders of 2 x 3 in. dimensions were found too small to have the expressivity of the mix's consistency and workability, so 20 gms. of the polystyrene beads

were used for all the mixes with the correspondent values of the cement and sawdust. The quantities of sawdust were determined by weight, according to its density and the density of the beads used. In the trial mix using beads type (1) and sawdust of 0.30 times the volume of the beads, the weight of cement of 22.5 times the weight of beads was found to be a suitable initial value to produce a concrete mix of a reasonable strength.

For demonstrating the effect of water content on the mix workability and the concrete strength and density, four or five different values of water content were used for each of the twelve mixes made by using beads type (1) table (2.4). The quantity of water to give the required workability was determined experimentally for each value of the cement content of the twelve mixes. The influence of water content on concrete strength and density was studied using beads type (2) for all the mixes of sawdust of volume 0.20 times the volume of the beads - group II - and three mixes of group III - of cement content 380, 570, 760. The water required to give workability in these mixes was determined according to the results obtained from the mixes made using beads type (1). All the mixes made by beads type 3 (table 2.4) and the remaining mixes of group III beads type 2 were made only to determine the quantity of water required for workability according to the method which was being developed.

All the mixes were made, and the concrete was cast and cured in the way mentioned before in 2.3. The density of the samples was measured using the method described before in 2.4. The compression tests of all the cylinders - three from each

Table (2.4) : The cement content according to sawdust used in the mixes investigated to show the effect of water/cement ratio on the mix properties.

Type of beads	Cement/beads in weight proportion	Cement content (wt. of cement in kg. per cubic metre of aggregate) according to the ratio of sawdust in the mix.		
		Mix I	Mix II	Mix III
1	22.5	400	370	340
	30.0	535	490	450
	37.5	670	615	565
	45.0	805	735	680
2	22.5		305	285
	30.0		410	380
	37.5		515	475
	45.0		615	570
	52.5		720	665
	60.0		820	760
3	22.5		305	-
	30.0		410	380
	37.5		515	475
	45.0		615	570

mix - made in this procedure were carried out on the Tensometer Type E at an age of 7 days with a load rate of about 2 MN/m^2/min. using the special cage for the compression test.

2.6.2 Results and discussions

2.6.2.1 Mixes' compression strength and density

The concrete compressive strength and the saturated density versus the total water/cement ratio used were graphed in figures (2.3 - 2.8) for all the mixes made by using bead types (1) and (2) respectively. The mixes were designed using a range of water contents to produce concrete characteristics between wet and dry mixes. It can be seen from the graphs of the compressive strengths - figures (2.3a - 2.8a) - that all the mixes show similar behaviour, where the compressive strength increased with increasing water content up to a certain value, beyond which further increase in the water content causes a decrease in strength. The influence of water content on the concrete density can be seen in figures b. It can be considered (neglecting the very dry mixes) that the density is reduced with increasing water content. However, the effects of water content on the concrete strength and density gave the expected results. The behaviour can be attributed to the amount of the water required to form the cement paste as follows:

- The water used in this concrete consists of that required to saturate the aggregate - especially sawdust - and to wet the surface of the aggregates and that required to form the cement paste to a suitable consistency.

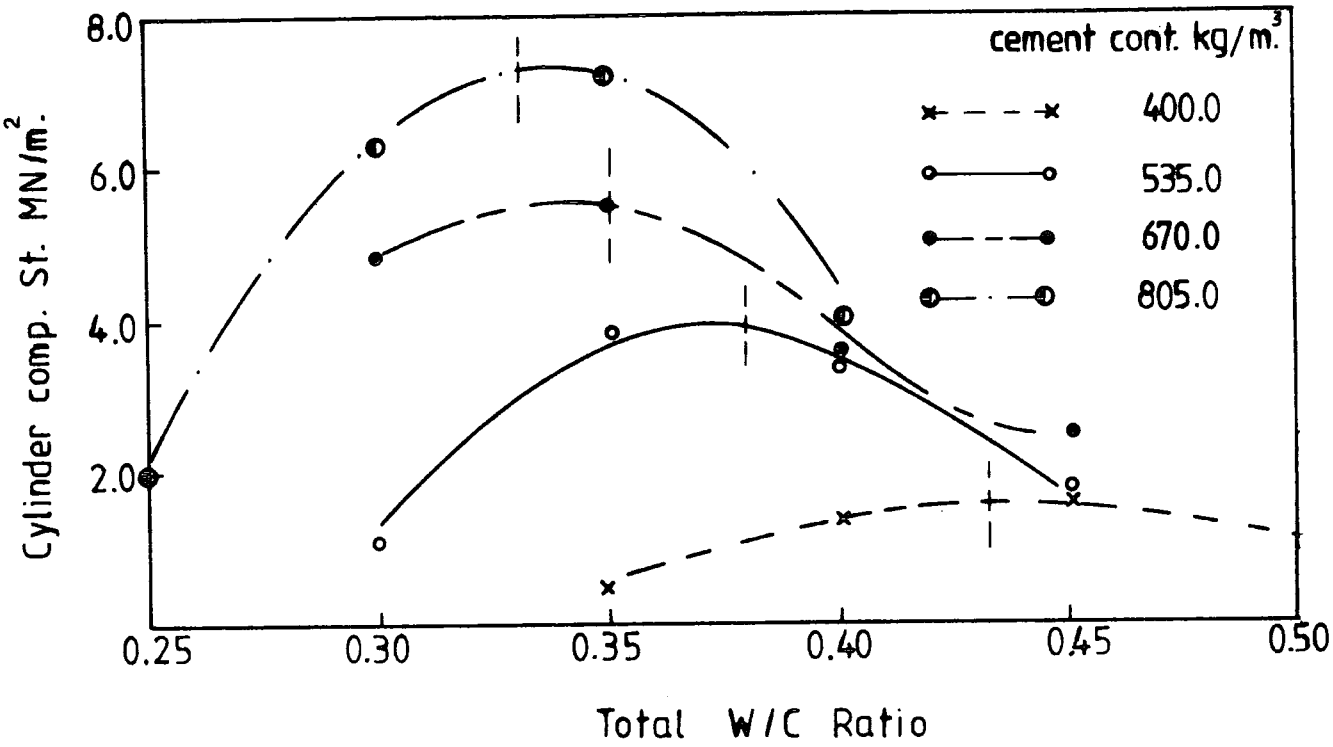

Fig. (2.3a)

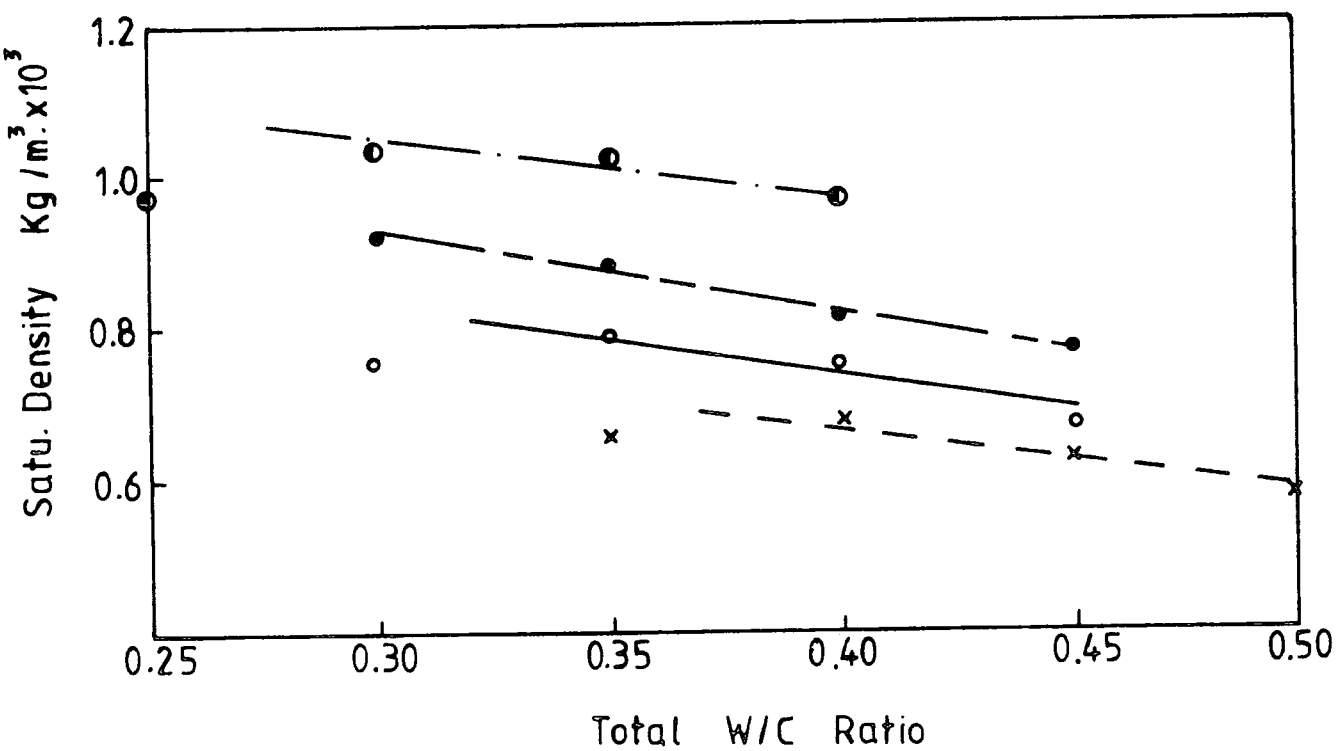

Fig. (2.3b)

Figure (2.3) Cylinders compressive strength and density versus the total water/cement ratio used for mix I.

(Beads type 1)

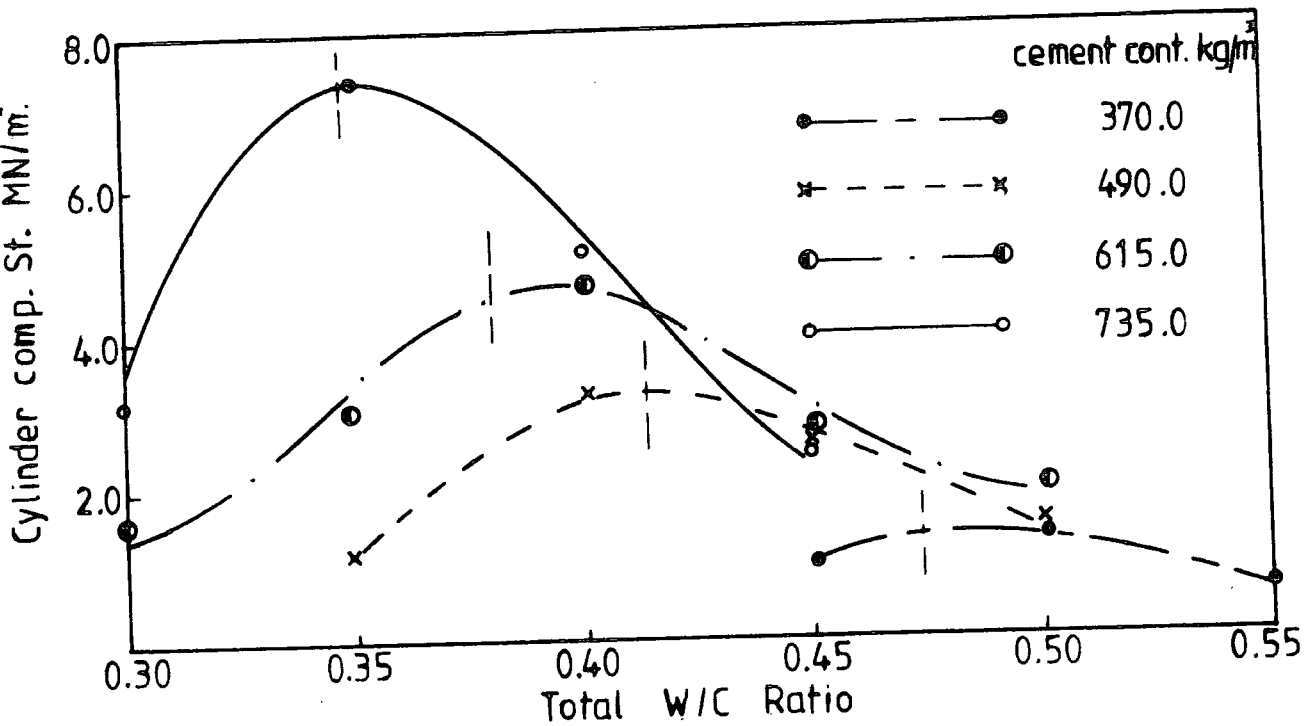

Fig. (2.4a)

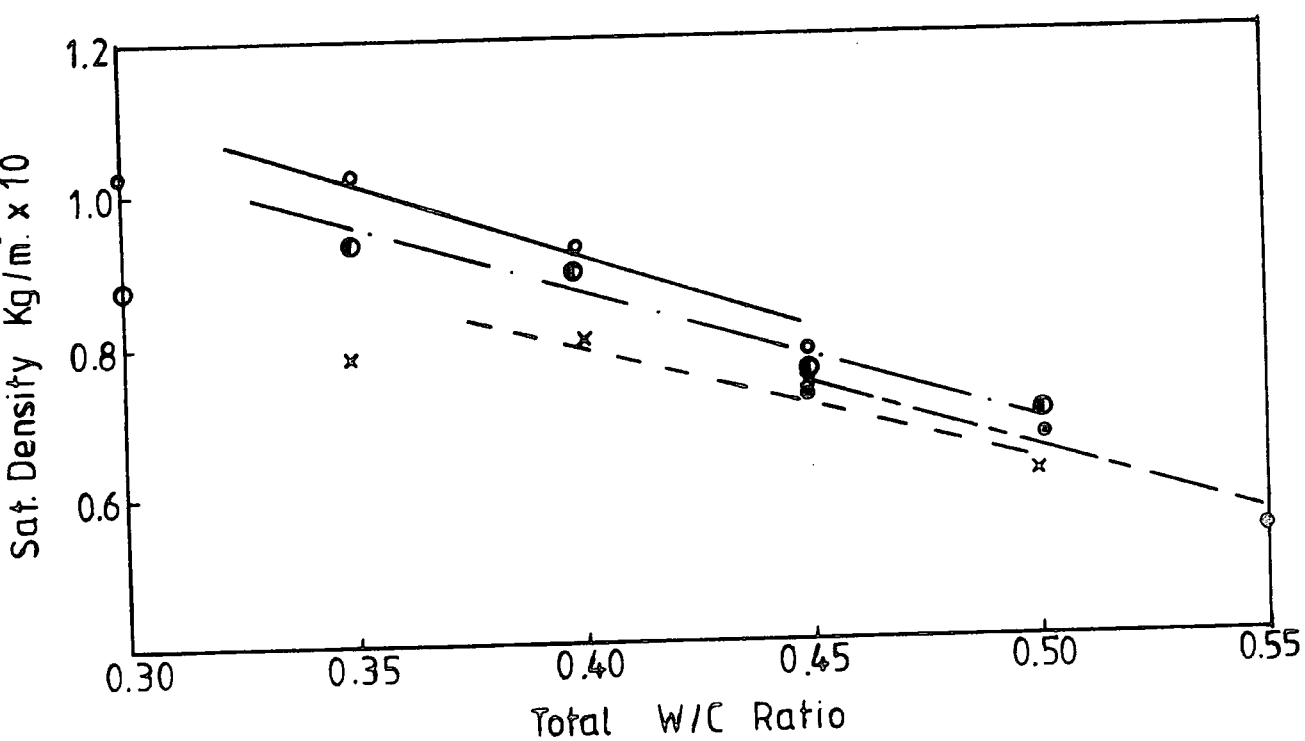

Fig. (2.4b)

Figure (2.4) Cylinders compressive strength and density versus the total water/cement ratio used for mix II.

(Beads type 1)

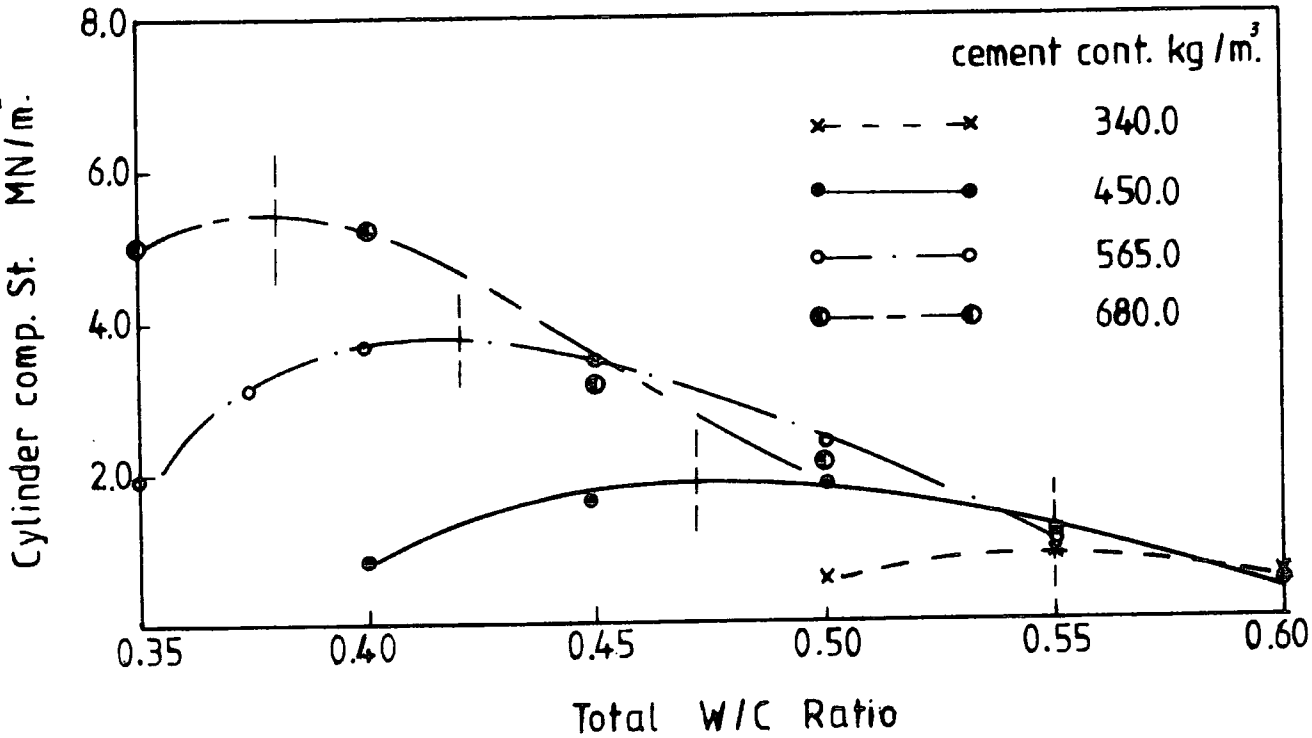

Fig. (2.5a)

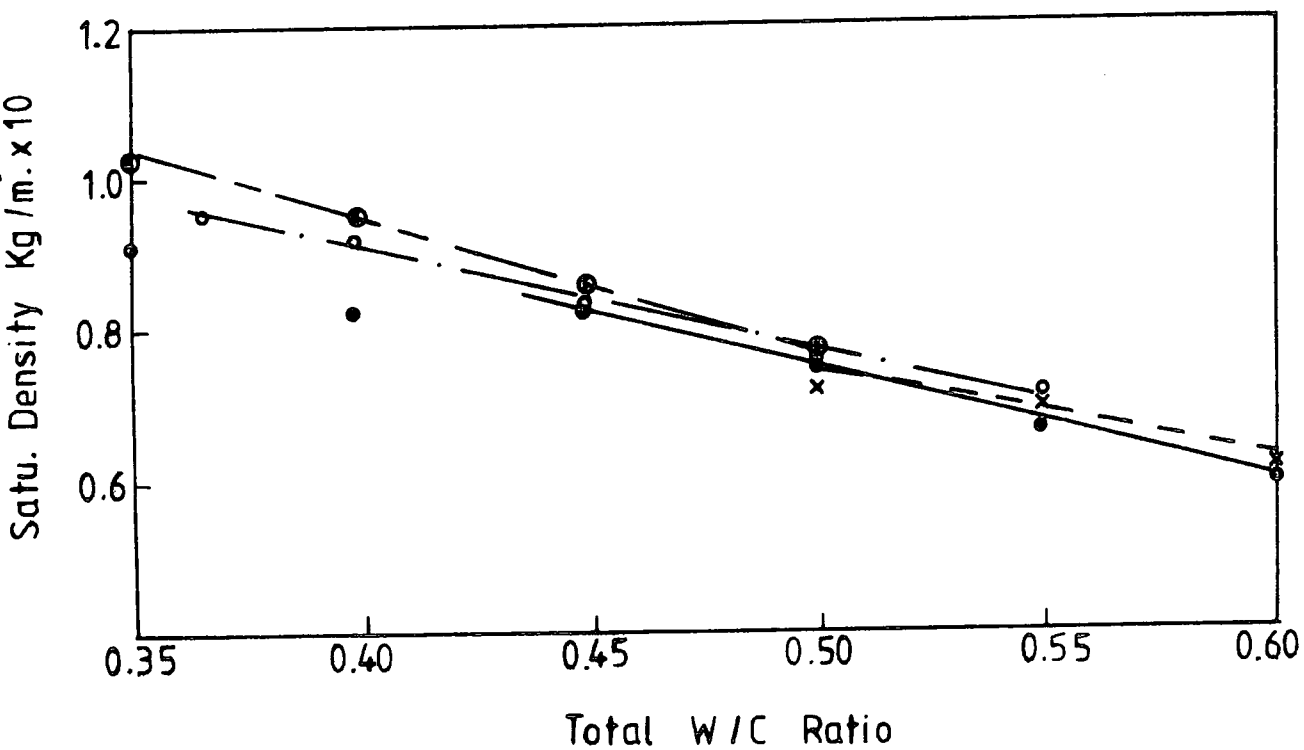

Fig. (2.5b)

Figure (2.5) Cylinders compressive strength and density versus the total water/cement ratio used for mix III. (Beads type 1)

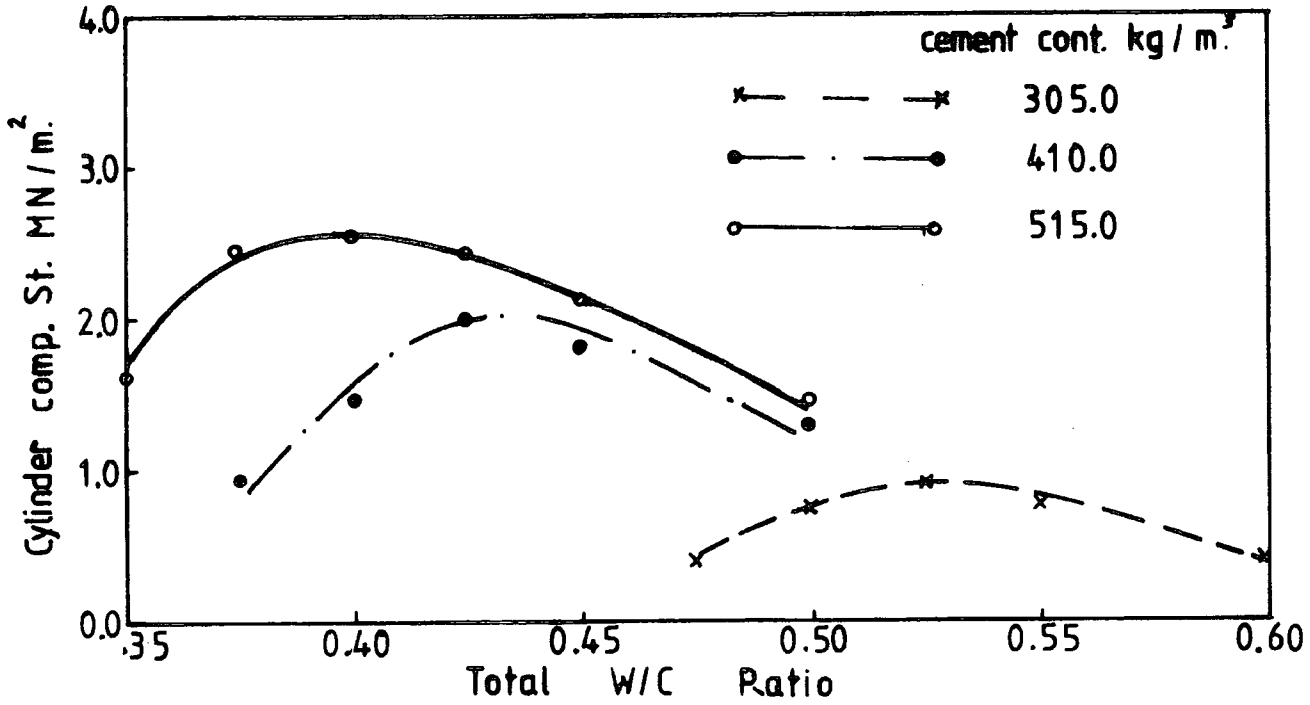

Fig. (2.6a)

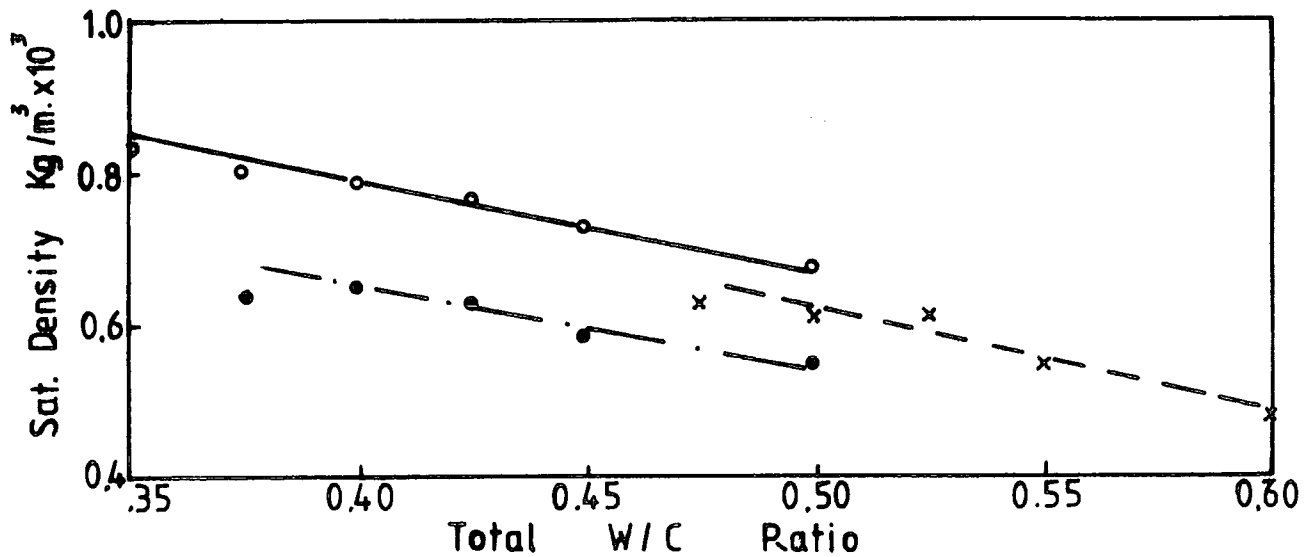

Fig. (2.6b)

Figure (2.6) Cylinders compressive strength and density versus the total water/cement ratio used for mix II. (Beads type 2)

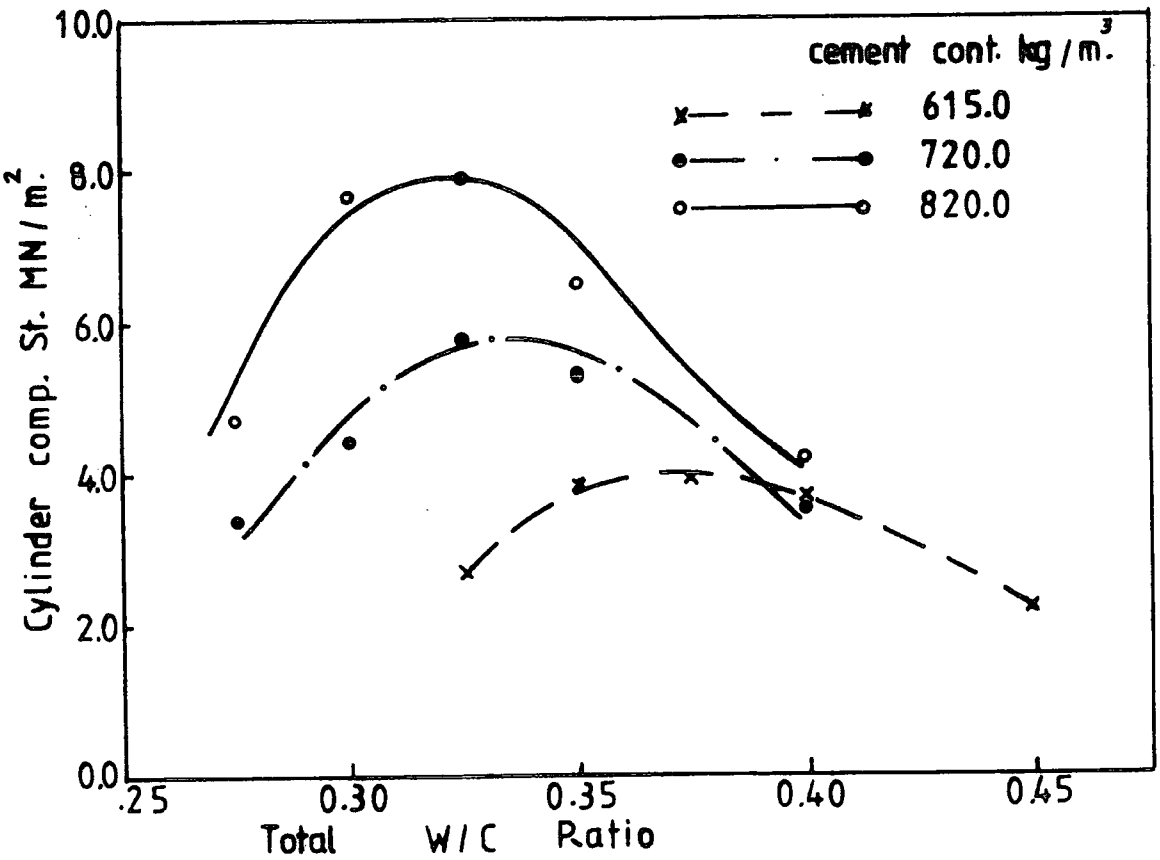

Fig. (2.7a)

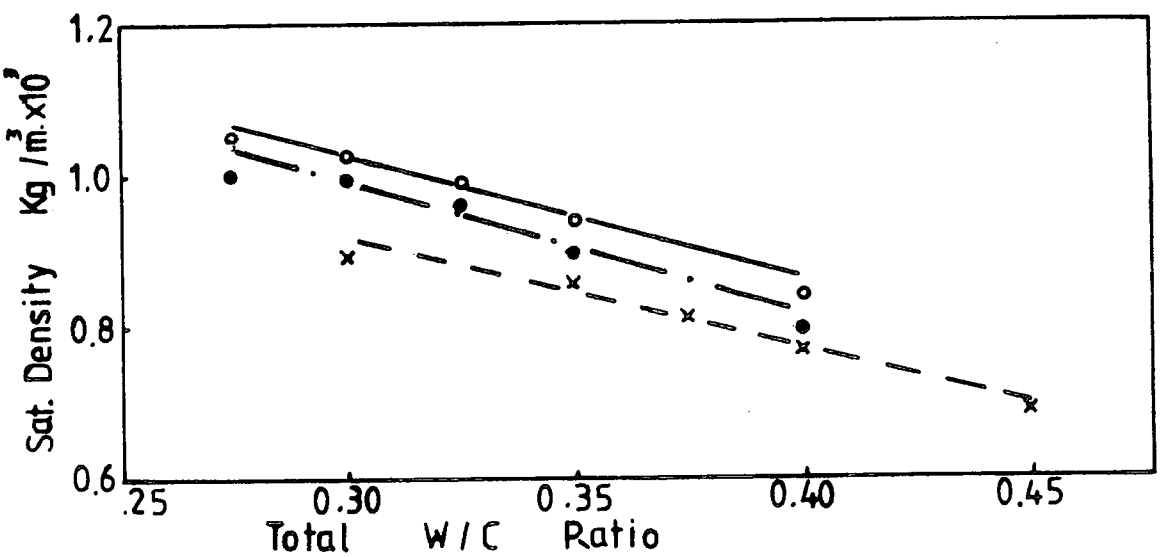

Fig. (2.7b)

Figure (2.7) Cylinders compressive strength and density versus the total water/cement ratio used for mix II.

(Beads type 2)

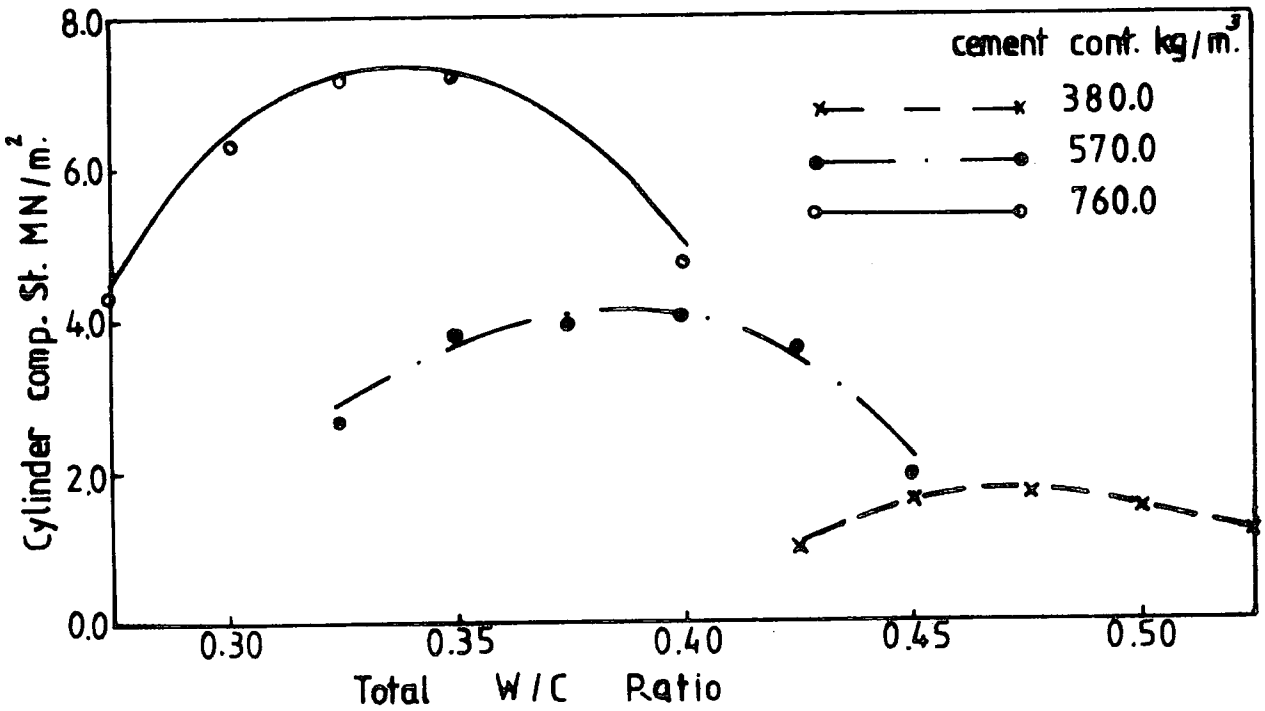

Fig. (2.8a)

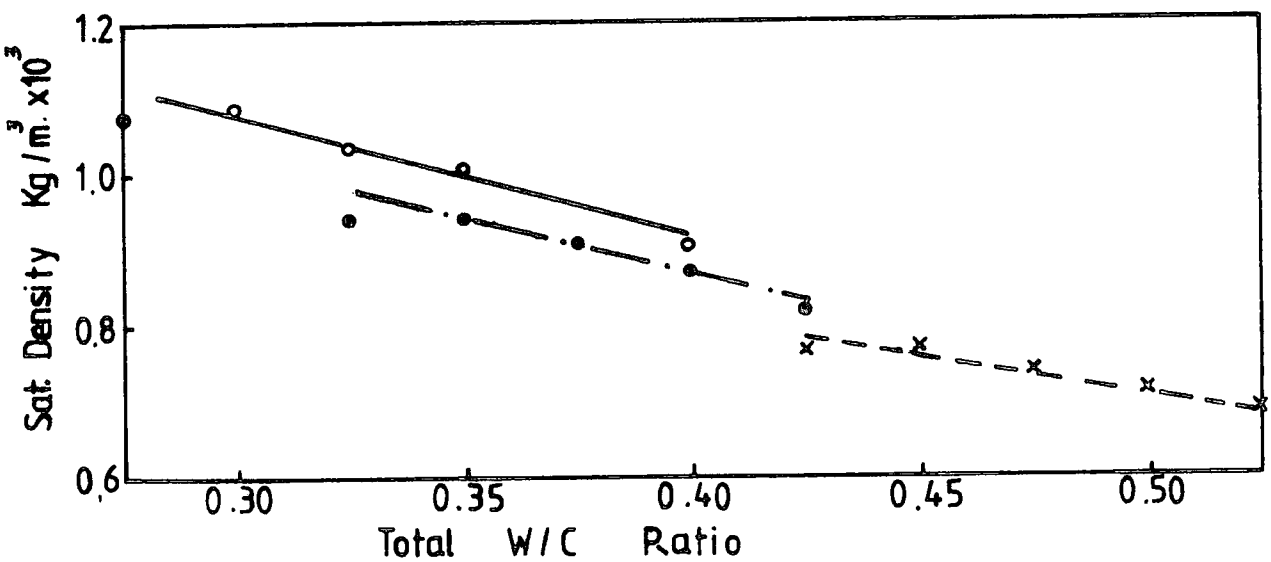

Fig. (2.8b)

Figure (2.8) Cylinders compressive strength and density versus the total water/cement ratio used for mix III.

(Beads type 2)

- When the amounts of water used are small the sawdust absorbs the water, leaving the cement without enough water to cause the chemical interaction and finally produce a concrete of poor adhesion - weak strength - and high density.

- When the water content is higher than that required, the addition water occupies space inside the cement paste causing reduction in both strength and density.

The results of the tests on all mixes as reported here, indicate that the concrete maximum strength and density are affected mainly by the cement content and the variation of both seem proportional to the variation of the values of the cement content. However, these variations are discussed in greater detail in the light of the test results described in chapter 3.

2.6.2.2 The water/cement ratio for workability

Determining the quantities of water required for workability is one of the most important points which was interesting in this procedure. The total water/cement ratios for greatest workability which were determined experimentally for the mixes made by using beads type (1) were recorded in table (2.5). When these ratios were marked on the strength curves (the vertical lines) figures (2.3a - 2.5a), fortunately they were found to coincide with the optimum points of the strength, or were very close to the optimum value. It was found also that the total water/cement ratio was reduced by increasing the cement content to achieve the required workability, but the quantities of the water itself increased. This is because the volume of the aggregate is the same and the cement and the water are the only changeable factors. The water which was

added to account for the additional cement could be considered the net water/cement ratio to form the cement paste for determining that ratio. The quantities of the water and cement used and subsequently the additional water and cement added to the mixes made by using bead type (1) were calculated and recorded in table (2.5). Figure (2.9) is a graph to show the water increment versus the cement increment. From table (2.5) and figure (2.9), the rate of water increment due to the cement increment could be written in the following formula:

$$\Delta W = 0.229 \quad \Delta C \qquad (2.1)$$

where ΔC = the increment in the cement content

and ΔW = the increment in the water due to the increment in cement of ΔC

According to these results, the quantities of water required for workability can be determined in one of the following two methods :

(1) using saturated aggregates and the net water/cement ratio deduced previously. This method is not recommended for two reasons; the first is the difficulty of saturating the sawdust exactly without any water to be more or less than that required for this specific purpose. Secondly; saturating the aggregates before mixing leads to concrete of strength about 10 per cent lower than when dry aggregates are used at the same cement content.

(2) The second method, which it is advisable to use, depends on making a trial mix of suitable cement

content with the ratio of sawdust designed, the quantities of water to give the required workability being determined experimentally. If a subsequent increase, or decrease, in the strength is required, the water added for any additional cement may be calculated using the formula mentioned before.

The total water/cement ratios for workability of the mixes made by beads types (2) and (3) were determined by the second method as shown in table (2.6). The mixes of cement contents of 410 and 380 kg. were used in the trial mixes for groups II and III respectively. Determining the total required water/cement ratios from the curves of strength of the mixes in figure (2.6a - 2.8a) was found to give results close to the optimum points of the strength, thus confirming the applicability of the method. Both the mixes of cement content 305 and 285 kg/m^3. of groups II and III respectively need a higher water content to give required workability than to give the maximum strength.

Table (2.5) : Calculating the net water/cement ratio from the total water for the required workability

(Beads type 1)

Mix Symbol	Cement cont.kg.for cubic meter of agg. C	Tot.water/ cement ratio for suitable workab- ility	Weight of tot. water W kg.	Increase in the cem- ent cont. (ΔC) kg	Increase in the water (ΔW) kg	The net water/cem- ent ratio ΔW/ΔC
Mix I	400	0.430	174.0			
	535	0.380	205.0	135	31.10	0.231
	670	0.350	236.0	270	62.25	0.231
	805	0.330	267.0	405	93.30	0.230
Mix II	370	0.475	175.7			
	490	0.415	203.4	120	27.7	0.230
	615	0.380	233.7	245	58.0	0.236
	735	0.350	257.3	365	81.6	0.224
Mix III	340	0.550	184.3			
	450	0.470	211.5	110	27.2	0.246
	565	0.420	235.2	225	51.0	0.227
	680	0.38	257.0	340	72.7	0.214
Average net water/cement ratio = 0.229						

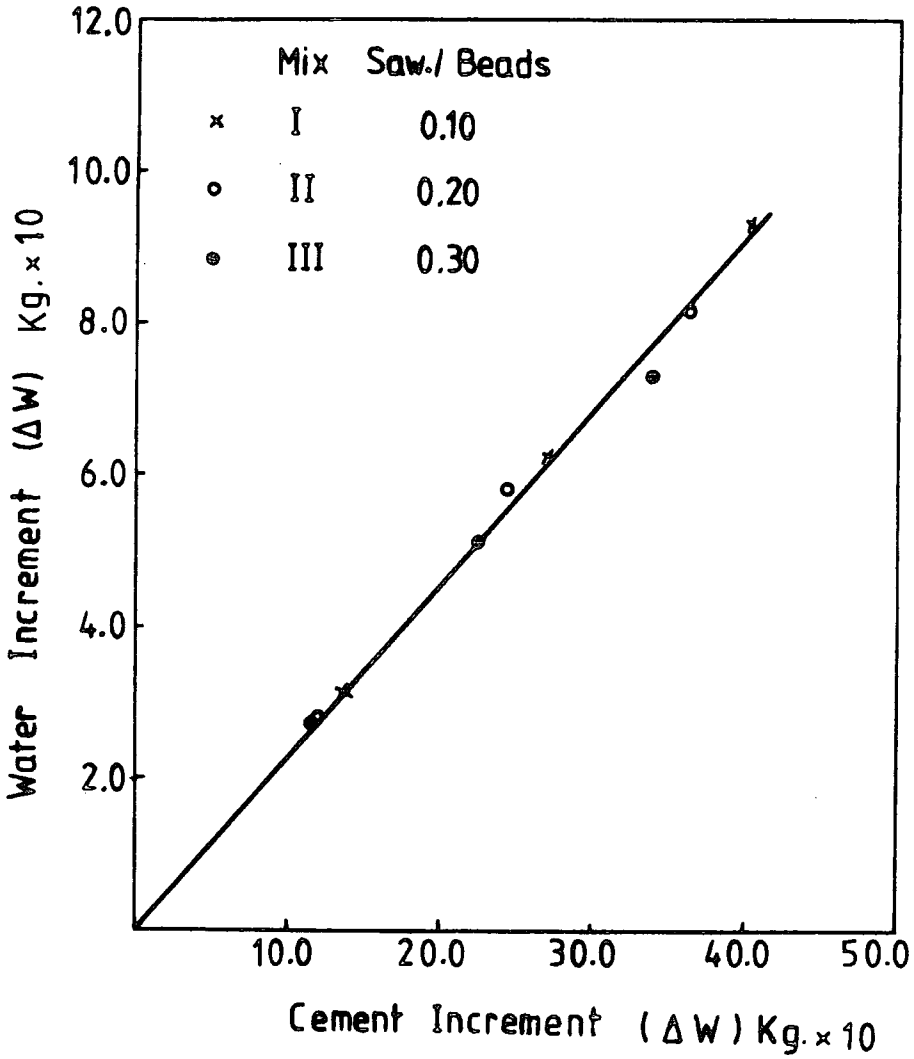

Figure (2.9) Water increase versus cement increase.

(Mixes made from beads type 1)

Table (2.6) : Determining the total water/cement ratio for the required workability for the mixes made using beads type (2) and (3) according to the developed method

Mix Symbol & beads type	Cement cont. kg. for m^3 of aggr. (C)	Cement cont. increment in kg. (Δ C)	Water incr. for cement inc. in kg. (Δ W) $=0.229\Delta$ C	Tot. water req. for workability $=W_i + \Delta W$	Tot. water/ cement ratio
Initial mix	410			$W_i=174.7$	0.426
II Beads type (2)	515	105	24.05	198.75	0.386
	615	205	47.00	221.70	0.360
	720	310	71.00	245.70	0.340
	820	410	94.00	269.0	0.328
Initial mix	380			$W_i=183.00$	0.475
III Beads type (2)	475	95	21.76	204.76	0.427
	570	190	43.51	226.51	0.394
	665	285	65.26	248.26	o.370
	760	380	87.00	270.00	0.353
Initial mix	410			$W_i=179.0$	0.435
II Beads type (3)	515	105	24.00	203.0	0.395
	615	205	47.00	226.0	0.370
Initial mix	380			$W_i=184.0$	0.485
III Beads type (3)	475	95	22.00	206.0	0.435
	570	190	46.00	230.0	0.405

CHAPTER THREE

STRUCTURAL PROPERTIES OF POLYSTYRENE CONCRETE

3.1 Introduction

The experimental works which have been done, and the test results described in this chapter, were planned to demonstrate the structural properties of the polystyrene cement under the circumstances of the manufacturing techniques which have been mentioned in Chapter 2.

At the convenient water/cement ratios and with the suitable values of sawdust content, the influence of cement content on the concrete compressive strength, density, modulus of elasticity and rigidity has been demonstrated. The values were expressed in empirical formulae including all the relevant factors.

3.2 Concrete compressive or crushing strength and density versus cement content

The results which were obtained and recorded in (2.6) showed clearly that strength and density of concrete of suitable workability mainly depend on the cement content of the mix. Because the samples tested in (2.6) are not of standard dimensions and to increase the dependability and comparability of the results, the experimental work carried out in this procedure was planned to examine more precisely the influences of the cement content on the concrete strength and density in standard samples.

The ultimate compressive strength - or crushing strength - of concrete is determined by testing cubes or cylinders of

standard dimensions. Cylinders are believed to give a greater uniformity of results for similar specimens as their failure is less affected by end restraint of the specimens. The stress distribution on horizontal planes in the cylinders is more uniform than on specimens of square cross-section, so the cylinder is preferred to the cube for research purposes (28). In the case of polystyrene concrete the use of cylinders is more preferable, because they are cast and tested in the same position, while in cubes the line of action of the load is at right angles to the axis of the cube as cast.

3.2.1 The sample dimensions, manufacture and testing procedures

The cylinders tested in this section have been made to be one of two dimensions; 150 x 300 mm. or 102 x 204 mm. According to the dimensions of the polystyrene beads used as a coarse aggregate in this research and with reference to the results carried out by others, the cylinders of the dimensions 102 mm. diameter and 204 mm. length can be considered standard samples, in the sense that the results may be compared with findings by other workers (27, 32).

Three cylinders were made for each mix of the thirty-one mixes recorded in table 2.4, using the quantities of water to give the required workability as determined before in (2.6.2). The moulds used for these samples are those mentioned and described before in (2.5.1). The cylinders of dimensions of 102 x 204 mm. were used for all mixes of beads types (1) and (3), and the 150 x 300 mm. samples have been made for all the twelve mixes of beads type (2).

All the cylinders made in this procedure were cast in three layers each of about a third of the cylinder's length and vibrated for about 20 seconds using a tamp weight of about 6 gm/cm^2. The cylinders were cured in the curing tank for 5 days. After removing the samples from the tank for 10 minutes, the dimensions of each cylinder were measured to determine the volume (bulk volume) using a micrometer giving an accuracy of $\pm$0.02 mm. The cylinder was weighed to find the saturated density of the concrete. The samples were capped by using plaster of Paris and were kept in the control room till testing.

All the cylinders that have been made for this purpose were tested at an age of 7 days in the Denison Testing machine model T42 B4 in the way mentioned before in (2.5.1) with load of rate about 2 $MN/m^2/min$.

3.2.2 Results and discussions

The compressive - or crushing - strength and the density of the concrete (the average of the three samples) have been obtained using the polystyrene beads type (2) in the standard cylinders of 150 x 300 mm. dimensions, and were graphed in figure (3.1) against the approximate cement content used. The data also were recorded in table (3.1). Since the same type, and the same volume of aggregate was used for each group with water to keep all the mixes at the same workability, and the same degree of tamping and vibration was used for all the mixes, variations in the strength and the density then are attributed only to the cement content. It can be seen from the results obtained in group II, when the cement content was increased from 410 kg/m^3 to be 615 kg/m^3 - i.e. 50 per cent - the com-

pressive strength increased 112 per cent and the density was found to be only 28 per cent higher. Using cement content of 820 kg./m.^{3} - i.e. double - led to strength more than triple and 50 per cent increment in the density. The results which were recorded from the mixes of group III were found to be approximately similar to those of group II. The graphs indicate that the relationship between the cement content and the average strength is linear for each group figure (3.1a), and the average density - cement content relationship also is linear, as shown in figure (3.1b). It can be observed that the increase in the compressive strength of the mixes of group III is accompanied by an increase in the mixes density. However, the rate of stress increment was found to be more than 3 times the rate of density increment for the two groups.

The compressive strength and density of the concrete of beads type (1) and made in the cylinders of 102 x 204 mm. dimensions were graphed in figure (3.2), and the data also were recorded in table (3.2). It was found that the strengths and densities of the mixes of groups II and III were approximately similar, while the results of the mixes made in group I are of the lower strength and density as shown in figure (3.2). The results obtained from the mixes of groups II and III were found nearly equal to the average results of the same groups which were made by beads type (2). The little variation in the results of the two types may be attributed to the change in the size of the samples used in each; i.e. when the beads were equal in size, the variation in their density is negligible.

The results obtained from the concrete made by using

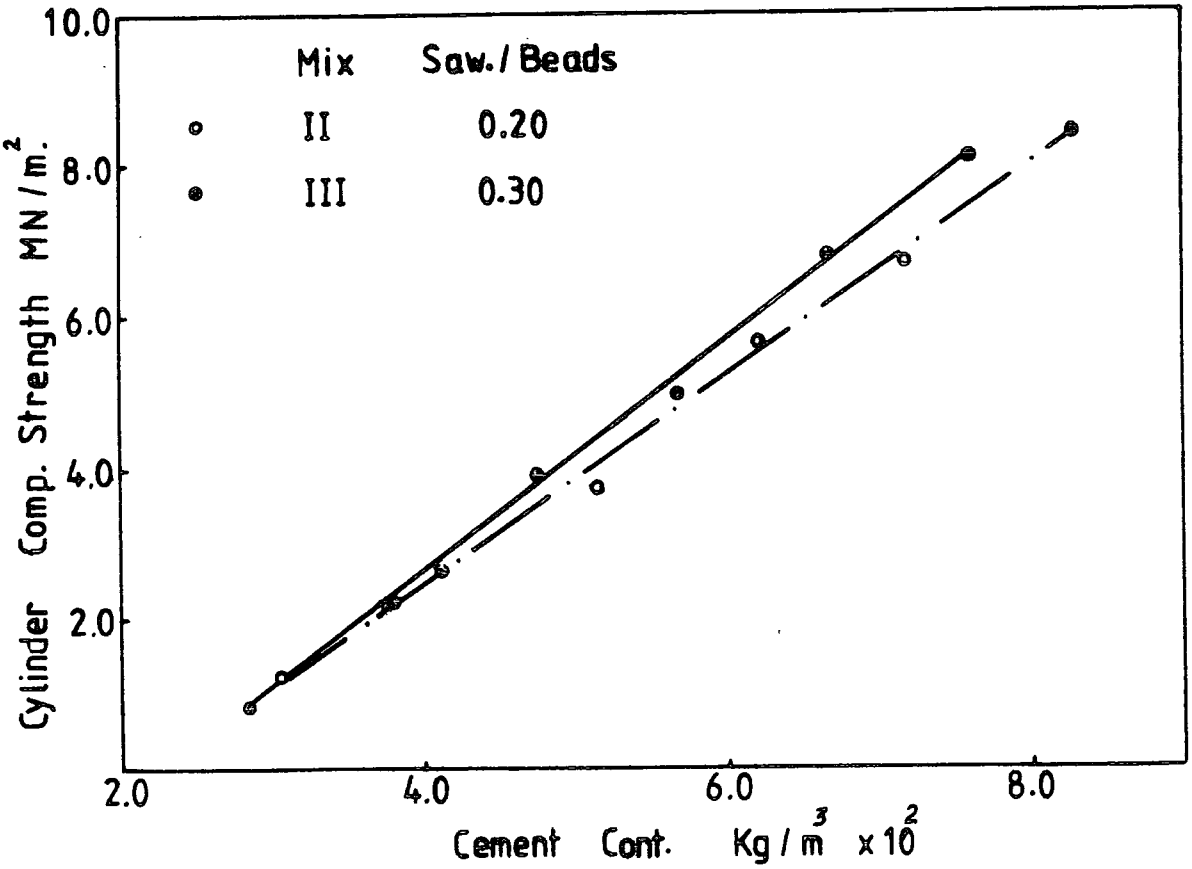

Fig. (3.1a)

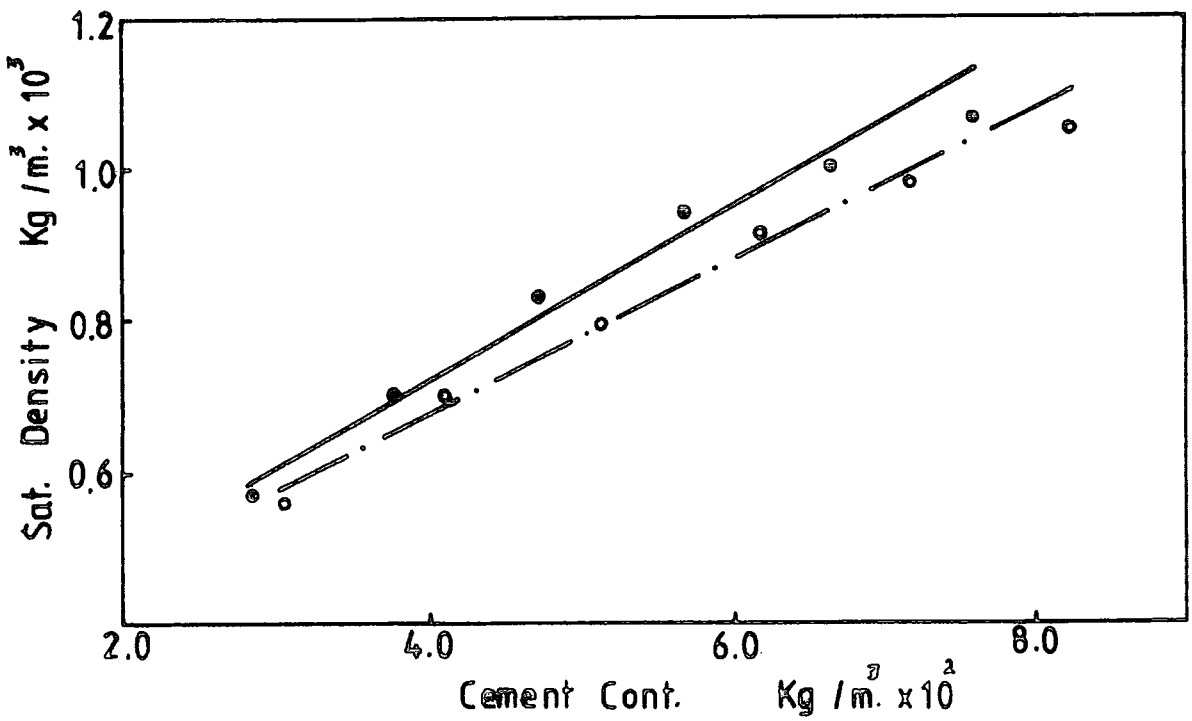

Fig. (3.1b)

Figure (3.1) Compressive strength and saturated density versus the cement content of cylinders of 150 x 300 mm. dimensions.

(Beads type 2)

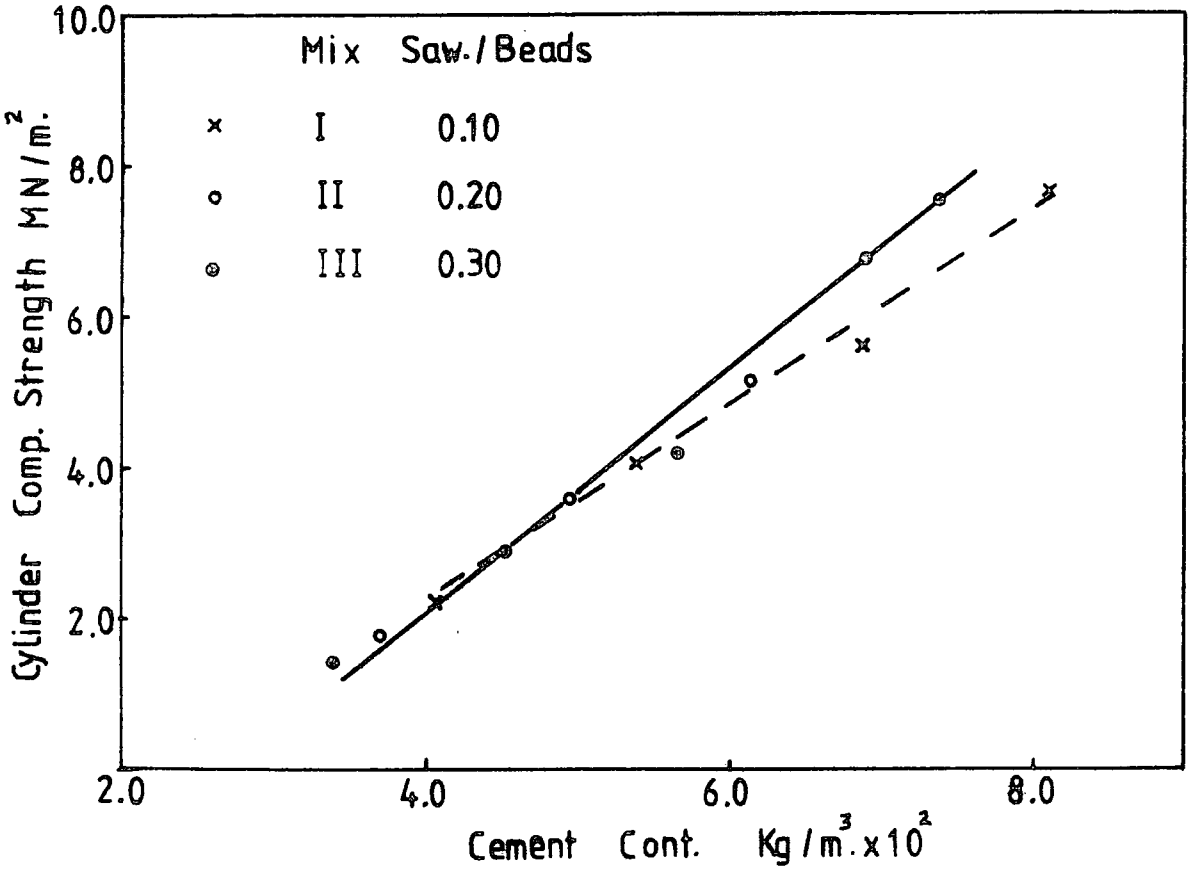

Fig. (3.2a)

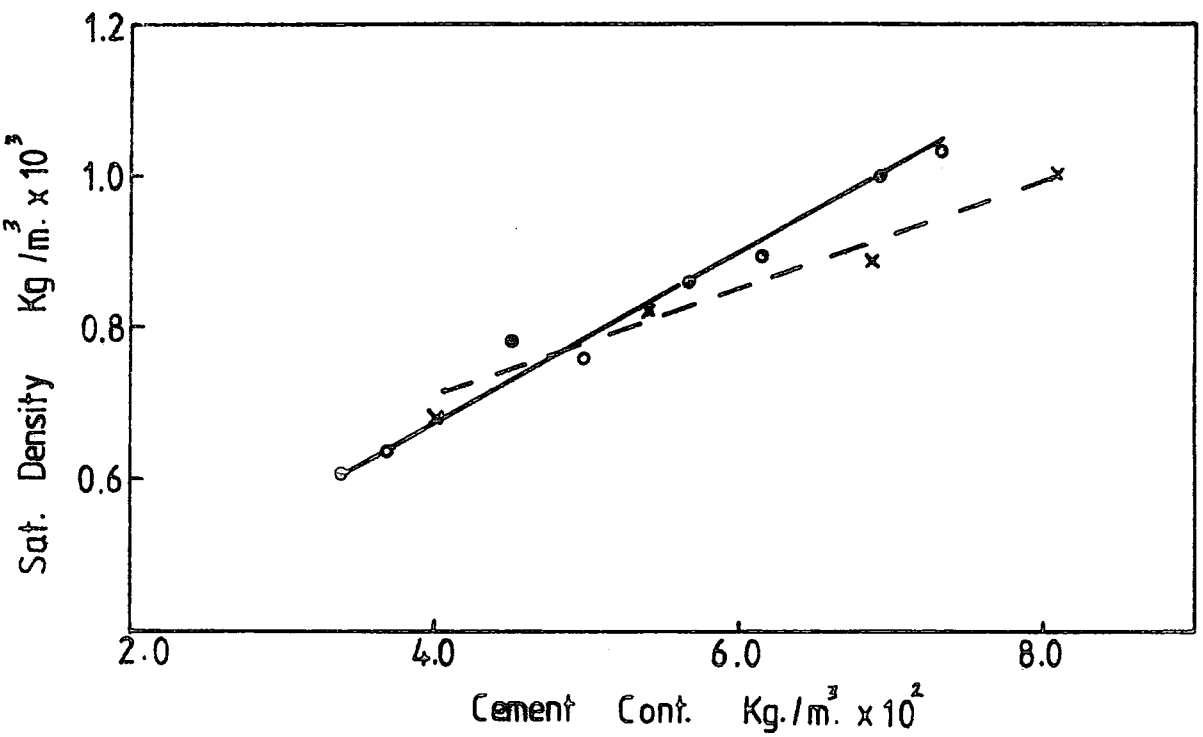

Fig. (3.2b)

Figure (3.2) Compressive strength and saturated density versus the cement content of cylinders of 102 x 204 mm. dimensions.

(Beads type 1)

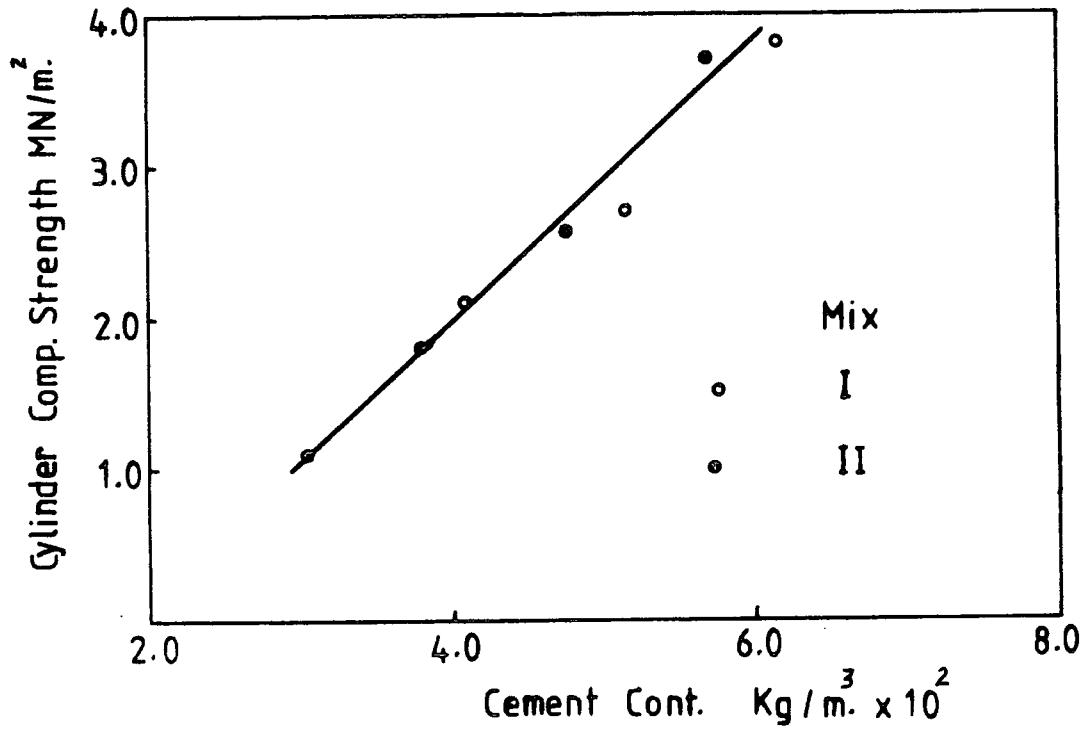

Fig. (3.3a)

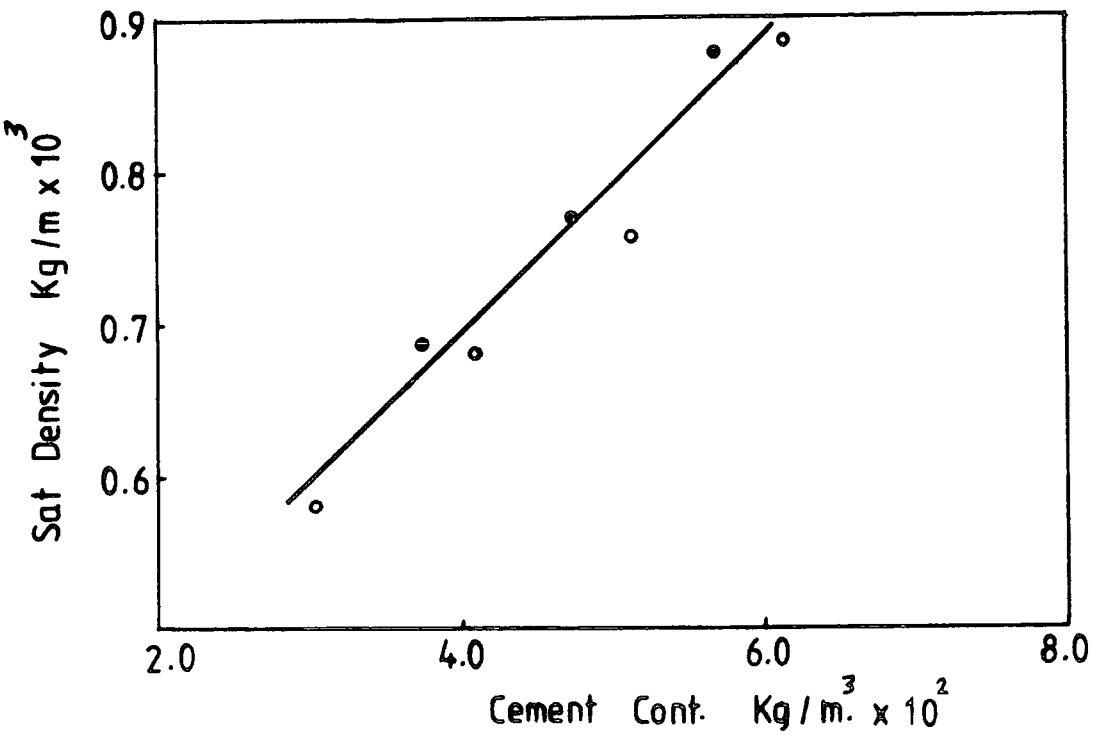

Fig. (3.3b)

Fig. (3.3) Compressive strength and saturated density versus the cement content of the concrete made from beads type 3.

beads type (3) - the beads of bigger size table (2.1) - were graphed in figure (3.3). The strength and the density of the two mixes II and III were found also of a linear relationship with the cement content as shown in figures (3.3a) and (3.3b). The mixes of more sawdust - mixes of group III - were found of the higher density also. The compressive strength of the mixes made by these beads were found to be about 30 per cent lower than those which were made using the smaller beads at the same cement content, while the reductions in the densities are only about 5% less. The reduction in the strength of this concrete may be attributed to the increasing of the water content to form the mix of the required workability, and also the increase in the size of the voids owing to the large size of the beads inside the cement matrix. The workability of the concrete was found to be less than that of the concrete which was made using the smaller beads.

The conclusion of the work and the results obtained in this procedure are summarized as follows:

(1) The use of polystyrene beads of a specific size as coarse aggregate gives the same results in spite of considerable variation in the density. The strength may be predicted by the method of design used in this research; i.e. relating the weight of cement to the aggregate's volume.

(2) Using polystyrene beads of larger size leads to strengths lower than the strength of samples made from the smaller size at the same cement content, and the workability, also, is reduced by increasing the beads size at the same sawdust content.

(3) The compressive strength of the polystyrene concrete mainly depends on the cement content used and partially on the density of the concrete.

(4) The density of concrete in a suitable state of workability and in a specific regime of compaction depends on the cement content mainly and less sensitively on the sawdust content.

(5) The percentage of the increment rates in the compressive strength and density were found about 1.85 and 0.60 times respectively the rate of the cement content increment.

3.2.3 The compressive strength for unit density

The results of the compressive strength and density investigations of the polystyrene concrete were described and were discussed in (3.2.2). These indicate that the density is one of the factors which affects the concrete strength, i.e. at the given cement content, when the density increased, the compressive strength also increased. For demonstrating the effects of the cement content only on the concrete strength, figure (3.4) was drawn to show the relationship between the cement content and the compressive strength for unit density of the concrete made by beads type (2). The graph shows that the mixes of the two groups II and III, have the same linear relationship. The results of the three groups of specimens made using beads type (1) were found to fulfil the same linear relationship. The equation of that linear relationship can be written as follows:

$$F_c/\rho_s = K\,(C_c - 110) \qquad (3.1)$$

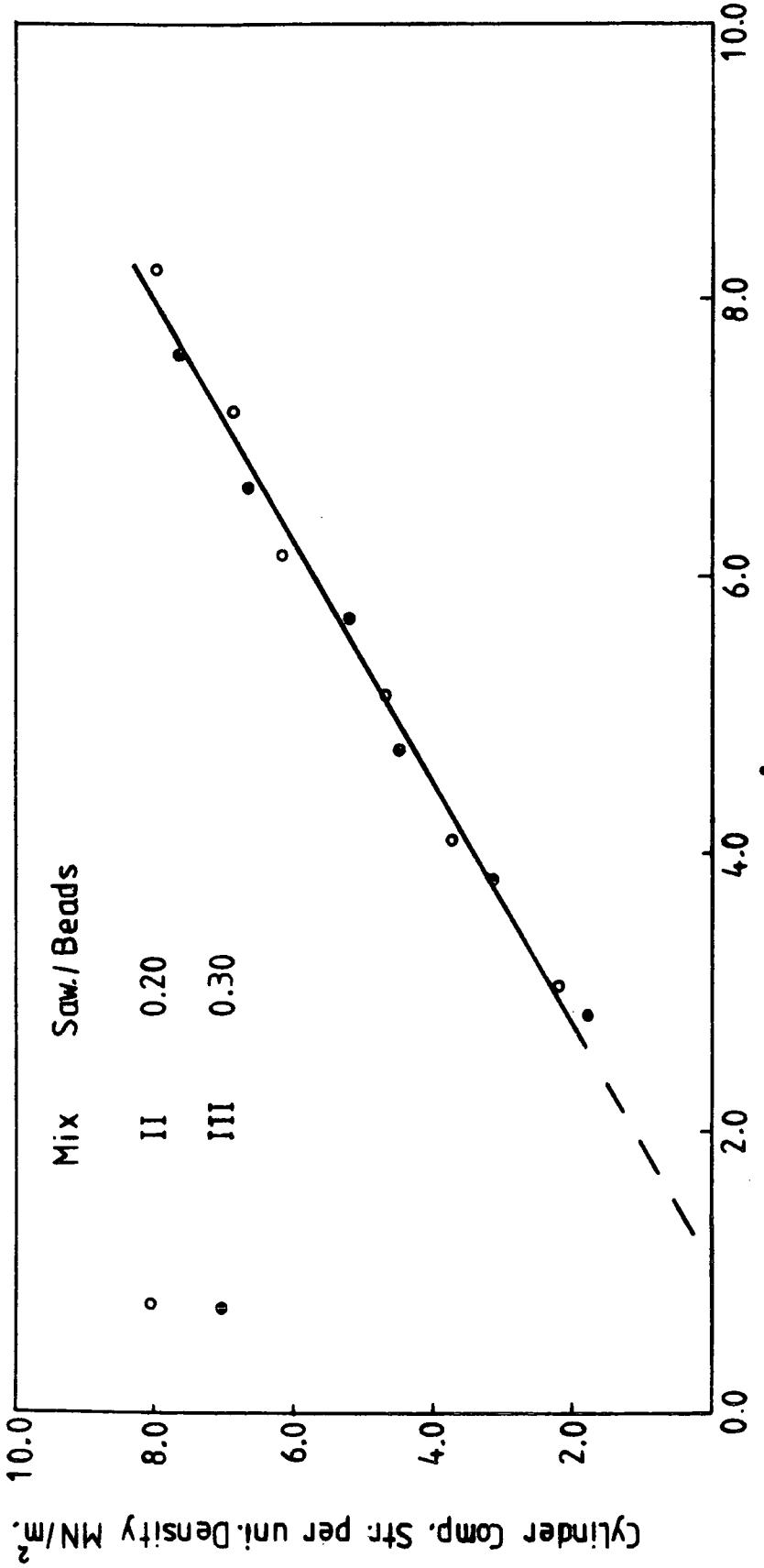

Figure (3.4) Relationship between the cement content and the compressive strength for unit density (1 t/m^3) of the concrete made from beads type 2.

(Test results carried out on cylinders of 150 x 300 mm. dimensions)

where:

F_c is the cylinder compressive strength in MN/m^2.

ρ_s is the concrete saturated density in kg/m^3.

K(Const.) = slope of straight line (for these specimens and units K = 0.0116)

C_c is the cement content in kg. for each cubic meter of aggregate (bulk volume)

to simplify:

$$F_c = \frac{1}{8.6} 10^{-4} . \rho_s (C_c - 110) \qquad (3.2)$$

The compressive strength of all the mixes made from beads (1) and (2) were calculated according to the concrete density and the cement content using equation (3.2), and recorded in tables(3.1) and (3.2) respectively. The error due to the use of that formula was calculated in per cent compared with the experimental recorded strength. It can be seen in the results of the mixes of group II table (3.1), the maximum error is only about 6 per cent. In the mixes of group III the maximum error was found also less than $\pm$ 5 per cent. Neglecting the poor mix - the first mix of this group - the average error of each group is less than $\pm$ 1%. In the results of the mixes made by using beads type (1) and cylinders of 102 x 204 mm., the maximum error was found not more than $\pm$ 7.5 per cent.

[Note : In 'imperial' dimensions equation (3.2) is:

$$F_c = \frac{1}{2.3} \rho_s (C_c - 6.8) \qquad (3.2)$$

where:

F_c = cylinder compressive strength in lb/in^2.

ρ_s = the concrete saturated density lb/ft^3.

C_c = cement content in lb for each cubic ft of aggregate]

Table (3.1) : The saturated density and compressive strength experimentally and calculated and the error of the calculation according to the cement content

(Beads of type (2) in cylinder 150 x 300 mm.)

Mix Symbol	Cement con. kg. for each m^3 of agg.	Concrete sat.density(ρ_s) kg/m^3.	Cylinders comp. strength (MN/m^2.)		Error % due to using the formula	Average error %
			Experimental results	Calculated by the dev.formula		
II	305	560	1.20	1.27	+ 5.8	+0.87
	410	700	2.60	2.44	- 6.1	
	515	790	3.67	3.72	+ 1.4	
	615	900	5.53	5.28	- 4.4	
	720	980	6.66	6.95	+ 4.3	
	820	1050	8.32	8.67	+ 4.2	
III	285	570	0.99	1.16	+17.0	-0.72
	380	700	2.19	2.20	+ 0.5	
	475	830	3.70	3.52	- 4.8	
	570	940	4.86	5.03	+ 3.5	
	665	1000	6.64	6.45	- 2.8	
	760	1060	8.00	8.01	-	

Table (3.2) : The saturated density and compressive strength experimentally and calculated and the error of the calculation according to the cement content

(Beads of type (1) in cylinder 102 x 204 mm.)

Mix Symbol	Cement con. kg. for each $m.^3$ of agg.	Concrete sat.density (ρ_s) $kg/m.^3$	Cylinders comp. strength ($MN/m.^2$)		Error % due to using the formula	Average error %
			Experimental results	Calculated by the dev. formula		
I	400	680	2.28	2.30	+0.90	+3.2
	535	826	4.00	4.10	+2.50	
	670	890	5.51	5.80	+5.26	
	805	983	7.63	7.94	+4.12	
II	370	640	1.81	1.93	+6.6	+0.95
	490	760	3.60	3.36	-6.7	
	615	895	5.05	5.26	+4.2	
	735	1030	7.50	7.48	-0.3	
III	340	610	1.51	1.60	+6.0	+4.95
	450	795	2.90	3.10	+6.9	
	565	860	4.23	4.55	+7.5	
	680	1000	6.67	6.63	-0.6	

The compressive strength for unit density - (F_c/ρ_s) - of the concrete made from the polystyrene beads of the bigger size - beads type (3) - was found to be of lower value than would be calculated from the relationship in figure (3.4). Therefore figure (3.5) was drawn to show the relationship of F_c/ρ_s and cement content when the beads are of that size. The graph indicates that the linear relationship of that concrete is of inclination lower than the relationship of the concrete which was made by the polystyrene beads of smaller size. However, the expression of the cylinder strength, saturated density and the cement content of the concrete made by beads of that size is:

$$F_c = \frac{1}{11} \times 10^{-4}. \rho_s (C_c - 110) \qquad (3.3)$$

It can be seen from equations (3.2) and (3.3) that the cylinder compressive strength of the polystyrene concrete according to the cement content used in kg. per $m.^3$ of aggregate, and the saturated density of the concrete, without compacting so as to destroy the spherical shape of the beads can be written in the expression :

$$F_c = \frac{1}{K} \times 10^{-4}. \rho_s (C_c - 110) \qquad (3.4)$$

where :

K is a factor which depends on the polystyrene beads' size and increases with the beads size increment.

ρ_s is the concrete saturated density in $kg./m.^3$

C_c is the cement content kg. per $m.^3$ of aggregate.

F_c is the cylinder compressive strength in $MN/m.^2$

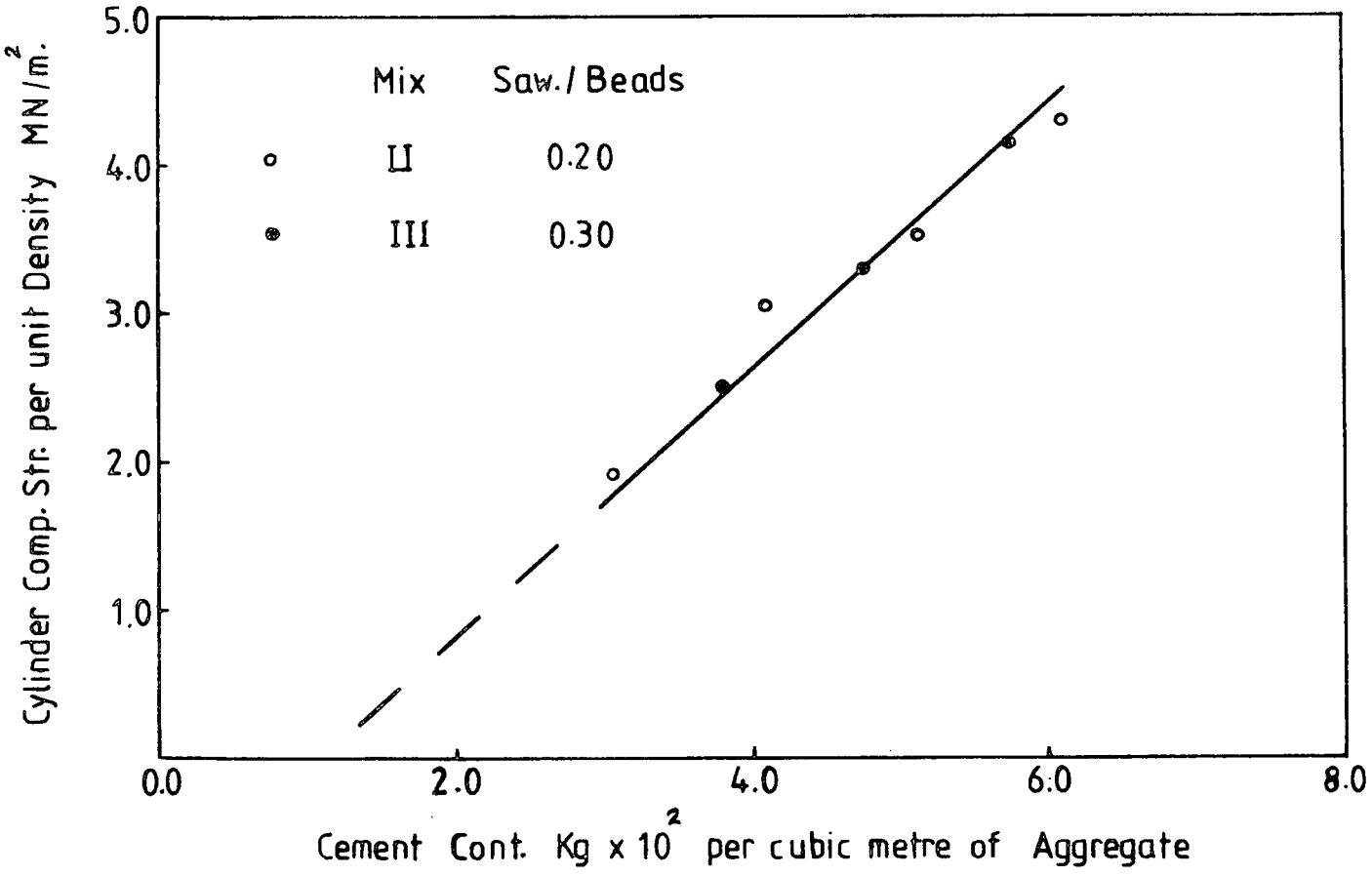

Figure (3.5) Relationship between cement content and the compressive strength per unit density (F_c/ρ_s) of the concrete made from beads type 3.

3.2.4 Examination mixes

The accuracy of measurement of the polystyrene concrete's consistency is still difficult to attain because, in practice, it may change from one job to another, i.e. the mixes may be in some cases a little drier or wetter than the mixes made in this research, and to test the reliability, two experimental programmes were carried out.

In the first programme, two mixes were made using beads type (2) group II at the cement content 615 kg. with different consistencies. The two mixes were designed to be of total water/cement ratio 0.35 in one and 0.37 in the other, i.e. respectively drier or wetter than the workability used in this research as determined before in (2.6.2.2). Two standard cylinders of 150 x 300 mm. dimensions were made and tested from each mix. The concrete was mixed, cast, cured and tested with all the conditions identical to the compression test mentioned before. The average saturated density of the cylinders made by the lower water content was found to be 930 kg./m.^{3}, and their average recorded strength was 5.78 MN/m.^{2} The compressive strength given by equation (3.2) according to the cylinders density is 5.46 MN/m.^{2} i.e. the error in the calculating strength is only 6 per cent lower than the experimental strength. The concrete which was made from the mix of greater water content was found, as expected, to be of lower density and strength. The average density and strength recorded from the two cylinders of this mix was 865 kg./m.^{3} and 4.98 MN/m.^{2} respectively. The calculated strength corresponding to that density is 5.10 MN/m.^{2} i.e. the strength by the formula is accompanied by an error of only 2.2 per cent higher.

In this programme another two mixes were made at a cement content of 410 kg./m.^{3} The error in the calculated strength was found to be 6.6 per cent lower in the dry mix and about 4 per cent higher in the wet mix. It can be seen from the results of tests carried out in this programme that the strength expressions which were developed are available to be used when the mixes consistency is in the limit of workability with probable error of about $\pm$ 6 per cent. When the mixture of the polystyrene beads is quite different, equation (3.4) is the recommended one.

The experimental work carried out in the second programme was planned to find out how to deal with the polystyrene concrete, using equation (3.4) for determining the compressive strength, when the beads size is not one of the gradings used in this research. The polystyrene beads which are used for making the concrete tested in this programme were a mixture of equal parts from beads type (2) and type (3). Three mixes were made with cement contents 410, 615 and 820 kg./m.^{3} and with sawdust of volume 0.20 times the volume of the beads. The water contents used for these mixes have the same values used for group II table (2.6). Two standard cylinders of 150 x 300 m. were made and tested from each mix in the same way as was described previously. The average density of the two cylinders was found for the three mixes to be 690,900 and 1,030 kg./m.^{3} respectively, and the recorded strengths were 2.17, 4.75 and 7.5 MN/m.^{2} for the three mixes respectively. Calculating the compressive strength by equation (3.2) produced a value having an error of about 12 per cent higher than the recorded strength in the mixes, and the use of equation (3.3)

also was not suitable where the calculated strength is about 11 per cent lower. In that case, equation (3.4) is the more suitable expression to be used where one of these mixes is considered as a trial mix for determining the K value in the equation, and this value is used for calculating the strength of the other mixes. For instance, assuming the mix of cement content 410 kg./m.^{3} is the trial mix, the value of K according to the results obtained is equal to 9.54. When the compressive strengths of the two other mixes were calculated by equation (3.4) with K = 9.54, the error in the calculated value was found to be less than 3 per cent between the two mixes.

From these results, it can be seen that equation (3.4) can be used for concrete using polystyrene beads of any size while doing a trial mix at any value of cement content not less than 400 kg./m.^{3} , and from the density and strength of this mix the constant K is determined. The strength of any mix then can be calculated by equation (3.4) by using the constant K which is calculated from the results of the trial mix.

3.3 Modulus of elasticity

The mix proportion in ordinary concrete is the most important factor affecting the modulus of elasticity, because the aggregates generally have higher modulus than the cement paste. In lightweight aggregate concrete, where the modulus of the lightweight aggregate differs little from the modulus of the cement paste, the mix proportions usually do not affect the modulus of elasticity.

In polystyrene concrete, where the aggregate used is

very weak relative to the cement paste, the modulus of elasticity then will depend mainly on the cement content used. However, experimental work was carried out which was planned to determine the influence of the cement content on the polystyrene concrete modulus. The experimental results obtained also will be discussed with reference to the current codes formulae for lightweight concrete, which determine the relationship between the compressive strength and the modulus of elasticity.

3.3.1 Schedule of mixes, sample's preparations and testing

Three cylinders were made from each one of the mixes of group II and III recorded in table (3.3). The concrete was mixed and the cylinders were poured - or cast - in the way mentioned previously. The moulds used are the same moulds used for the compression test according to the beads type as mentioned in (3.2). All the cylinders were removed from the curing tank after 5 days immersion, and the saturated density was determined as mentioned before. Two cylinders at least, of density approximately equal to the density of the test cylinders were tested for compressive strength and when there was poor agreement a third was tested also. The cylinders were left after capping in the control room for at least 7 hours to dry, and to allow for the curing of the glue fastening the demec points onto the specimens' sides. Three vertical lines were marked on the surface of each cylinder at 120 intervals around it. On the cylinders, of 150 mm. diameter and 300 mm. height, three pairs of demec gauge points

Table (3.3) : Shows the cement content and the average density of the mixes which were made and tested for determining the modulus of elasticity, according to the beads used and the sawdust content.

Dimension of cylinder and type of beads (as classified in table 2.1)	Cement content and density according to the mix designation			
	Mix II		Mix III	
	Cement cont. (kg./m.^{3})	Sat. density (kg./m.^{3})	Cement cont. (kg./m.^{3})	Sat. density (kg./m.^{3})
150 x 300 mm. beads type (2)	305	570		
	410	705	385	710
	515	785	575	930
	615	900	765	1050
	720	975		
	820	1050		
102 x 204mm. beads type (1)	490	755	450	790
	615	890	565	865
	735	1020	680	995
102 x 204mm. beads type (3)	305	575		
	410	680	380	685
	515	760	475	770
	615	885	570	885

were attached on the three lines, using araldite adhesive. A demec gauge of 150 mm. gauge length was used for all the cylinders of these dimensions. For the cylinders of 204 mm. length, a demec gauge with 2 in. (50.8 mm.) gauge length was used, where three demec gauge points were attached on each line for taking two readings on each line, one above and one below the middle of the length.

All the cylinders were tested during the next day - i.e. at an age of 7 days - under compression in a Denison testing machine model T 42B4. The load was applied on the cylinders of 150 mm. diameter at 5 kN. intervals for all the concrete of cement content less than 600 kg./m.^{3} , and at 10 kN. for the cylinders made with a higher cement content. On the cylinders of 102 mm. diameter, the load was applied with increments half of the values mentioned for the big cylinders. The readings of strain were taken from each pair of gauge points using the demec gauge after about 20 seconds of the load application.

3.3.2 Results

The average strains from the three readings (or the six in the case of the small cylinders) were taken at each load increment and then the stress - strain curve was graphed. The modulus of elasticity was determined by taking the inclination of the initial tangent line, i.e. the modulus of elasticity recorded in this research is the initial tangent modulus. Typical stress-strain curves of the mixes of group II which were made in the cylinder of 150 x 300 mm. dimensions by beads type (2) can be seen in appendix (I-b).

The average results of the modulus obtained were compared with the cement content used in tables (3.4, 3.5, 3.6) according to the type of the polystyrene beads used and the sawdust content. It can be seen from the results of all types that, the modulus of elasticity of the polystyrene concrete mainly depends on the cement content, and partially on the sample density. The concrete made using beads of the same size gives approximately the same results, and using standard cylinders of the larger size - 150 x 300 mm. - improves the results with an increment of about 6 per cent. The concrete made using beads of the large size - beads type (3) - gives the results shown in table (3.6), and has a modulus of about 20-25% lower than the concrete made using smaller size beads at the same cement content. In general, the modulus of elasticity of the concrete displayed behaviour similar to the compressive strength, but with an increment less than the compressive strength increment. However, the relationship between the modulus of elasticity and the compressive strength of concrete is discussed in the next section, and the modulus of elasticity will be related to the compression strength in one formula.

3.3.3 Relationship between modulus of elasticity and compressive strength

3.3.3.1 Discussion of the current codes formulae

With both ordinary and lightweight concrete, all the current codes relate the modulus of elasticity to the compressive strength in empirical formulae.

The British code of practice for the structural use of concrete cp 110 : 1972 gave the relationship between

modulus of elasticity E_c in GN/m.^{2} and the cubic strength in MN/m.^{2} when the density (ρ) is between 1400 and 2300 kg./m.^{2} by the expression

$$E_c = 0.85 \rho^2 \sqrt{u} \times 10^{-6}$$

The Comité Européene du Beton expression for lightweight aggregate concrete differs primarily in taking the influence of density to the power of 3/2, as is the American approach. The Comité Européene du Beton recommends the value of Modulus in GN/m.^{2} as:

$$E_c = \frac{1}{1.8} \times 10^{-4} \rho^{1.5} \sqrt{F_c}$$

Where F_c is the cylinder strength in MN/m.^{2}

The ACI Building Code gives E_c in pounds per square inch for lightweight concrete. When density (ρ) is different from 145 lb./ft.^{3} (assumed to be the value for normal weight concrete) by the expression

$$E_c = 33 \rho^{1.5} \times \sqrt{F_c}$$

Where F_c is the compressive strength of the cylinders in pound per square inch.

Because all the densities of the polystyrene concrete made in this research are less than 1100 kg./m.^{3} , the formulae may not be acceptable because of the density specification. However, the results of the compressive strength and modulus of elasticity which were obtained experimentally will be discussed to show the relevance of the formulae which can be used for concrete of this nature. Because the compressive strength tests were carried out in this research on cylinders - not cubes - the results are discussed in the context of C.E.B.

and the A.C.I. formulae only.

Using the C.E.B. formulae to calculate E_c according to density and the cylinder strength gives results in the range between 12 and 35 per cent higher than the experimental recorded modulus. The average error for the concrete made in cylinders of 150 x 300 mm. dimensions is more than 20 per cent, as shown in table (3.4), and is about 28 per cent for the concrete made in cylinders of 102 x 204 mm. It can be seen from these results that the error in some mixes was as high as +35 per cent, i.e.The European formulae in that form is not suitable to be used with that concrete. The factor which needs to change - or to be reduced - is the power of density (ρ); for two reasons, the increase in density due to the moisture content, and the greater weakness of the aggregates used, since the formula was derived for lightweight concrete using aggregates of reasonable strength. When the power of (ρ) was calculated by the formulae using the experimental results of E, ρ_s and F_c, it was found to be between 1.485 and 1.455 with an average of 1.47. When the modulus of elasticity was calculated by the formula with ρ_s to power of 1.47, neglecting the first mix of group II in table (3.4), the error then was found to be about $\pm$9 per cent in the concrete made in the big cylinders, and not more than 12 per cent in the concrete made in the cylinders of 102 x 204 mm. table (3.5); i.e. using an expression similar to the one in the Comité Européene du Beton, the expression must be modified as in the following formula:-

$$E_c = \frac{1}{1.8} \times 10^{-4} \cdot \rho_s^{1.47} \sqrt{F_c} \qquad (3.5)$$

Table (3.4) : Discussion on the compression modulus of elasticity with the empirical formula of Europeene du Beton for lightweight concrete, mixes made in the cylinders of 150 x 300 mm. dimensions

(Beads type 2)

Mix Symbol	Cement cont.for cub.metre of aggr. (kg.)	Modulus of elas., exper., calculated and error%				
		E_c Experimentally ($GN/m.^2$)	E_c by the formula ($GN/m.^2$)			
			with f to power 1.5		with f to power 1.47	
			E_c	Error %	E_c	Error %
II	305	0.720	0.827	+15.0	0.668	-16.9
	410	1.500	1.676	+12.0	1.368	- 8.8
	515	2.100	2.340	+11.5	1.917	- 8.7
	615	2.800	3.530	+26.0	2.876	+ 2.7
	720	3.450	4.360	+26.0	3.550	+ 2.9
	820	4.100	5.450	+33.0	4.425	+ 7.9
III	385	1.350	1.556	+15.0	1.28	- 5.4
	575	2.600	3.470	+33.0	2.82	+ 8.6
	765	3.960	5.345	+35.0	4.34	+ 9.6

Table (3.5) : Discussion on the compression modulus of elasticity with the empirical formula of Europeene du Beton for lightweight concrete, mixes made in the cylinders of 102 x 204 mm. dimensions

(Beads type 1)

Mix Symbol	Cement cont. for cub. metre of aggr. (kg.)	Modulus of elas., exper., calculated and error %				
		E_c Experimentally (GN/m.^{2})	E_c by the formula (GN/m.^{2})			
			with ρ to power 1.5		with ρ to power 1.47	
			E_c	Error %	E_c	Error %
II	490	1.72	2.19	+27.0	1.795	+ 4.4
	615	2.65	3.32	+25.0	2.707	+ 2.2
	735	3.63	4.92	+35.0	4.030	+11.0
III	450	1.60	2.10	+31.0	1.716	+ 7.3
	565	2.50	2.88	+16.0	2.365	- 5.4
	680	3.26	4.50	+38.0	3.66	+12.0

Table (3.6) : Saturated density, cylinder's compressive strength and modulus of elasticity according to cement content used of the concrete made from beads type (3)

Mix Symbol	Cement cont. for cub.met. of agg. in kg.	Concrete sat. density ρ_s ($t/m.^3$)	Cylinders Comp.str. F_c ($MN/m.^3$)	Modulus of elasticity E ($GN/m.^2$)
II	305	0.580	1.10	0.72
	410	0.680	2.10	1.25
	515	0.760	2.68	1.58
	615	0.885	3.80	2.07
III	380	0.685	1.81	1.00
	475	0.770	2.56	1.42
	570	0.885	3.73	2.00

Calculating the modulus of elasticity E by the A.C.I. expression was found for this concrete to be much better than the European formula, as shown in tables(3.7), (3.8 and (3.9). The results of the cylinders of 150 m. diameter, table (3.7), indicate that the errors due to using the formula are reduced with the mixes of the higher density. Neglecting the weak mix - the first mix of group II - the average error is about 4.5 per cent lower than that experimentally recorded. In the results of the concrete made in the cylinders of 102 x 204 mm. dimensions, the errors were found to be lower, especially in the mixes of group II. The average error of the two groups is about 0.65 per cent lower. The value of cement content, density and the experimental modulus mentioned in tables (3.7), (3.8) and (3.9) were converted from tables (3.4), (3.5) and (3.6) from metric dimensions to imperial dimensions.

All the values of the cylinder compressive strength F_c used in these calculations are the compression strength obtained before in the compression testing, where the mixes have the same cement content and approximately the same density.

Using the dry density to be substituted in the European formula with (ρ) to power 1.5 was found to be unsuitable, where the calculated E_c was accompanied by error which reached about 16 per cent lower than the recorded value, especially at the mixes of cement content lower than 600 kg. The error in the mixes of cement content higher than 600 kg. was found about -3.5 in the mix of cement content 615 kg. and about +6 per cent in the mix of 820 kg. cement content. However, this method is not practical.

Table (3.7) : Discussion on the compression modulus of elasticity with the empirical formula of A.C.I. Building Code for lightweight concrete, mixes made in cylinders of 150 x 300 mm. dimensions

(Beads type 2)

Mix Symbol	Cement cont. for cubic ft. of agg. (lb)	Modulus of Elasticity (lb./in^2. x 10^3)		Error of calc. in per cent of the experiment
		Experimentally	Calc. by the formula	
Mix II	19.00	104.4	92.4	-18.0
	25.60	217.0	187.0	-13.5
	32.15	304.0	261.0	-14.0
	38.40	406.0	394.0	- 2.9
	45.00	500.0	488.0	- 2.3
	51.20	595.0	608.0	+ 2.2
Mix III	24.00	196.0	173.3	-11.6
	36.00	377.0	387.6	+ 2.8
	47.75	574.0	579.2	+ 4.0

Table (3.8) : Discussion on the compression modulus of elasticity with the empirical formula of A.C.I. Building Code for lightweight concrete, mixes made in cylinders of 102 x 204 mm. dimensions

(Beads type 1)

Mix Symbol	Cement cont. for cubic ft. of agg. (lb)	Modulus of Elasticity ($lb./in^2$ $x10^3$)		Error of Calc. in per cent of the experiment
		Experimentally	Calc.by the formula	
Group II	30.6	249.0	243.0	-2.4
	38.4	384.0	370.0	-3.6
	46.0	526.0	553.0	+5.2
Group III	28.0	232.0	234.0	+1.0
	35.0	362.0	324.0	-10.4
	42.0	472.0	502.0	+6.4

Table (3.9) : Discussion on the compression modulus of elasticity with the empirical formula of A.C.I. Building Code for lightweight concrete, mixes made using beads type (3)

Mix Designation	Cement cont. for cubic ft.of agg. in lb.	Modulus of Elasticity ($lb./in.^2 \times 10^3$)		
		Experimentally	Calc. by the formula	Error % due to using the formula
Group II	19.00	104.0	90.8	-13.0
	25.60	181.3	159.3	-12.0
	32.15	229.2	210.5	- 8.0
	38.40	300.2	318.2	+ 6.0
Group III	24.0	145.0	149.7	+ 3.2
	30.0	206.0	212.0	+ 2.9
	36.0	290.0	312.4	+ 7.7

3.3.3.2 Empirical formula according to the experimental results

The discussion in 3.3.3.1 indicates that using the European formulae after modification, or the A.C.I. formula to express the relationship between the modulus of elasticity and compressive strength for the polystyrene concrete, may be accompanied by error of more than 10 per cent, higher or lower. Because these formulae were derived empirically, the results of the compressive strength and modulus of elasticity obtained in this research were used to derive a relationship between them with a formula giving greater accuracy for polystyrene concrete.

The relationship between $\sqrt{F_c}$ and E_c of the results obtained experimentally from the concrete made using beads (1) and (2) were graphed in figure (3.6). The equation of a linear relationship from this diagram is:-

$$E_c = 2\,(\sqrt{F_c} - 0.88) \qquad (3.6)$$

if the formula is to be similar to the current codes formulae i.e. including the density (ρ) in the expression. The relationship between $\sqrt{F_c}$ and (E_c/ρ_s) were graphed in figure (3.7), for the mixes which were made in the cylinders of 150 x 300 mm. dimensions. It can be seen from the graph that the straight line of the average linear relationship passes through the origin, and its equation, which expresses the relationship between the modulus of elasticity and the cylinder compression strength is:

$$E_c = 1.36\ \rho_s \sqrt{F_c} \qquad (3.7)$$

Where:

E_c is the compression modulus of elasticity in (GN/m^2)

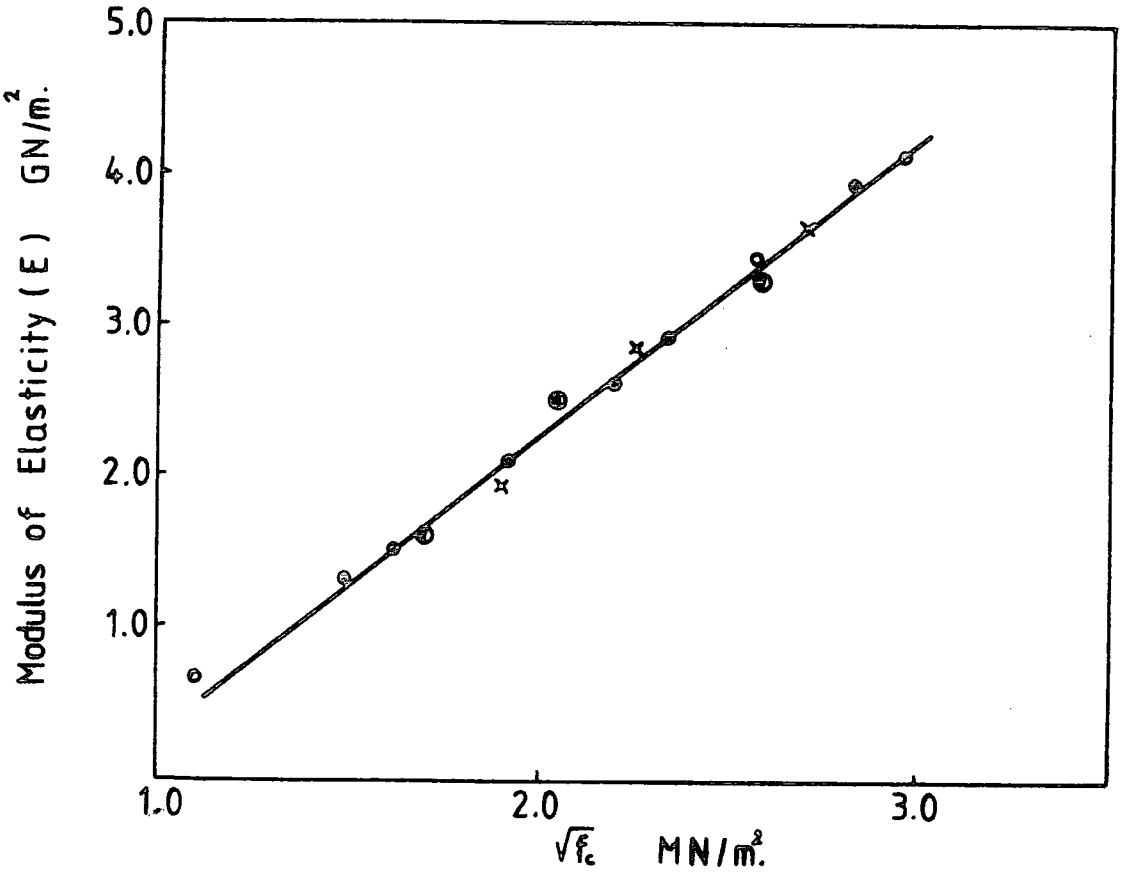

	Group	Cylinder dim.
⊙	II	150 x 300
⊛	II	102 x 204
○	III	150 x 300
◉	III	102 x 204

Figure (3.6) Relationship between the compressive strength and modulus of elasticity of the mixes made from beads types 1 & 2.

When the relationship between the compressive strength and E_c were plotted figure (3.8) for the concrete made using beads (1) (tests carried out on cylinders of 102 x 204 mm. dimensions) the expression (3.7) was found:

$$E_c = 1.28 \rho_s \sqrt{F_c} \qquad (3.7)$$

i.e. using cylinders of these dimensions caused reduction in E_c of about 5.6 per cent.

Figure (3.9) was graphed also to show the relationship between the compressive strength and the modulus of elasticity of the concrete which was made using the polystyrene beads of larger size - beads type (3) - the expression of the relationship for that concrete from the graph is:

$$E_c = 1.2 \rho_s \sqrt{F_c} \qquad (3.8)$$

It can be seen from the results obtained from the three types of beads that the relationship between the modulus of elasticity E and the cylinder compressive strength of the polystyrene concrete can be expressed in the following empirical formula :

$$E_c = K \cdot \rho_s \sqrt{F_c} \qquad (3.9)$$

Where

K is the factor which depended on the size of the beads used and it increased with using beads of smaller size and using cylinders of 102 x 204 m. may be accompanied by a reduction in E of about 6% than when cylinders of 150 x 300 mm. are used.

F_c is the cylinder compressive strength in $MN/m.^2$

E_c is the compression modulus of elasticity in $GN/m.^2$

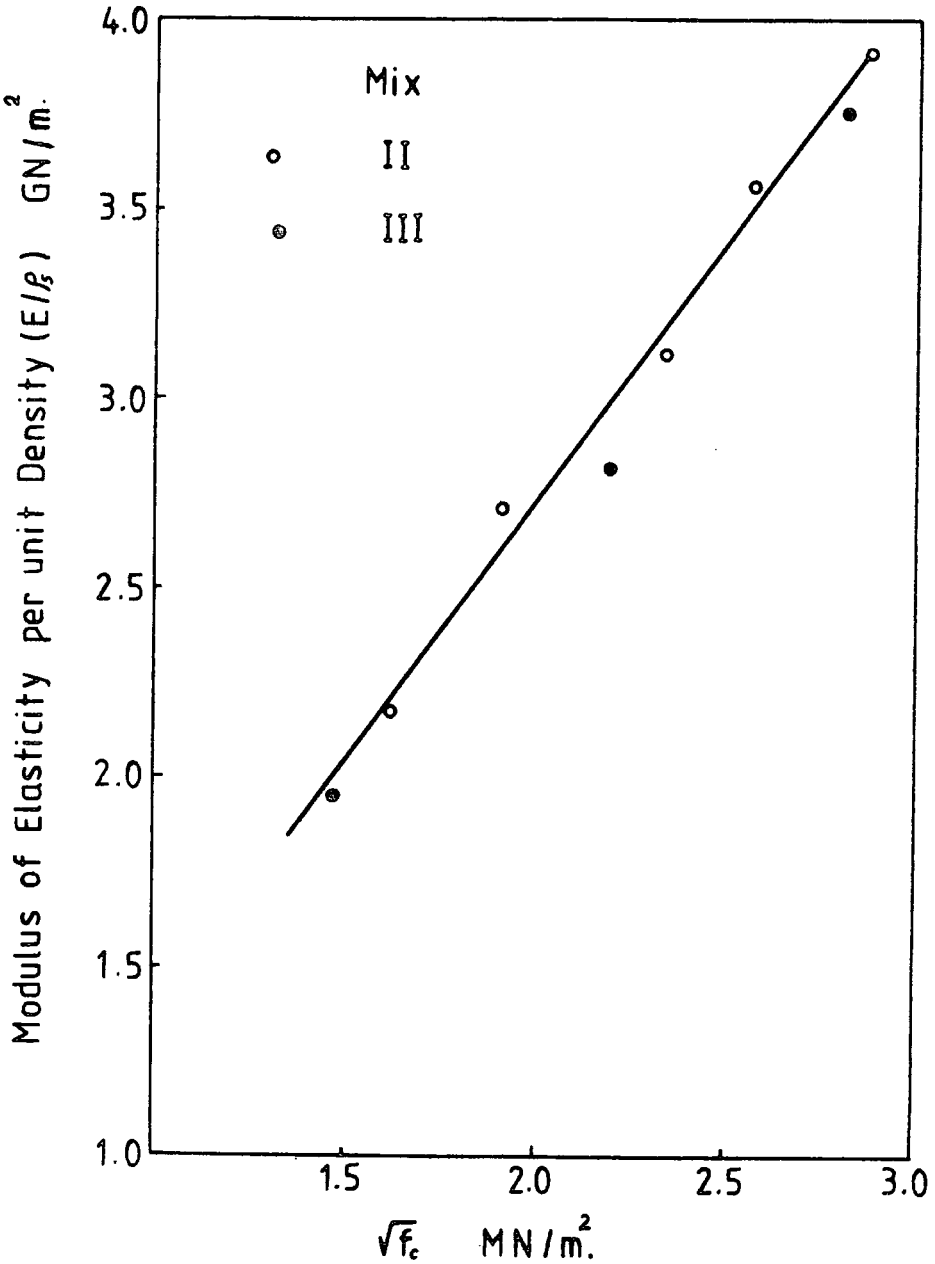

Figure (3.7) Relationship between the compressive strength and modulus of elasticity per unit density of the mixes made from beads type(2) in cylinders of 150 x 300 mm.

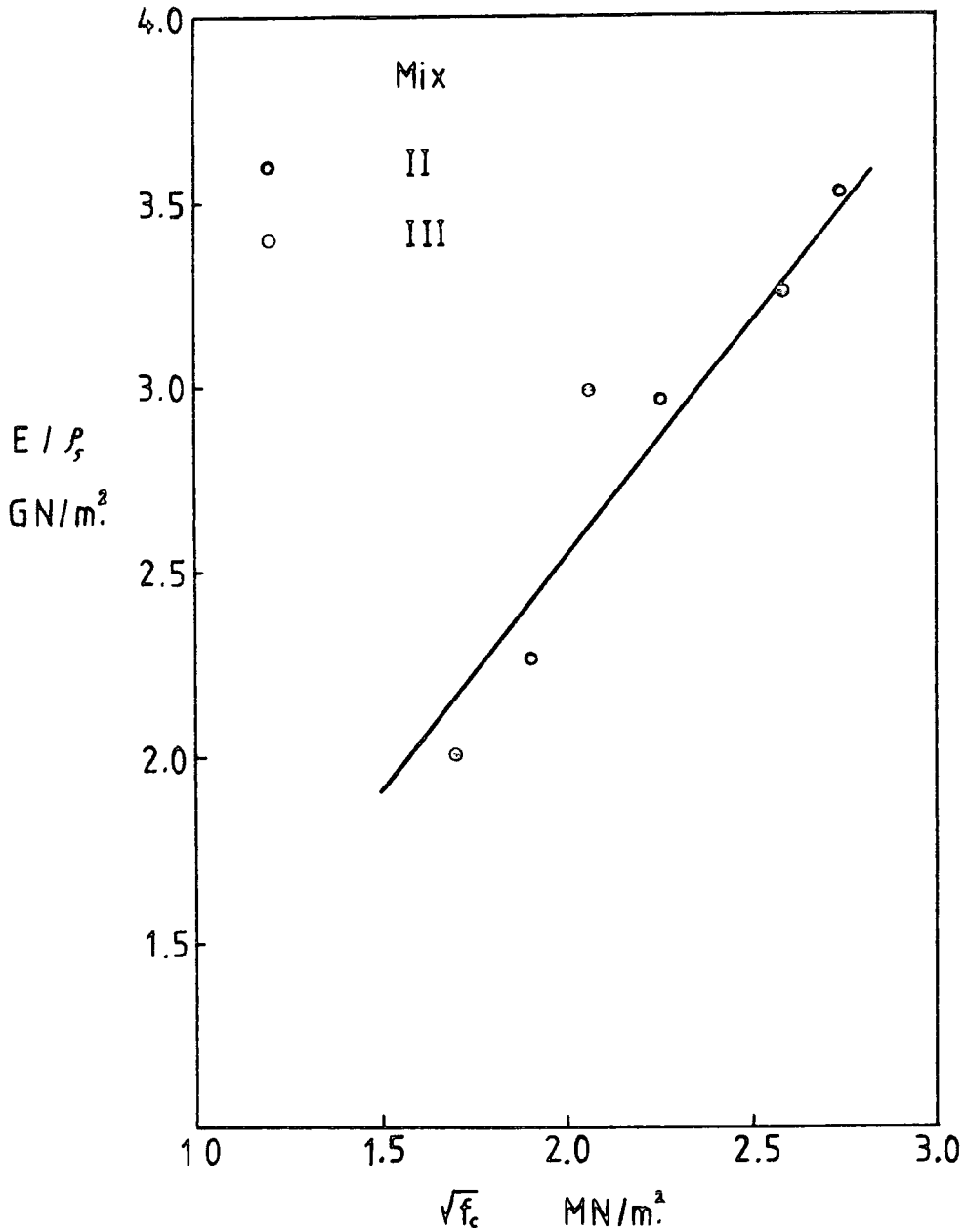

Figure (3.8) Relationship between the compressive strength and modulus of elasticity per unit density of the mixes made from beads type(1) in cylinders of 102 x 204 mm.

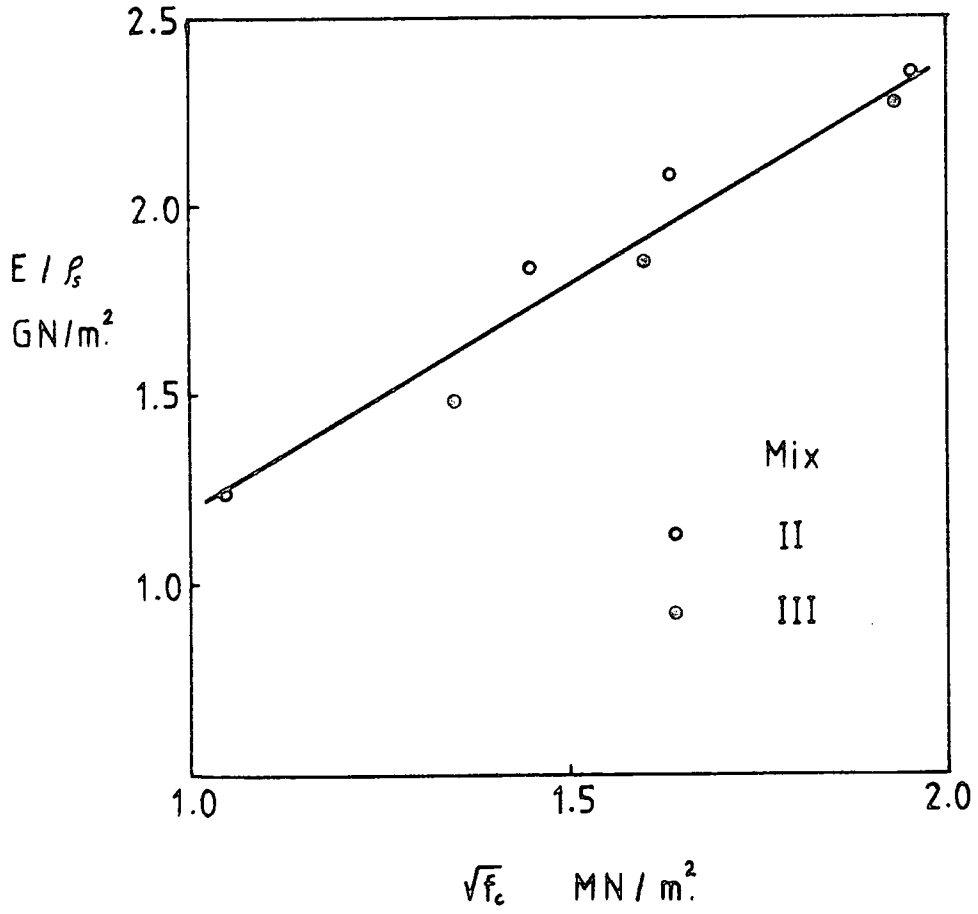

Figure (3.9) Relationship between the compressive strength and modulus of elasticity per unit density of the concrete made from beads type 3.

3.4 Modulus of rigidity (shear modulus)

The shear modulus of some mixes of the polystyrene concrete was determined using a torsion test on cylinders, where the relative angle of twist of two circles on the cylinder with a fixed gauge length between them was measured. The effect of cement content on the shear modulus has been demonstrated and the relationship between the modulus of elasticity and the shear modulus also has been demonstrated by the results obtained.

3.4.1 The mixes tested and samples' dimensions

The results of tests carried out on the polystyrene concrete and reported in this chapter showed clearly that the mixes which were made using the beads of smaller size are of the higher efficiency in terms of workability, strength and modulus of elasticity. The quantity of sawdust in the mix occupying a volume of 0.20 of the volume of the beads is that recommended to be used. This principle is followed in the six mixes of group II which were made using beads type (2) as shown in table (3.3) and are the mixes tested in torsion.

The cylinders which were tested in this procedure were designed to be of dimensions 102 mm. diameter and 300 mm. length. The moulds used were made from plastic rainwater pipe, and have been described previously in (2.5.1), but in this instance they were longer. The total water/cement ratio, mixing, casting and curing have been done in the way used for the compressive and modulus of elasticity samples. Five samples were made from each mix, and the three-cylinders, or in some cases the two-cylinders which were tested were chosen

to be of average density nearly equal to the cylinders tested for modulus of elasticity at the same cement content.

3.4.2 Experimental procedure

When a solid circular shaft - or cylinder - is under equal and opposite torque T at each end of a shaft, so that it is twisted about its longitudinal axis one may make the following assumptions :

(1) That radial planes will remain planar

(2) That elastic strain will be proportional to the radius.

(3) That straight generator lines will be rotated by a constant angle.

From this the well-known torsion relationship may be deduced (10) :

$$\frac{T}{I_p} = \frac{\tau}{r} = \frac{G\theta}{L} \qquad (3.10)$$

Where :

θ is the relative angle of twist between two cross-sections on the cylinder of L between them

(See list of definitions)

For measuring the relative angle of twist between two cross-sections on the cylinder, two jubilee clips were used, where a steel arm - or plate - of cross-section 2.0 x 10 mm. and 110 mm. length was welded to each one as shown in appendix (VI.a.2). The two clips were tightened on the cylinder with 200 mm. between them, and the two arms were kept in the same line. Two steel clamps were made to fit in the two sides of the twisting machine, and the cylinder was fixed between

these clamps or bases (Appendix IV.a.2). The bases could be removed for cleaning. A dental plaster paste was used for fixing the cylinders into the bases as follows : the steel bases were fitted into the machine first. After the clips were tightened onto the cylinder with 200 mm. between them the dental plaster paste was put on the ends of the cylinder, the cylinder was then fixed into the bases in the machine. The cylinder was rotated during the fixing to keep the steel arms in a horizontal position, this being checked with a spirit vial. The movable part of the machine was gently pushed inwards to keep the cylinder firmly in contact with the bases. After 2 hours the dental plaster was thoroughly solidified and the cylinder was firmly fastened to the steel bases.

Two dial gauges of accuracy 0.01 mm. were fixed so as to touch the horizontal arms at equal distances (90 mm.) from the surface of the cylinder as shown in figure (3.10). The dial gauge readings were recorded before loading was started. The load was applied and controlled gently by hand till the cylinder failed. The dial gauge readings were recorded at every 100 lb. in torque. An Avery Torsion Tester machine of capacity 7500 lb.in. was used.

3.4.3 Results and relationship to the elasticity modulus

From the relative vertical displacement of the Dial gauges and their distance from the centre-axis of the cylinder, the relative angle of rotation between the two cross-sections was determined at each load. Assuming the concrete to be an elastic material especially in the first stages of load, the

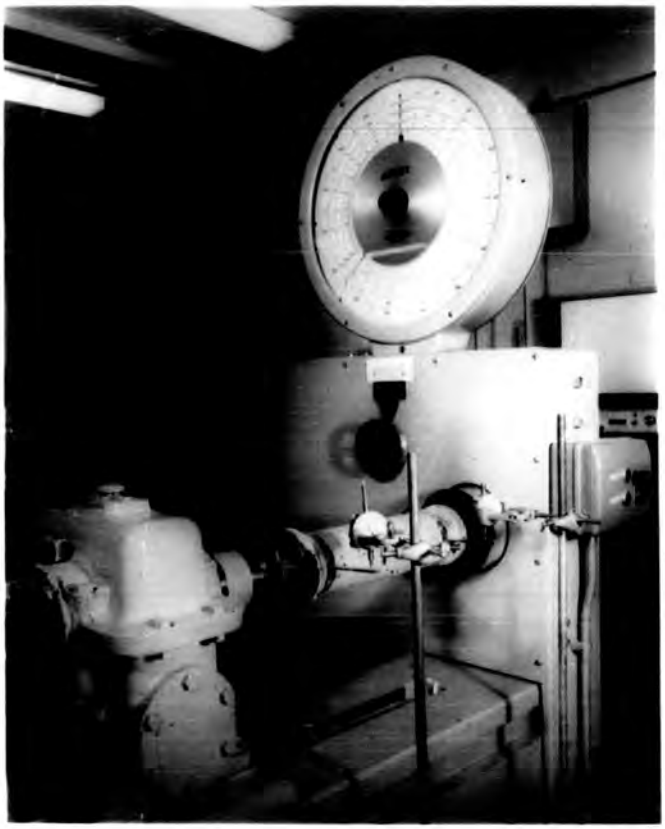

Figure (3.10) : Cylinder in Torsion testing machine.

Figure (3.11) : Typical Torsion failure.

equation mentioned before can be used. From equation (3.10) when the relationship between θ and $\frac{T.L}{I_p}$ was plotted with θ as the absissa and $\frac{T.L}{I_p}$ as the ordinate, the rigidity modulus G was taken to be the slope of the initial tangent line to the curve. The typical curves of this relationship and their tangent can be seen in (Appendix I.c).

The values of the shear modulus of the mixes made in this procedure obtained against the cement content and the concrete density were recorded in table (3.10). It can be seen from the results that the modulus of rigidity of the polystyrene concrete depends mainly on the cement content, i.e. the shear modulus behaves approximately in the same manner as the compressive strength and the modulus of elasticity. However, the shear modulus per unit density was plotted in figure (3.12) against the cement content. The expression of this linear relationship is

$$G = \frac{1}{54.5} \times 10^{-4} . \rho_s (C_c - 70) \qquad (3.11)$$

Where :

ρ_s is the saturated density of the concrete in kg./m^3

C_c is the weight of cement for m.^{3} of aggregate in kg.

G Shear modulus in GN/m^2.

Figure (3.13) was plotted also to show the relationship between E and G, from the graph the relationship between E and G is :

$$G = 0.42 \; E \qquad (3.12)$$

and the relationship is notably constant.

Table (3.10) : Shear modulus and maximum shear strength according to the cement content and density of the mix (mixes made from beads type (2) group II)

Cement Content kg. per cubic metre of agg.	Concrete saturated density (kg/m.^{3})	Shear modulus (GN/m.^{2})	Maximum shear strength (MN/m.^{2})
305	575	0.31	0.482
410	700	0.64	0.780
515	770	0.83	0.895
615	900	1.19	1.100
720	970	1.44	1.242
820	1050	1.72	1.520

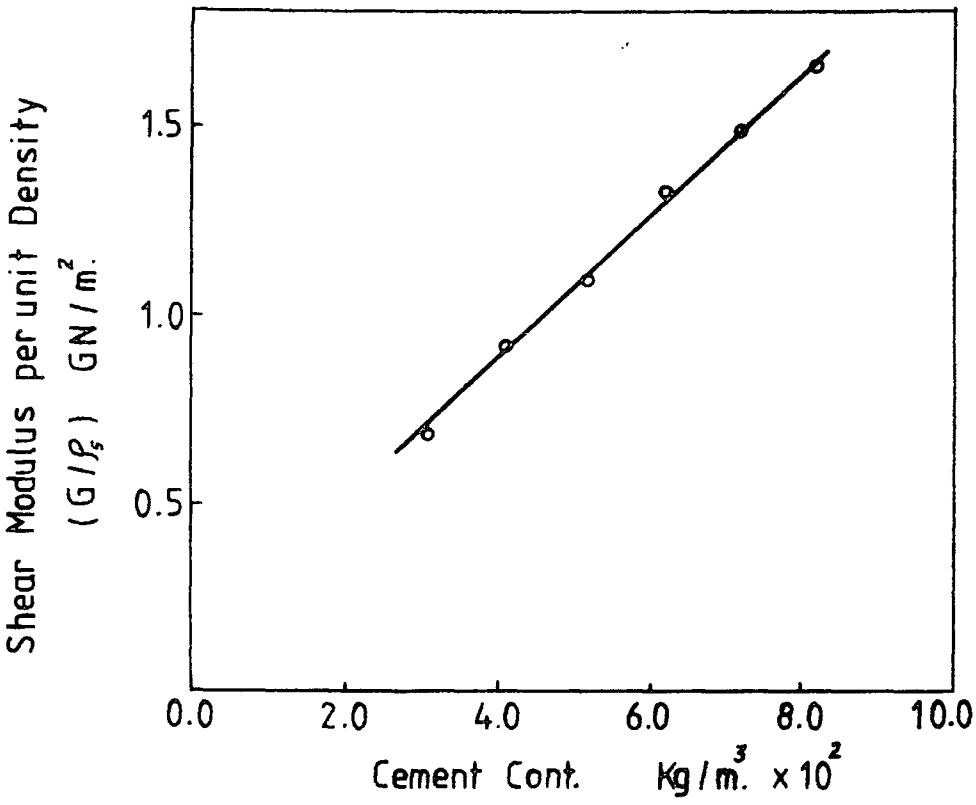

Figure (3.12) Relationship between the shear modulus per unit density and the cement content of concrete made from beads 2 (mixes II).

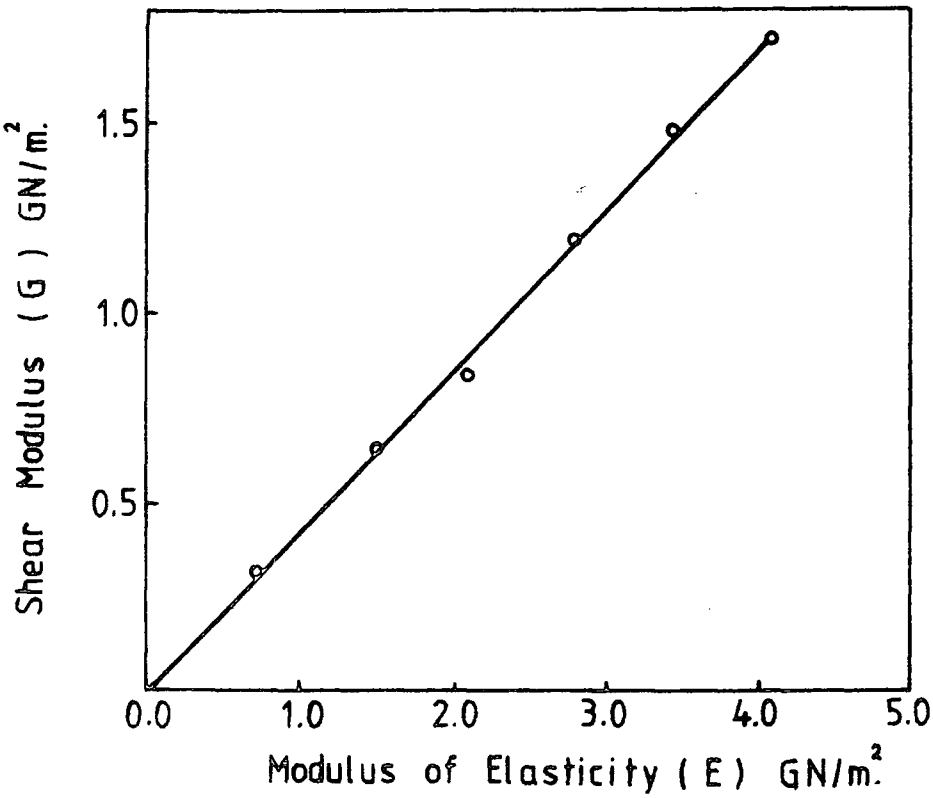

Figure (3.13) Relationship between the shear modulus and modulus of elasticity.

3.5 The saturated and dry density for designs used

The compressive strength, modulus of elasticity and shear modulus of the polystyrene concrete made in this research were related to the saturated density to avoid the difficulties involved in defining and determining the moisture contents, and also it is more useful practically. The saturated density is not the condition in which the concrete would remain in construction. The oven-dry density is only of academic interest because the concrete, naturally, is never fully dry. The concrete which is semi-dry (air-dry) is the case which is interesting to the structural designer.

To determine the dry density and for measuring the moisture content according to the cement content in the mix, three cylinders of 2 x 3 in. dimensions and two of 102 x 204 mm. were made from each mix of the six mixes of group II which were made using beads type (2) and the four mixes made using beads type 3 (table 3.3). The cylinders were put in an oven of 55°C temperature till there was no further loss in weight. The samples of 2 x 3 in. took about 3 weeks to dry, while the samples of 102 x 204 mm. took about 6 weeks. The losses in the weights due to drying was found to be affected by the cement content, where the higher value in the weight's reduction were recorded in the poor mix. In this procedure the losses in the weights were found to be of varying value, from 18 per cent in the mix of cement content 305 to 14 per cent in the mix of cement content 820 kg/m^3. This behaviour is related to the sawdust content increment when the lower value of cement is used, because most of the moisture movements are related to the sawdust. Some mixes also were made and were left in the control room to become air dry and the average

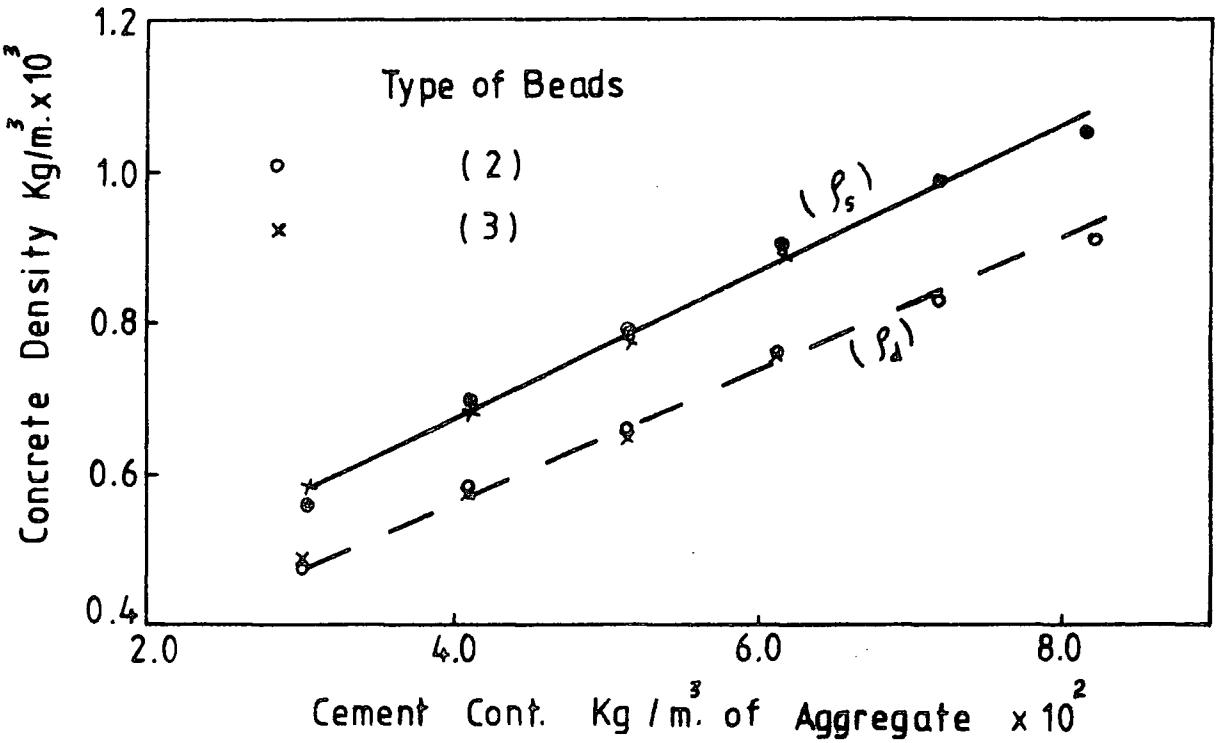

Figure (3.14) Relationship between the cement content and the saturated and dry density of the concrete made from beads type 2 (Group II) and beads type 3 (Group II)

losses through 8 weeks was found to be about 10-12 per cent.

Figure (3.14) was plotted to show the relationship between the cement content and the saturated density for the six mixes of beads 2 and the four mixes of beads 3 (group II). The oven-dry density of all these mixes were graphed also in the same figure. The relationship involving the saturated density can be written for the concrete made from the two types of polystyrene beads used in the following expression :

$$\rho_s = 0.95 \quad C_c + 300 \qquad (3.13)$$

and the dry density expression is :

$$\rho = 0.89 \quad C_c + 200 \qquad (3.13)$$

(see list of symbols)

3.6 Comment and mix design

The most practical methods of mix design in lightweight concrete have been based upon empirical rules derived from experimental research and the author agrees with the view. It follows, then, that the method of mix design of the polystyrene concrete developed and described in this section also was based on the experimental results obtained and with reference to the empirical formulae developed during this research.

Tests carried out in this research showed that at certain values of cement content the change in the grading of the polystyrene beads changed the concrete strength, modulus of elasticity and shear modulus according to the density of the concrete obtained. The change in the density is mainly as a result of alteration in the water ratio required to maintain a

given workability, and also due to changes in the size of the voids in the concrete owing to the beads' size.

Because the oven-dry density is not of real practical interest and the moisture content of the concrete is changeable due to the existence of the sawdust, the method design is based upon the saturated density obtained as the tests were carried out.

The following is a sequence of instructions on the procedure of mix design which may be used in conjunction with the results of this research:-

(1) The quantity of sawdust recommended to be used is 0.20 times the bulk volume of the polystyrene beads when the maximum size of the beads' grading is less than 4 mm.. If the larger size of beads is used, the sawdust volume should be between 0.2 and 0.3 of the bead bulk volume.

(2) The cement content to be used is given in kg. per cubic meter of the bulk volume of aggregates.

(3) When a certain density is required, the cement content for that concrete may be determined from equation (3.13) taking into consideration that the air dry density after 4 weeks is about 90 per cent of the saturated density, i.e. if the required dry density is specified, then the saturated density is about 1.1 times the air dry density.

(4) Because the beads' size and/or the sawdust moisture may be different from the value used in this research, a trial mix of cement content not less than 400 kg./m^3 is required to be done first, for determining the quantity of water required for workability and three standard

cylinders should be cast and tested in compression from that concrete.

(5) The quantities of water for workability for the required mix are determined using equation (2.1) as follows:-

$$W_t = W_i + 0.229 \Delta C \quad \text{(See list of symbols)}$$

(6) The cylinder's compressive strength can be calculated by equation (3.4), where the constant k. is determined first according to the density and compressive strength of the cylinders made from the concrete of the trial mix and the formula can then be used with the known value of k.

(7) The modulus of elasticity also can be estimated using equation (3.9) and the constant k varies in the range between 12 and 14 according to the beads' size, where the higher values are used for the beads of smaller size.

(8) The rigidity modulus also can be estimated by equation (3.11) or (3.12).

In this method of design the maximum error due to using the empirical formulae mentioned will not be more than $\pm$10 per cent, with the manufacturing conditions described in this research; i.e. without compacting so as to distort the spherical shape of the beads. A compacting weight applied so as to impose a load of about 6 gm./cm.^{2} should be used during vibration.

CHAPTER FOUR

PROPERTIES OF TENSION AND COMPRESSION FACES

4.1 Introduction

In the reinforced concrete beam, due to the poor tensile strength characteristic of cement, the capacity of the beam in flexural tension is attributed to the cross-sectional area of reinforcement in the tension side. In a sandwich beam the flexural tension is expressed by the tensile force of the whole face. The types of reinforcement which can be used in a thin concrete face of thickness about 10 mm. thick so that the whole face acts in tension as one unit - i.e. as a homogeneous section - are fibre reinforcement or steel wire mesh. Faces were reinforced by alkali resistant glass fibre or steel fibre with the reinforcement in such density as would give mixes of acceptable workability. They were found to be of modulus and tensile strength much lower than could be acceptable (33).

All the faces of the sandwich beams made in this research were reinforced by expanded steel wire mesh. The experimental work which produced the results presented in this chapter was planned to demonstrate the influence of the mesh cross-sectional area on the face characteristics.

Since the stiffness of the sandwich beams and their analysis depend mainly on the faces' properties, compression and direct tension tests have been done for samples of thickness equal to their thickness in the beams. The purpose of these tests is to determine both the compression and tension modulus of elasticity and the ultimate strength according to the mesh size and dimensions used. For determining the flexural stiffness

of the faces with the different meshes, bending tests have been carried out also on all cases of reinforcement used.

In order to increase the tensile strength and the tension modulus of elasticity of the faces, some samples were made and tested where steel fibre was used along with the mesh.

4.2 Face materials

4.2.1 Proportions of the concrete mix

The faces of the sandwich beams made in this research - as mentioned before - consist of a concrete mix reinforced with an expanded steel mesh. According to the dimensions of the diamonds of the meshes used and the thickness of the faces (10 mm.), a fine concrete was required to go easily through the mesh and surround it. Because of this, the ordinary building sand was found of grading size suitable for use in all the faces made. Tests were carried out and the results reported in this chapter for all the faces of the sandwich beams studied in this research. A typical sieve analysis of the sand used according to B.S test sieves was recorded in table (4.1) and graph (4.1) was plotted to show the grading.

The water content of the sand is supposed to be constant for all the faces made and tested in this procedure, and also the faces of the sandwich beams. Because the sand is delivered to the laboratory in a wet state and its water content changes with time, all the sand used was dried in the dry-oven one week before using and was kept in the control room in buckets. The moisture measurement of the sand, at different times of using, was found to be between 0.20 and 0.40 per cent. The moisture

Table (4.1)

Sieve No.	% passing by weight	Sieve No.	% passing by weight
3/16	96.0	52.0	30.85
7	75.0	72.0	22.10
14	62.0	100.0	13.80
18	54.4	170.0	3.90
25	49.6	200.0	2.50
40	37.8		

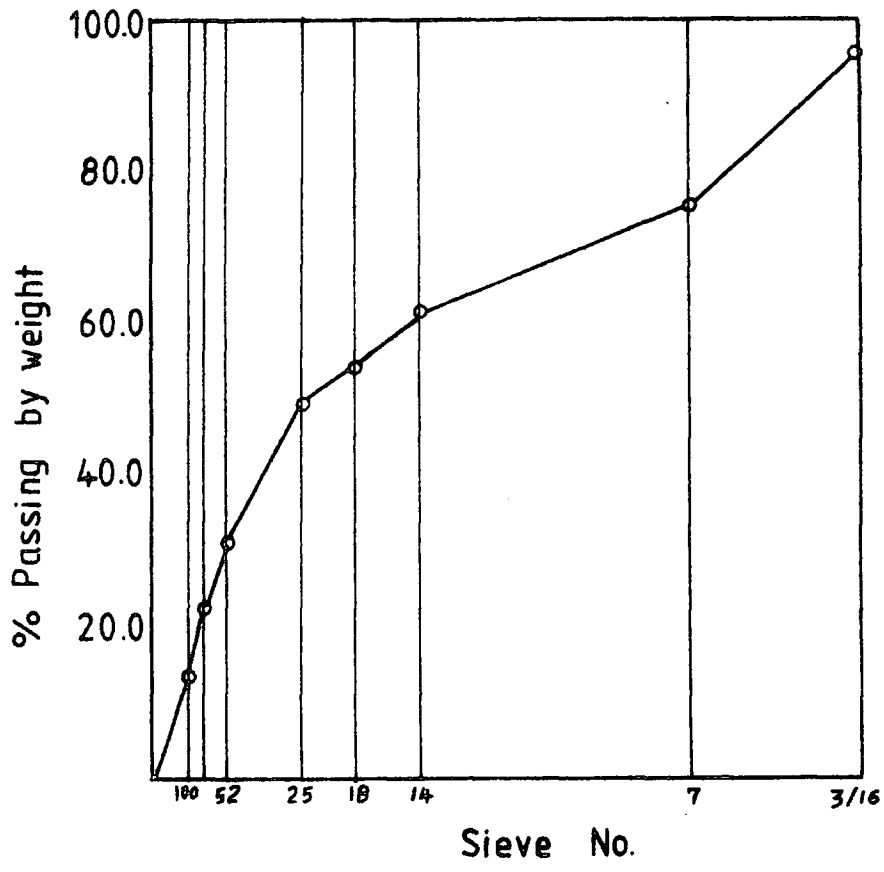

Figure (4.1) Grading Curve of Sand (B.S. 410)

was determined by Moisture tester type D.1.

In the concrete faces of sandwich structures such as these the strength of the concrete used is one of the factors which affects the face stiffness and strength. Since the faces were required to be of high stiffness and as strong as possible, their concrete mix was selected from four mixes. The four mixes were made first to achieve the best proportions of the sand-cement giving concrete of suitable strength with high modulus of elasticity. The sand-cement proportions used for these mixes can be seen in table (4.2). The value of water/cement ratio was chosen for each mix - as shown in table (4.2) - so that the workability was within the required range.

Three standard cubes of 150 mm. side were made and tested in compression from each mix. For more data in comparison, six cylinders of 150 x 300 mm. dimensions were made also from each of the four mixes. Three of them were tested in compression to determine the modulus of elasticity of the mix, and the other three were tested to determine indirectly the tensile strength of the mix. The compression and the indirect tensile strength tests were carried out with reference to B.S specifications (8). The modulus of elasticity (initial tangential) was determined from the compression stress-strain curve. The strains were measured at each load increment (50 KN) by demec gauges with 150 mm. gauge length through three pairs of demec gauge points attached on the surface of each cylinder. Typical stress-strain curves from different samples can be seen at appendix (II.a).

All the specimens were cured in a tank for six days and

Table (4.2) : Concrete for faces, the mix proportions and corresponding strength and modulus

Mix Symbol	Mix proportions		Test results		
	Sand/cem. by wt.	Water/cem. ratio	Comp.str. (N/mm^2)	Modulus of elasticity (N/mm^2)x10^3	Indirect tensile st. ($N/mm.^2$)
M_1	0.33	0.310	73.0	21.0	3.89
M_2	0.50	0.320	78.4	21.5	4.13
M_3	1.00	0.350	73.0	21.5	4.46
M_4	2.00	0.410	54.0	20.6	3.78

they were tested at 7 days' age in a Denison testing machine model T1B/M.C, 200 ton capacity. A Denison Rate-of-load pacer was used during the compression and indirect tensile strength tests for adjusting the rate of the load as required.

Rapid hardening Portland cement was used for all these four mixes and also forthe concrete of the faces made and tested in this research.

The results obtained in this procedure were recorded in table (4.2). It will be seen that the mix of the highest sand/ cement ratio (Mix M_4) was found to have the lowest strength and modulus. The increase of mix's cement content (Mix M_1) was not accompanied by an increase in the concrete strength and modulus in the same proportion. The two mixes M_2 and M_3 were found to have the highest efficiency, since the highest values of compression strength were recorded from mix M_2 and the indirect tensile strength of mix M_3 was found to have the highest value. The modulus of elasticity of the two mixes was found to be the same. In view of the requirement of economy the concrete of mix M_3 was chosen to be used for the faces in this research.

4.2.2 Reinforcement

All the sandwich beam face specimens, of which the test results are recorded and discussed in this chapter, were reinforced - as mentioned before - with expanded steel mesh. The meshes used were chosen from those produced by Expamet Industrial Products Limited, Hartlepool, and were provided by them (17). Seven different grades of meshes were used for the work carried out in this research, where eight different degrees of reinforcement have been used. They were selected to provide the faces with reinforcement of cross-sectional area in the range

between 40 and 120 mm.^{2} cross sectional area with widths approximately equal to the face width (120 mm.). All the meshes used were chosen also to be of total thickness which can be embedded completely in the thickness of the face, which, according to the beam dimensions used in these experiments, was of 10 mm. thickness. The faces were designated as shown in table (4.3) according to the mesh Ref. No. and the cross-sectional area of the reinforcement in the face.

The meshes were supplied in sheets each of 1220 x 2440 mm. dimensions. All the sheets were cut into strips, each 1220 mm. in length with the longer across the diamond in the mesh running parallel to the strip length. All the strips were cut to have only complete strands. The meshes of smaller diamond size (No. 1598, 1597 and 1595) were found to be of 14 strands to provide the face with reinforcement of about 115 mm. width, and 10 strands in strips made from the mesh of large size were approximately of the same width (see figure (4.2)). The No. of strands (9 and 8) of the mesh which was used to reinforce respectively the faces S_4 and S_6 were determined to provide the face with reinforcement of the cross-sectional area required to fill the gaps between the other faces. In other words the reinforcement of these two faces was determined to provide the missing increments between the cross-sectional area of reinforcement in the other faces.

The dimensions of the mesh size (S.W and L.W) were found by laboratory measurements to be approximately equal to the production specifications. The measurements of the strand dimensions indicated that the mesh of the Ref.No. 2091 has different dimensions. The width and the thickness of this mesh

Table (4.3) : Faces' designation according to the mesh and area of reinforcement and the dimensions of the meshes used

Face Designation	Mesh Ref. No.	Mesh size mm.		Strand size mm.		θ^{o}	No. of strands in the face	A_s (mm^2)
		S.W	L.W	Width	Thickness			
S_1	1598	12.7	38.1	2.31	1.20	18.43	14	41.0
S_2	1597	12.7	38.1	2.41	1.58	"	14	56.0
S_3	1595	12.7	38.1	3.10	1.58	"	14	72.5
S_4	2093	19.05	50.8	3.18	1.58	20.55	9	48.3
S_5	2091	19.05	50.8	2.22	2.82	"	10	67.0
S_6	2089	19.05	50.8	3.12	3.10	"	8	82.6
S_7	2089	19.05	50.8	3.12	3.10	"	10	103.3
S_8	2088	19.05	50.8	4.04	2.75	"	10	118.0

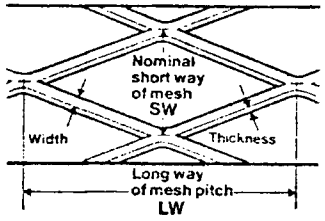

$$A_s = \frac{\text{width x thickness}}{\text{Cos. } \theta} \text{ x No. of strands} \quad (mm^2)$$

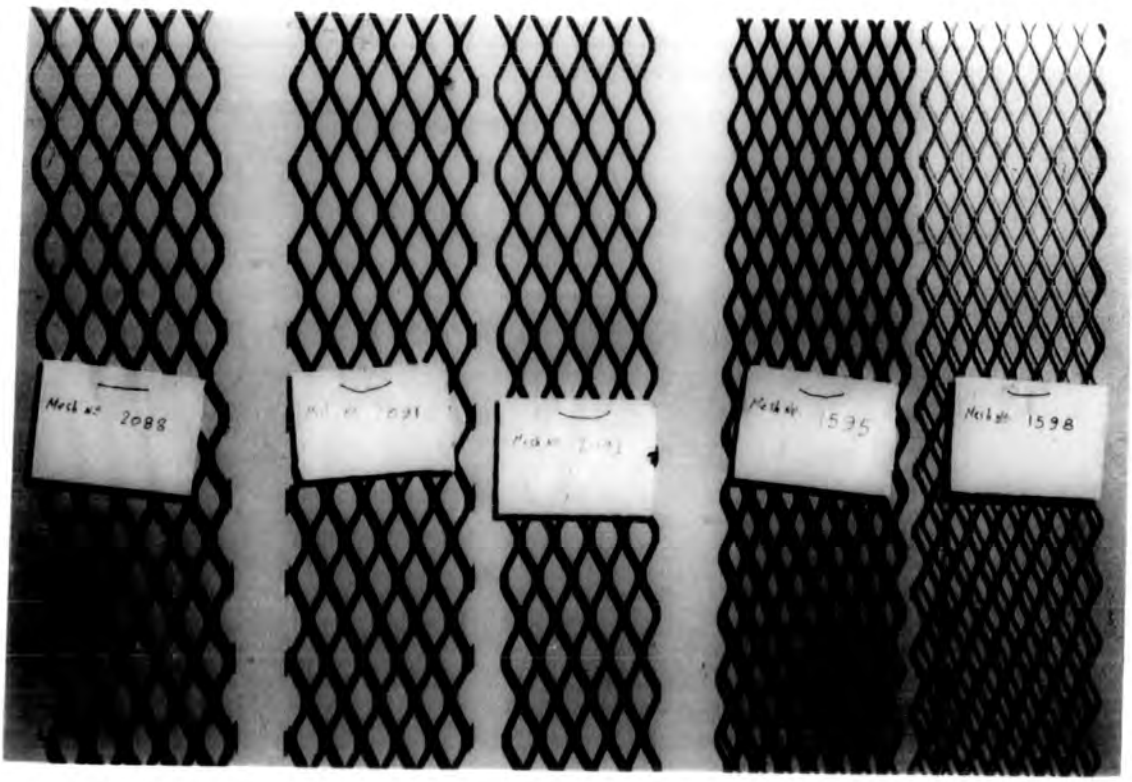

Figure (4.2) shows photographs of strips of the mesh from the two sizes used.

were found respectively 2.22 mm. and 2.82 mm. instead of the 2.51 and 2.50 given in the table of the production specifications. The strand of the mesh of the Ref. No. 2088 was found also by measurements to be of thickness 2.75 mm. instead of 3.10 mm. The dimension of the strands of the other meshes were found to be approximately equal to the specified dimensions. However, the dimensions and the cross-sectional area of all the meshes which were recorded in table (4.3) were determined by practical measurements to an accuracy of 0.01 mm. and were approved by the manufacturer (44). The areas of steel (A_s) were recorded in table (4.3), and are the cross-sectional areas of the reinforcement in the faces normal to the face length.

Because the meshes were oiled at delivery, the strips were washed with paraffin and well brushed during washing. After 24 hours the steel was washed again with water. (2.07×10^{11} $N/m.^2$) is the modulus of steel used.

4.3 Strength and modulus of faces

The faces in the efficient sandwich beam are supposed to act principally in direct compression and tension. Therefore, it is appropriate to determine their properties in compression and tension tests. The modulus of elasticity of the reinforced concrete section in compression can be determined theoretically according to the modulus of elasticity of both concrete and reinforcement used.

In this research the faces (according to the dimension of the sandwich beams studied) are required to be of 10 mm. thickness. Since the characteristics of these relatively thin faces and with such reinforcement may be affected by the mesh's

size, the dimensions of strand and the conditions of the mesh's surface, calculating the compression modulus of elasticity theoretically is suspect. The face mechanics with this type of reinforcement in tension is not easy to determine theoretically.

For the reasons mentioned, and for results of greater accuracy in the beam's calculation and analysis, the moduli of elasticity of all the faces in compression and in tension were determined experimentally. All the eight faces were made and tested with cross-sectional dimensions similar to their dimensions in the sandwich beams (10 mm. thickness and 120 mm. width).

4.3.1 Faces in compression

The compression test on such a thin sheet as a single face is rather difficult and impractical. It would not be possible to complete the test without premature failure due to elastic instability. So that the faces would be tested until their failure in compression, and would be in a situation similar to their position in the sandwich beams, the sample was made to have two faces on either side of a core of 40 mm. thickness made from polystyrene concrete. The dimensions of the sample can be seen in figure (4.3a).

Wooden moulds were made for casting two samples together at the same time. The casting and curing process of such sandwich samples was described with full details in chapter 5 at section (5.3).

All the samples were tested at age 7 days and were removed from the tank for 24 hours so as to be in the same condition as the sandwich beams. Six pairs of demec gauge points

were attached on each sample. Two pairs were fixed at the external side of each face, and one pair at each side of the cores and shown in figure (4.3a).

Four samples were made from each one of the eight degrees of reinforcement which were mentioned in table (4.3). Two of them were tested to determine the compression modulus of elasticity and then other two were tested to determine the ultimate strength of such faces. The compression tests were carried out on a Denison testing machine model T42 B4, 500 KN. capacity, using the scale disk of 250 kn. Two steel plates with two pieces of plywood were used to spread the load on the sample.

For the compression modulus the load was applied at each sample from zero till failure. At each 10 KN. increment and after about 30 seconds of the load application, the compression strains were measured from the four pairs of demec gauges which were fixed on the two faces. The strain of the core was taken also from the two pairs fixed on the two sides of the core. A demec gauge with 200 mm. gauge length was used. When the strain measurements of the two faces of the sample were found of values varying with more than 10 per cent, the results of such a sample were disregarded.

At each load increment, the compression load carried by the core was calculated with reference to the modulus of elasticity of the core mix used and its strain measurements. The compression load carried by the two faces then was calculated. The relationship between the compression strength of the two faces and the correspondent strain (the average of four readings) was graphed for each sample. The modulus

of elasticity was determined from the initial tangential line of the stress-strain curve. Typical graphs of the stress-strain relationship of some samples can be seen in Appendix (II.b). The values of the modulus which were determined experimentally for the eight faces (average from two samples not varying by more than 10 per cent) were recorded, according to the cross-sectional area of the reinforcement used, in table (4.4). The young's moduli of the faces were calculated also theoretically with reference to the modulus of the concrete mix used and the young's modulus of the steel used and the values were recorded in table (4.4). They were calculated by the expression :

$$E_{Fc} = \frac{A_s}{A_F} E_s + \left(1 - \frac{A_s}{A_F}\right) E_c \qquad (4.1)$$

It can be seen from the results recorded in table (4.4) that the modulus of elasticity of all the faces which were determined experimentally were found, as expected, of values lower than the calculated values. The experimental moduli of all the faces were found in the range between 81-85 per cent of the calculated modulus. Because all the results were approximately in the same range in spite of the change in the mesh's size and the dimensions of strands, the reductions then are attributed to the face's dimensions. The gap between the experimental and the calculated modulus is expected to be reduced with increase in the thickness of the face. The expression (4.1) which may be used for calculating the faces' young's modulus can be written in the next formula:

$$E_{Fc} = \phi \left[\frac{A_s}{A_F} E_s + \left(1 - \frac{A_s}{A_F}\right) E_c \right] \qquad (4.2)$$

Where :

ϕ is a factor which depends on the dimensions of the face (with the dimensions of the faces tested in this research, ϕ = 0.81 - 0.85; average, ϕ = 0.83)

However, the values of the modulus of elasticity which were determined experimentally were considered to be the more reliable values for the beam's calculation and analysis.

Two samples from each degree of reinforcement were tested in compression to determine the ultimate strength. The results (average of the two samples) were recorded in table (4.4). The failure came due to the destruction of the faces themselves as shown in figure (4.5a). This type of failure was very interesting, since the faces reached their ultimate strength without buckling in spite of the core mix used being the weakest mix used in the sandwich beams, i.e. the bond characteristic of the polystyrene concrete as the core of the sandwich beam was satisfying the recommended condition of the core.

4.3.2 Faces in tension

The direct tension test of the reinforced concrete elements is one of the most difficult to perform. The faces of the sandwich beams made in this research were required to be tested in direct tension with cross-sectional dimensions the same as their dimensions in the beams (10 mm. thickness and 120 mm. width). Several attempts have been made to produce suitable forms for the samples and to achieve the best method for such testing without any bending or load eccentricity on the sample. The best results were obtained from the samples of the form shown in figure (4.3b).

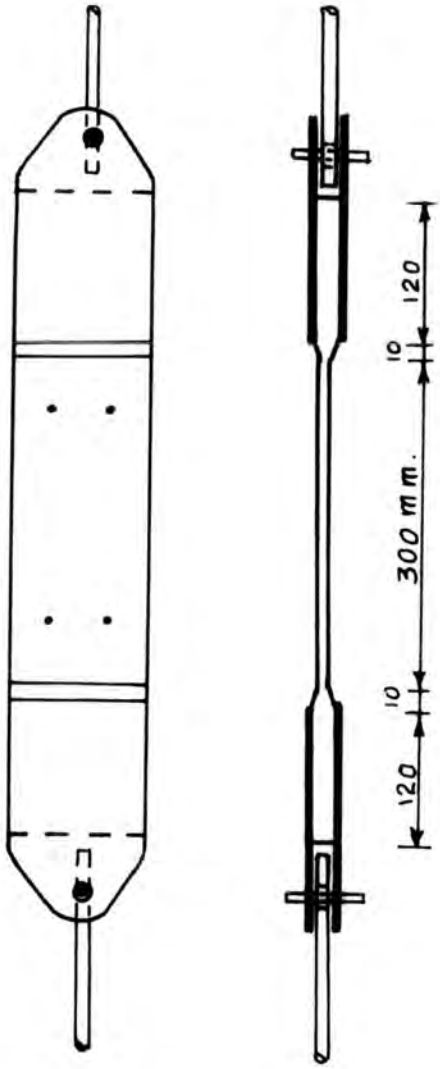

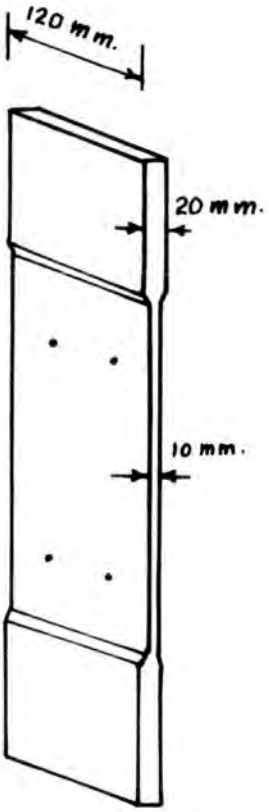

Fig.(4.3b)

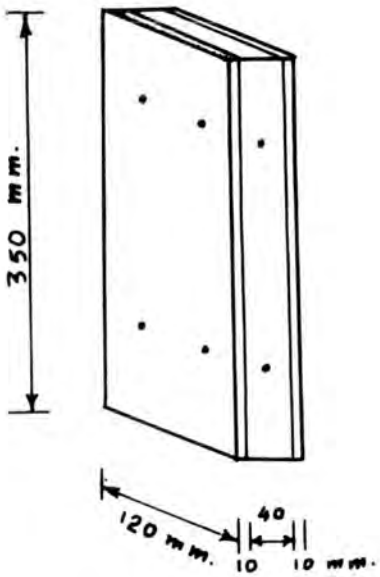

Fig. (4.3a)

Fig.(4.3c)

Figure (4.3) Dimensions of the compression and tension samples of the faces and tension test arrangement.

Wooden moulds were constructed for producing the tension samples. The details of these moulds can be seen in Appendix (IV.b). The moulds were prepared to provide each sample with three holes near each end (see Figure 4.5b). The positions of these holes were chosen as being in the diamond of the mesh without cutting any of its strands. Also, they were chosen to be symmetrical about the centre line of the sample. The additional thickness at each end was reinforced by steel mesh, also, so as to be stronger than the body of the sample and to avoid the early appearance of cracks and/or the earlier failure which may happen due to the existence of the holes.

All the tension samples were cured by the same method used for the compression samples and the sandwich beams. After removing the samples from the curing tank, two pairs of demec gauge points were fixed at each face of the sample, using araldite adhesive. The tension tests were carried out on all the samples at age 7 days in the Denison testing machine model T42 B4. Four steel plates with two round bars were used to transfer the tension load from the machine to the sample, Figure (4.3b). Two plates were well tightened around the thick part at each end by three bolts passing through the three holes. Round bars were joined to the two plates by hinge joints. These were used for fixing the sample into the two jaws of the machine, as shown in Figure (4.3c). The tension load was applied on the sample in equal increments until failure and the strains were measured from the four pairs of demec gauge points at each load increment. The load increments were adjusted according to the areas of reinforcement used, these being 1.5 kN. for face S_1 and 3.0 kN. for faces S_6, S_7 and S_8, and they were taken to be

2.0 kn. for the other faces. A Demec gauge of 200 mm. length was used for all the measurements carried out in this procedure. It was difficult to position the samples precisely enough for the demec gauges to give the same readings. When the strains were found to vary with a range of more than 20 per cent, the results of the samples were not used. Typical values of the acceptable results from sets of two samples made from different meshes can be seen in Appendices (II.ℓ 1 & 2).

The stress-strain relationship was graphed for each sample giving acceptable results, and the tension modulus was determined. Appendix(II.c) shows the stress-strain curves of some samples. The values of the young's modulus of the faces (average from two samples not varying by more than 12 per cent) were recorded in table (4.4). The results indicate that the increase in the tension modulus of the faces is approximately proportional to the increase in the cross-sectional area of reinforcement being used.

Since all the faces were made using the same concrete mix and there was no evidence of change in the results due to the variation of the mesh diamond size, the variation of the tension modulus can be attributed to the area of steel mesh (A_s) used. Figure (4.4) was plotted to show the relationship between the tension modulus (E_{Ft}) and the cross-sectional area of the mesh (A_s) being used. The graph showed that the relationship (on average) is linear and the equation of this linear relationship is :

$$E_{Ft} = 1.28 \times 10^2 A_s \qquad (4.3)$$

Where:

E_{Ft} is the tension modulus of elasticity of the face as reinforced by steel mesh in $N/mm.^2$

A_s is the cross sectional area of the mesh normal to the face length (acting length) in $mm.^2$

The modulus of elasticity of the concrete with this type of reinforcement affects the face strain and subsequently the tension modulus, because it may change from one job to another; the relationship for this type of reinforcement, generally, can be expressed :

$$E_{Ft} = K A_s \qquad (4.4)$$

Where:

K is a constant factor changing according to the concrete mix used and it may also be affected by the face thickness.

The samples were watched carefully during the tension test procedure and when the initial crack appeared the tension load was recorded. The values of the tension stress at crack appearance and the ultimate strength (average) are stated for all the eight faces in table (4.4).

It can be seen from the compression and tension test results that the tension modulus is lower than the compression modulus and on average it is about one third of the compression modulus. The results also indicated that the ultimate tensile strength varies between about ($\frac{1}{3}$ - $\frac{1}{2}$) the ultimate compression strength. For such faces and reinforcement, according to the results obtained, it can be deduced that the range of the varation between the compression and tension modulus and the ultimate strength is reduced by increasing the area of reinforcement being used.

Table (4.4) : Face's characteristics in compression and tension according to the mesh and the area of reinforcement used

Face designation	Area of reinforcement (A_s) mm^2.	Faces characteristics in compression			Faces characteristics in tension		
		Modulus of elasticity N/mm^2. x 10^3		Ultimate strength N/mm^2.	Modulus of elasticity N/mm^2. x 10^3	Crack st. N/mm^2.	Ultimate strength N/mm^2.
		Theoretical	Experimental				
S_1	41.0	27.95	23.40	34.0	5.71	5.0	11.0
S_2	56.0	30.60	24.90	39.0	7.76	7.50	14.58
S_3	72.5	32.90	28.40	43.0	9.77	10.50	16.25
S_4	48.3	29.16	24.10	35.8	6.48	5.50	12.10
S_5	67.0	32.10	26.90	41.7	8.73	8.33	15.83
S_6	82.6	34.59	28.70	43.0	10.30	11.67	20.00
S_7	103.3	37.88	30.20	44.5	12.60	13.80	23.75
S_8	118.0	40.20	32.70	46.0	14.84	15.70	25.40

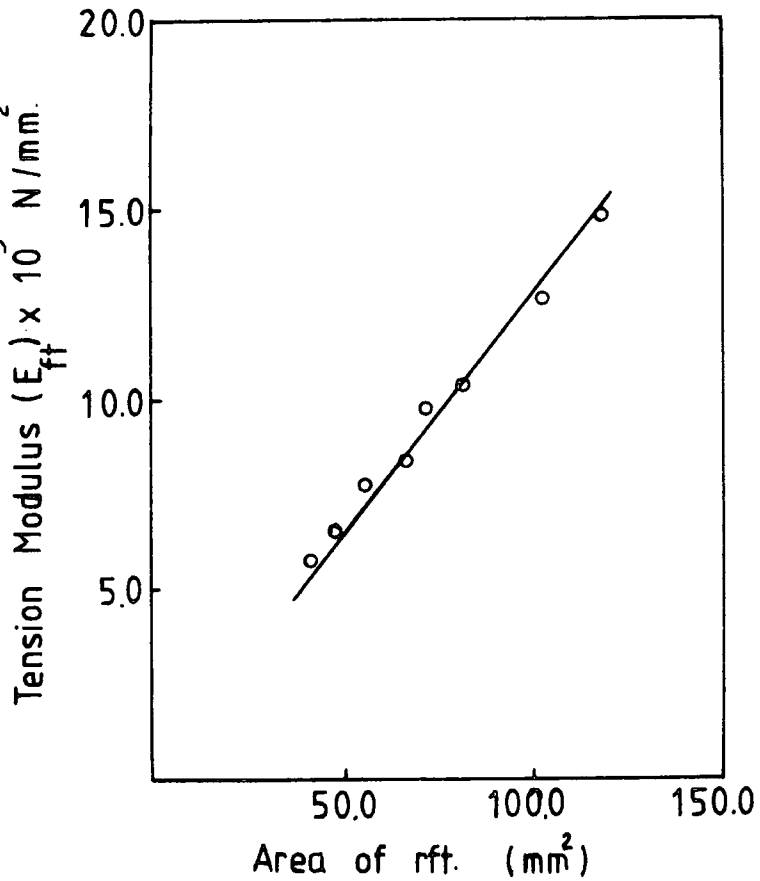

Figure (4.4) Relationship between tension modulus and area of mesh reinforcement (A_s) in the faces.

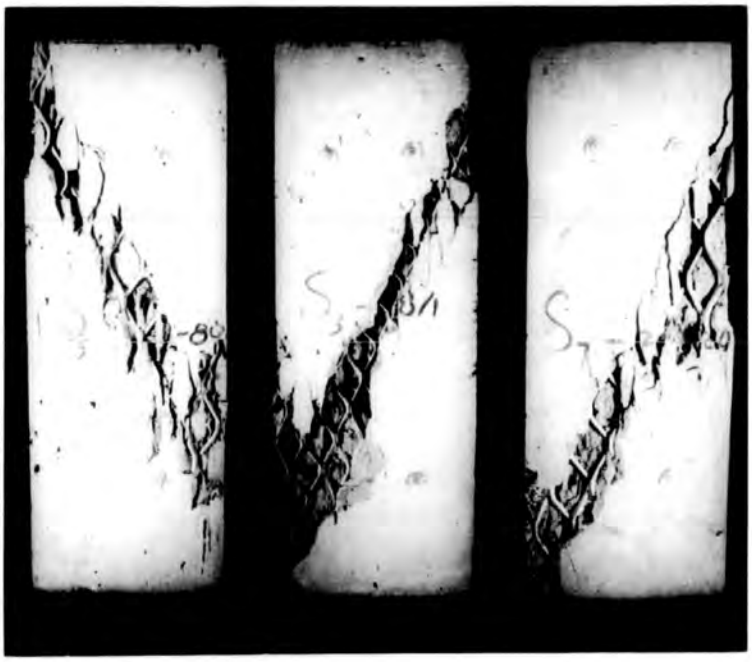

Figure (4.5a) : Typical compression failure of faces for samples reinforced by different meshes.

Figure (4.5b) : Typical modes of face failure in tension.

The faces failed in one of two ways; mesh snapping or concrete crushing. The faces S_1 and S_4 (of reinforcement of cross-sectional areas less than 50 mm.^{2}) failed due to steel snapping and the others failed with the concrete crushing. Figure (4.5b) shows the two types of failure for two samples from the faces S_4 and S_8.

4.4. Flexural stiffness of faces

The flexural stiffness of the face is one of the factors which constitutes the sandwich beam stiffness, so, the flexural stiffness of the face is required to be determined exactly. In relatively homogeneous materials like steel or aluminium sheets, the flexural stiffness is determined easily by measuring the dimensions of the face and with reference to the modulus of elasticity of the materials in tension. This may not provide accurate results for the face of inhomogeneous material such as the reinforced concrete faces, and in these cases the flexural stiffness must be determined by direct experimental measurements.

For determining the flexural stiffness with sufficient accuracy, three samples were made from each one of the eight faces mentioned before in table (4.4). The specimens were made to have the same cross-sectional areas as the faces in the sandwich beams (10 mm. thickness and 120 mm. width). All the samples were cured by the same method and under the same conditions as the compression and tension samples and the beams. The faces were tested at age 7 days in the Denison testing machine model T42 B4, using the load disk of 10 KN. capacity. The sample was tested as a strip by means of a four-point load test (1)

as shown in Figure (4.6a). The two equal loads W were applied on the sample by using a wooden bridge (see Figure 4.6b). Three dial gauges with 0.01 mm. divisions were fixed at mid-span point and at two points of equal distance around the mid-span point as the graphs show. The loads were applied on the samples with equal increments (100 N.) and at each increment the readings of the three dial gauges were taken.

According to the load conditions used, the central region of the sample is, therefore, subjected to uniform bending moment of value equal to Wb. As a result it bends in an arc of a circle of curvature $1/R = Wb/EI$. At the values of small deflections, the flexural stiffness of the face is determined by the expression:

$$EI = \frac{Wbc^2}{2\Delta} \qquad (4.3)$$

Where:

Δ is the deflection of the mid-span point with respect to the line between the two points where the deflection was measured (the line CE in figure (4.6a)).

b & c are the distances shown in the graph.

For more accurate results the load W was plotted against Δ for the earlier stage of load (range of load of the elastic stage) and the slope W/Δ was inserted in equation (4.3) for calculating the value of EI. Typical W-Δ curves of some samples can be seen in Appendix (II.d).

The values of Δ measurements versus W (average from three samples) were recorded in the table stated in Appendix (II.e.3) for all the eight faces were defined before. The results, as

shown, indicate that the average of measurements of Δ from the samples of face S_1 is approximately equal to the results which were recorded from the samples of S_4 in spite of the cross-sectional area of the mesh of the first being less. The recorded results from S_2 samples were found also approximately the same as, or close to, the results which were recorded from S_5 and S_3 samples. The behaviour of such cases mainly is attributed to the position of the mesh in the face cross-section which is affected by the width of strand and mainly by the thickness of the slices used to put under the reinforcement. In view of the fact that the meshes used for the faces S_1 and S_2 are of smaller width, and with the thickness of slices used, most of the reinforcement occupies a lower position in the face cross-section leading to faces of higher stiffness. Accordingly, it may be advisable for such reinforced concrete faces, to improve the flexural stiffness, to keep the reinforcement as far as possible in the lower part of the face's section, but this situation is not recommended because of the compression and tension stress distribution on the face.

The values of the flexural stiffness (EI) of the eight faces as defined previously were recorded in table (4.5). The results, as shown, indicate that the flexural stiffness of the faces increases by using mesh - or reinforcement - of large cross-sectional area, but this increment is not proportional to the reinforcement increment. Because the flexural stiffness (as demonstrated) may change according to the mesh width and its position in the face section, expressing its value according to the area of steel used is suspect. It is advisable to determine the flexural stiffness for each face experimentally.

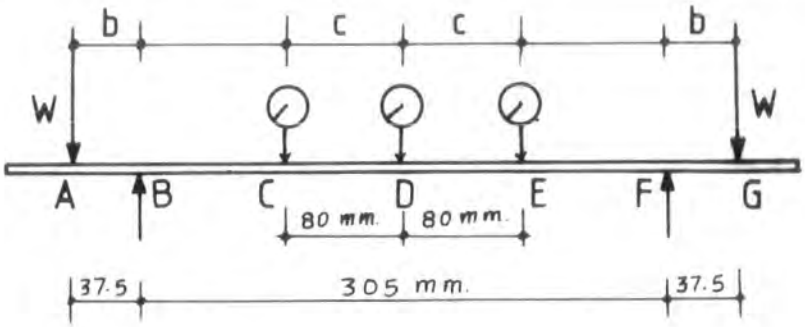

Fig. (4.6a)

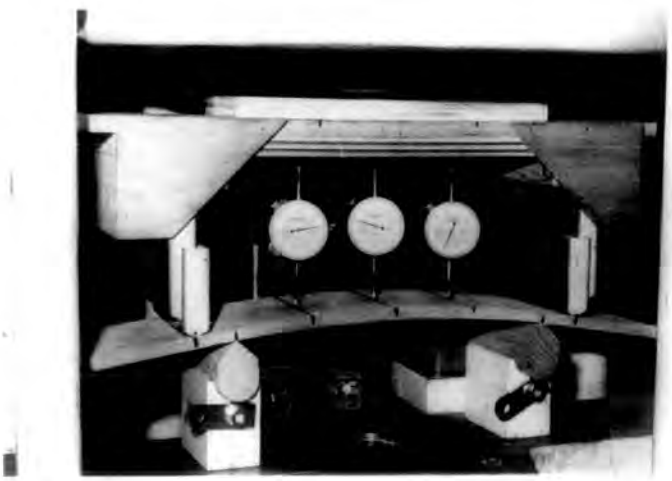

Fig. (4.6b)

Figure (4.6) : Testing for flexural stiffness of faces.

Table (4.5) : Flexural stiffness of faces typical to their symbol

Face designation	Flexural stiffness (EI) x 10^7 N.mm^2.
S_1 & S_4	7.62
S_2, S_3, S_5	8.94
S_6	9.8
S_7	11.1
S_8	11.76

4.5 Steel fibre addition to the face with mesh reinforcement

The form of the reinforcement (mesh) used to reinforce the faces made in this research allows the concrete to act in lateral compression when the face is in tension, i.e. in such a case of reinforcement the concrete in each diamond can be supposed to be under compression force which is due to the mesh deformation, and is perpendicular to the action line of the face. Accordingly, splitting forces are developed on the concrete diamonds parallel to the face length. When this splitting force is increased due to increasing longitudinal tension force and the concrete becomes unable to resist it, the failure will occur. One way to improve the tensile characteristic of the cement-based material (or the concrete) is to add steel fibre to the concrete.

The effects of steel fibre on the concrete tensile characteristic have been widely studied by others. Most of the research work has been done to demonstrate the effects of steel fibre (types and dimension) on concrete crack propagation, width

and tensile strength for beams or elements reinforced by steel bars.(13,14,37) Since there was no previous data from experiments carried out on samples of such reinforcement or geometry as is used in this research, some experimental work has been done in an attempt to improve the face tension modulus and strength with fibre reinforcement. According to the results of other work (13), the length of steel fibre (or in other words the aspect ratio) is the major factor determining the fibre efficiency. Because the shape of steel fibre is also one of these factors, three types were used for the work carried out in this section. The dimensions of steel fibre used are:

(1) Crimped : of 0.32 mm. diameter and 25 mm. length
(2) Straight round : of 0.42 mm. diameter and 32 mm. length
(3) Straight round : of 0.29 mm. diameter and 56 mm. length

The steel fibres were added to the concrete mix before mixing started as percentage of the weight of cement used. The mix proportions used in this procedure were the same as were used for the face manufacture mentioned before. The experimental work done in this procedure was carried out on the face of the highest reinforcement (S_8). The faces were cured and tested by the method mentioned before in the section on the face tension test (4.3.2).

Since the length of all the fibres used is longer than the dimensions of the diamond of the mesh and it was required to be well distributed in the cross-section of the face, the faces were cast in two layers. The first layer was cast before putting the mesh in the mould, and the second layer was poured after the mesh was placed. Casting processing of this kind

was found to be very difficult, especially with the thickness of the face and type of reinforcement of the dimensions being used.

The test results indicated that using the longest fibre (stated No.3) led to the best results. For fibre of weight 2% of the cement the modulus of elasticity of the face in tension increased by about 8 per cent as did the ultimate strength. Using fibre of ratio higher than 2% was found to produce difficulties in mixing. For the faces which were made with 4% and 6% from the crimped fibre, the modulus was found to be only about 5 per cent higher and the ultimate strength increased by only 4%. The improvement of the faces which were made from the fibre No. (2) with 4% and 6% is negligible. However, according to the results obtained, and the difficulty of manufacture, the addition of the steel fibre for such cases (face thickness and dimensions and size of the mesh) is not advisable. For meshes of larger size, the results may be improved. However, the point needs more attention, considering the mesh width, the strand dimensions and the face thickness.

It can be seen from the results of the work carried out in this chapter that the face characteristics in compression are quite different to those in tension. Since the improvement of the face's tension characteristics due to adding fibre is very small and is not enough to be satisfactory rather than the difficulty of manufacture, fibre will not be used in the faces of the beams made in this research. However, the variation of the face modulus in compression and in tension will be considered in the beam analysis and calculations.

CHAPTER FIVE

SANDWICH BEAMS, DIMENSIONS AND CONSTRUCTION

5.1 Introduction

The sandwich beam was defined in chapter 1 and some of its characteristics and advantages were described. The desirable properties of the core and face materials were discussed briefly in Chapter 1, also, and it was explained how difficulties could arise when attempts are made to produce such structures in concrete. Subsequent chapters have reported on the development and the characteristics of materials and composites which may be used for the separate components of the sandwich beam or slab, i.e. for the core and the faces. This chapter describes the assembly of the components into the complete sandwich structure, and proceeds to describe the behaviour and properties of a range of sandwich beams.

All the sandwich beams made and studied in this research were cored by polystyrene concrete mixes conforming to the general specifications and design methods described in chapters 2 and 3. Their faces were reinforced by expanded steel mesh in configurations described in chapter 4.

This part of the research has been planned - as mentioned before - in order to construct, and to demonstrate the properties of such sandwich beams which may be used as load-bearing elements in structures. Because the properties of sandwich beams are affected by the properties of the core and the face materials, several groups of beams were made having different combinations of a range of core and faces. The beams were made to have variation in either the core mix or the face reinforcement

so as to give a suitable variation in modulus and strength. The dimensions and the schedule of the beams made and studied in this procedure are given in the next section of this chapter (5.2).

Due to the wide disparity in the density of the core and face materials, the casting procedure described in section (5.3) has been adhered to strictly so as to produce beams which could be compatible and repeatable.

5.2 Dimensions and schedule of the beams

All the sandwich beams made for study in this research were constructed to have a square cross-section of 120 mm. x 120 mm. and were 1.25 m. long. Each beam was constructed with two faces of the same reinforcement and the same thickness, which was 10 mm. at both top and bottom. Accordingly the rest of the cross-section was the core, which, therefore, had dimensions of 120 mm. width and 100 mm. depth.

The schedule of the sandwich beams investigated in this experimental programme includes 24 sets, each consisting of three beams; i.e. 72 beams were made and tested in all. The three beams of each set were made to have the same faces, core mix, manufacture, curing conditions and testing procedures. The twenty four sets were classified according to the properties of the core mix and the faces used to construct the beams of each set.

Three mixes of polystyrene concrete of different properties were used for making the core. With each of the core mixes, all eight of the face reinforcements were used, described

Table (5.1) : Properties of the polystyrene concrete mixes used for cores of sandwich beams made and studied in this research

Core mix Symbol	Sawdust/ beads in vol.	Cement Con. kg.per cub. metre of agg.	Water/ Cement ratio	Concrete dens. kg/m.^{3}		Cylinder compress-ive str. MN/m.^{2}	Modulus of elasticity GN/m.^{2}	Shear rig-idity GN/m.^{2}	Max shear stress MN/m.^{2}
				Saturated	Dry				
G_1	0.20	410	0.425	700	580	2.60	1.50	0.64	0.78
G_2	0.20	615	0.360	900	760	5.33	2.80	1.19	1.10
G_3	0.20	615	0.325	1050	910	8.33	4.10	1.72	1.52

in chapter 4. These are listed in tables 4.3, 4.4 and 4.5.

The three mixes used to constitute the cores were chosen from the polystyrene concrete mixes of group II made using beads type 2 which were investigated and their test results described in chapter 3. However, the properties of these three mixes are listed in table (5.1). The first mix, as shown in table (5.1), was chosen to be of the lowest density having reliable strength and modulus. The other two mixes were chosen to have modulus of elasticity and shear modulus approximately double and triple the values of the first one.

Rapid hardening Portland cement was used for making all the beams (faces and cores) constructed and studied in this research, thus maintaining the practice of chapters 3 and 4.

5.3 Method of construction

Each of the three beams of one set which have the same faces and the same core were cast together at the same time. Three identical wooden moulds were made to provide beams of the required dimensions. The details of these moulds were given in Appendix (IV.C).

The reinforcing mesh was cut as mentioned before into strips each about 115 mm. wide and 1220 mm. in length (see section 4.2.2 of chapter 4). Steel spacers were made from flat mesh of thickness about 2.4 mm. They were of cramped shape, and were used to fix down the mesh in order to keep it in the mid-thickness of the face as well as possible. They were about 6 mm. wide and were cut to be about 60 mm. in length.

The beams were constructed in the following manner:-

The internal sides of the moulds were greased first with mould oil. Four or five steel spacers were tightened onto the bottom of the three mesh sections of the lower faces by fine wire. The meshes were then placed in the moulds so as to be central across the beam width and length. The mesh was only 3 cm. shorter than the finished beam to ensure that the reinforcement continued over the supports with the same length at each end.

The quantities of cement, sand and water required for the three faces were weighed out. 6 kg. of cement, the same weight sand and 2.1 kg. water gave the required amount and with little to spare. These proportions were determined according to the results of the work carried out before (see section 4.2.1 of chapter 4). The cement and sand were mixed in the dry state first for about one minute. Then the water was added slowly, and the mixing continued for about 3 minutes after the water was added until the mixture became totally homogeneous. A HOBART MODEL AE.200 was used for concrete mixing for the face mixes.

A third of the mixture was spread on the bottom of each mould on the top of the reinforcing mesh and, using a trowel, the paste was distributed through and over the reinforcement. The moulds were then vibrated on a vibration table and during vibration they were held down and the reinforcement mesh was lifted slightly to allow the concrete paste to circulate around the mesh. After about 40 seconds of vibration the mixture was well distributed on the bottom of the mould. A wooden float was constructed to hang exactly 10 mm. above the base of the moulds to check that the lower face was 10 mm.thick.

After this check on the thickness and the removal of the excess concrete, the moulds were vibrated again for a short period (about 10 seconds) to flatten the upper surface of the lower faces. Then the drum of the mixer was cleaned and allowed to dry.

The quantities of polystyrene beads, sawdust and cement for the core of the three beams which had been weighed out during the previous day were placed, in the order stated, in the drum of the mixer; i.e. the cores of the three beams of one set were made together in one batch. An Electric Liner Mixer type 3415 was used. The polystyrene beads alone occupied the same volume as the finished cores of the three beams, and therefore their required weight could be calculated from the bead density in table (2.1) to weigh about 730 gm. Because the batch usually is made to have a greater volume than is required, to ensure that enough remains for casting control specimens, 850 gm. of beads was used. The quantity of sawdust was determined by weight to have a volume of 0.20 of the beads' volume. The amount of sawdust used was in accordance with the conclusions reached in the polystyrene concrete investigation (see section 2.2.2 in chapter 2). The weight of cement changed according to the type of core, as indicated in table (5.1) and chapter 3, section 5. The required water was weighed out just before mixing commenced, and the mixing operation was done in the way described before in section (2.3.1) of chapter 2. The mixing operation started 15 minutes after the bottom faces had been cast.

The cores were cast in three layers, each layer being about a third of the core depth. Three wooden plates each of

dimensions 115 mm. width, 1240 mm. long and 12.5 mm. thick were used to rest on the top of each layer during vibration, weighted to give the required compacting force, which is about 6 kg/cm^2 as determined before (see section 2.3.2, chapter 2 and section 5, chapter 3). Each layer was vibrated for about 25-30 seconds. For the final layer wooden plates were made to enable the finished surface of the core to be exactly 10 mm. down from the top surface of the moulds' sides. A wooden block of T section with a drop of 10 mm. was used for checking. All the wooden plates used were covered or wrapped in polythene sheets to prevent the adhesion of the cement paste to the wood. After the cores had been cast, the moulds were removed from the vibration table and all their top edges were well cleaned and the top surfaces were covered with wet sacks. The casting operation of the core of three beams took about 20-25 minutes.

Three and half hours after casting the core, its top surface was firm to the touch. Then the top layers of reinforcing mesh were placed in the correct position using suitable steel spacers. The materials for the concrete of the upper faces were weighed out, these being exactly the same quantities as were used for the bottom faces. After placing concrete and using a trowel to distribute the cement paste on the mesh, each beam was vibrated individually four times, each period being for about 4-5 seconds. The vibration was necessary in short periods of time to avoid the movement of the beads from the top surface of the core to the upper face, and also so as not to disturb the firmness of the core itself. After vibration a level surface was achieved by using a float.

This method was successful in producing sandwich beams

with faces and core of the thickness as designed. The experience could be considered an important factor in planning future work.

A similar method was used for constructing the compression samples of the faces. However, because the core of these samples was only 40 mm. thick, it was cast in one layer.

5.4 Curing of beams

The concrete mix used for the faces was in a slurry-like state. This was necessary because of the manufacturing process. Because of the relative softness of the material the top surfaces of the beams were not covered by wet sacking until twenty minutes after casting. The moulds were kept in the control room, where the temperature was $22^{\circ}C \pm 1^{\circ}C$. On the following day the moulds were stripped in the morning and the beams were cleaned of mould oil using paper hand towels. Two hours later the beams were put in the curing tank, where the temperature was kept at $20^{\circ}C \pm 1^{\circ}C$. A set of weights was used to keep the floating beams down below the top surface of the tank. All the beams were cured in the tank for 5 days.

5.5 Control specimens

Two types of specimens were used to check the core mix properties. One of these consisted of four cylinders of dimensions 102 x 204 mm., which were made from each batch of the polystyrene concrete mix. Two of the cylinders were tested to determine the compression strength of the mix and the others were used to find the modulus of elasticity. All these cylinders

were cast, cured and tested by the method used and described before. (see sections 2.3.2 and 2.5.1 of chapter 2 and sections 3.2.1 and 3.3.1 of chapter 3). The results of the compressive strength and modulus of elasticity tests recorded from these samples were found to have values in a range between +2 and -7 per cent of the values obtained before for such mixes and recorded in table (5.1). This average reduction is relatively small and may be attributed to the size of the samples tested. The tests on mixes were carried out before in cylinders of 150 x 300 mm., the mixes were considered to have the properties for which they were designed.

The second type of control specimen was used to test the homogeneity of the core after the beams had set. In this test, three cylinders of 2 in. diameter were drilled horizontally from some beams at the top, mid-height and the lower layer of the core. When these cylinders were weighed, they were found to have approximately the same density and the variation was negligible. These cylinders also were tested in compression and there was no evidence of variation in their strength.

CHAPTER SIX

SANDWICH BEAMS TESTING AND ANALYSIS

6.1 Beam's preparation for testing and testing procedure

After the beams had been immersed in the curing tank for 5 days, they were removed from the water early in the morning of the sixth day and left in the control room to dry. Eight hours later the surfaces of the beams (faces and core) were cured-dry, allowing application of the glue (Araldite) for fastening the demec points onto the faces and the sides of core. The need for exactly repeating the procedure of loading and deformation measurements with each beam necessitated careful marking. Thus, all the beams were marked to have the same effective span (points of supports), points of load, demec gauge points and the points of deflection measurements. The points of support were marked so as to be symmetrical around the centre of beam length with 1.14 m. distance between them, i.e. all the beams tested in this programme have effective span 1.14 m. The beams were marked to be loaded at two points which divide the beam span into three equal parts, each 380 mm. as shown in Fig. (6.1a).

Two pairs of demec gauge points were fixed at the top surface of the upper face and the further two at the bottom surface of the lower face of each beam. Each pair was fastened at distance 30 mm. from the edge of the surface and symmetrical around the mid span. On one of each set of three beams five pairs of demec points were fastened to each side of the beam on the top part of the beam symmetrical about the midspan. Three pairs also were fixed at each side in the lower part of the beam.

On the following day the beams were tested at age 7 days, having similar age and curing conditions, and having both cores and faces which had been made and studied before. Tests were carried out on a Denison testing machine model T1B/M.C 200 ton capacity on the flexural frame tester using a system of four point loading figure (6.1c). A steel beam with two steel rollers, each 35 mm. diameter and 120 mm. length (equal the beam width) were used to transfer the machine load to the beam.

After the beam had been placed in the frame of the machine and its roller supports were adjusted to be lined with the points of beam supports as marked, the steel rollers were placed in the correct position. Two thin sheets of metal each 25 mm. width and 120 mm. length were placed under the rollers to spread the load. The steel beam then was put over the rollers in a central position. The steel beam was prepared as shown in figure (6.1c) to provide clear distance between its bottom and the top surface of the beam to allow the Demec strain gauge for reading the upper surface strain measurements.

A dial gauge of $\frac{1}{100}$ mm. divisions was fixed under each point of load touching the bottom surface of the beam at the centre of its width which was marked before. Another two dial gauges were fixed also at the points of support. A special steel frame was constructed to connect with the lower face of the beam for measuring the deflections at midspan by means of two dial gauges which were fixed touching the frame at the two sides of the beam with equal distance from the beam sides fig. (6.1b). This method was necessary for measuring the beam's deflection and the strain on the bottom surface of the lower face at midspan in the same time. It was also of benefit to

show whether the beam twisted during the test procedure.

A load cell of capacity ten thousand pounds, of which the calibration was confirmed from time to time, was used to control and measure the applied load precisely.

The initial readings from the demec points and the dial gauges were taken before the load application. The load was applied on each beam slowly with approximately constant rate of increase, which was controlled by Direct Reading Transducer Meter type C52. At each 200 pounds increment the load was kept constant for about 30 seconds until the readings of the dial gauges became constant. Then their values were recorded and the demec gauge readings also were recorded.

The tension crack load was estimated according to the face used, from the previous test, when its crack strength had been obtained and recorded before (table 4.4). The beam was carefully watched before reaching this estimated crack load and when the first crack was observed the load at that stage was recorded as the cracking load. After the cracks appeared the continuous application proceeded with the same range and rate, with recording of the dial gauge readings and the demec gauge strain readings at each 200 pound load also. Two or four hundred pounds before reaching to the beam's ultimate load, which was calculated both according to the face ultimate strength and the maximum shear strength of the core mix used, the dial gauges were removed and the strain measurements were no longer recorded. The loading then continued slowly until the beams failed. The failure load and the type of failure were recorded. Two beams were tested in the morning and the third one was tested in the afternoon of the same day.

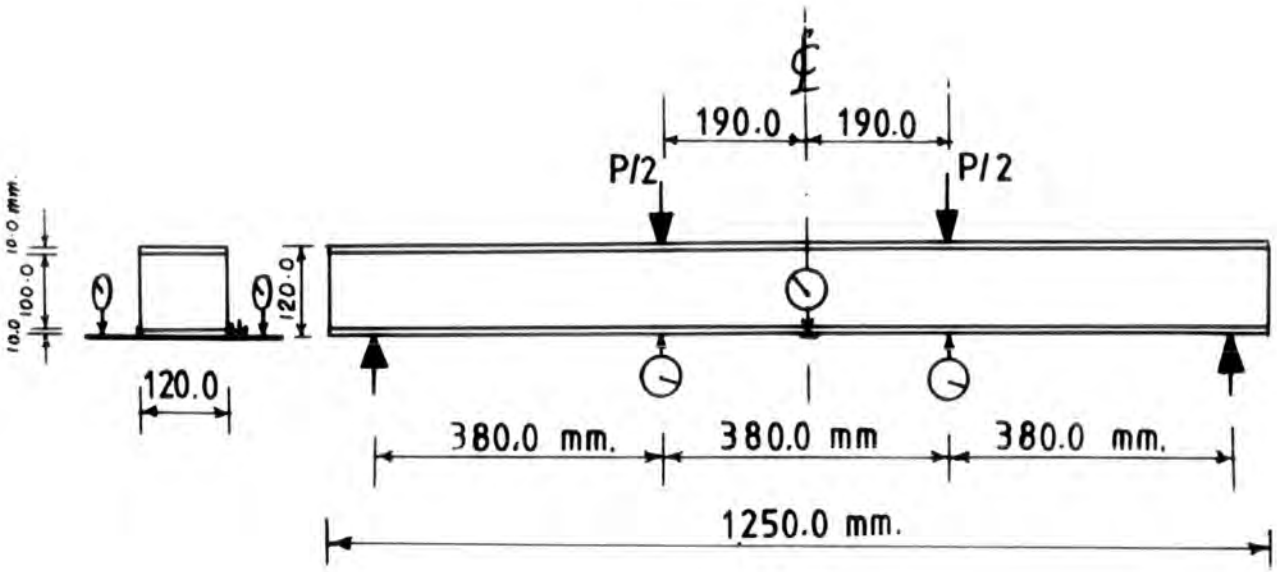

Fig.(6.1a)

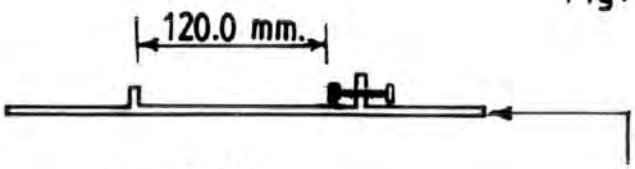

Fig.(6.1b)

steel frame constructed to connect to the bottom face to read dialguage (12 mm.width)

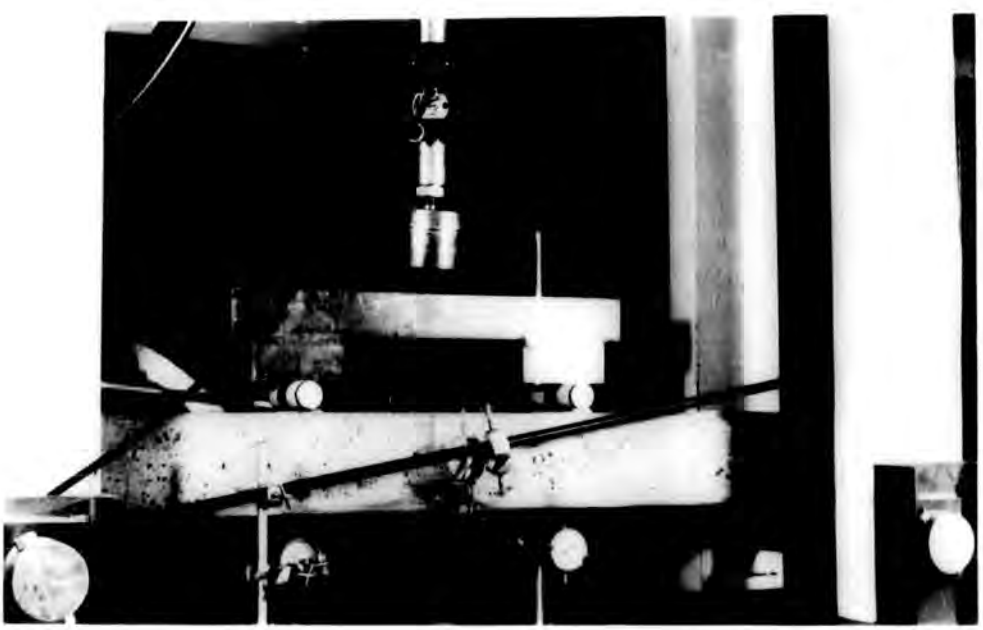

Fig.(6.1c)

Figure (6.1) : Beam arrangement for testing.

6.2 Beams' deflections

In this section, at the different values of the reinforcement used in the faces with each one of the three cores used, the behaviour of the experimental deflection is compared with the theoretical predictions taking into consideration the factor of the variation between the face and core moduli.

The object is to discuss the relationship between the bending stiffness and the shear stiffness of the beams in theory and in practice.

6.2.1 Theory

The deflection of beams is composed of two components; that caused by bending moment and that caused by shear force due to the applied load. Its value is affected both by beam bending stiffness and shear stiffness. Deflection at any point on the beam generally is written as the following expression:-

$$\Delta = \Delta_b + \Delta_s \qquad (6.1)$$

Where:

Δ_b is bending deflection and Δ_s is shear deflection

It could also be written as in this formula:-

$$\Delta = \frac{1}{D_b} \times K_b + \frac{1}{D_s} \times K_s \qquad (6.1')$$

Where:

D_b and D_s are the bending and shear stiffness respectively,

and K_b and K_s are variables which are calculated from the beam bending and shear according to the type of loading and the point at which the deflection is required to be calculated.

The system of loading (symmetrical four points loading) which was used for testing the sandwich beams studied in this research resulted in the central portion of the beam having no shearing force. It follows that the change of slope throughout the midspan section was caused by bending alone while the change of slope between the supports and the loads was the result of bending and shearing together, so that the total deflection over the mid-span section is due to the bending deflection plus the shear deflection of the outer section only. Neglecting the beam's own weight and the weight of the steel beam, considering the total load acting on the beam is equal to P and the distance from the load points to supports is a, from the bending moment the value of K_b is :

At midspan section $K_b = \frac{23}{48} Pa^3$

and At loaded points $K_b = \frac{5}{12} Pa^3$

Since the thickness of the core is 10 times the thickness of the face it is reasonable for the beams to be considered as "sandwich beams with thin faces" (1, 31). This assumes that the core carries no longitudinal normal stress (for simplicity) and accordingly the shear stress in the core is constant throughout the cross-section of the beam, with value :

$$\tau = \frac{Q}{A} \qquad \because \quad Q = \frac{P}{2}$$

$$\therefore \quad \tau = \frac{P}{2A} \qquad (a)$$

The deflection due to shear under the loaded points was determined by considering the strain energy due to shear as:

$$U_s = \frac{1}{2} \frac{\tau^2}{G} \times (\text{volume of beam at shear span}) \qquad (b)$$

Since the strain energy is equal to the work done by the load :

$$\text{i.e.} \quad U_s = \frac{1}{2} \frac{P}{2} \Delta_s$$

$$\therefore \quad \Delta_s = \frac{4 \ U_s}{P} \qquad (c)$$

Substituting U_s from (b) in equation (c) with the value of τ from (a)

$$\therefore \quad \Delta_s = \frac{P a}{2AG}$$

Since AG is equal to the beam shear stiffness (D_s) and A = b x(c + f)for the relative value of these face and core dimensions of these sandwich beams (1, 3, 22, 31)

$\therefore$ for such loading $K_s = \frac{P a}{2}$;

finally the deflection at midspan is

$$\Delta = \frac{23 \ Pa^3}{48 \ D_b} + \frac{P a}{2AG} \qquad (6.2)$$

and at the loaded points

$$\Delta = \frac{5 \ Pa^3}{12 \ D_b} + \frac{P a}{2AG} \qquad (6.3)$$

The method to calculate the bending stiffness D_b is mentioned later at section (6.2.2.2).

6.2.2 Results and discussions

6.2.2.1 Deflection diagrams for midspan

A graph was plotted showing the values of the deflection at midspan against the total load P for the twenty four sets of beams (figs. 6.2 - 6.9). Each value of the deflection in these

diagrams is the average of 6 readings recorded from the six dial gauges connected to each of the groups of three beams tested as mentioned before. Each graph includes three diagrams showing the results for the three core mixes used with each one of the eight faces.

In their deflection, all the beams generally behaved in the same manner. As the graphs indicated, the load-deflection diagram of each set can be classified into two stages in behaviour. The first stage, before the appearance of cracks, shows the beam behaving elastically, and the second stage is after the cracks appeared. It can be seen in all diagrams that the load-deflection relationship is approximately linear throughout the first stage, i.e. the beams behaved elastically. In this stage of loading - as the graphs show - the deflection was found to have a lower rate of increment when a core mix of higher stiffness was used. This trend seems to be attributed to the increasing shear stiffness of the beams, owing to increase in the shear modulus of the core mix. The value of this reduction in deflection is unpredictive. It was found more remarkable in the beams made using faces of low moduli than the beams made with stronger faces.

In this research, according to the shear modulus of the three core mixes used and the beam dimensions, following the simple assumptions mentioned above, the deflections due to shear are supposed to be 5.51, 3.18 and 2.28 per cent of the total deflections for the beams faced by face S_1 (of A_s = 41 mm^2.). For the beams made with the strongest face (i.e. face S_8 of A_s = 118 mm^2.) the bending stiffness was approximately double (see the table at appendix (III.2)), the shear deflections

are = 11.2, 6.4 and 4.45 per cent of the total supposed deflection typical of the three core mixes used. It can be seen that the deflection caused by shear is relatively small compared to that caused by bending, especially for those beams which were cored by the core mixes G_2 and G_3. Consequently the variation produced by changing the core could be supposed to remain small especially when the stronger faces were used. Since all the beams were constructed using faces of steel area and moduli between these two cases and the same core mixes were used, the gaps between the three deflection diagrams could be expected to be similar in all cases, with probably slight increments in favour of the beams of stronger faces.

The deflection diagrams of the beams faced by faces S_6, S_7 and S_8 which are graphed respectively in figures (6.7, 6.8 and 6.9) were found to be close to the expected behaviour. The relation between the three diagrams of the beams made by face S_3 of A_s = 72.5 mm^2. (figure 6.6) can be considered with full reservation for the results of the set cored by the core mix G_3. In figure (6.5) of the sandwich beams made using faces of lower modulus (face S_5 of A_s = 67 mm^2.) the deflection diagram of the beams cored by mix G_2 may be considered to have some possibility of error but within an acceptable range. The results of the beams cored by the stronger core (G_3) are not seen to be following previous expectations since their deflection diagrams were found to be separated by wider gaps. Whenever the reinforcement of the faces was reduced (i.e. their moduli became less) the gaps between the deflection diagrams of the beams increased due to the use of stronger cores, see figures (6.2, 6.3 and 6.4). It follows that it is very doubtful that

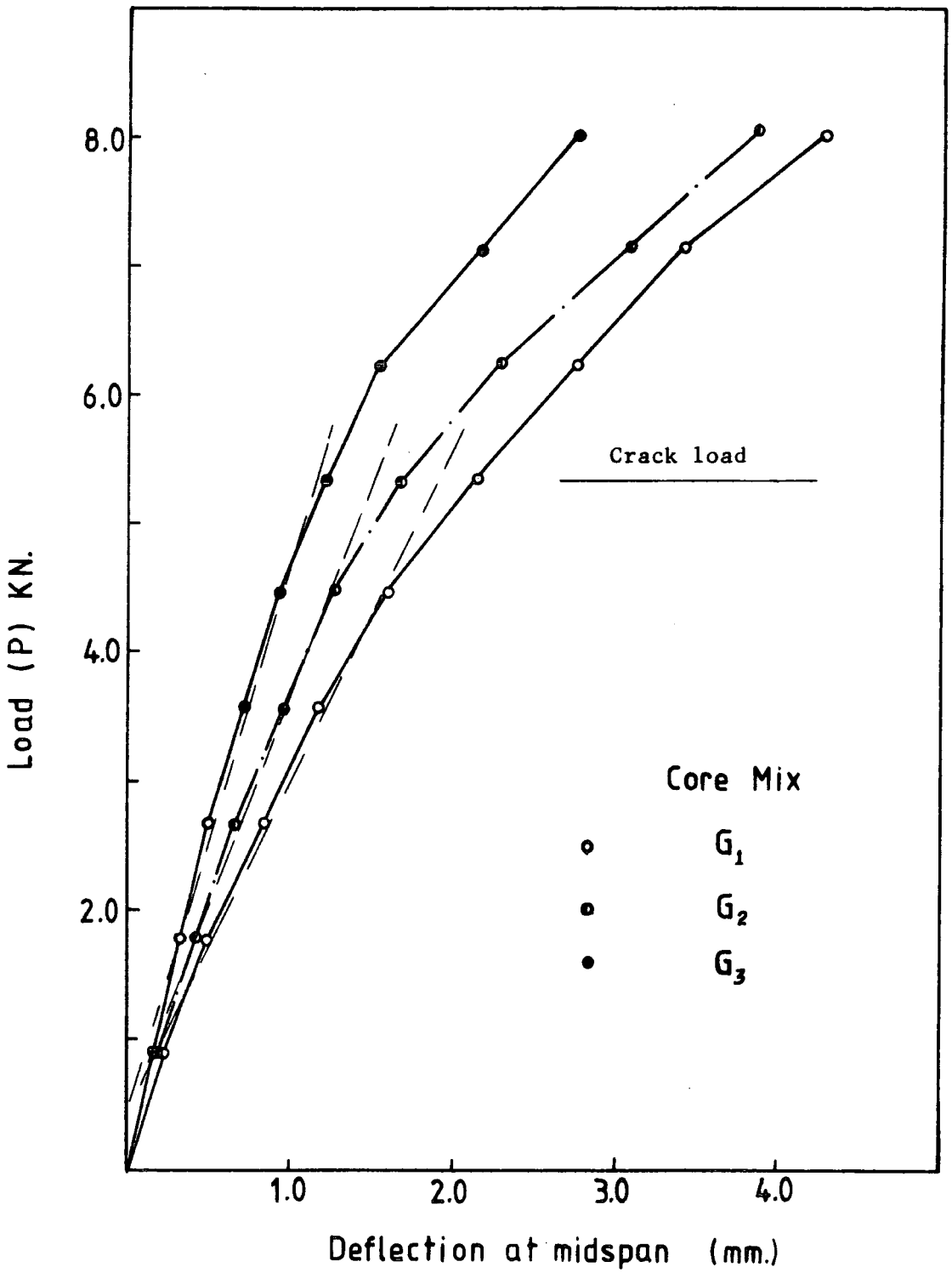

Figure (6.2) Midspan deflection vs. the load P for beams made with face of A_s = 41.0 mm.^{2}

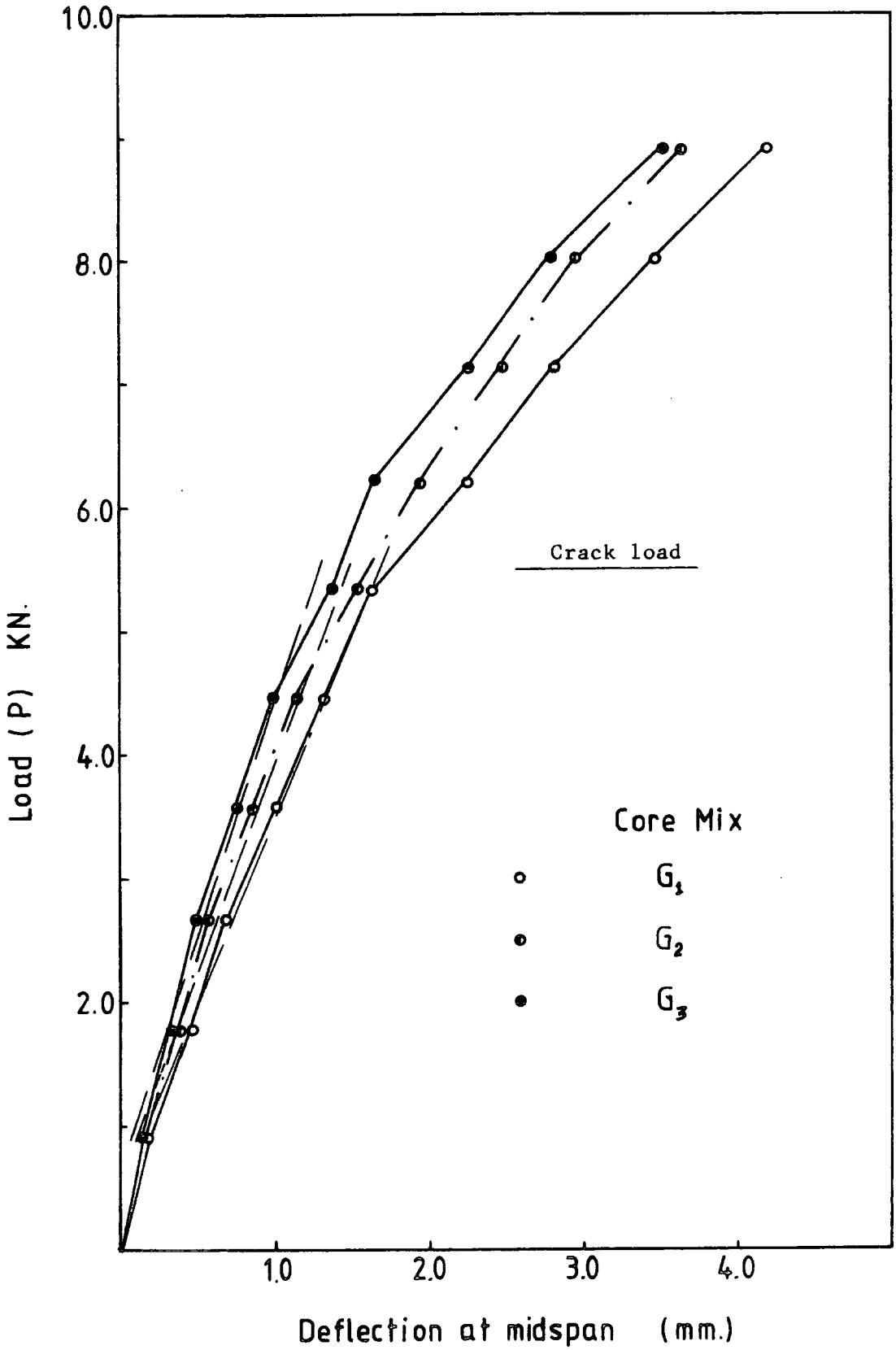

Figure (6.3) Midspan deflection vs. the load P for beams made with face of A_s = 48.3 mm.^{2}

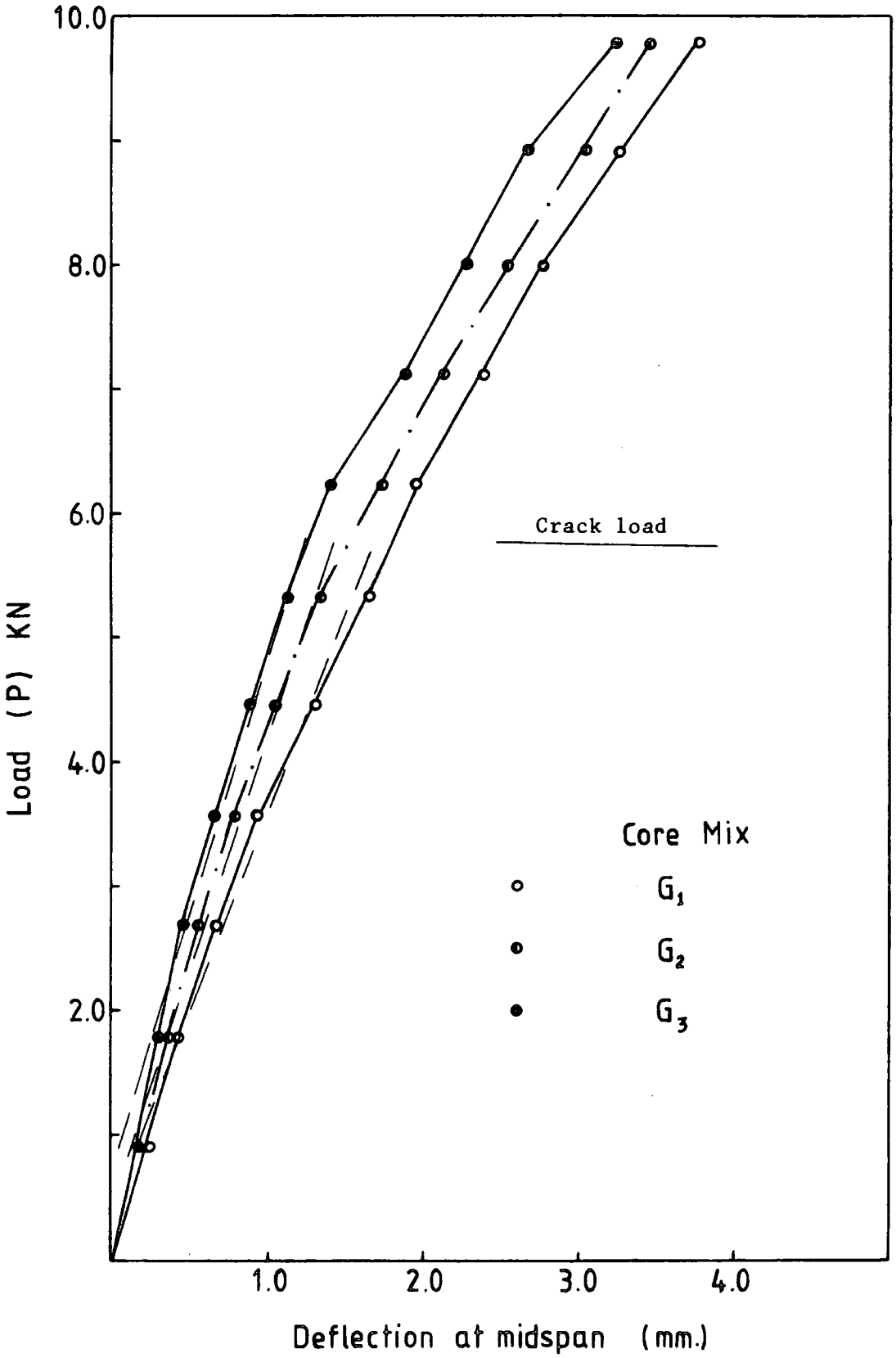

Figure (6.4) Midspan deflection vs. the load P for beams made with face of A_s = 56.0 mm.^{2}

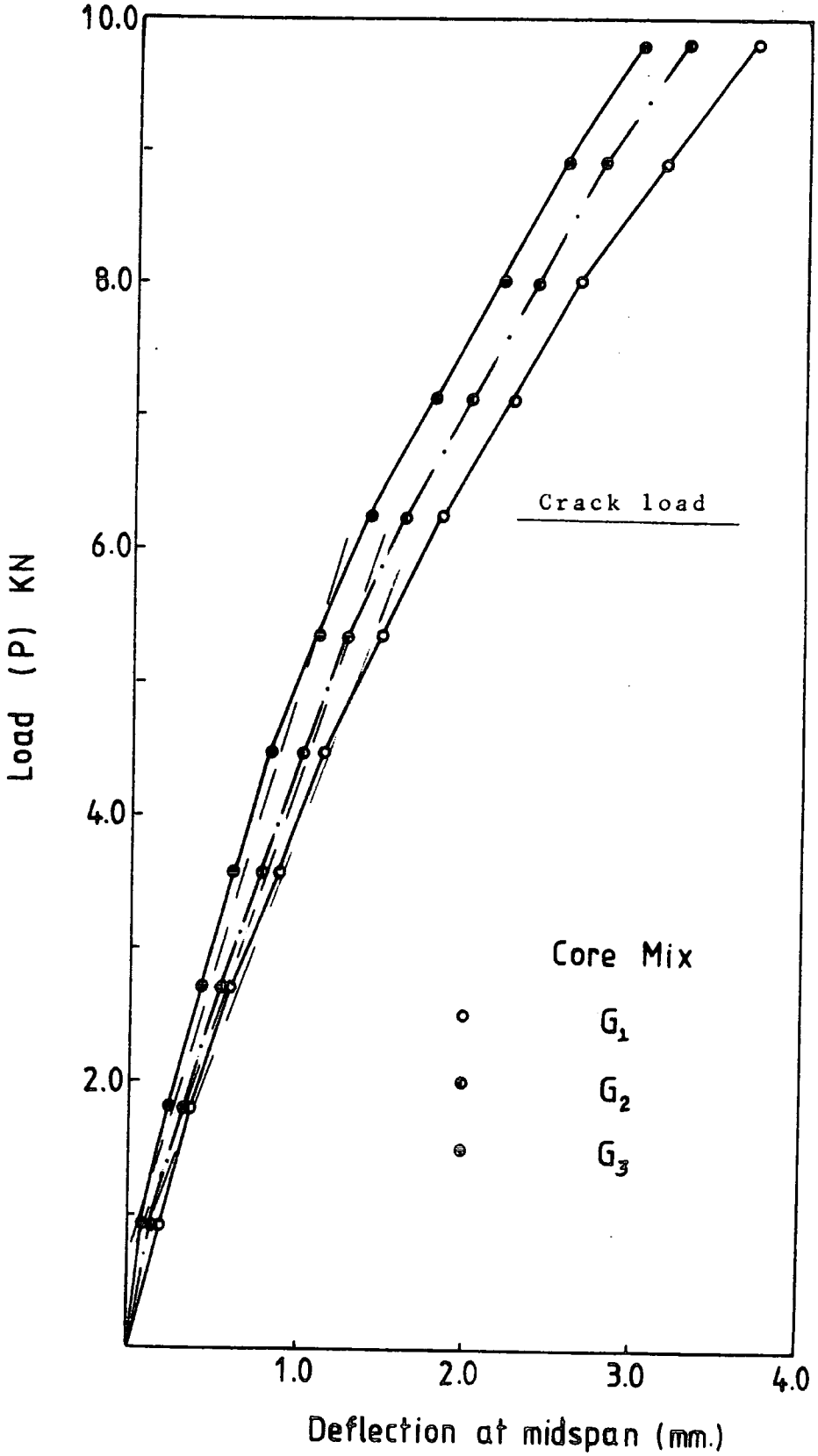

Figure (6.5) Midspan deflection vs. the load P for beams made with face of A_s = 67.0 mm.^{2}

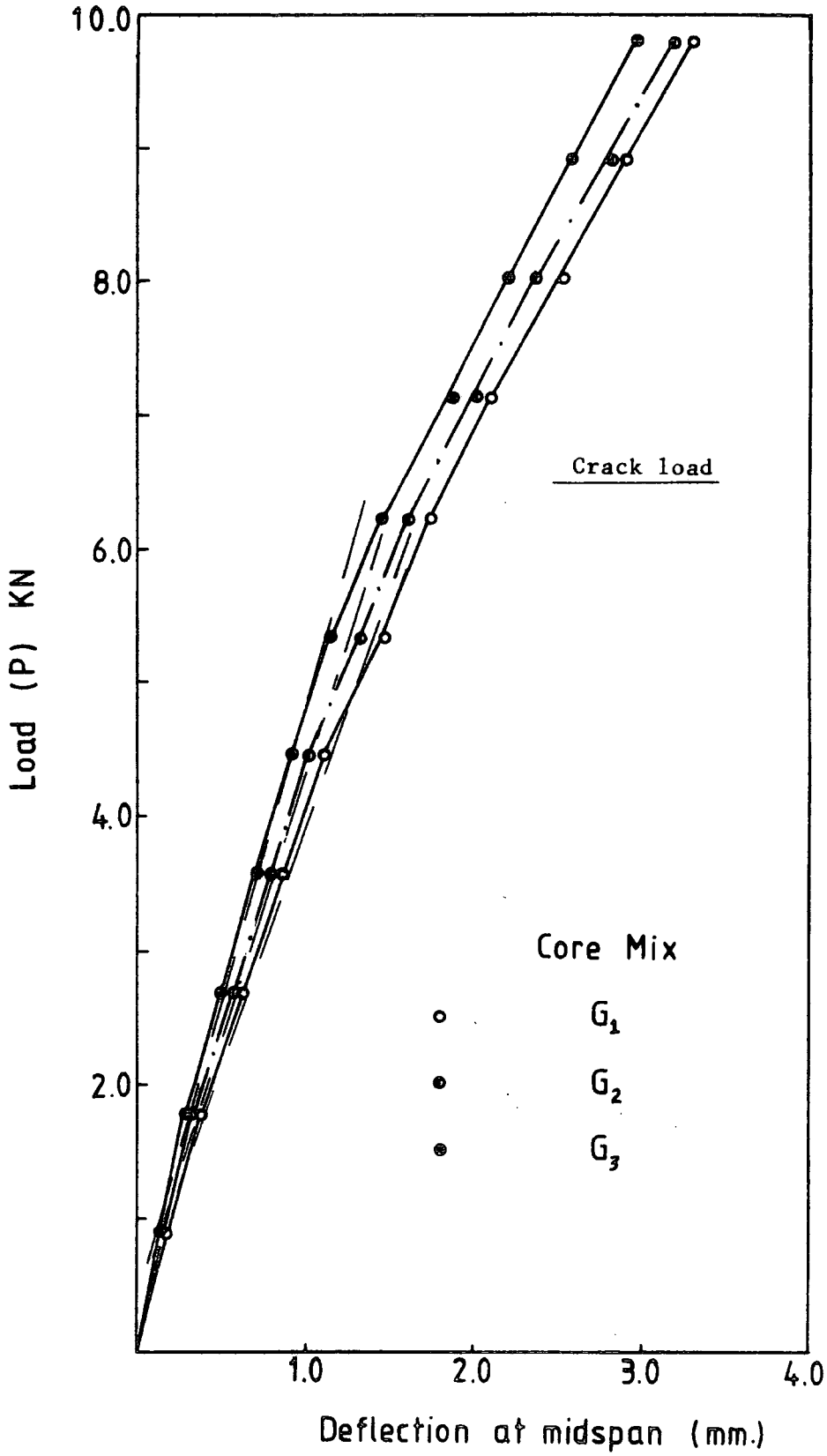

Figure (6.6) Midspan deflection vs. the load P for beams made with face of A_s = 72.5 mm.^{2}

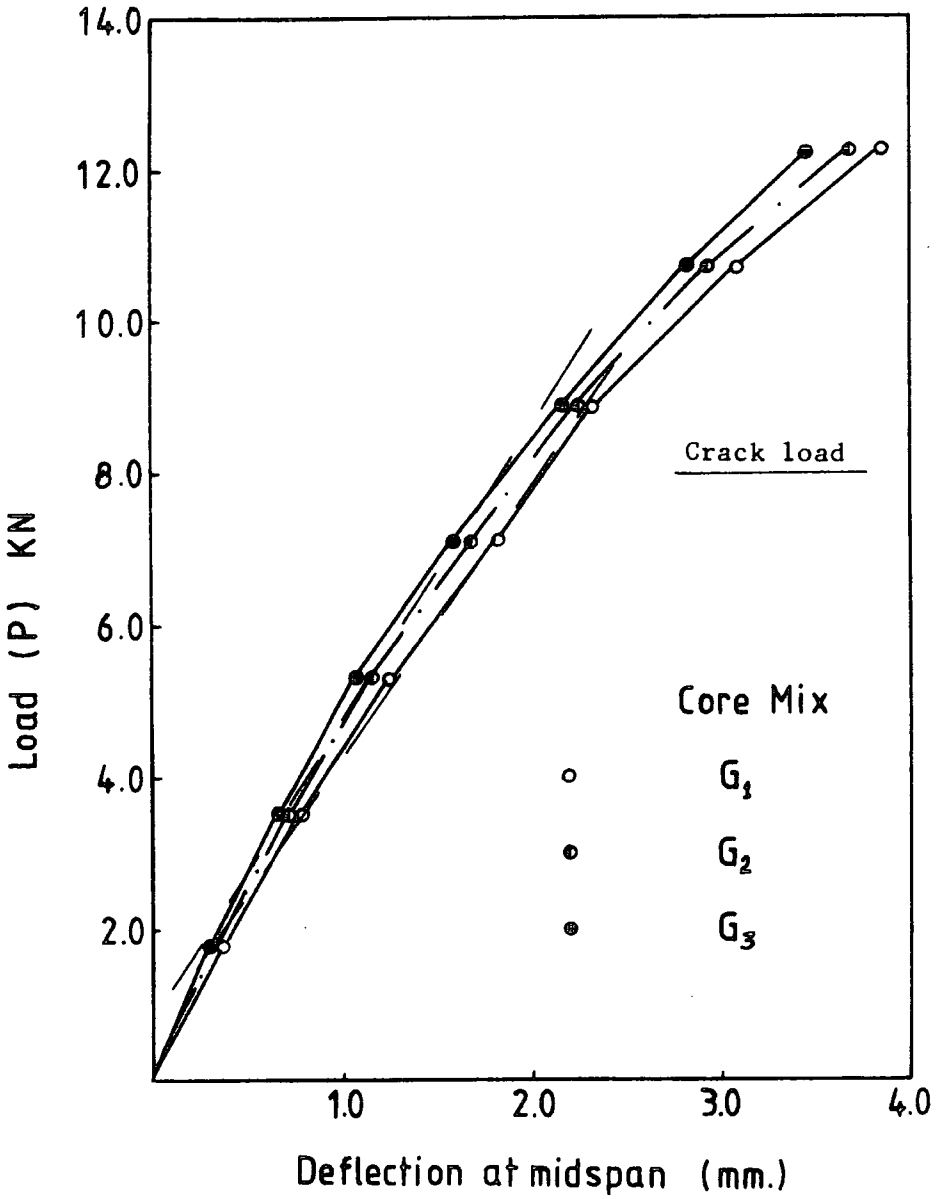

Figure (6.7) Midspan deflection vs. the load P for beams made with face of A_s = 82.6 mm.^{2}

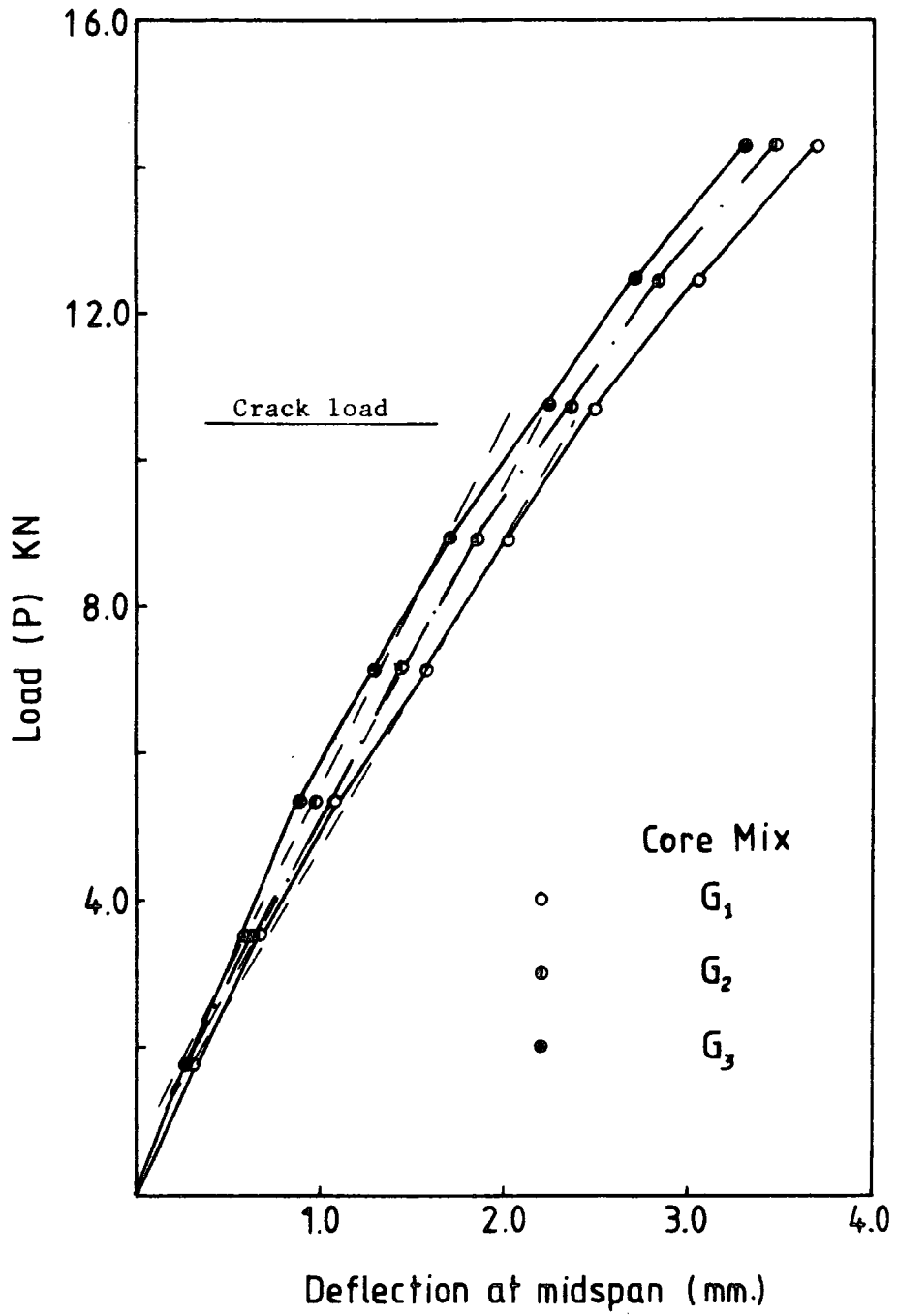

Figure (6.8) Midspan deflection vs. the load P for beams made with face of A_s = 103.3 mm.^{2}

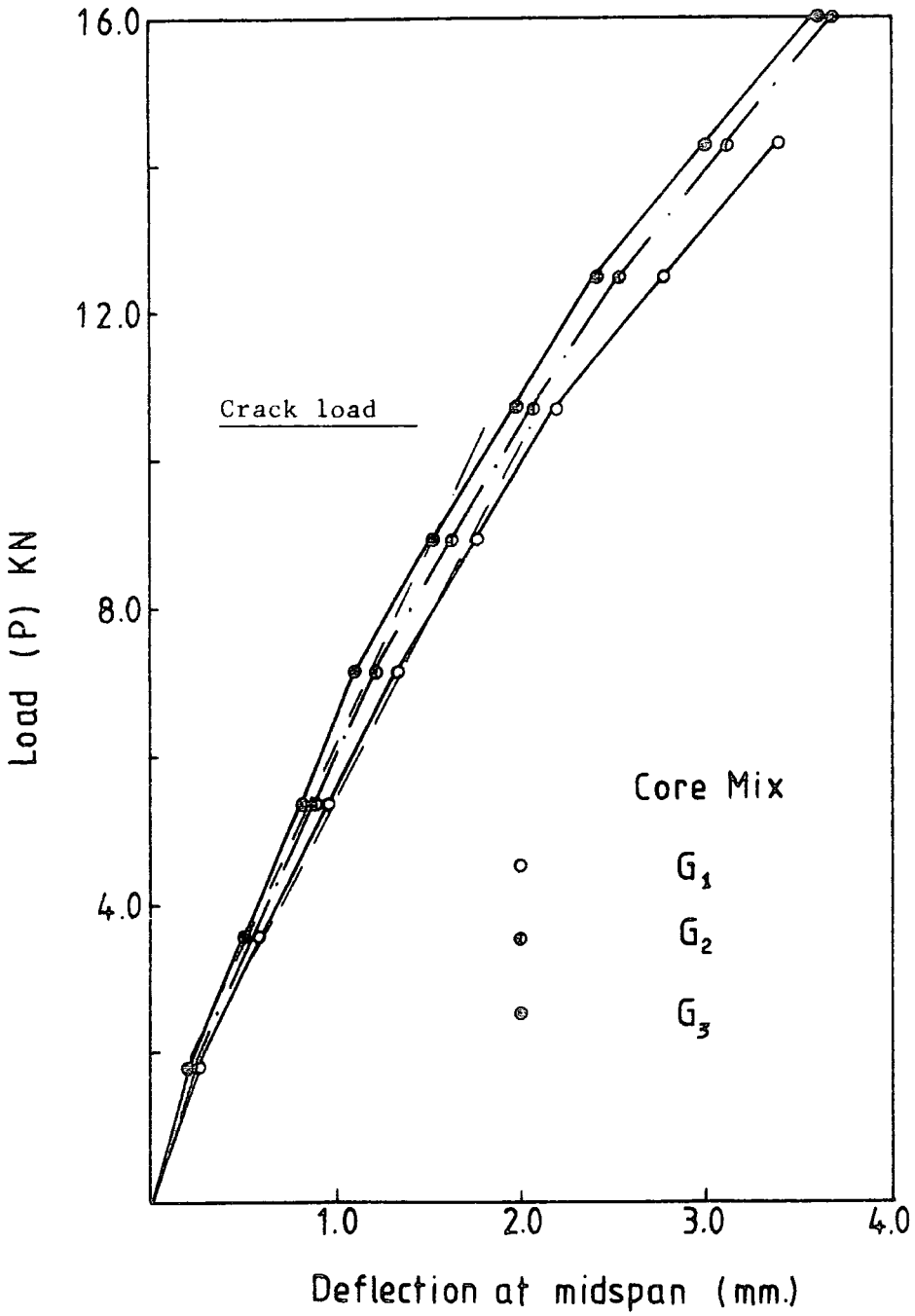

Figure (6.9) Midspan deflection vs. the load P for beams made with face of A_s = 118.0 mm.^{2}

beams with these results may be considered to follow the theory with the simple assumptions mentioned above.

There will be further discussion of the more remarkable phenomena associated with this stage in the deflection of the sandwich beams in section (6.2.2.2).

After the cracks appeared in the lower face, it can be seen in all the graphs that the slope of the graphs of deflection versus the load increased at a higher rate. In this stage of loading, in most cases the three diagrams seem nearly parallel, i.e. the deflection increased approximately at the same rate in the three cases of core.

6.2.2.2 Deflection per unit load

The discussion of beam deflections in the previous section (section 6.2.2.1) was based upon a study of the attitude of the deflection diagrams, and their relationship to each other. It was found - as mentioned before - that the experimental deflection of some beams is not predictable by the theory as described in section (6.2.1). Since the analysis is more reliable in the elastic stage, i.e. where the faces and the core behaved elastically, the discussion in this section deals with the beam's deflection during this stage of loading.

Figures (6.10, 6.11 and 6.12) were graphed to show the deflections of the beams in the elastic stage per unit load experimentally and theoretically corresponding to the three mixes used for cores. The experimental values were taken equal to the inclinations of the straight lines which were plotted expressing the average slope of the load-deflection diagrams [the dotted lines in figures (6.2 - 6.9)]. Because the faces have unequal

moduli in compression and tension (see table 4.4 in chapter 4), in calculating the theoretical deflection one needed to know the position of the neutral axis on the beams' cross sections to determine the bending stiffness of the beams. From the strain measurements recorded during the beam's testing, the position of the N.A. can be determined and its position relative to the top surface of each beam was listed in the table in appendix (III.1). It was found to move towards the top side of the cross-section, as expected due to increase in the modulus of the face in compression compared with its modulus in tension. The bending stiffness of the beam, according to the simple condition mentioned in (6.2.1) is determined by the following expression -

$$D_b = D + 2D_F \qquad (6.4)$$

Where:

D_F is the bending stiffness of the face about its N.A = $(EI)_F$

D is the 2nd moment of the faces about N.A of the beam due to their virtual area.

$$= A_F \; E_{Fc} \; (d_c)^2 + A_F \; E_{Ft} \; (d_t)^2 \qquad (6.5)$$

d_c and d_t are the distances from N.A of the beam to the centre of the upper and lower faces respectively.

Because the value of D_F is very small relative to the value of D (D_F is about 0.1% of D) it is neglected and the bending stiffness D_b of the beam was taken as equal to D. The values of D_b of all beams were calculated and listed in the table in appendix (III. 2) according to the position of the N.A and the compression and tension moduli of the faces as determined before in chapter 4. The bending stiffness of the beams due to the

compression zone of the core (D_c) were calculated also and listed in the same table, where

$$D_c = \frac{b(d_c - f/2)^3}{3} E_c$$

The theoretical values of the deflections were calculated at the midspan of the beams using equation (6.2) with regard to the data provided for bending stiffness due to the face used and the shear modulus of the core mix used. The relationship between the theoretical and experimental deflection can be seen in figures (6.10, 6.11 and 6.12) typical of the three core mixes used and the area of reinforcement (A_s) in each face.

Figure (6.10) shows the theoretical and the experimental deflection diagrams per unit load of all the beams which were cored by the core mix G_1, in $\frac{mm}{N}$. It can be seen that the two diagrams intersect at the point where $A_s = 66\ mm^2$; the experimental deflections are of higher values for the beams of faces of A_s greater than 66 mm^2. and become lower when A_s is less. The graph indicates that there is no remarkable deviation between the two diagrams when the area of steel increased. The variations between the two diagrams grow only when the faces of lower A_s are used. Generally, the two diagrams of this group could be considered conformable with each other with probability of error in an acceptable range, which increases with the faces of lower reinforcement.

In figure (6.11) of the beams made using a core of higher modulus (mix G_2), the intersection point of the two diagrams was found to be at a higher value of A_s. The variation between the two deflection diagrams is observed to be most remarkable for the beams of faces having reinforcement less than 67 mm^2.

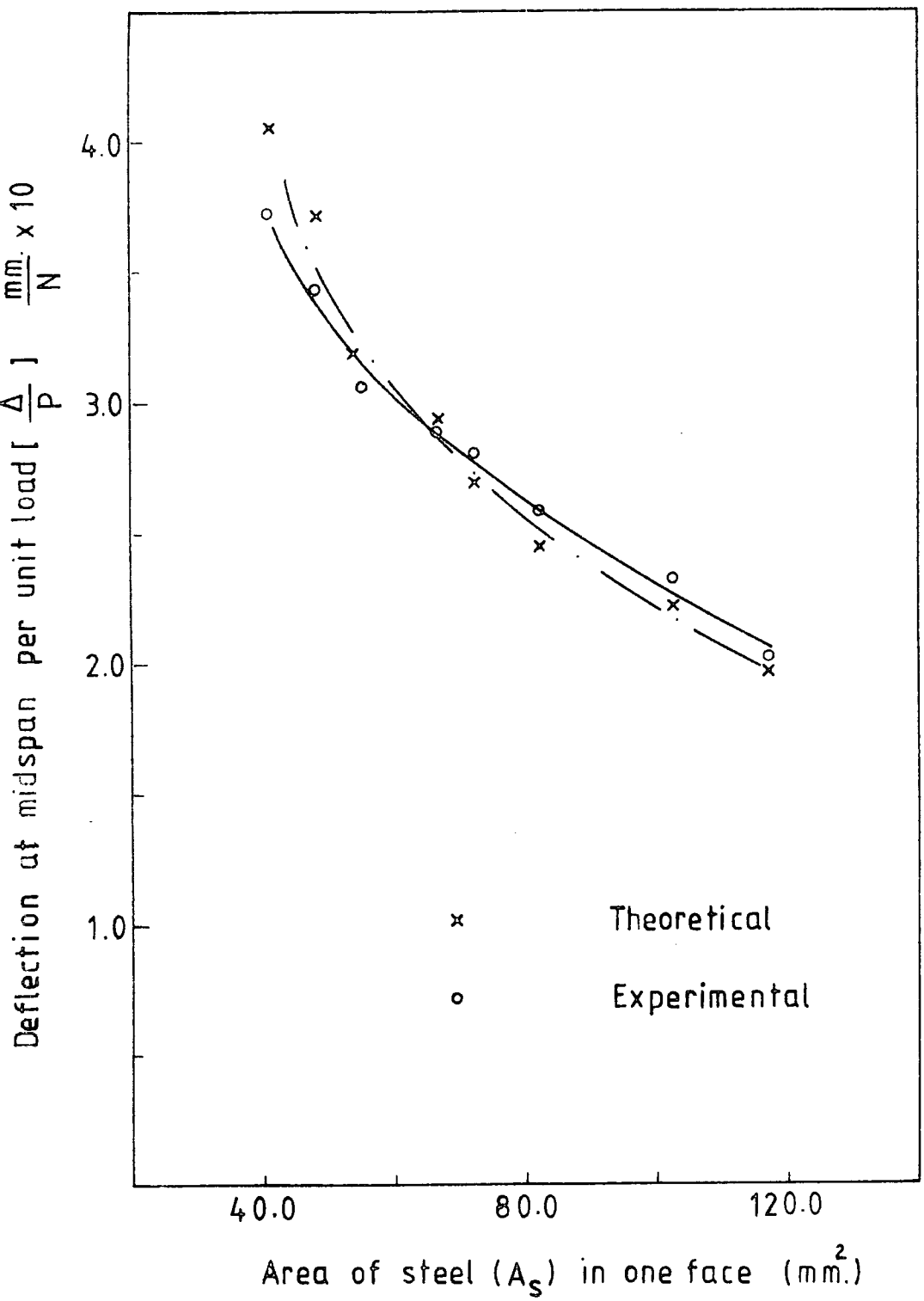

Figure (6.10) Theoretical and experimental deflection per unit load at midspan versus the area of reinforcement (A_s) in each face for beams made using core mix G_1.

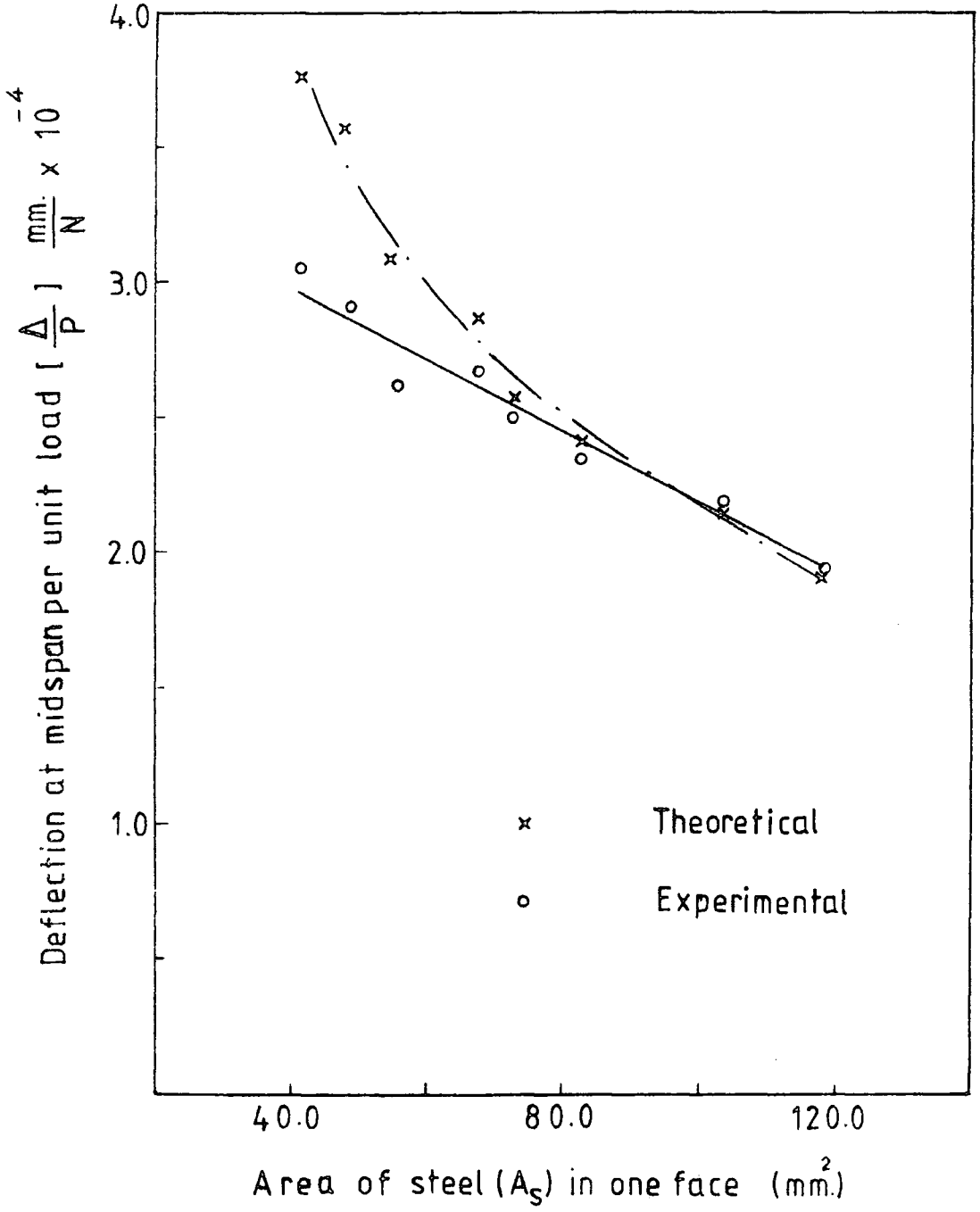

Figure (6.11) Theoretical and experimental deflection per unit load at midspan versus the area of reinforcement (A_s) in each face for beams made using core mix G_2.

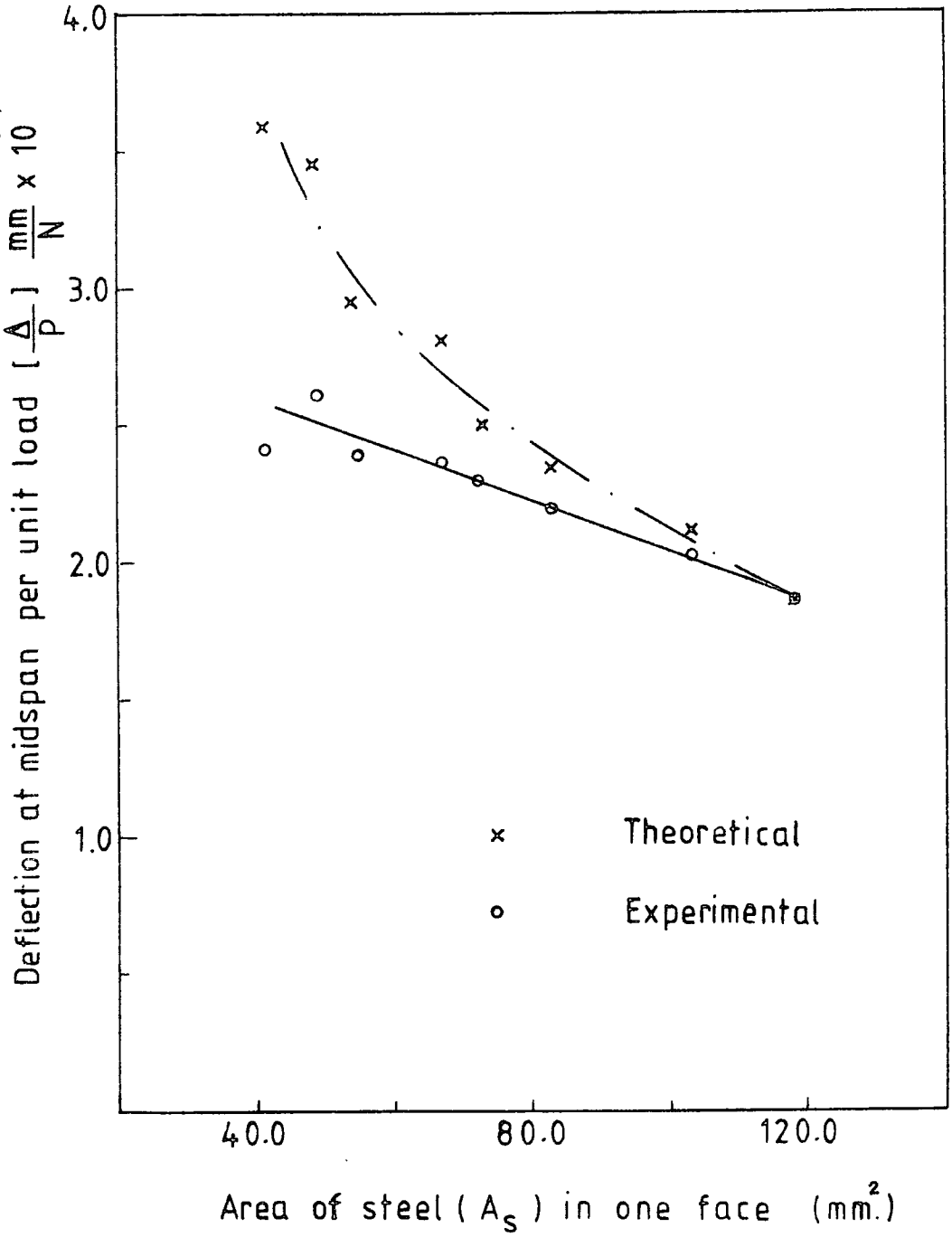

Figure (6.12) Theoretical and experimental deflection per unit load at midspan versus the area of reinforcement (A_s) in each face for beams made using core mix G_3.

When the beams using the strongest core (G_3) are examined, the closing point of the two diagrams was found moving up to A_s = 118 mm^2. and the variation between them became greater, as shown in figure (6.12). In the results of this group it can be seen that all the experimental diagram is below the theoretical one and the deviation between them is reduced with increasing cross-sectional area of reinforcement. In these three graphs the reduction of the theoretical deflection diagrams due to the increase of the area of reinforcement seems non-linear. There is some difficulty in explaining these results because the reduction in the theoretical deflection must be linear with the increase of the bending stiffness.

Table (6.1) shows the values of the experimental and theoretical deflection per unit load and the error between the experimental and theoretical values as a per cent of the theoretical value for each of the twenty four sets of beams. From table (6.1) and figures (6.10, 6.11 and 6.12) it can be seen that using a core mix of higher stiffness needed the bending stiffness of the beam to increase in order to achieve experimental results conformable to the theory. It is evident that over part of the range of the relationship between the beam's bending stiffness and shear stiffness the behaviour of the experimental deflection of the beam (in the elastic stage) can be predicted by the theory in its simple form (considering the core has no normal stress). Several attempts had been made to find out a suitable expression for the limits of that relationship. The ratio between D_b and D_s, including the tension modulus of the face [(D_b/D_s) E_{Ft}] was found a convenient possible formula for this expression. It seemed particularly appropriate to include the modulus of elasticity of the face in tension (E_{Ft}) in the expression. It is

affected by the percentage of reinforcement more than the compression modulus and can be seen to vary considerably in consequence. Clearly it affects the position of the neutral axis and has much to do with the evaluation of the crack load, which determines the limit of the elastic stage of deformation. The values of $[(D_b/D_s)\ E_{Ft}]$, which is referred to by the symbol μ, were listed in table (6.2) for all the twenty four sets of beams according to the area of reinforcement in the face and the core mix used. Because the bending stiffness is affected by the depth of the core as well as the area of steel in the face A_s and the shear stiffness also is affected by the area of the core in addition to the shear modulus of the mix, the values of the ratio between A_s and the area of the core A_c, which is referred to by the symbol η , are calculated and listed also in table (6.2).

From tables (6.1) and (6.2) it can be observed that the variations between the experimental and theoretical deflections were reduced due to increasing μ value. It can be seen also that the error approximately disappeared when μ had a value of about 90 in all the core mixes used. It became negative for the beams of μ lower than 90 and positive for the beams of the higher values. With reference to the three figures (6.10, 6.11 and 6.12) it can be seen that the intersection points of the experimental and theoretical diagrams are at values of A_s giving μ a value of about 90. This method of analysis indicated also that the beams having μ of values less than 42 are accompanied by an error in values of more than 10 per cent. It can be seen, also, that whatever the increase in the value of μ the probable error will remain less than 5 per cent [see the results of the group made by core G_1 in tables (6.1 and 6.2)].

Table (6.1) : Beam deflections at midspan per unit load $(\frac{\Delta}{P})$ $\frac{mm.}{N} \times 10^{-4}$ experimentally and theoretically and the difference between them as a percent of the theoretical values

Area of rft. (A_s) in one face (mm^2.)	Core mix G_1			Core mix G_2			Core Mix G_3		
	Deflection Δ (mm.)		Error %	Deflection Δ (mm.)		Error %	Deflection Δ (mm.)		Error %
	Experimental	Calculated		Experimental	Calculated		Experimental	Calculated	
41.0	3.70	4.05	-8.6	3.03	3.79	-(20.0)	2.41	3.59	-(32.3)
48.3	3.43	3.72	-7.8	2.90	3.57	-(19.0)	2.60	3.45	-(25.0)
56.0	3.07	3.24	-5.1	2.65	3.12	-(15.0)	2.39	3.07	-(22.0)
67.0	2.90	2.95	-1.7	2.67	2.85	-6.4	2.33	2.80	-(16.9)
72.5	2.82	2.69	+4.6	2.50	2.56	-2.3	2.29	2.50	-8.4
82.6	2.60	2.51	+4.0	2.38	2.46	-3.0	2.18	2.38	-8.0
103.3	2.33	2.24	+4.0	2.19	2.14	+2.3	2.01	2.10	-4.3
118.0	2.04	1.98	+3.0	1.93	1.88	+2.6	1.85	1.85	-

Table (6.2) : The values of the possible expression of the bending/shear stiffness including the tension modulus of the face according to the core mix and area of reinforcement (A_s) used

Area of rft. (A_s) in one face ($mm.^2$)	$\eta = A_{st}/A_c$ per cent	Values of $\lvert (D_b/D_s) \times E_{ft} \rvert \times 10^6 = (\mu)$		
		Core mix G_1	Core mix G_2	Core mix G_3
41.0	0.34	42.3	(24.0)	(17.4)
48.3	0.40	52.5	(28.0)	(20.0)
56.0	0.47	73.0	(39.5)	(27.5)
67.0	0.56	90.0	48.0	(34.0)
72.5	0.60	111.0	61.0	43.0
82.6	0.69	124.0	67.4	47.4
103.3	0.86	177.0	95.0	65.0
118.0	0.98	238.0	128.0	89.0

When the core is considered to take a direct normal stress the beam's bending stiffness is increased and there follows a reduction in the theoretical value of deflection. Consequently the variation between the theoretical and experimental deflection is seen to be reduced. The bending stiffness of the core may be considered in one of the two following methods:

(1) Considering the compression zone of the core only.

(2) Considering the compression and tension zone together.

The increase of the beam's bending stiffness due to the first method is relatively small (see the table in appendix III.2) and consequently the reduction in the theoretical deflection is also small. Indeed the change in the results of analysis with this method is too small to improve any of the suspected or the refused cases.

In the second method, the effect of the core on the beam's bending stiffness will be considered as described later in section (6.3.2) (where the bending moment carried by the core is determined) see table in appendix (III.3). However, in following this method for deflection analysis, the results of two refused sets only are improved where the error between the theoretical and experimental values becomes less than 10 per cent (beam of A_s = 56 mm^2. at group 2 and beam of A_s = 67 mm^2. group 3).

It can be seen from the results and discussion carried out in this section, that the ability of concrete sandwich beams of this type to have a deflection behaviour predictable by the theory depends on the relationship between the faces moduli and the core moduli. For results to be satisfactory in any of the methods of analysis suggested above, using the expression relating the bending and shear stiffness (μ), the value of μ is recommended

to be more than 50.

Because the deflection measurements under the loaded points were found to have values not noticeably different from the values of deflection at midspan, they were not used in discussion in this chapter. The justification for this will be shown clearly later in chapter 7.

6.3 Faces' strains

6.3.1 Theory

With the type of loading used (four point load) and the assumption of neglecting the beam self-weight, the central portion of the beam will be considered to carry constant bending moment M. With the simplified condition (mentioned before) of assuming the core takes no direct stress due to bending, the total bending moment M is resisted by a couple of normal forces N, equal in magnitude, acting on the centre of the faces, and two local bending moments in the upper and lower faces, as shown in figure (6.13a). These forces can be expressed by the following equation:

$$M = N(C + f) + M_{Fu} + M_{Fl} \qquad (6.6)$$

The local bending moment of the lower face will be in the same direction as the beam bending, i.e. a sagging bending moment. The upper face is likely to have a bending moment in the same direction as the lower face under the load but may have hogging bending moment on either side of the load due to compression of the core directly under the loaded points. This possibility is illustrated in figure (6.13c).

Assuming the normal force N is distributed uniformly over

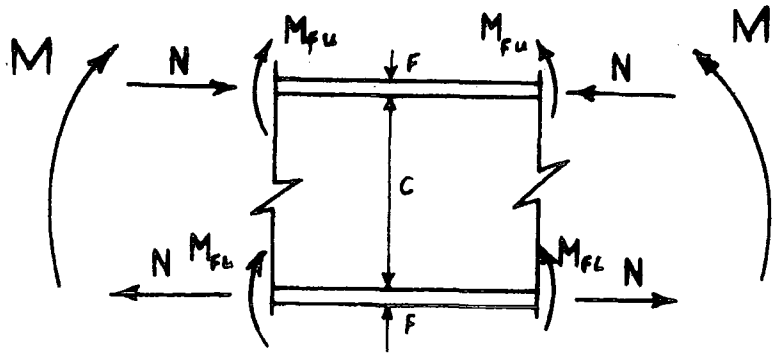

Figure (6.13a) Forces and moments acting on an element at midspan of sandwich beam.

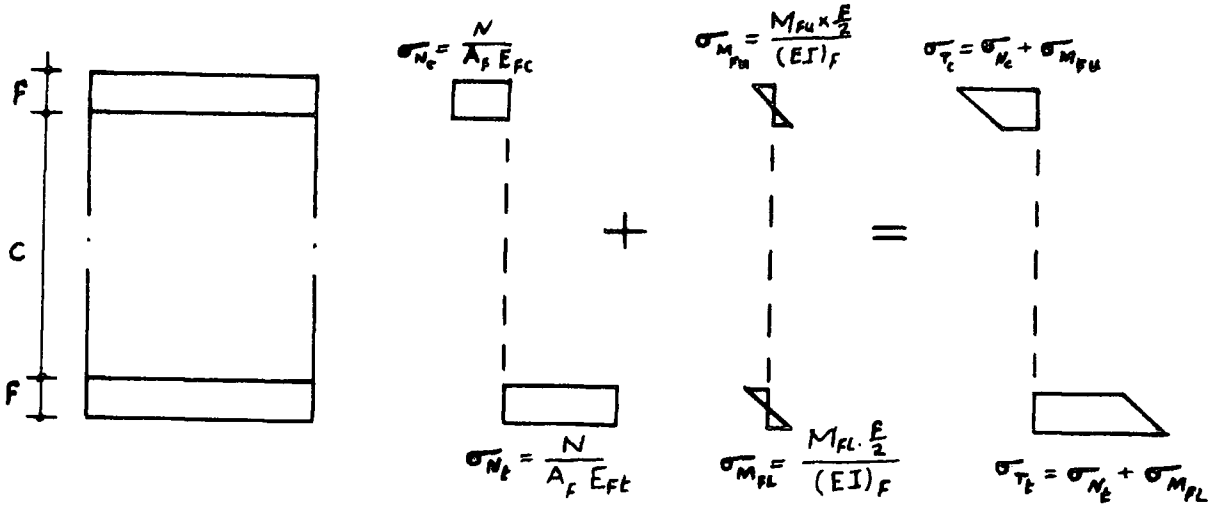

Figure (6.13b) Stress distribution on the faces due to the normal force and local moments.

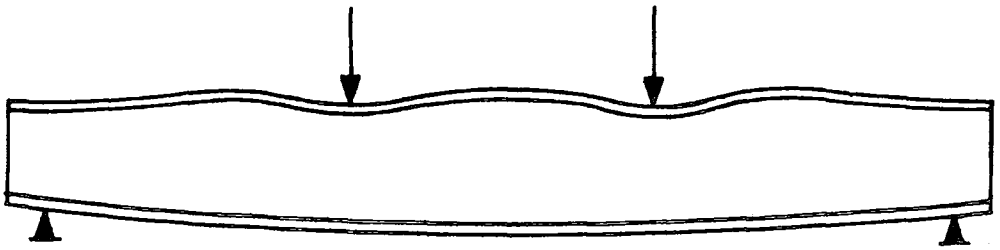

Figure (6.13c) Shows the possible hogging moment which may happen to the upper face due to core compression under the load points.

the cross-section of the face, the distribution of the normal stresses on the upper and lower faces is likely to be caused by the normal forces N and the local bending moment ds shown in figure (6.13b). Accordingly the maximum stresses are on the top of the upper face and the bottom of the lower face, and are:-

$$\overline{\sigma_T} = \overline{\sigma_N} + \overline{\sigma_{M_F}} \qquad (6.7)$$

Consequently, in the elastic stage the strain at the top and the bottom of the upper and lower faces respectively is :

$$\left.\begin{aligned} \xi_T &= \xi_N + \xi_{M_F} \\ \text{or} \quad \xi_T &= \frac{N}{A_F E_F} + \frac{M_F . f}{2D_F} \end{aligned}\right\} \qquad (6.8)$$

i.e. the face strain is dependent on the normal and bending stiffness of the face as well as the normal force and local bending. The relationship between the magnitude of the two values will not be the same for the two faces due to the variation in the modulus of elasticity of the faces in tension and in compression.

The values of the local bending moments are of particular importance in a sandwich beam with a very flexible core, since sudden changes of shear force cause sharp changes in the slope of the beam, resulting in local areas of acute bending in both the faces. However, when the shear deflection accounts for only a small proportion of the total deflection, as in these cases, the problem is not so troublesome.

6.3.2 Results and discussions

The total strains (ξ_T) measured on the surfaces of the faces as described before in section (6.1) were plotted against the total acting load (P) for the twenty four sets of beams tested, in figures (6.14 - 6.21). Figures (a) show the strains on the top of the upper faces and figures (b) show strains on the bottom surfaces of the lower faces. Each figure was drawn - as shown - to include the results of the beams cored by the three different core mixes used with each one of the eight faces, i.e. in the same way that the deflections were displayed.

All the strains measured on the top of all upper faces were compressive and were found to be tensile on the bottom surfaces of the lower faces. The curves of the upper faces' strains approximate well to straight lines in most cases, while the strain curves of the lower faces show a distinct change of gradient after 'cracking load'. The change of slope in the strain curves of the upper faces is observed to accompany the beams made using faces of lower reinforcement area.

It can be seen from each figure that the lower faces strain is approximately twice the upper faces strain. The lower faces' strain is more affected by changing the core mix used than is the upper faces' strain and that is most noticeable whenever the cross-sectional area of the reinforcement in the face was low, i.e. the beams made by faces of lower moduli. However, in all cases, as the graphs show, the load-strain relationship is approximately linear in the stage of loading before crack appearance, i.e. the beams behaved elastically in this stage, as considered before in the deflection analysis.

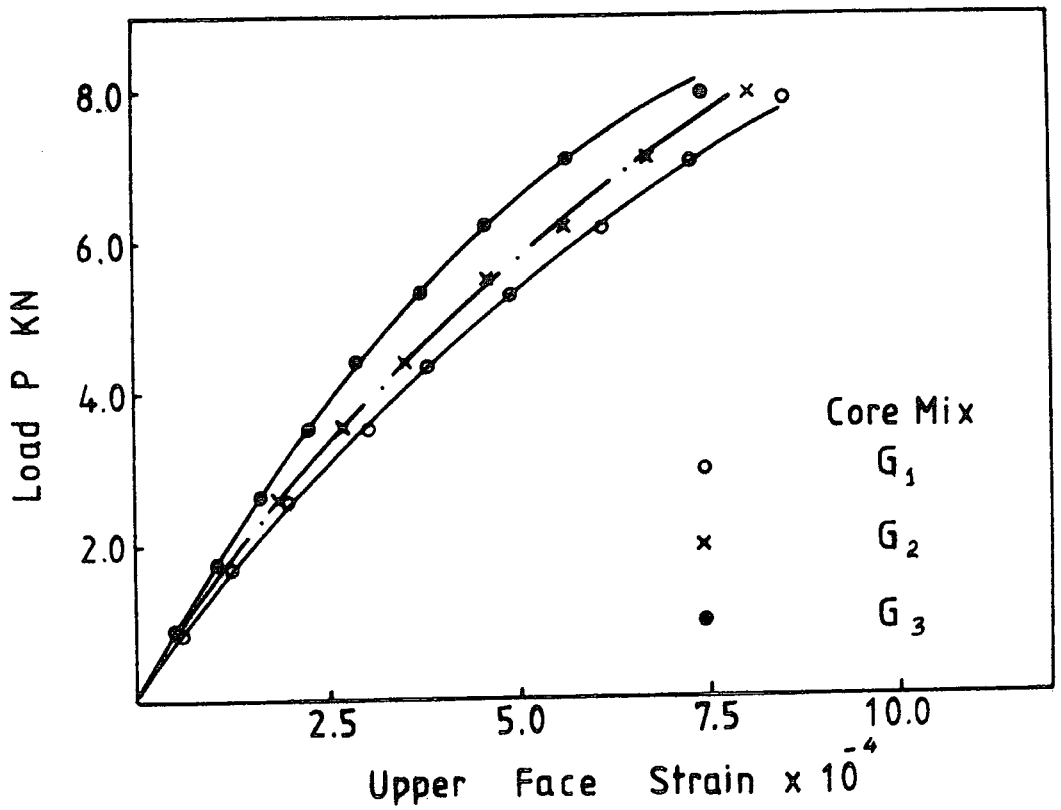

Fig. (6.14a)

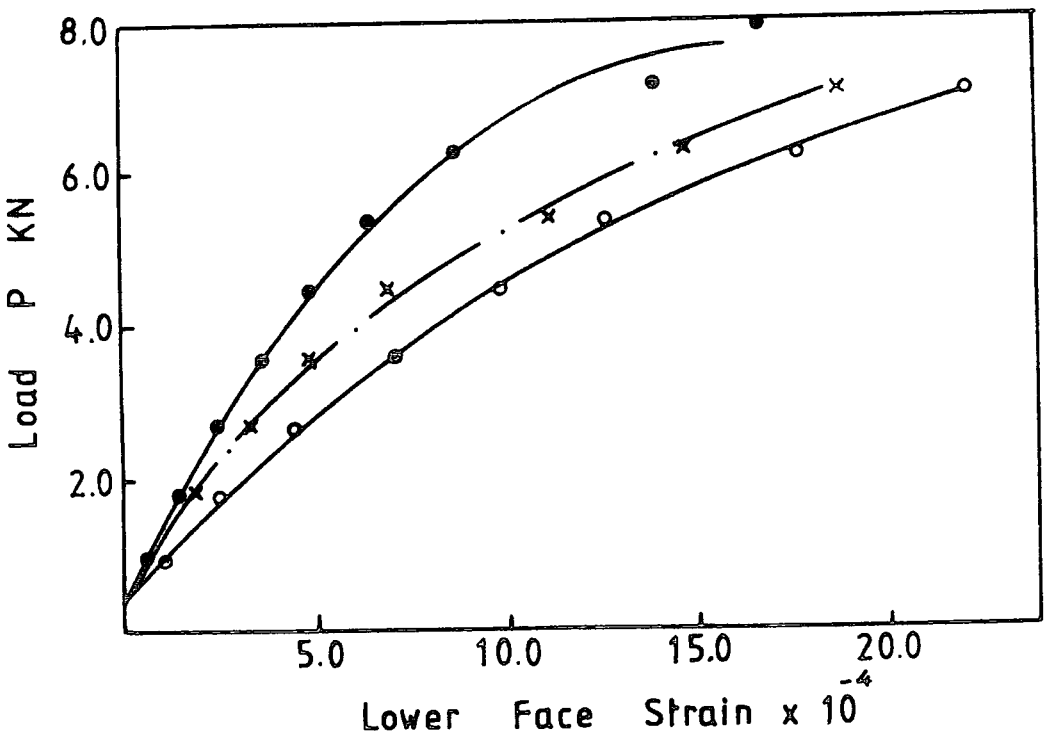

Fig. (6.14b)

Figure (6.14) Relationship between the total load P and the face strain for beams made using faces of A_s = 41.0 mm.^{2}

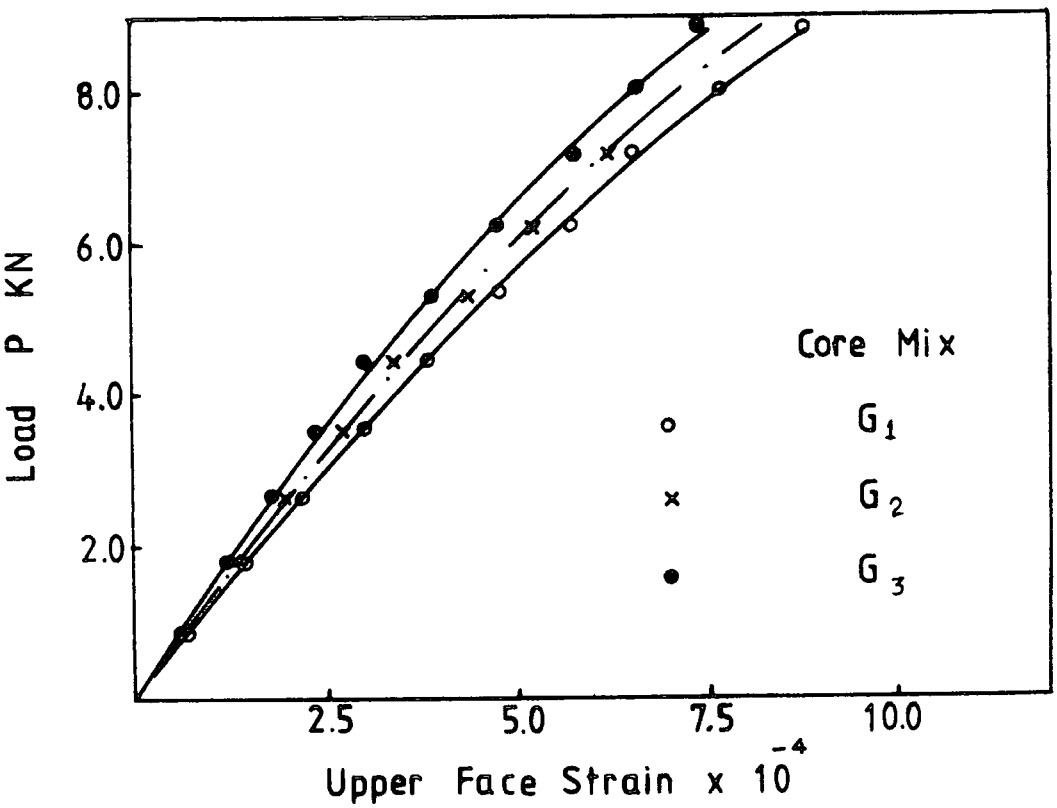

Fig. (6.15a)

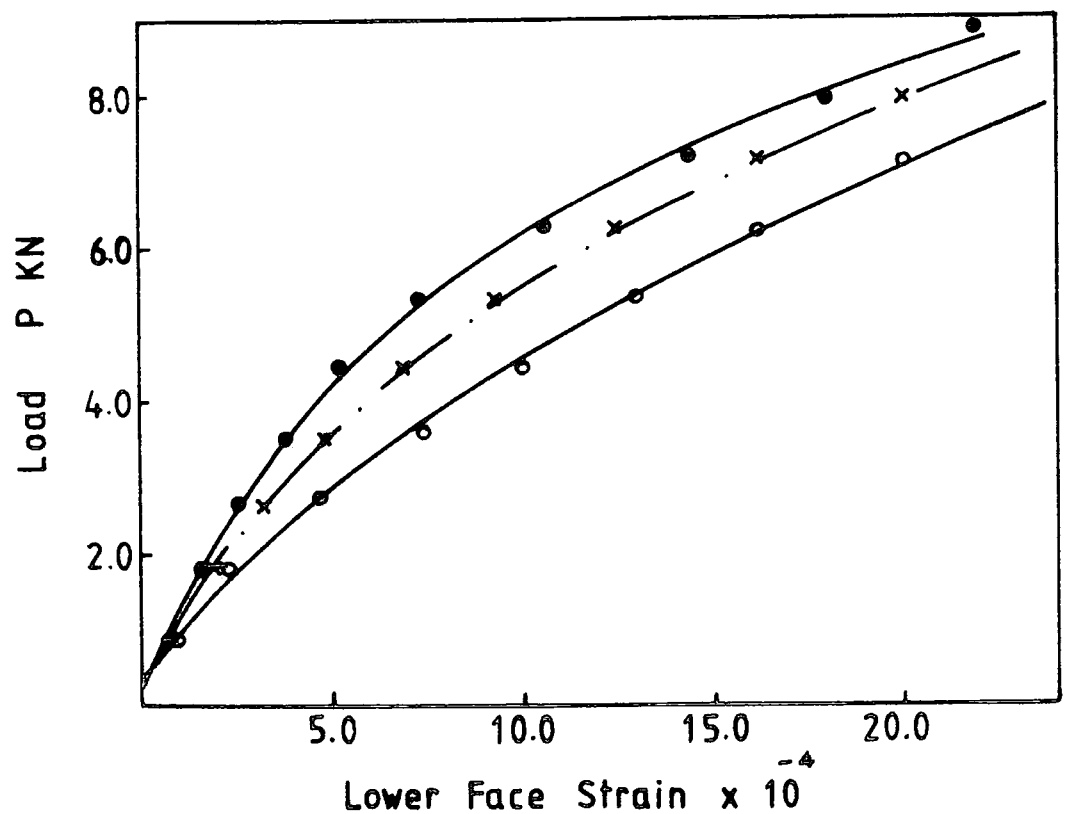

Fig. (6.15b)

Figure (6.15) Relationship between the total load P and the face strain for beams made using faces of A_s = 48.3 mm.^{2}

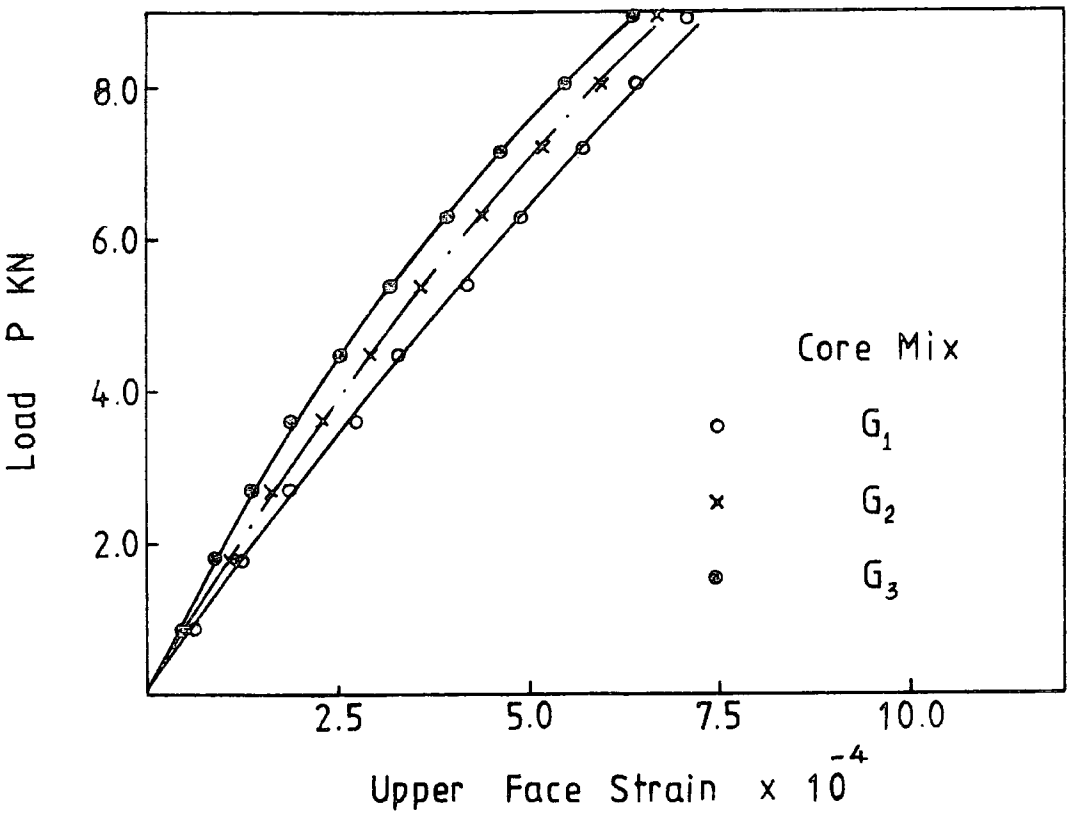

Fig. (6.16a)

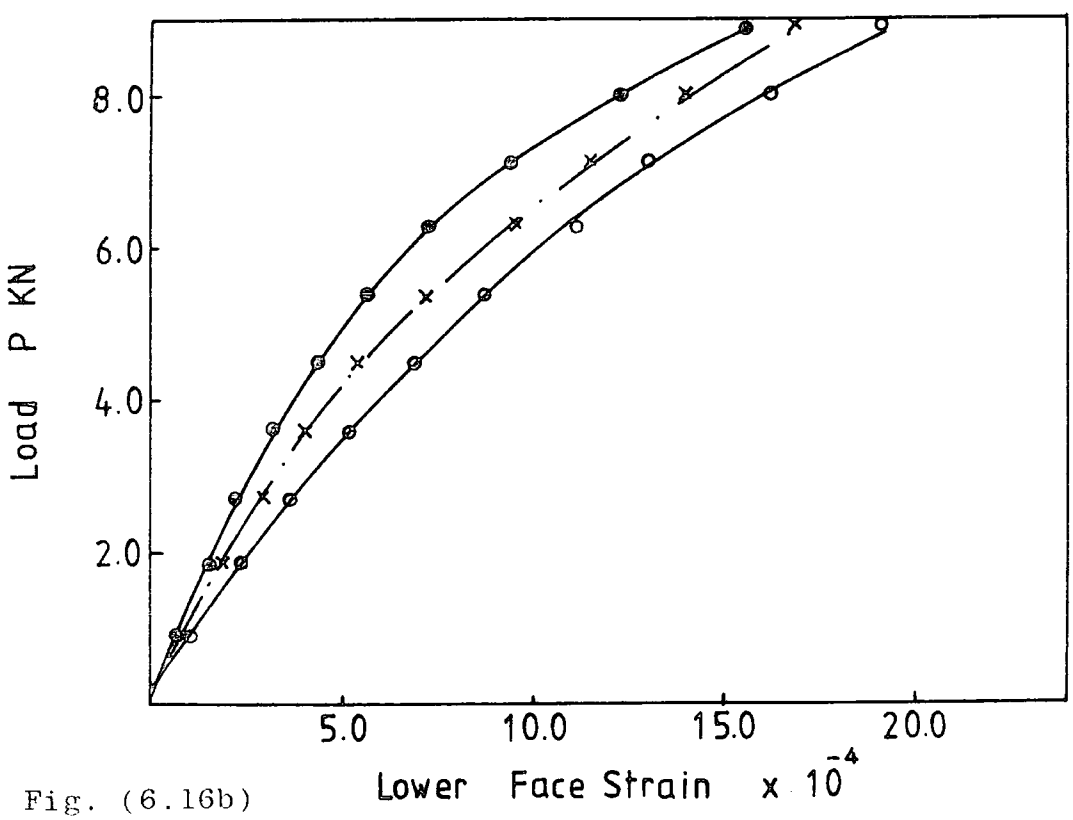

Fig. (6.16b)

Figure (6.16) Relationship between the total load P and the face strain for beams made using faces of A_s = 56.0 mm.^{2}

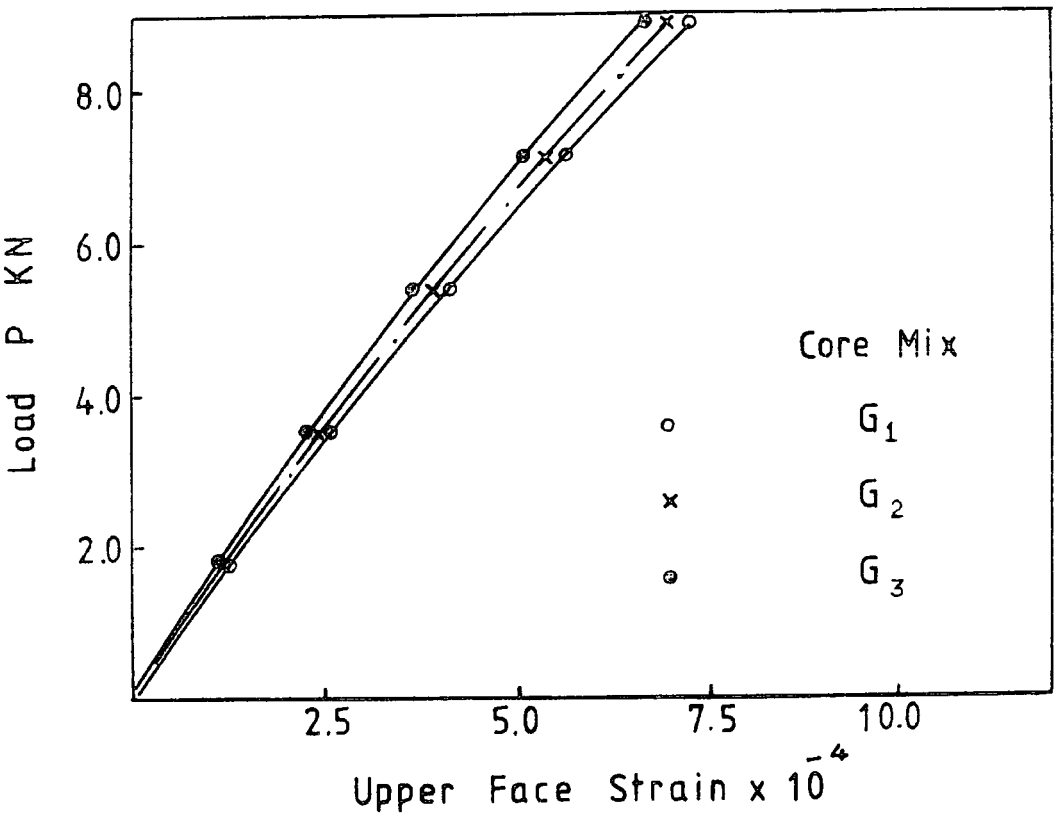

Fig. (6.17a)

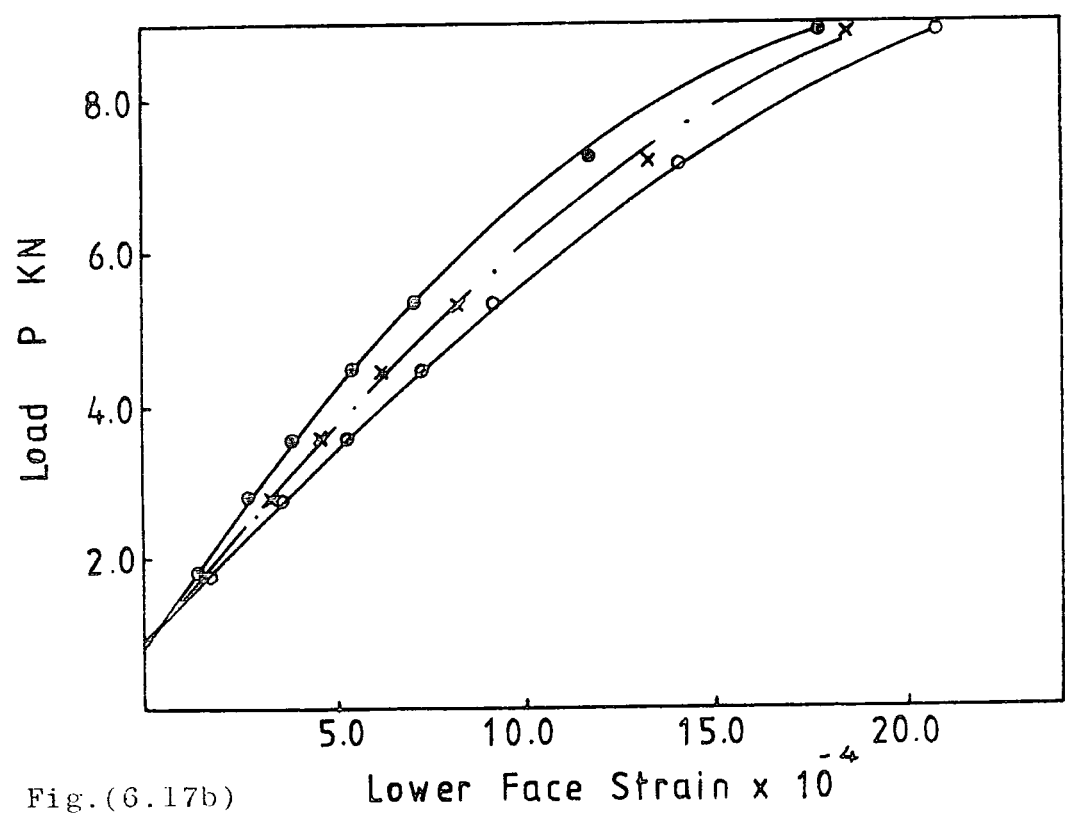

Fig.(6.17b)

Figure (6.17) Relationship between the total land P and the face strain for beams made using faces of A_s = 67.0 mm.²

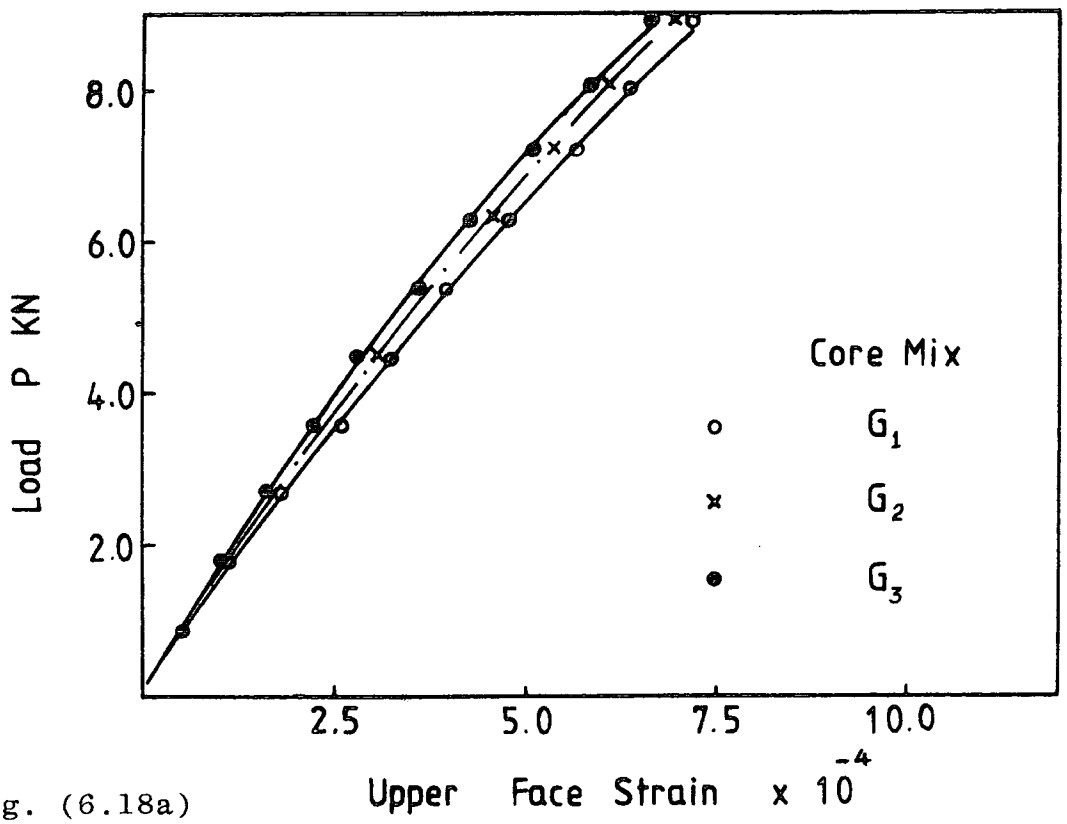

Fig. (6.18a)

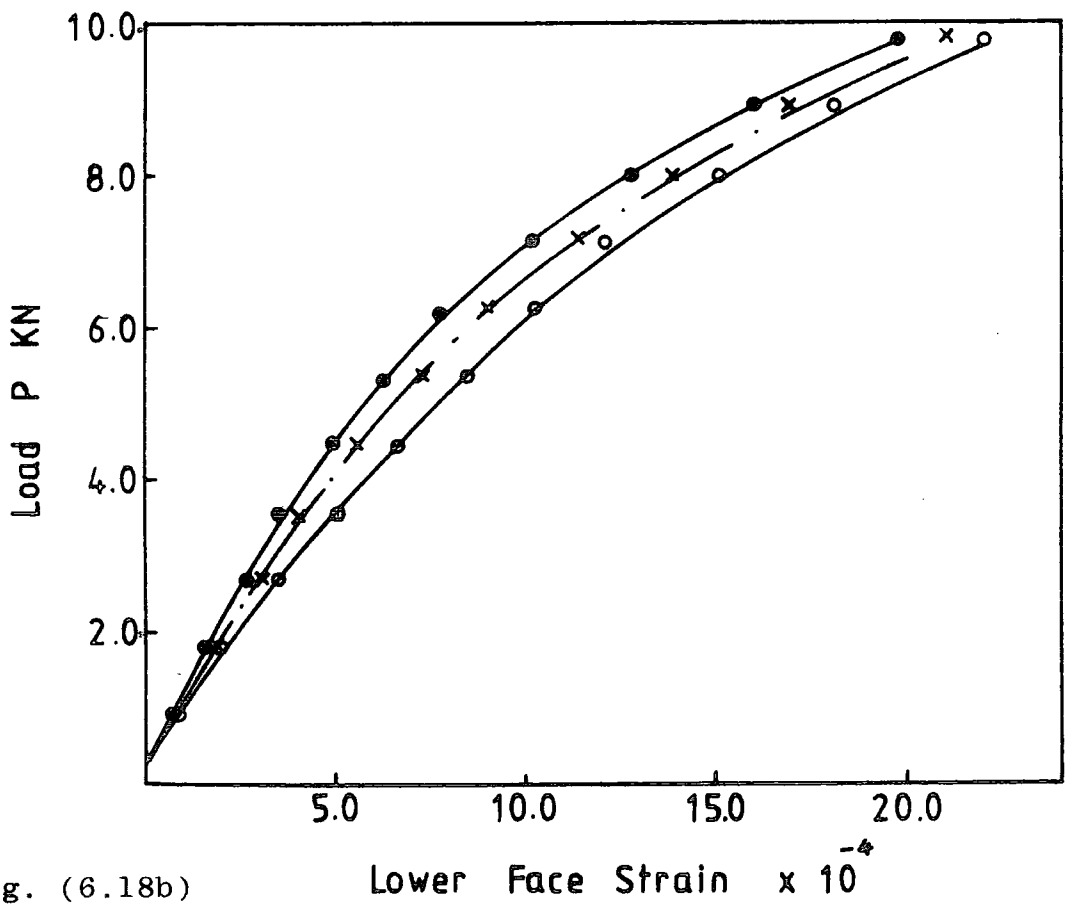

Fig. (6.18b)

Figure (6.18) Relationship between the total load P and the face strain for beams made using faces of A_s = 72.5 mm.^{2}

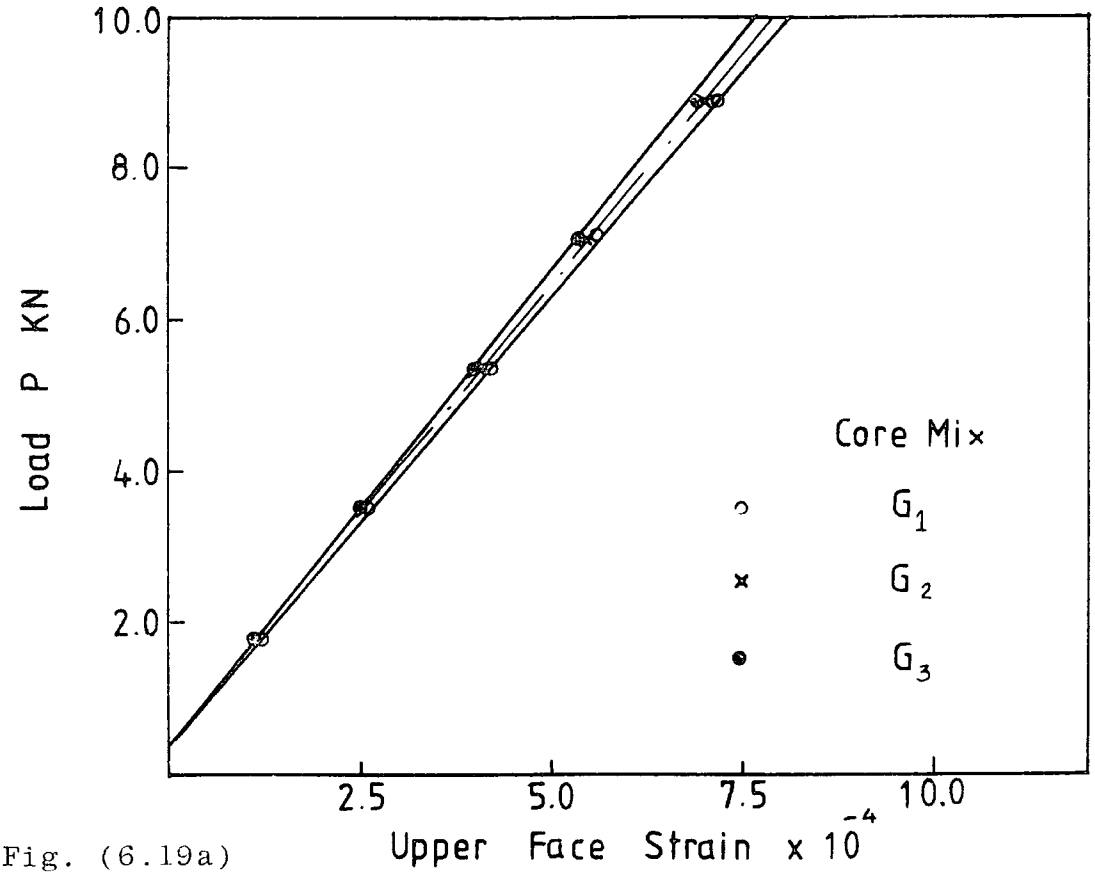

Fig. (6.19a)

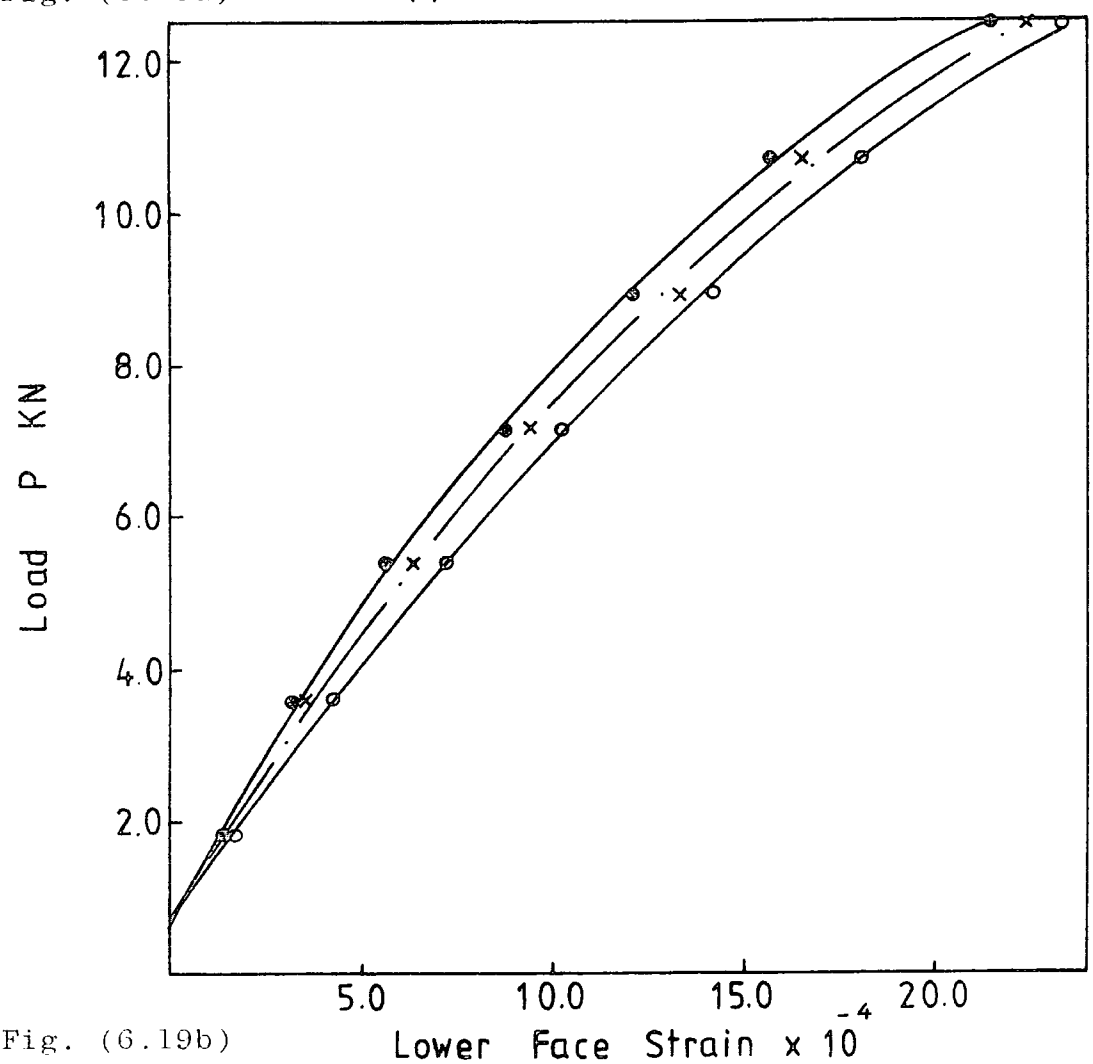

Fig. (6.19b)

Figure (6.19) Relationship between the total load P and the face strain for beams made using faces of A_s = 82.6 mm.^{2}

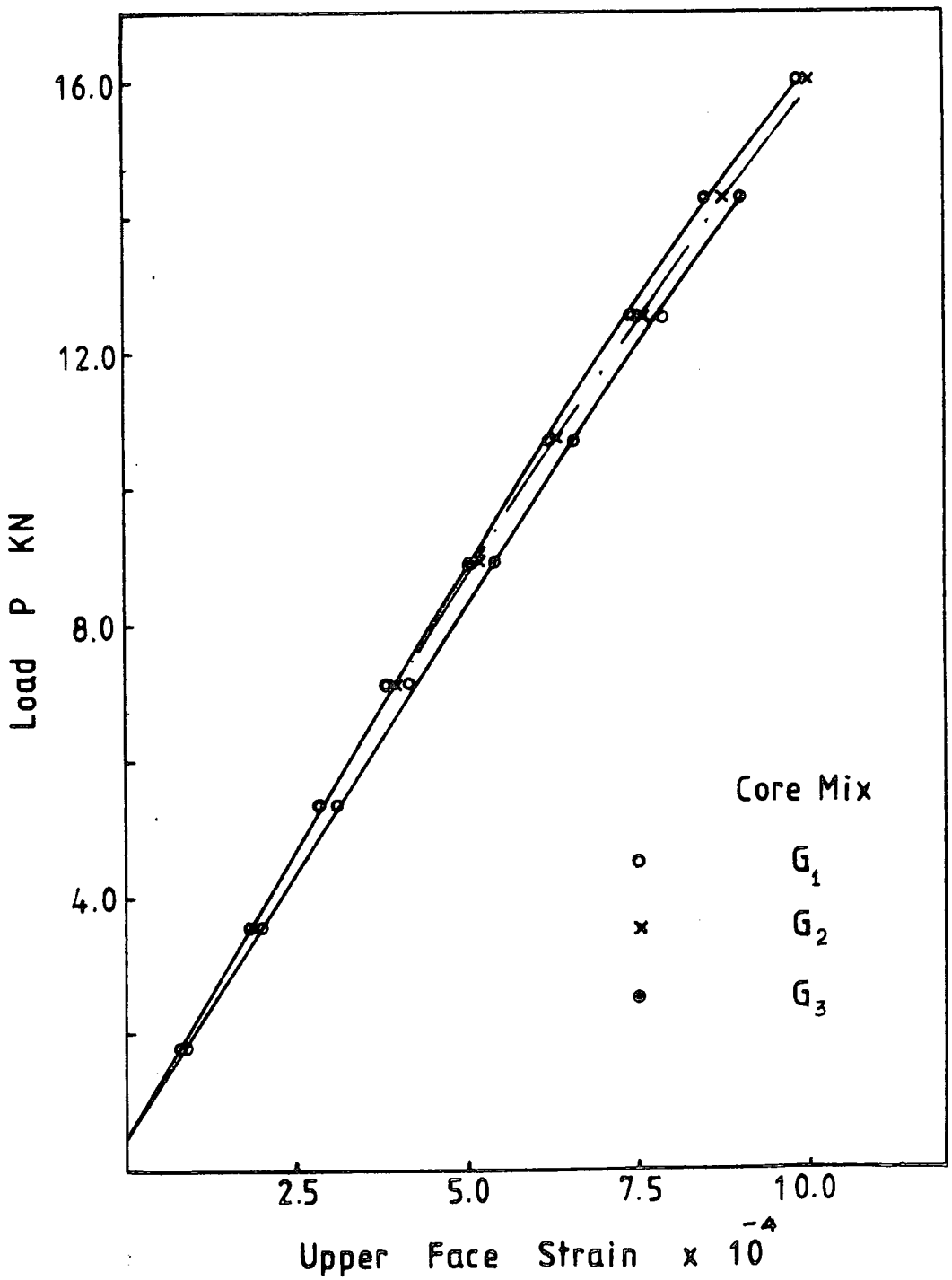

Figure (6.20a) Relationship between the total load P and the upper face strain for beams made using faces of A_s = 103.3 mm.^{2}

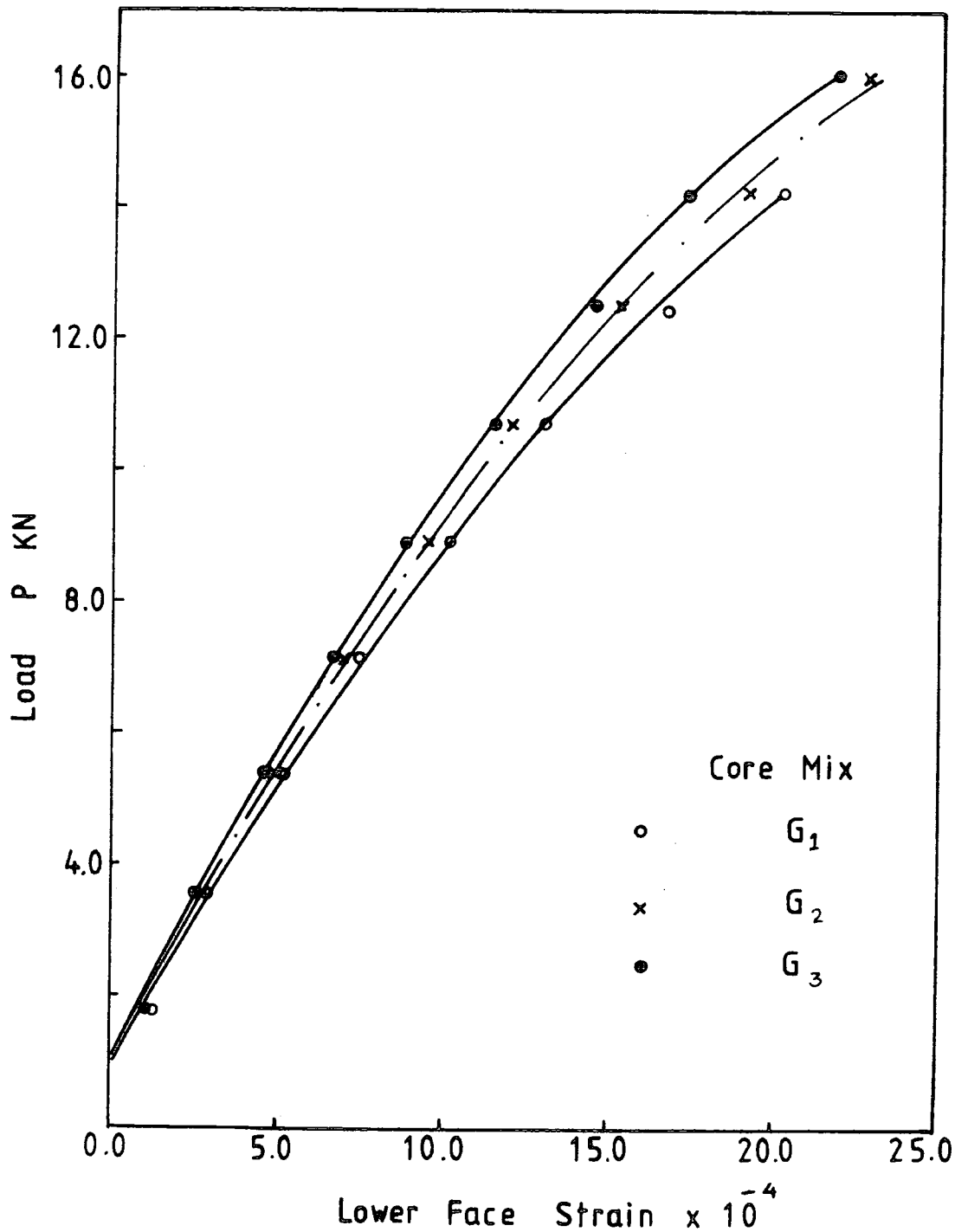

Figure (6.20b) Relationship between the total load P and the lower face strain for beams made using faces of A_s = 103.3 mm^2.

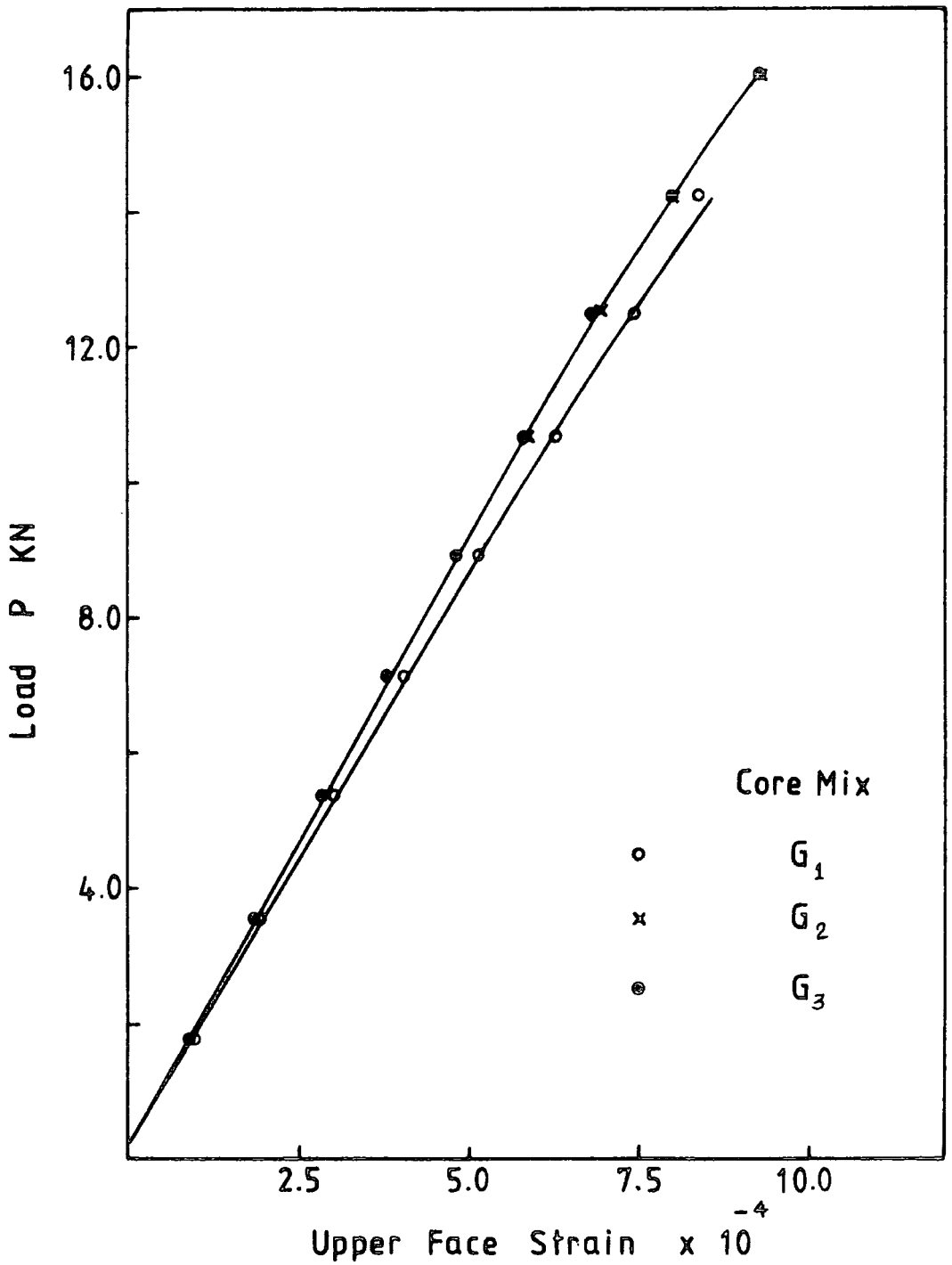

Figure (6.21a) Relationship between the total load P and upper face strain for beams made using faces of A_s = 118.0 mm.^{2}

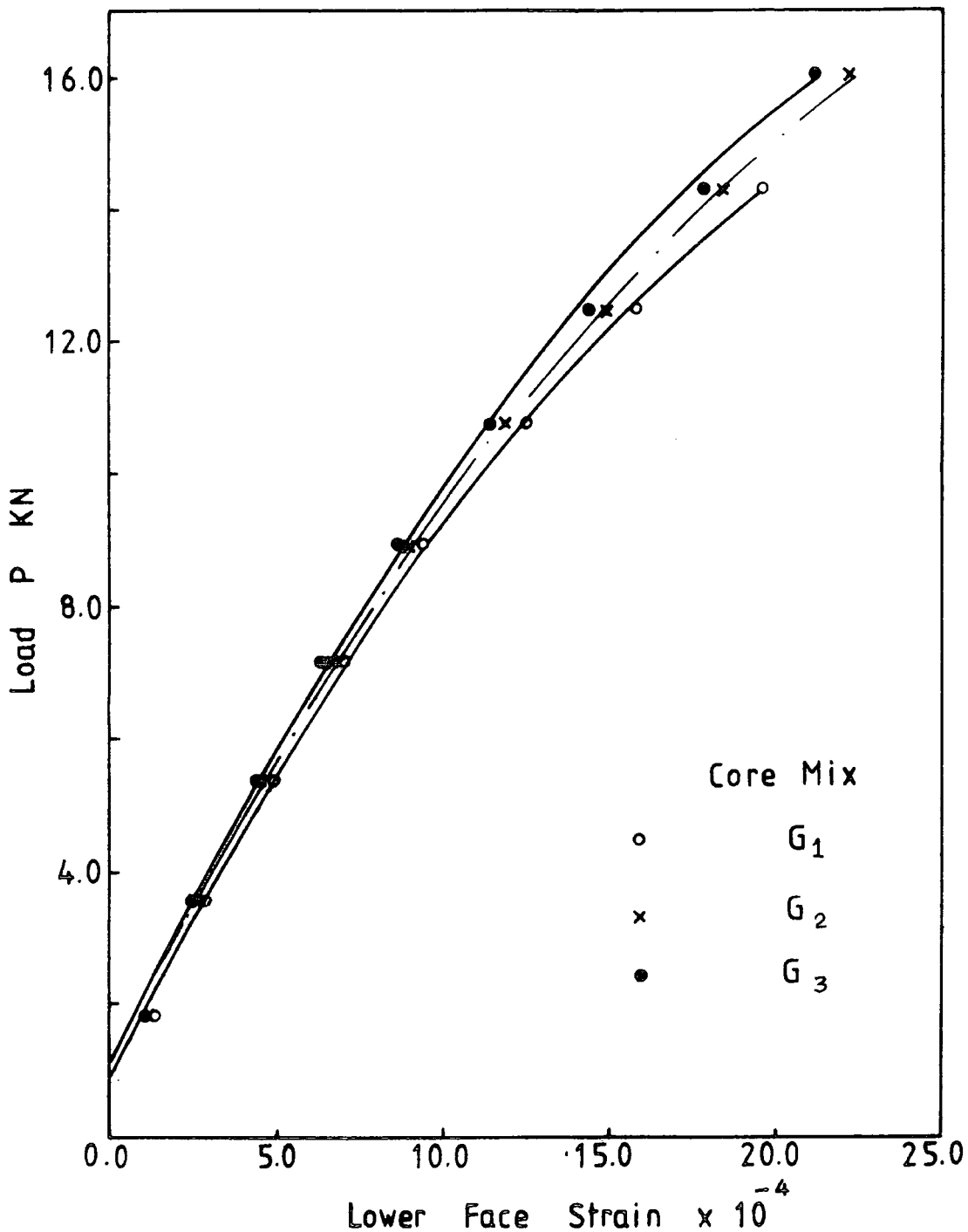

Figure (6.21b) Relationship between the total load P and the lower face strain for beams made using faces of A_s = 118.0 mm.^{2}

Strain per unit load $\frac{\xi_T}{\kappa N}$ was taken from the straight line of the linear relationship throughout the elastic stage of each curve. The values obtained are listed against the area of steel reinforcement in each face in tables (6.3, 6.4 and 6.5) typical to the three core mixes (G_1, G_2 and G_3) used in the same sequence. For a unit load ($P = \kappa N$) the normal force (N) acting on each face was calculated from equation (6.6) neglecting the local bending moment in the faces (M_{Fu} and M_{FL}) due to their relative insignificance. The strains in the faces due to $N(\xi_N)$ were calculated with regard to their moduli, as previously obtained (chapter 4, table 4.4), and their values recorded also in tables (6.3, 6.4 and 6.5). From the total strain measured and the strain caused by the normal force $N(\xi_N)$, the strain due to the local bending moment was estimated according to equation (6.8).

According to this method of analysis (of assuming the core takes no direct normal stress) the normal force N acting on the faces is of the same magnitude for all the different cores, and it follows that the strain caused by the local bending moment will be related to the effectivness of the cores. This can be seen in the results in the three tables where ξ_{M_F}/ξ_N ratios are recorded. The values ξ_{M_F}/ξ_N have no constant ratio in the upper or lower faces, and this may be attributed to the surface condition of the face and the position of the mesh reinforcement in the face. Further to that, when the slice of the mesh used to reinforce the face was narrow, as in the beams made by face S_6 of A_s = 82.6 mm^2. (see table 4.3 in chapter 4) the ratio ξ_{M_F}/ξ_N was of higher value in the upper face strain.

The results of the upper face strains indicated that in all cases the faces had a sagging bending moment and there was

no indication of possible hogging bending moment, as was imagined due to compression of the core and illustrated in figure (6.13c).

Surprising results were obtained when the strains due to the local bending moments in the lower faces were calculated in the same way and under the same simple assumption. The strains due to M_{Fl} were found approximately nonexistent in some beams or of negative values in some others. This means that such faces have no appreciable bending or have a hogging bending. The latter is unlikely to be true, and the lower face, in all cases, had a sagging moment according to the deflection measurements recorded. The suspect results approximately disappeared when the ratio between the bending stiffness of the beam and its shear stiffness (μ in table 6.2) increased. The strange values accompanied the beams of smaller μ. (i.e. values which were negative or less than half of the value given by the local moment in the upper face).

However, according to the results obtained the faces' strain for such sandwich beams cannot be considered to conform to the analysis if one makes the assumption that the core takes no direct normal stress when the beams are of μ less than 55. Whenever the beam had a μ of higher value the analysis becomes more satisfactory. This is shown in the results of the beams made by core mix G_1 (table 6.3), where the local bending moments of the upper and lower faces are of similar values. This suggests that the expression $\mu = (D_b/D_s)\, E_{Ft}$ is a suitable way of defining the limit of appliability of sandwich beam analysis and is suitable for both deflection and strain analysis.

After the surprising results obtained for the lower face strains, it is of some interest to examine the effect of including

Table (6.3) : Face strain per unit load (P = 1 KN) as experimentally obtained (ξ_T), calculated due to the normal force (ξ_N) and local B.M for beams made using core mix G_1.

(Core assumed takes no direct normal stresses)

A_s in one face ($mm.^2$)	Upper face				Lower face			
	Strain per unit load x 10^{-5}			M_{Fu}	Strain per unit load x 10^{-5}			M_{Fl}
	ξ_T	ξ_N	$\xi_{M_{Fl}}$	(N.mm.)	ξ_T	ξ_N	$\xi_{M_{Fl}}$	(N.mm.)
41.0	9.30	6.15	3.15	480	24.00	25.20	-1.20	
48.3	8.60	5.97	2.63	400	24.40	22.20	2.20	333
56.0	7.83	5.78	2.07	369	18.50	18.50	-	-
67.0	8.20	5.35	2.85	508	20.34	16.48	3.85	687
72.5	7.80	5.07	2.73	478	18.55	14.73	3.82	680
82.6	8.20	5.01	3.18	623	16.56	13.97	2.59	506
103.3	6.39	4.77	1.62	359	12.92	11.42	1.50	332
118.0	6.00	4.40	1.60	374	12.00	9.70	2.30	538

Table (6.4) : Face strain per unit load (P = 1KN) as experimentally obtained (ξ_T), calculated due to the normal force (ξ_N) and local B.M for beams made using core mix G_2.

(Core assumed takes no direct normal stresses)

A_s in one face (mm^2)	Upper face				Lower face			
	Strain per unit load x 10^{-5}			M_{Fu}	Strain per unit load x 10^{-5}			M_{Fl}
	ξ_T	ξ_N	$\xi_{M_{Fl}}$	(N.mm.)	ξ_T	ξ_N	$\xi_{M_{Fl}}$	(N.mm.)
41.0	8.80	6.15	2.65	404	18.80	25.20	-6.40	-(975)x
48.3	7.92	5.97	1.95	297	19.00	22.20	-3.20	-(488)x
56.0	7.22	5.78	1.44	257	16.0	18.50	-2.50	-(447)x
67.0	7.89	5.35	2.54	454	18.90	16.48	2.42	433
72.5	7.60	5.07	2.53	452	15.80	14.73	1.07	191
82.6	8.00	5.01	2.99	586	15.50	13.97	1.53	300
103.3	6.10	4.77	1.33	295	12.0	11.42	0.58	129
118.0	5.62	4.44	1.18	276	11.1	9.70	1.40	328

Table (6.5) : Face strain per unit load (P = 1 KN) as experimentally obtained (ξ_T), calculated due to the normal force (ξ_N) and local B.M for beams made using core mix G_3 .

(Core assumed takes no direct normal stresses)

A_s in one face ($mm.^2$)	Upper face				Lower face			
	Strain per unit load x 10^{-5}			M_{Fu} (N.mm.)	Strain per unit load x 10^{-5}			M_{Fl} (N.mm)
	ξ_T	ξ_N	$\xi_{M_{Fl}}$		ξ_T	ξ_N	$\xi_{M_{Fl}}$	
41.0	7.32	6.15	1.17	178	13.34	25.2	-11.85	-(1087)x
48.3	7.05	5.97	1.08	165	14.90	22.2	- 7.30	-(1112)x
56.0	6.34	5.78	0.56	100	13.45	18.5	- 5.05	-(903) x
67.0	7.50	5.35	2.15	384	16.62	16.48	+ 0.14	(25)
72.5	7.50	5.07	2.43	217	14.30	14.73	- 0.43	- (77) x
82.6	7.76	5.01	2.75	539	14.30	13.97	+ 0.33	(65)
103.3	5.83	4.77	1.06	235	11.30	11.42	- 0.12	(27)
118.0	5.62	4.40	1.22	285	10.85	9.70	+ 1.15	269

in the analysis some force contribution from the core when calculating the beams' resistance moment. According to the position of the N.A, as determined by the strain measurements on the core sides at the compression Zone - as described before in section (6.1) - the compression forces carried by the cores (N_c) were calculated with regard to the modulus of elasticity of the core used. The values of N_c are listed in the table in appendix (III.3) against the area of reinforcement in each face for the three core mixes.

For simplicity, the core in the tension Zone will be assumed to take normal tension force of magnitude equal to the normal force carried by the compression Zone (N_c), where each acts on the centre of the triangular stress block for each part. Consider that the beam's resistance moment consists of two component moments; one carried by the normal forces of the core and the remainder carried by normal forces acting on the two faces. (In this case neglect the value of M_{Fl} and M_{Fu}, because of their relative insignificance, as mentioned before). The moment carried by core (M_c) has been calculated and its ratio to the total moment (M), per cent, can be seen in the same table in appendix (III.3) (all values of M_c and M are calculated for unit load P = 1.0 ⌀N.). From equation (6.6) the values of N were calculated by substituting $M = M-M_c$. The strains due to N (ξ_N) were determined and subsequently ξ_{M_F} and M_F in the lower and upper faces respectively, as described before, and the results obtained by this method were listed in tables (6.6, 6.7 and 6.8) typical to the three core mixes used (G_1, G_2 and G_3) in the same sequence.

From table (6.6) of the beams cored by the weakest core

(mix G_1), in most cases local moment in the lower face is higher than it is in the upper face. The suspect result in this group is given by the beam of lowest reinforcement (A_s = 41 mm^2.) where M_{Fl} is very small relative to M_{Fu}. The result of the set of faces reinforced by A_s = 56 mm^2. also suggests rather strange behaviour i.e. it is probably the result of error in the lower face strain which may be attributed to the surface condition or may be owing to the position of the reinforcement in the face.

When the beams were cored by a stronger core (G_2), the result recorded in table (6.7) show the local moment in the lower faces of the three sets of beams made using faces of lower reinforcement are of negative value. In the other five sets the local moments in the lower faces are positive and in some beams were more, and in others were less than the local moment in the upper faces. It can be seen in the results of the three unsatisfactory cases (of negative M_{Fl}) that the value of the negative moment in the lower face is decreased with increase in the area of reinforcement in the faces (i.e. increase the face modulus and thus the beam's bending stiffness). Using the strongest core (G_3), the local negative moments in the lower faces of the three first sets were found to be increased and remarkable reductions were found also in the local moment of the upper faces of these three sets. In all other five cases the values of M_{Fl} are positive and in most of them the local moment in the lower face (M_{Fl}) is less than in the upper face (M_{Fu}). When the average value of M_{Fl}/M_{Fu} is calculated, (omitting the unsatisfactory and the suspected cases, i.e. the crossed cases in the tables), it was found to be 1.27, 1.05 and 0.836 in the three core mixes G_1, G_2 and G_3 respectively.

Table (6.6) : Face bending taking into consideration core resistance

(Beams made using core mix G_1)

A_s in one face ($mm.^2$)	Upper face strain and B.M				Lower face strain and B.M			
	Strain per unit load (KN) x 10^{-5}			M_{Fu} (N.mm.)	Strain per unit load (KN) x 10^{-5}			M_{Fl} (N.mm.)
	ξ_T	ξ_N	$\xi_{M_{Fl}}$		ξ_T	ξ_N	$\xi_{M_{Fl}}$	
41.0	9.30	5.84	3.46	527	24.00	23.90	0.10	(15)x
48.3	8.60	5.736	2.86	436	24.40	21.35	3.05	465
56.0	7.85	5.51	2.34	418	18.50	17.69	0.81	145
67.0	8.20	5.11	3.09	552	20.34	15.74	4.60	822
72.5	7.80	4.84	2.96	529	18.55	14.07	4.48	800
82.6	8.20	4.75	3.45	676	16.56	13.24	3.32	650
103.3	6.39	4.55	1.84	407	12.92	10.91	2.01	446
118.0	6.00	4.20	1.80	421	12.00	9.28	2.72	636

Table (6.7) : Face bending taking into consideration core resistance

(Beams made using core mix G_2)

A_s in one face (mm^2.)	Upper face strain & B.M				Lower face strain & B.M			
	Strain per unit load x 10^{-5}			M_{Fu}	Strain per unit load x 10^{-5}			M_{Fl}
	ξ_T	ξ_N	$\xi_{M_{Fu}}$	(N.mm.)	ξ_T	ξ_N	$\xi_{M_{Fl}}$	(N.mm.)
41.0	8.80	5.48	3.32	505	18.80	22.47	-3.675	-(560)x
48.3	7.94	5.46	2.48	378	19.00	20.32	-1.32	-(201)x
56.0	7.22	5.29	1.93	345	16.00	16.97	-0.97	-(173)x
67.0	7.89	4.89	3.00	536	18.90	15.08	3.82	687
72.5	7.60	4.58	3.02	540	15.80	13.30	2.50	447
82.6	8.00	4.46	3.54	694	15.50	12.43	3.07	600
103.3	6.10	4.37	1.73	384	12.0	10.48	1.52	338
118.0	5.62	4.07	1.55	363	11.1	8.96	2.14	506

Table (6.8) : Face bending taking into consideration core resistance

(Beams made using core mix G_3)

A_s in one face (mm.^{2})	Upper face strain & B.M				Lower face strain & B.M			
	Strain per unit load x 10^{-5}			M_{Fu}	Strain per unit load x 10^{-5}			M_{Fl}
	ξ_T	ξ_N	$\xi_{M_{Fu}}$	(N.mm.)	ξ_T	ξ_N	$\xi_{M_{Fl}}$	(N.mm.)
41.0	7.32	5.18	2.14	326	13.34	21.16	-7.82	-(1192)x
48.3	7.04	5.20	1.84	280	14.90	19.29	-4.39	-(669)x
56.0	6.34	5.12	1.22	218	13.45	16.43	-2.98	-(533)x
67.0	7.50	4.65	2.85	510	16.62	14.32	2.30	411
72.5	7.50	4.29	3.21	574	14.30	12.45	1.85	330
82.6	7.76	4.19	3.56	699	14.30	11.68	2.62	513
103.3	5.83	4.20	1.63	362	11.30	10.08	1.22	271
118.0	5.62	3.90	1.72	400	10.85	8.60	2.25	526

In the sandwich beam theory (1,31), the two faces are supposed to have the same sagging moment and consequently the same local bending moment, especially if the upper face moment was not increased due to core compression (which it was not in these cases). Accordingly the results of the beams cored by mix G_2 are the most satisfactory. However, the other two groups could be considered to give acceptable results by this method of face strain analysis for such concrete sandwich beams, especially with this type of the reinforced concrete face. The increase of M_{F1} in cases of using core G_1 (the weaker) and its decreasing with the strongest core (G_3) may be attributed to the value of the tensile normal force N, assumed to be taken by core. It may be of smaller value for the weaker core and of greater value for the stronger core mix.

As a result of the comparisons made above it can be seen that the behaviour of some of the beams cannot be modelled satisfactorily by the simplified "sandwich beam" method; in particular their face strains are not compatible with the simplified analysis. The bending and shear stiffness formulae (μ in table 6.2) developed here appear to be expressions which describe the behaviour of these sandwich beams and give results which are compatible with the experimental values.

6.4 Beams' ultimate load and failure mode

The sandwich beam's ultimate load is determined by the maximum strength of the face used or the maximum shear strength of the core material. The ultimate load must be calculated from both cases and the lower value is the beam capacity. Neglecting the values of the local moments in the faces, because they are

relatively small, as illustrated in section (6.3), the ultimate load P corresponding to the face strength is determined by the expression:-

$$P_F = 2\,\overline{\sigma}_{F\,max}\,\frac{A_F\,(c + f)}{a}$$

Where $\overline{\sigma}_{F\,max.}$ is the maximum strength of the weaker face.

Since all the concrete faces of the sandwich beams made in this research are weaker in tension than in compression, the beams' ultimate loads are determined by the maximum tensile strength of the faces, i.e. the failure could be tension failure or shear failure and the compression failure is unlikely to happen.

According to the thickness of the core and faces, and following the simplest form of the sandwich beam theory, the distribution of the shear stress is constant over the cross-section of the core (1, 3, 22, 31) and the beam ultimate load due to shear then is:

$$P_Q = 2\,\tau_{cf}\,b\,d$$

Where $d = c + f$ for the relative values of these face and core dimensions (1, 3, 22, 31)

The failure load of the beams of each set was calculated, using the maximum tensile strength of its face as obtained in the tension test procedure (which was described before at section 4.3.2 and the results are recorded in table (4.4)). The values of these calculated ultimate loads were graphed in figure (6.22) against the cross-sectional area of reinforcement in each face of the beam, thus producing a theoretical flexural failure

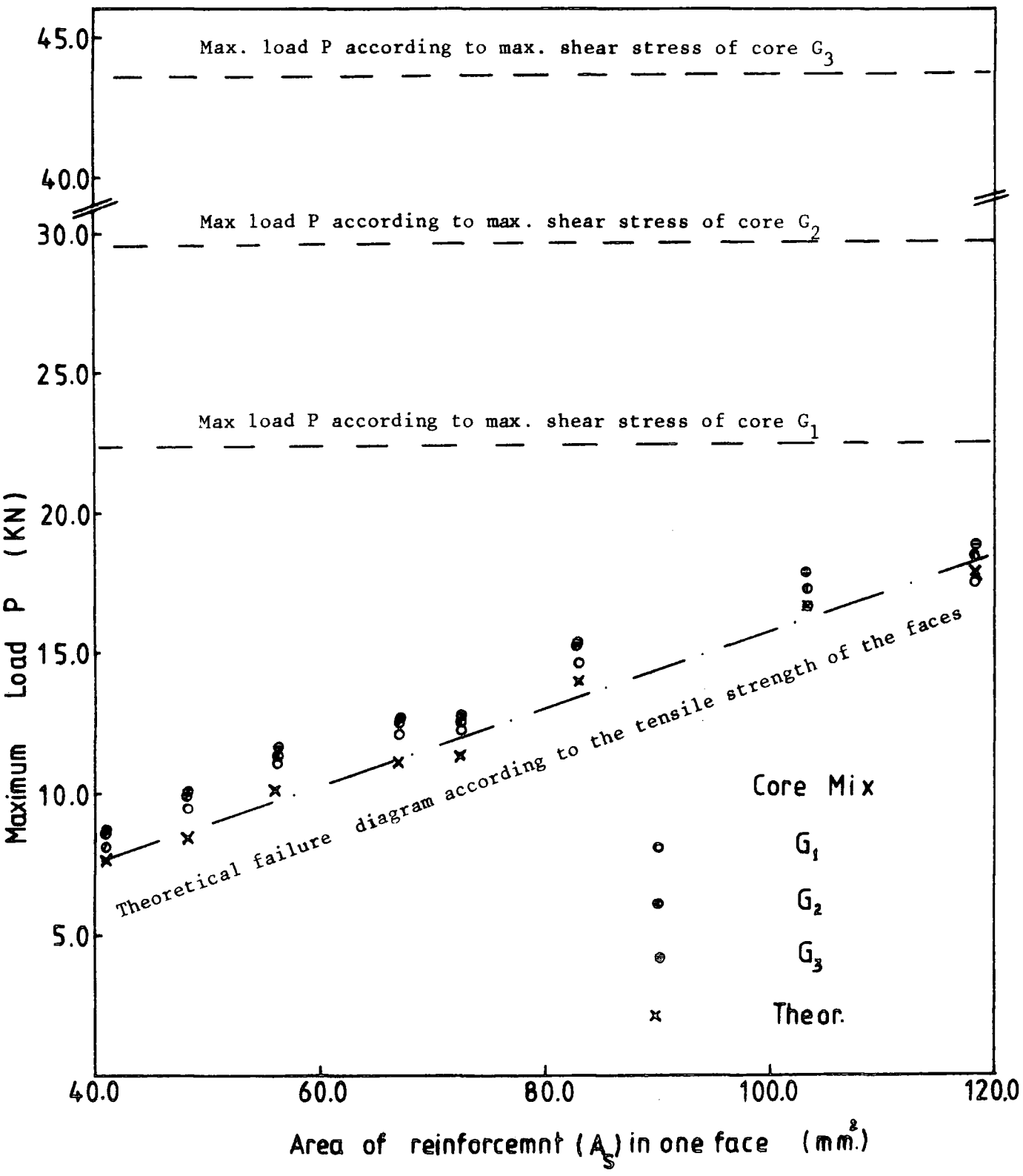

Figure (6.22) Beams' ultimate load according to the area of reinforcement in each face and the core mix used (theoretical and experimental).

diagram. In this linear relationship the increase of the beams' ultimate loads is not proportional to the increase of the reinforcement in the face. This is because the reinforcement in the face (A_s) is not the only factor affecting the face failure, it is also affected by the concrete of the face, as described later. The beams' ultimate loads due to shear were determined also and plotted on the same figure for the three core mixes, using their maximum shear strength as obtained and recorded in table (5.1). It can be seen from this graph that the beams' failure can be expected to happen due to a face failing before the core fails in shear, i.e. all the sandwich beams made in this research are likely to fail in flexure rather than in shear.

The ultimate loads of the beams recorded from testing (average from the three beams of each set) were plotted also on the same graph. They were found to be approximately close to the values of the flexural failure diagram, i.e. in the way predicted by calculation. The beam's ultimate loads recorded experimentally in general are higher than the calculated values which may be attributed to increase the face tensile strength because it is built into a beam, and therefore its strength is greater than when it is tested singly. However, the increase of the beams ultimate loads are considered to be within an acceptable range. It can be seen also that the increase of the beam ultimate load due to using a stronger core in most cases is insignificant and could be considered negligible.

Each beam's failure was in one of three modes:

(1) Lower face reinforcement snapping at the centre portion.

(2) Lower face slipping on the core in the shear span portion.

(3) Failure due to the face's concrete destruction in the shear span.

This classification of the beams' failure was found in the following way and corresponds to the type of face failure in the tension test. It was found that the beams failing in the first mode are those made using faces which failed in the same way during the face tension test (faces S_1 and S_4 of A_s = 41 and 48.3 mm^2. respectively). This type of failure can be seen clearly in figure (6.23). The beams made using the other faces (of reinforcement of cross-sectional area greater than 48.3 mm^2.) were found to be in one of the other two failure modes, where the face failure in the tension test was caused due to the destruction of their concrete. Figure (6.24) shows photographs of some beams being in the second mode of failure which were made from different faces and symbolized by the face designation, the core mix symbol and the beam No. When the beams were cored by a stronger core (G_2 or G_3) the failure was found to resemble their failure using core G_1. i.e. the core has no effect on the mode of failure for the type of the sandwich beams tested in this research. This type of failure does not appear to be traditional shear failure (3) caused in the core due to it reaching the maximum shear strength of the core mix.

There are three reasons for this:-

(1) The calculated ultimate load of the beams according to the maximum shear strength of the core mixes are much greater than the experimental failure loads as shown in figure (6.22)

(2) There is an increase in the beams' ultimate loads for the same core mix when a stronger face is used (see figure (6.22) the experimental results).

Beam made using face S_1 (A_s = 41.0 mm.^{2}) and core G_1

Beam made using face S_4 (A_s = 48.3 mm.^{2}) and core G_1

Figure (6.23) : Typical tension failure due to snapping of the lower face reinforcement.

Beam of A_s = 56.0 mm^2 (face S_2) and core G_1

Beam of A_s = 72.5 mm^2 (face S_3) and core G_1

Beam of A_s = 82.6 mm^2 (face S_6) and core G_1

Beam of A_s = 103.3 mm^2 (face S_7) and core G_1

Beam of A_s = 118.0 mm^2 (face S_8) and core G_1

Figure (6.24) : Typical failure caused due to lower face slipping on the core in the shear span.

One of the beams made using face S_6 (A_s = 82.6 mm.^{2})

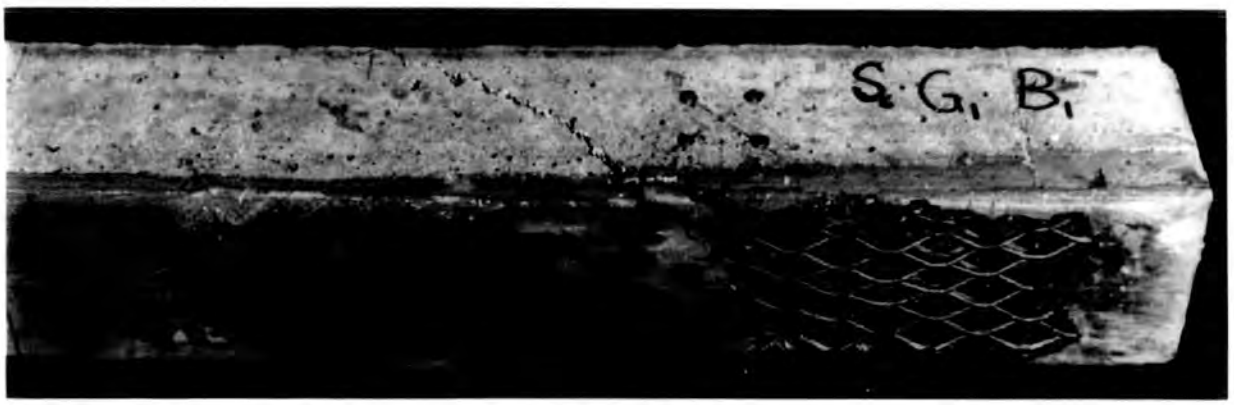

Figure (6.25) : Typical failure due to the face's concrete destruction.

(3) The existence of this type of failure at approximately the same load for each tension face in spite of using core mixes of higher shear stiffness.

This implies that the beams exhibit a particular type of failure which resembles a horizontal shear failure. It is considered to be caused due to the large growth in the tensile strain of the lower face throughout the shear span of the beam after the lower face exceeds the elastic stage. Such a failure becomes more acceptable if one understands the mechanism of the face with this type of reinforcement, which could be as follows:-

The concrete within each diamond of the mesh in the face under tension is exposed to longitudinal tensile stress and lateral compressive stresses owing to the deformation of the meshes' diamonds. In some cases, at certain values of reinforcement, the steel reaches its ultimate strength and snaps before the concrete's destruction occurs, thus exhibiting the first mode of failure. Due to an increase in the reinforcement area the failure of the face may happen due to destruction of the concrete, as obtained in the test results of the face in tension previously. When such a face is used in the sandwich beam its concrete in the shear span is exposed to shear stresses also. Since the lateral compression stresses increased due to an increase in the tensile strain, which causes an increase in the mesh diamond deformation. The increase of the tensile strain will be large when the beam is loaded beyond the elastic stage and the effect of the core shear may make the principle stress in the face concrete become greater in the shear span than the centre portion. Figure (6.25) shows the third mode of failure where the concrete of the tension face is destroyed in the shear span, emphasising the idea mentioned above, i.e. the face in tension

is the most important factor affecting the ultimate strength and failure made of these sandwich beams.

6.5 The "tied arch" theory of behaviour

In attempting to analyse the behaviour, and in particular the horizontal shear failure in the sandwich beams, reference is made to the most important and useful work reported by Swamy (38). In that research the work had been done with the purpose of finding out the necessary conditions for beam behaviour to be like a two-hinged tied arch. The work is based on a large amount of test data obtained from ordinary reinforced concrete beams. The beams were chosen - or designed- to have variation either of the load system, the shear span/depth ratio, or the reinforcement in rectangular or T section beams with bonded and unbonded reinforcement. The data included steel strain measurements of bonded beams under four point loading and of shear span/depth ratio of 3 or 4; i.e. in each case resembling the sandwich beams tested in this research. This work indicates that there is a large local increase in steel strain occurring in the shear span (see figure 3 of Ref. 38). In the same research the data of steel strain recorded from the unbonded beams showed that strain was approximately constant along the span (see figure 12 of Ref. 38).

If the lower faces in the sandwich beams tested in this research are assumed to replace the longitudinal reinforcement of the ordinary reinforced concrete beams tested in Swamy's research, the mechanism of the failure obtained may be better understood, in the context of the following considerations : When the bond between the lower face and core is effective, the distribution of strain along the lower face is likely to resemble

the strain of the longitudinal steel in Swamy's bonded beams, which may reach a maximum value in the shear span. It follows that crack propagation will weaken the already weak bond between the lower face and the core. When the face strain increases rapidly, the bond with the core may become very small or useless, and the beam then behaves like an unbonded beam, i.e. the strain becomes approximately constant along the face. At this stage the tendency is for the sandwich beam to behave like the tied two-hinged arch with the lower acting face as a tie (see fig.13 of Ref. 38). Accordingly, high tensile, compressive and shear stresses occur near to the support, resulting in a compound stress condition at the support which causes failure to occur here and propagate along the lower edge of the core. The lower face reinforcement was not anchored but was made to rely on its bond over its whole length in an attempt to build concrete sandwich beams similar to the usual sandwich panels or beams made from other materials. Thus it seems that this type of failure could be considered as a local failure in the form of a horizontal shear failure and was due to an increase in the face strain in the shear span.

CHAPTER SEVEN

BEAMS ANALYSIS WITH FINITE ELEMENT

7.1 Programme description

Finite element analysis is one of the methods which can be used to compare the experimental deflection or deformation of the beams with theoretical study. Using the structural property values of the sandwich components (core and face) which were obtained experimentally and recorded in the earlier parts of this thesis, a finite element analysis was done for the sandwich beams studied in this research and the results are reported in this chapter. The finite element analysis was carried out by means of the available "Irons-Quad" computer programme. The "Irons" programme was developed at Swansea University for general finite element analysis and the "Quad" developed at Durham University, i.e. the "Irons-Quad" computer programme is revised by Dr. G.M. Parton and his research assistants to compute stresses and displacements induced in structural elements affected by considerable shear deflections, therefore making possible the analysis of the sandwich plates and beams (see chapter 8 of Ref. No. 30).

When using this program the beam is divided into a mesh of elements of triangular shape as in figure (7.1). The load was applied so as to resemble the load position in the testing procedure and was distributed across the beam width to act on nodes located at the mid-length of the elements edges. This is illustrated in figure (7.1).

All the elements in the group are assumed to have the

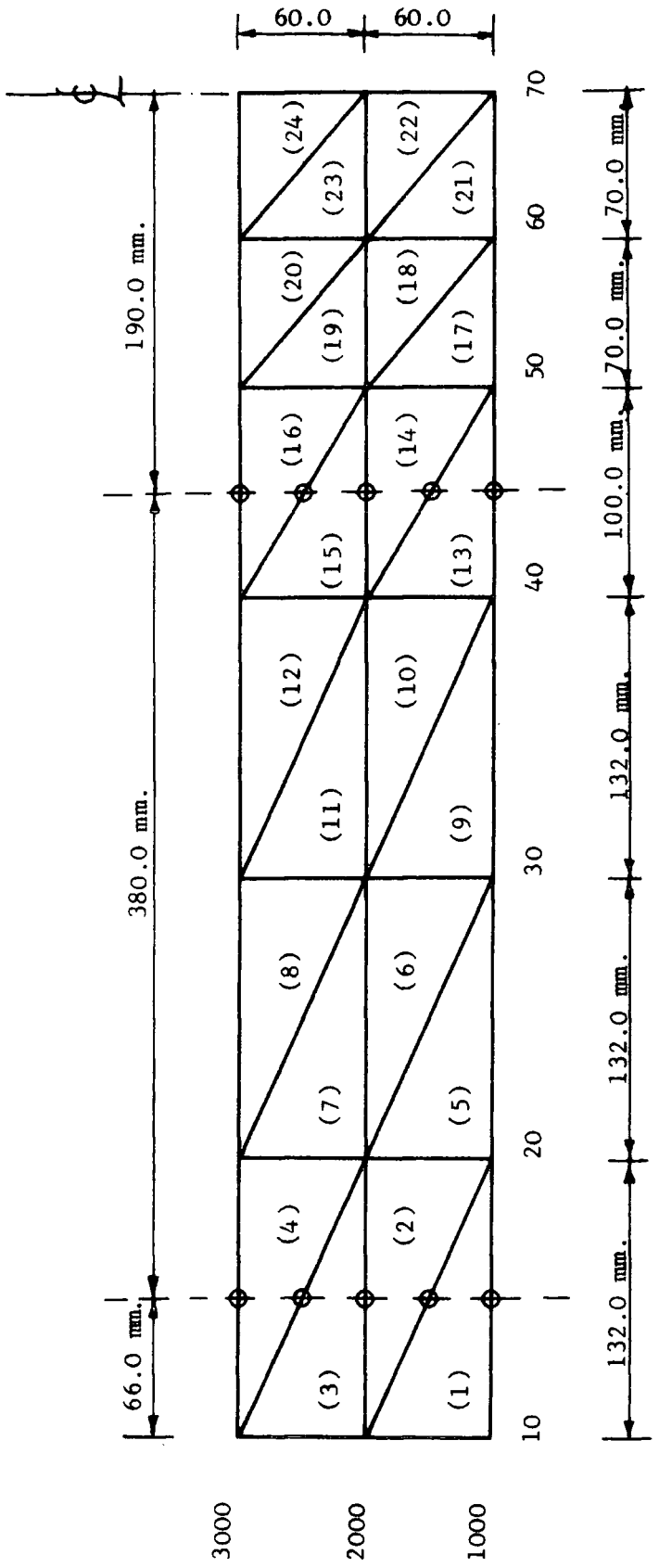

Figure (7.1) : Beam plan showing element layout for finite element analysis

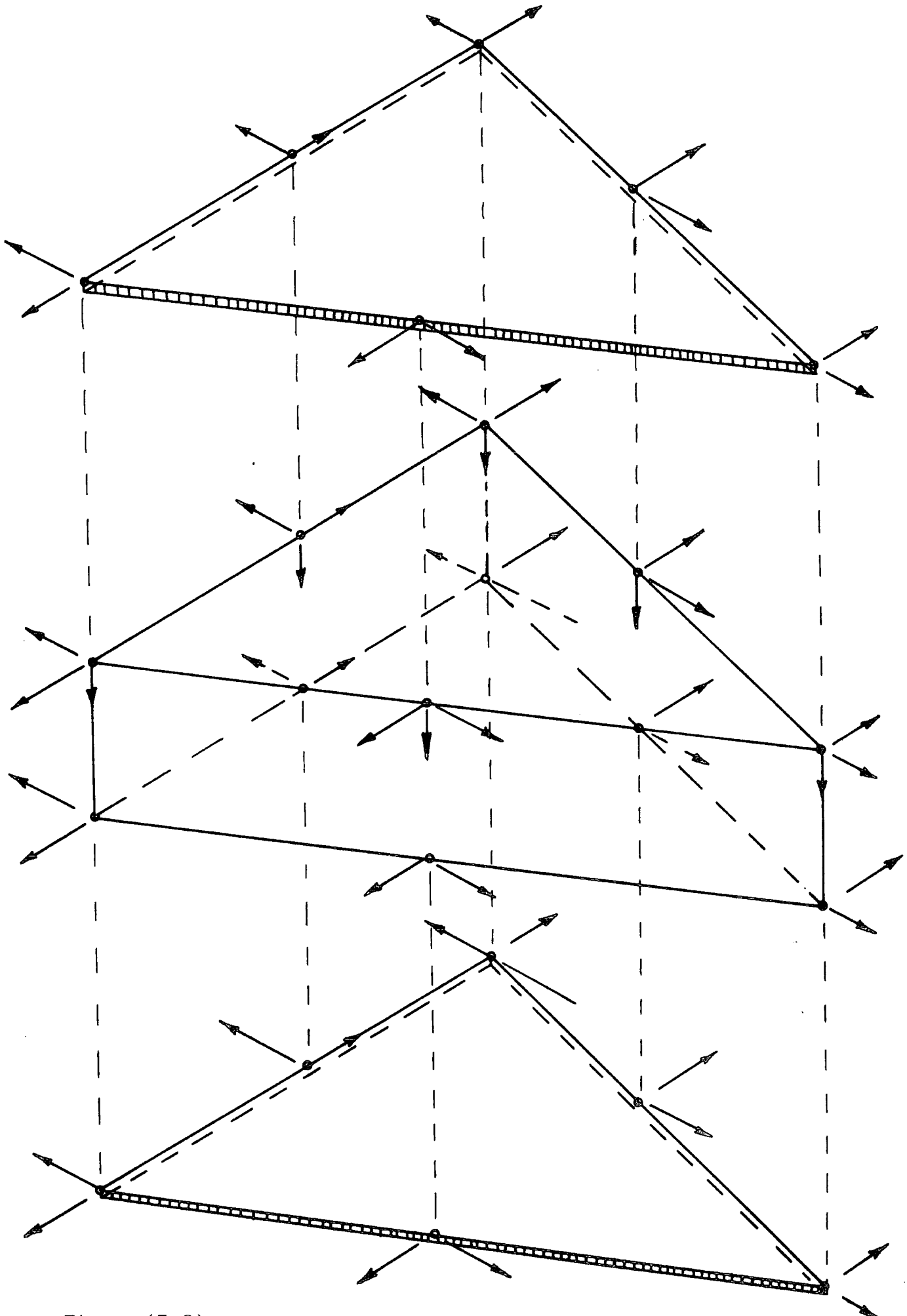

Figure (7.2)

same characteristic nodal freedoms. Each element consists of three initially separate components, which are put together to form the whole sandwich element. This is shown in figure (7.2) where the quadratic element appears showing its three components : upper face, core and lower face. The two faces are identical. Each has six nodes, (three corners and three mid-side nodes). Each node has two degrees of freedom, mutually at right angles, in the plane of the element. The core has twelve nodes, six top and six bottom, the latter initially perpendicularly below the former. Each node has two in-plane freedoms which correspond to the two freedoms of the face element. The top nodes only have a transverse freedom. In effect, this means that the element really has six compound nodes, each having five degrees of freedom, but the original conception of the element was in the form described and the element assembly routines in the programmes still treat it in this way, though the current forms of the programme assemble the total element first from its three components.

7.2 Beams' deflection profiles

From the computer output which gives the transverse displacement of the elements at their nodes (corners and mid-side node) the profiles of the beam centre line deflections are shown for three different cases in figures (7.3, 7.4 and 7.5). Each figure includes three graphs typical of the three core mixes used with the defined face. The values of the deflections at both midspan and the loaded point and which were recorded from the experimental procedure are illustrated also in each case, and an approximate diagram for the profile of the experimental

deflection is plotted in an attempt to show the variations of the beam centre line deflection both experimentally and theoretically in this method of theoretical study.

The analysis and discussion of the results of tests on the concrete sandwich beams reported in chapter 6, indicated that the lower face modulus and ultimate strength are the most important parameters affecting the beam deformation and strength. It was concluded that the weakness of the face in tension, both modulus of elasticity and strength, is the most sensitive factor affecting the characteristics of the concrete sandwich beams studied in this project. To confirm such conclusions and to show how much the modulus of elasticity of the face in tension affects the beam deflection, using the finite element method, some computer programmes were run to give the transverse vertical displacement of points along the beam centre line. For some cases, the tension modulus of the tension face in the beam is assumed equal to the face's compression modulus. From the computer output the profiles of the beams' centre line deflection (or vertical displacement) were plotted, figures (7.3, 7.4 and 7.5), the same graphs being used to show the behaviour of beams with faces of different modulus and similar beams but with the same modulus for both faces.

The results of the beams made using face S_1, of the lowest reinforcement and moduli (of A_s = 41 mm^2.), are shown in figure (7.3) with a deflection profile for each of the three core mixes used. All the three graphs shown in the figure indicate that the deflection diagrams based on the experimental results are of lower values than the values given by the theoretical method. With this face (S_1), the experimental values are less than the

theoretical by the following per cent : at midspan 14, 8 and 12.5; and at loaded points : 17, 9 and 16 respectively for the three core mixes used (G_1, G_2, and G_3). The theoretical deflection diagrams given for similar beams with the assumption that the face has tension modulus equal to its compression modulus ($E_{Ft} = E_{Fc} = 23.4 \times 10^3$ N/mm^2. i.e. isotropic face). are shown by the dotted lines in the graphs, and were found to have lower values of deflection everywhere on the span. The comparison between the two theoretical curves of deflection, given by the finite element method, indicate that using an isotropic lower face, the deflection in the three core mixes was approximately 55, 58 and 60 per cent the values of the deflection for these beams with their faces of different moduli.

The graphs in figure (7.4) were plotted also to show the comparison for the beams which were made using face S_5 (of $A_s = 67$ mm^2.). It can be seen from the graphs in this figure for the beams having faces of different moduli, that the variation between the experimental and theoretical deflection is seen most obviously in the case of the core of the lowest modulus (core G_1), where the experimental results are considerably less than the theoretical value. The deflection values with this core, which were obtained from the experimental procedure at both midspan and the loaded point respectively, are 16.7 and 18 per cent less than the theoretical values obtained by finite element method. In the results of the beams cored by the other two core mixes (Mixes G_2 and G_3) the variations, especially at midspan, are very small and may be considered negligible, and at the loaded point are less than 10 per cent in these cases. (The values are illustrated in the diagrams in figure 7.4). However, the experimental and theoretical curves of deflection

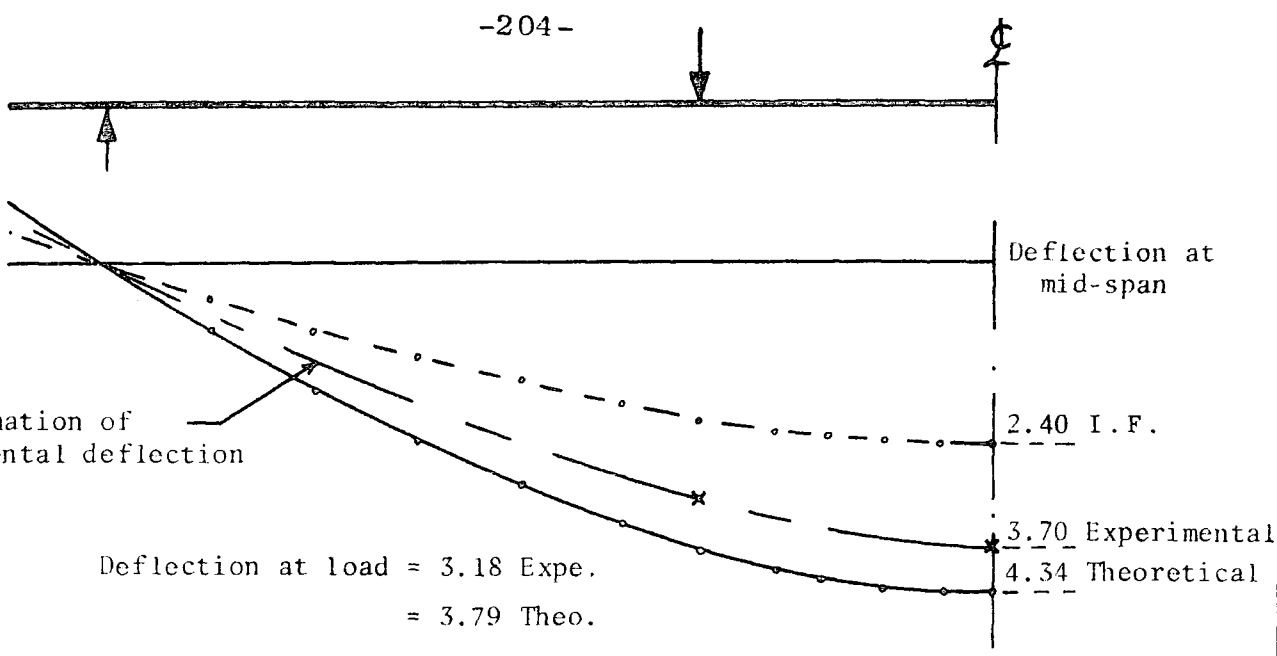

Fig. (7.3a) : Beams of core G_1

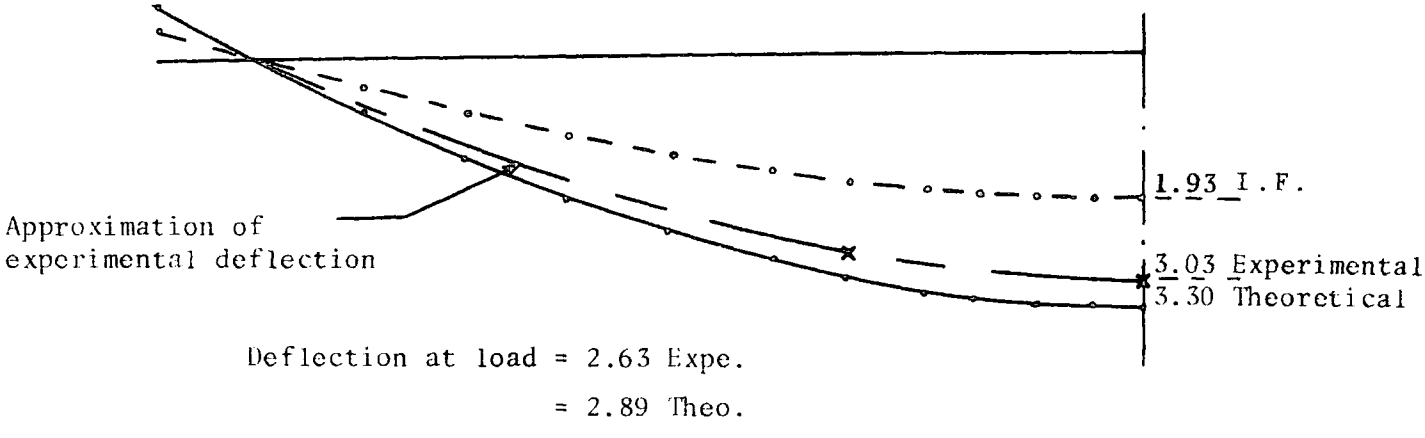

Fig. (7.3b) : Beams of core G_2

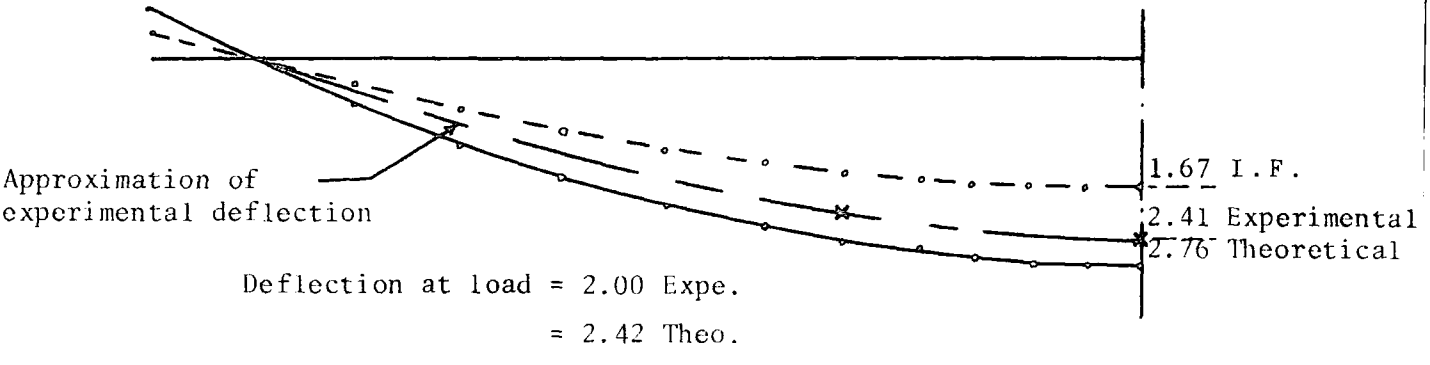

Fig. (7.3c) : Beams of core G_3

Figure (7.3) : Profile of beams' deflection experimentally, and theoretically by finite element method, for beams made using face S_1 (of A_S = 41.0 mm^2.); the dotted lines are given for beams of isotropic faces (labelled "I.F.")

(All values of deflection recorded are per unit load ($\frac{mm}{N}$.) x 10^{-4})

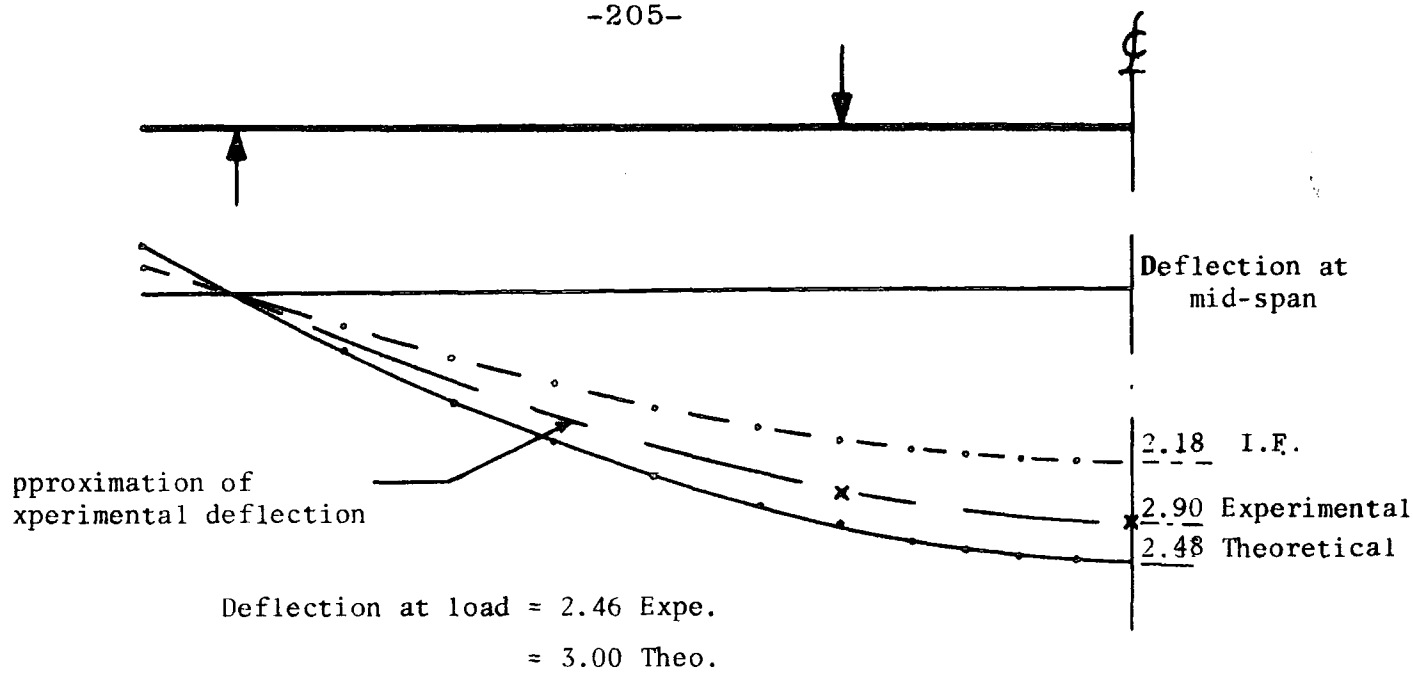

ig. (7.4a) : Beams of core G_1

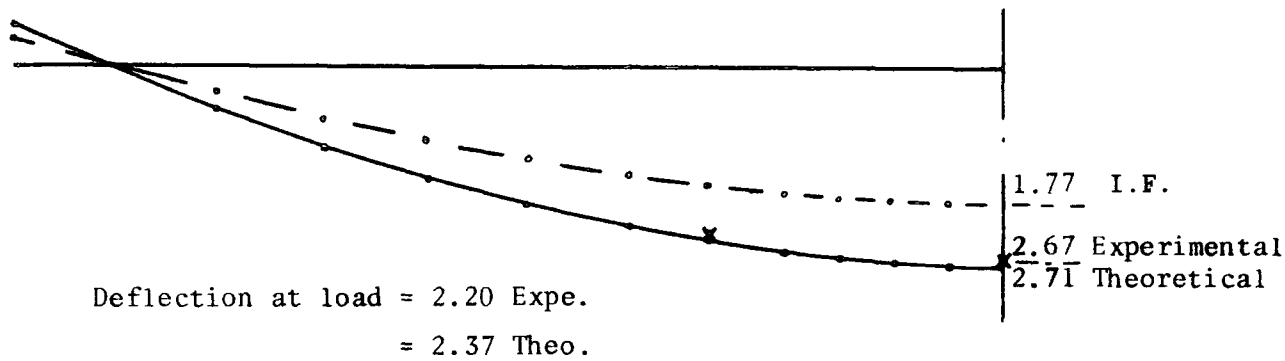

ig. (7.4b) : Beams of core G_2

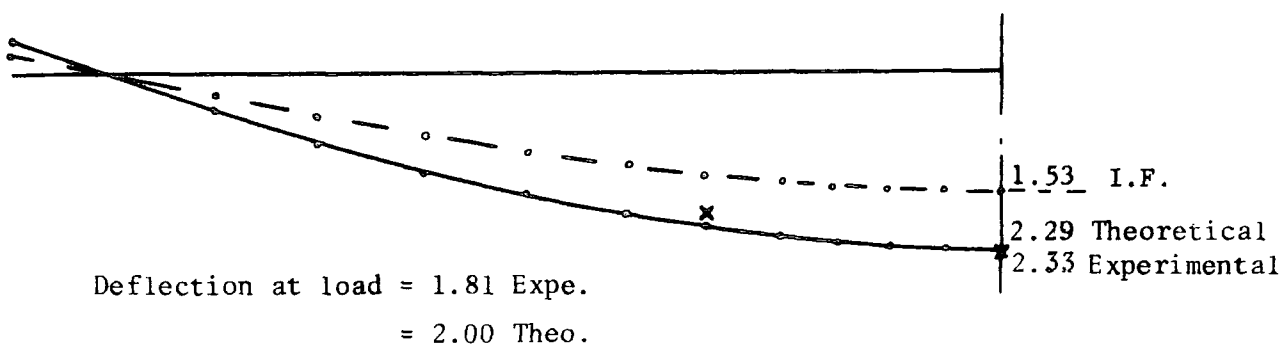

ig. (7.4c) : Beams of core G_3

gure (7.4) : Profile of beams' deflection experimentally, and theoretically by finite element method, for beams made using face S_5 (of A_s = 67.0 mm^2.); the dotted lines are given for beams of isotropic faces (labelled "I.F.")

(All values of deflection recorded are per unit load ($\frac{mm.}{N}$) x 10^{-4})

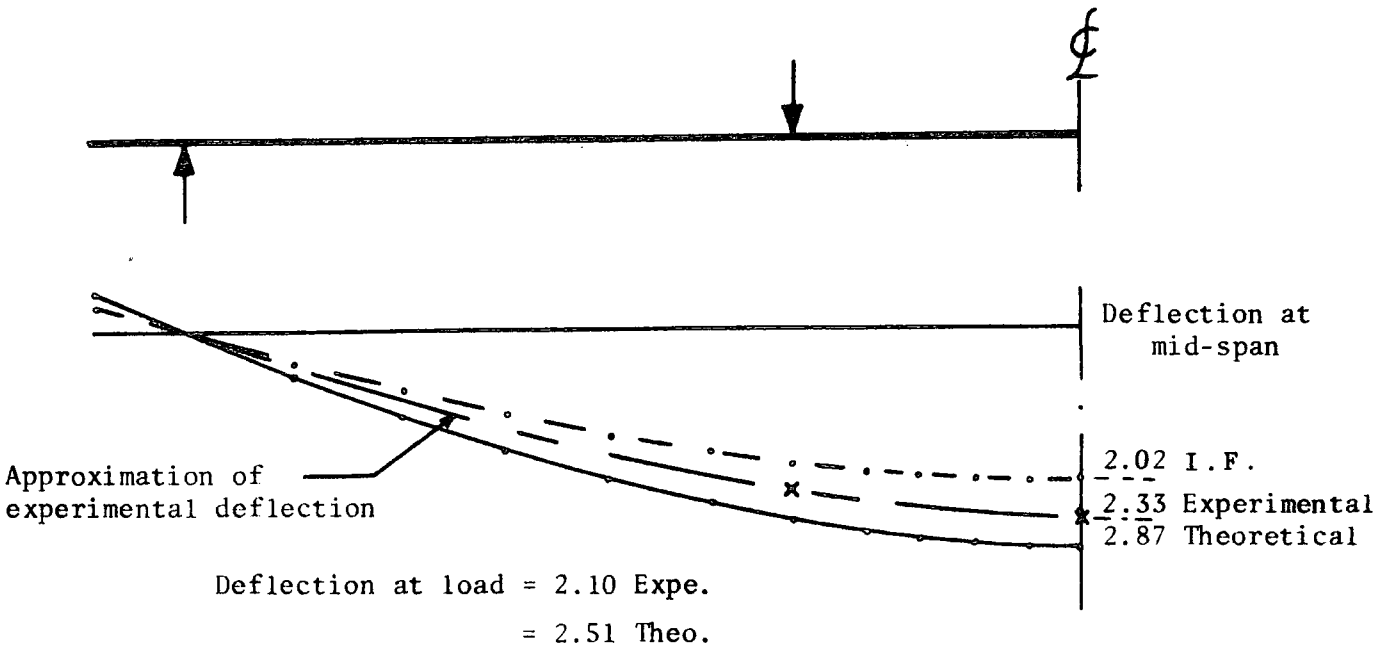

Fig. (7.5a) : Beams of core G_1

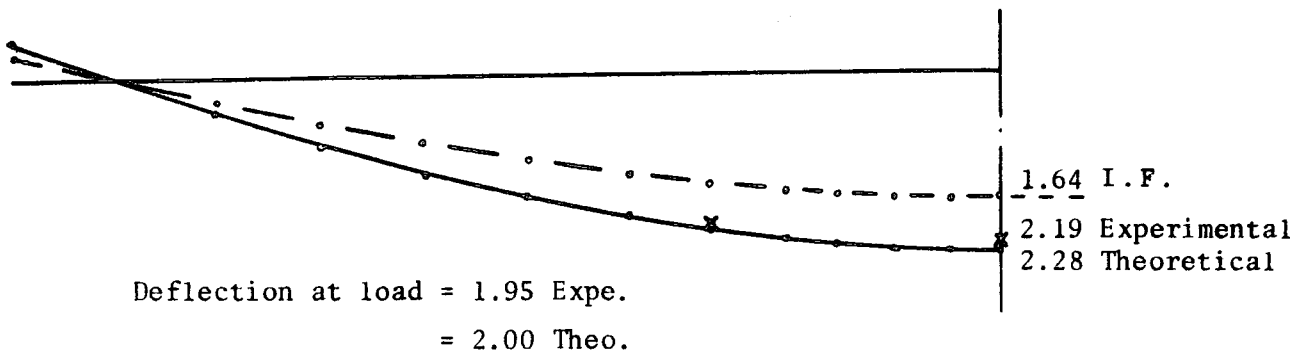

Fig. (7.5b) : Beams of core G_2

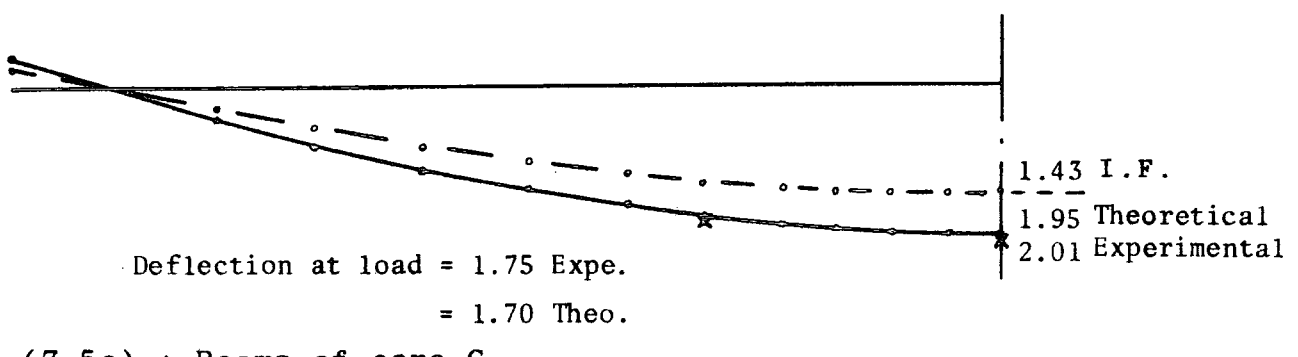

Fig. (7.5c) : Beams of core G_3

Figure (7.5) : Profile of beams' deflection experimentally, and theoretically by finite cement method, for beams made using face S_7 (of $A_s = 103.3\ mm^2$.); the dotted lines are given for beams of isotropic faces (labelled "I.F.").
(All values of deflection recorded are per unit load $(\frac{mm}{N}) \times 10^{-4}$)

of the beams made by these two core mixes are in close agreement with each other. From the two theoretical deflection diagrams of each core used with this face the deflections with two faces of modulus equal to the face's compression modulus (isotropic) is reduced to the values 63, 65 and 66 per cent the deflection values in the normal case for the three core mixes respectively.

The results of the beams made using face S_7 (of A_s = 103.3 mm^2.) were plotted in figure (7.5). The variation between the deflection diagrams of the theoretical and experimental results of these beams seems more to resemble the data given by the beams made using face S_5 and which were described in the previous paragraph. Equalization of the tension modulus of the lower face to the compression modulus of the upper face produce theoretical results of deflections of values 70, 72 and 73 per cent the deflection given using faces of the modulus as used, respectively for the three core mixes used with face S_7.

According to the work carried out in this section and the results presented here, the following points can be noted:-

1. a - The theoretical results obtained by the finite element method indicated that increasing the face modulus in tension to equal its modulus in compression would give a beam likely to have the same as or less deflection than the beam cored by a mix having three times the shear stiffness.

   b - The reduction in the deflection values become greater due to that equalization when the variation between the face moduli is greater (see figures 7.3a and 7.5a).

   c - This theoretical study was found to confirm the conclusion

which had been stated previously in chapter 6, that the tension modulus of the lower face is the most initial parameter affecting concrete sandwich beams (see section 6.2.2.2).

2. The deflection behaviour at the loaded point has not much more variation than at the midspan deflection. The experimental values at the loaded point are relatively smaller than at midspan. This may be attributed to the tendency for the bending stiffness of the faces themselves to smooth out the transition from centre section to shear span.

3. The variation between the experimental and theoretical deflection according to this method of analysis seems likely to be variable or changeable from one core to another. Because it may also be affected by the face used, the next section is introduced in order to find out with more reliability what, in fact, can be deduced for such kinds of sandwich beams using these methods of analysis.

7.3 Midspan deflection

The analysis carried out in this section, as mentioned before, aims to show clearly the evidence of the variations between the experimental and theoretical deflection of the sandwich beams at midspan. The averaged values of the deflection measured at midspan in the experimental procedure were compared with those given theoretically by finite element method at the same point. The comparison is presented in resemblance to the way of the comparison which were carried out before in section 6.2.2.2 of chapter 6. In this way the results of all beams made using the same core were put - or inserted - in one graph together. So,

figures (7.6, 7.7 and 7.8) were drawn to show that comparison for the three core mixes G_1, G_2 and G_3 in the same sequence.

The variations between the theoretical values of the deflection and those experimentally obtained are seen with core G_1 to be of greater value for all faces used (figure 7.6) than when the other two core mixes were used (figures 7.7 and 7.8). In the results of the beams cored by core mix G_1, the difference between the theoretical and experimental deflection seems approximately constant for all sets made. In the results of beams made using core G_2 (figure 7.7), the first three sets are seen to have the higher variation in this group, but generally the variation for this group is relatively small. From the diagrams, figure (7.8) which were plotted to show the comparison for the beams cored by the strongest core (G_3), it can be seen that the two diagrams (the experimental and theoretical) are in close agreement. The only case which may seem strange, in this group, is the result for the beams made using the face of the lower reinforcement, where the variation between the experimental and theoretical value was found to be greater than usual for cases in this group.

The results and comparison carried out indicated that the deflection obtained experimentally from the beams of the groups which were made using cores G_1 and G_2 are generally of values less than those obtained by theoretical method. The results of the beams of the third group (made by core G_3) are a reversal of this. However, the values of both experimental and theoretical deflection for all the beams are listed in table (7.1) according to the core mix used and the area of reinforcement in each face. The errors of the experimental results were calculated as per-

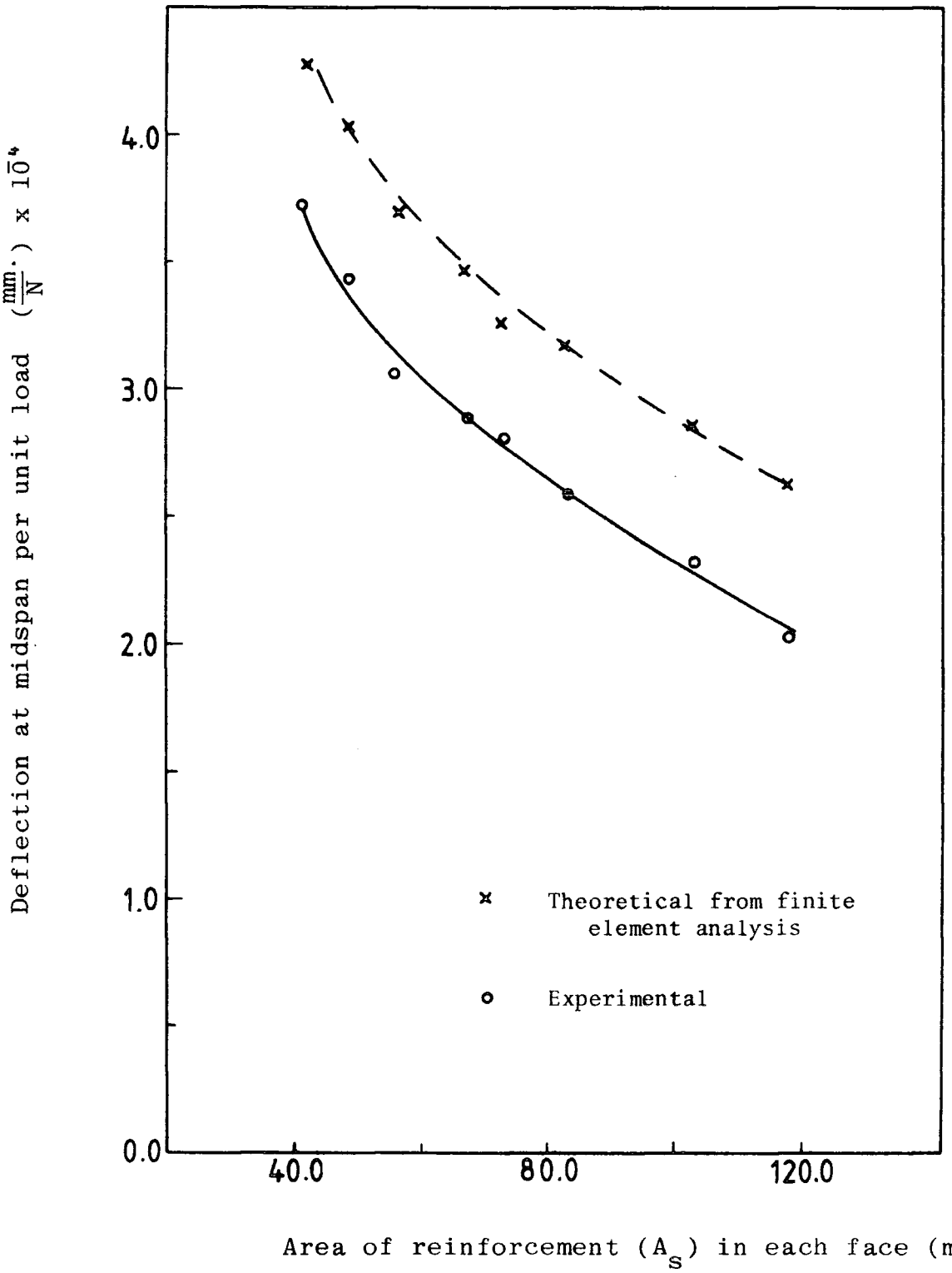

Figure (7.6) : Beams' deflection at midspan per unit load, experimentally and theoretically from finite element analysis, according to the area of reinforcement in each face.

(Beams made using core mix G_1)

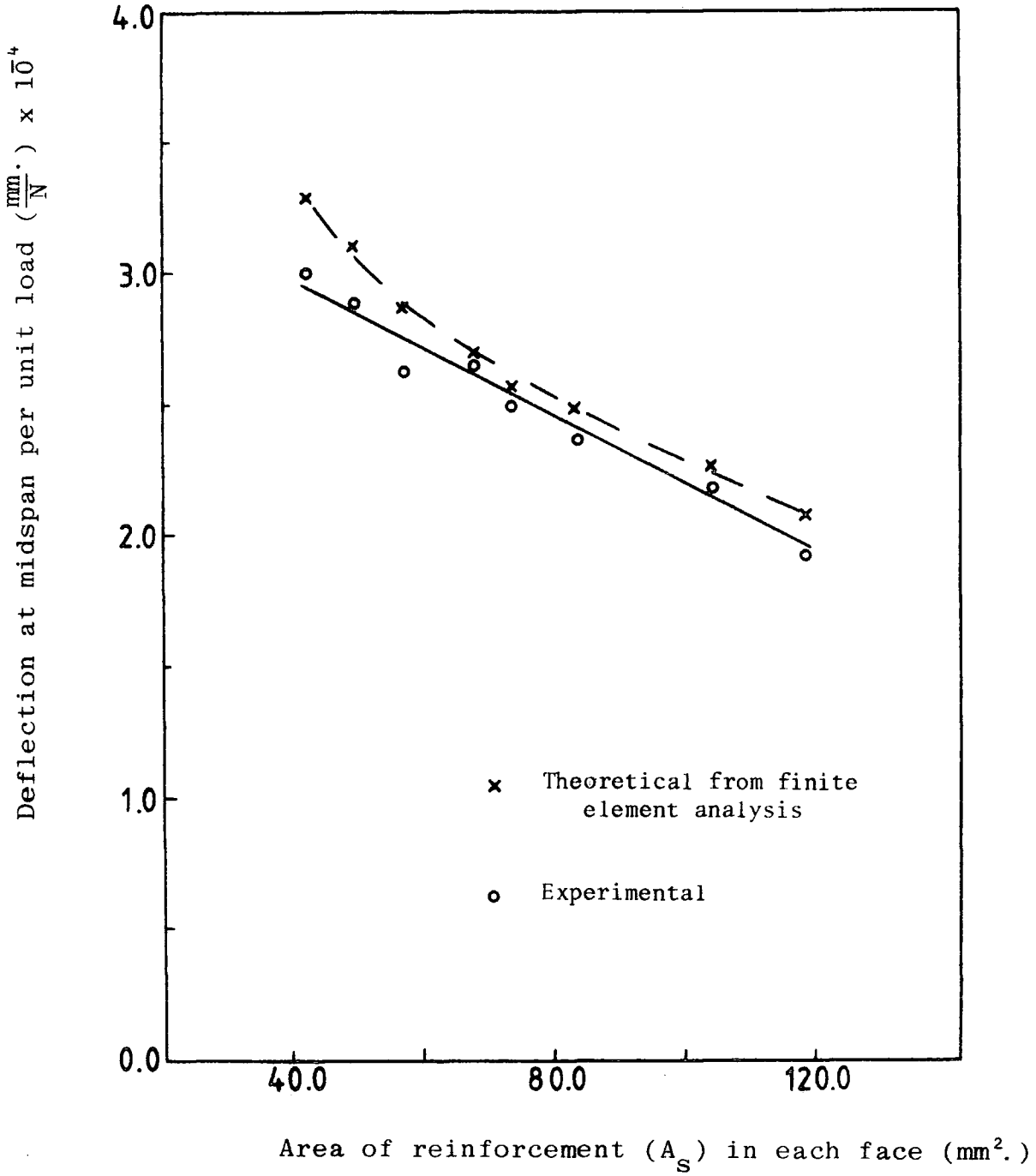

Figure (7.7) : Beams' deflection at midspan per unit load, experimentally and theoretically from finite element analysis, according to the area of reinforcement in each face.

(Beams made using core mix G_2)

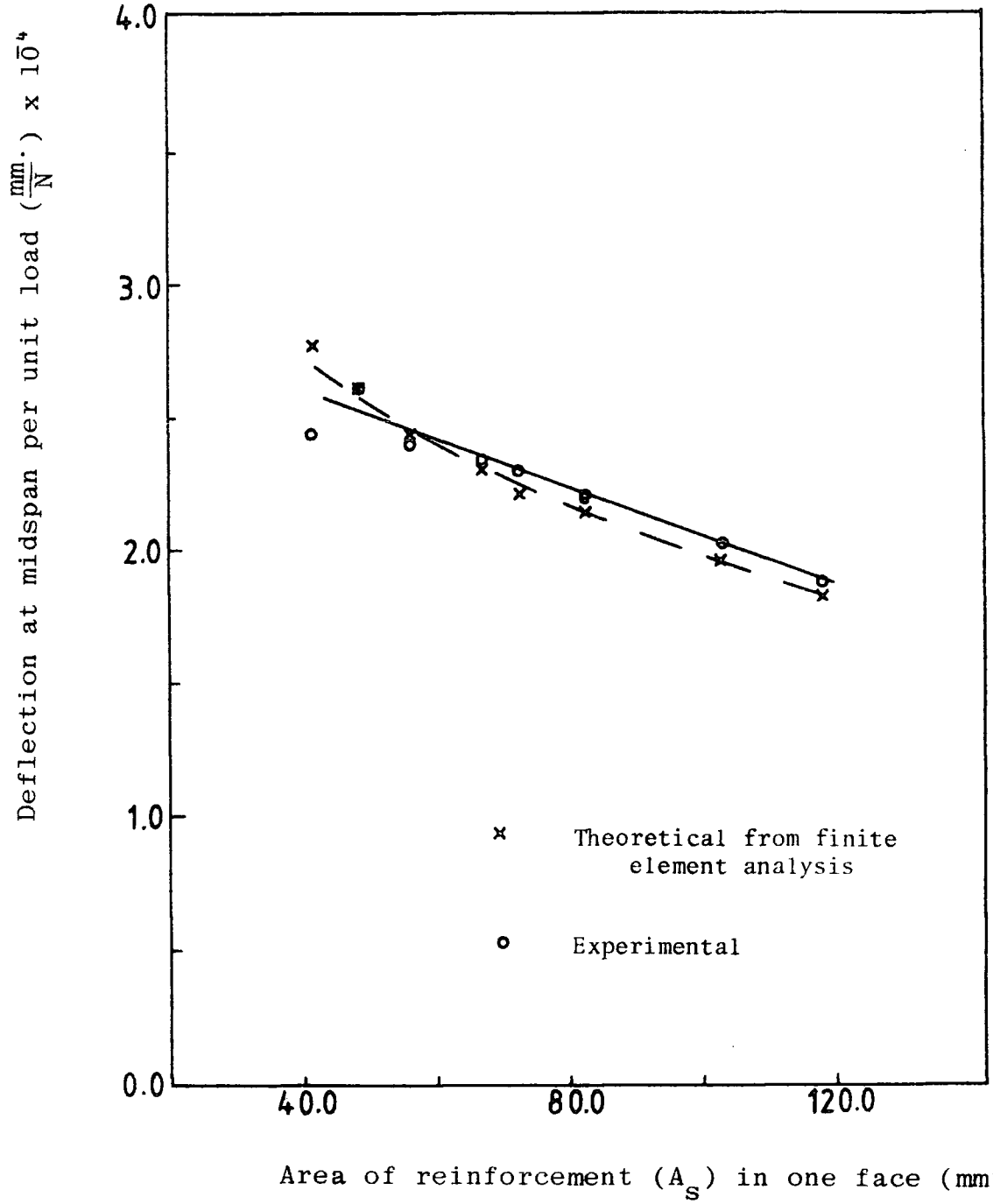

Figure (7.8) : Beams' deflection at midspan per unit load, experimentally and theoretically from finite element analysis, according to the area of reinforcement in each face.

(Beams made using core mix G_3)

centages of the theoretical values and recorded also in table (7.1).

From the comparison carried out and the error values (table 7.1), it can be deduced:-

1. The difference between the deflections obtained from the laboratory procedure and the theoretical one given by the finite element method on the computer, specially the beams cored by core G_2 and G_3, are within the error limits.

2. The higher values of error were found in the results of the beams made by core G_1, and because the error is approximately constant in all cases, it may be attributed to the approximation assumption in the programme which supposes the core only to resist the shear. In fact, the faces take part in shear resistance, and since the core G_1 is the weakest one in relation to the faces, the error then became greater.

Table (7.1) Deflection per unit load ($\frac{mm}{N}$) at midspan, experimental and theoretical by finite element method, and error as a per cent of the theoretical values.

A_s in each face (mm^2.)	Beams made using Core G_1			Beams made using Core G_2			Beams made using Core G_3		
	Deflection x 10^{-4}		Error %	Deflection x 10^{-4}		Error %	Deflection x 10^{-4}		Error %
	Experimental	Theoretical		Experimental	Theoretical		Experimental	Theoretical	
41.0	3.70	4.34	14.0	3.03	3.30	8.0	2.41	2.76	12.7
48.3	3.43	4.07	15.7	2.90	3.12	7.0	2.60	2.61	-
56.0	3.07	3.72	17.0	2.65	2.88	8.0	2.39	2.43	1.1
67.0	2.90	3.48	16.7	2.67	2.71	1.5	2.33	2.29	-1.7
72.5	2.82	3.27	13.7	2.50	2.57	2.7	2.29	2.18	-5.0
82.6	2.60	3.19	18.0	2.38	2.50	4.8	2.18	2.13	-2.3
103.3	2.33	2.87	18.0	2.19	2.28	3.9	2.01	1.95	-3.1
118.0	2.04	2.60	21.0	1.93	2.19	7.6	1.85	1.80	-2.7

CHAPTER EIGHT

CONCLUSIONS

The advantages possessed by both sandwich construction and cement concrete suggest the desirability of the application of sandwich elements in concrete structures. This was not achieved, in the past, due to the difficulties of producing a lightweight concrete which has the characteristics to satisfy the requirements for the core of a sandwich, such as homogeneity through the depth, low density, good bond with the face and reasonable shear stiffness.

Concrete sandwich beams of two thin faces having the same reinforcement, each 10 mm. in thickness, on the top and bottom of a core of 100 mm. thickness, made from lightweight concrete (polystyrene bead-concrete), were constructed and studied in this project. The conclusions drawn from the work carried out in this research on core material, faces and sandwich beams are summarized in the following sections:

8.1 On the core material

Using specified sizes of expanded polystyrene beads, a programme of testing has made possible the development of a design procedure which permits the production of polystyrene bead-concrete of the required density and strength for the core of concrete sandwich construction. The beads were used as aggregates for the purpose of producing what, in effect, are spongy voids in the cement paste, filling the majority of the core. This lightens the weight and improves the insulation characteristics of the sandwich element.

The density of the beads, which is much lower than that of the cement paste, causes problems in both mixing and casting procedures. It is difficult to produce homogeneous samples when the material is in a workable state. This necessitated the development of some special techniques in the design and handling of bead-concrete. One useful development was the addition of a filler material of low density and of a relatively high flexibility and resilience, so as to limit the brittleness of the final product concrete. The sawdust, of a suitable size, was found to be satisfactory in this respect.

8.1.1 In mixing, an adequate method has been achieved by putting the mix ingredients (beads, sawdust and cement) in the dry state into a pan mixer with about a third of the necessary water and adding the remaining water during the first 30 second of mixing. A total of three minutes of mixing was needed to produce a consistent material.

8.1.2 In casting, satisfactory compaction cannot be achieved either by the application of a large compressive force or by tamping, since both techniques distort the form of the beads. Successfully compacted samples have been made using a suitable constraining force accompanied by short bursts of mild, high frequency compaction.

8.1.3 The properties of the bead-cement mix and the resulting concrete have been classified according to the beads' size and the quantities of water, sawdust and cement used, and the following is a summary of these achievements:

(i) The use of beads of smaller sizes cause some increase in

workability, as might be expected, and improves the concrete characteristics, tending to improve strength and homogeneity.

(ii) The addition of sawdust to the mix should be constrained by the quantity which is required just to maintain the workability and homogeneity.

(iii) The density, compressive strength, modulus of elasticity and shear modulus of bead-concrete of specified bead size, and suitable in consistency to give adequate workability with the regime of the constrained compaction (about 6 kg./cm^2.), depend mainly on the cement content. For two specified bead sizes, these structural properties were expressed by empirical formulae which were based upon many test results obtained from laboratory procedures.

8.2 On faces

Several samples from the thin concrete faces (10 mm. thickness) used in the sandwich beams, which were made of fine concrete of high modulus and reinforced by expanded steel meshes, have been made and examined in laboratory procedures. In the context of this research, the object was to determine precisely the face moduli and strengths in both tension and compression and also the bending stiffness according to the mesh size or dimensions and the reinforcement content. This was needed to provide accurately the data used in the sandwich beams' analysis, and to determine what are the effects on the properties of such concrete faces. In the context of the laboratory results obtained, one may draw the following conclusions:

8.2.1 The face characteristics in compression, i.e. modulus of elasticity and strength, are much better than in tension when the same reinforcement is used in both cases.

8.2.2 Increase in the modulus of elasticity of the face due to increase in the reinforcement content is more noticeable in tension than in compression.

8.2.3 The bending tests on this type of concrete faces exhibited that they have a high resiliency, and their bending stiffness depends on the position of the reinforcement in the face cross-section and the width of the mesh as well as the reinforcement content.

8.3 On sandwich beams

Several sets of concrete sandwich beams having cross-sections of 120 x 120 mm. were constructed and tested in the simply supported state by means of a four point loading system, which divided the effective span to three equal parts, each 380 mm. in length. Taking account of the wide disparity between the densities of the faces and of the core materials, using a special manufacturing technique developed in the laboratory, beams of repeatable characteristics were made quite easily. The sets were designed to have a wide range in the relationship between the face and core moduli, where three core mixes of different moduli and strength were used with each one of eight degrees of reinforcement used in the faces.

This, in fact, has been done in order to classify the characteristics and behaviour of such sandwich beams according to the variations between the beam bending and shear stiffnesses.

8.3.1 Conclusion from comparisons of the test results with analysis using the theory of sandwich beams are:

(i) The characteristics of the face in tension, modulus of elasticity and maximum strength, are the most important initial parameters affecting the deformation and failure of these sandwich beams.

(ii) According to the results obtained experimentally from measuring the beams deflection and face strains and their comparison with the values given by the theory, the agreement between them is affected by the ratio between the bending and shear stiffnesses. A possible expression for this ratio, which includes the modulus of the tension face, has been suggested. This defines the range of values of experimental and theoretical results which are in close agreement.

8.3.2 The analysis carried out by the finite element method, leading to the results reported in the last part of this thesis, suggest the following conclusions:

(i) According to the theoretical results for the beams studied, the same decrease in deflection as would be achieved by increasing the core modulus by three times could be achieved by making the tension face modulus equal to the compression modulus.

(ii) If the weak core has enough shear strength to satisfy the load resisted by the isotropic faces, it is advisable to replace the weaker face by the isotropic one instead of using a stronger core. This is to maintain the sandwich

beam's lightweight and good insulation characteristics.

(iii) The comparison of the experimental and theoretical deflection in this type of theoretical analysis seems generally compatible with error in the experimental range. If the error is increased in some cases, it may be due to the approximation assumptions in neglecting the direct-strain modulus of the core and the shear contribution of the faces.

8.3.3 On the whole the concrete sandwich beams constructed and studied in this research had good performance in both stiffness and strength-to-weight ratios (their densities, in the saturated state were in the range between 0.9 and 1.15 t/m^3. according to the core mix used).

8.4 Further research

Since the failure and weakness in bending stiffness of the sandwich beams of such thin reinforced faces was found to be caused due to the weakness of the face in tension, the following suggestions are made to guide any subsequent work:-

(1) The beams' characteristics will be improved by using tension faces of higher moduli. This can be realized by either an increase in the reinforcement content or an improvement in its orientation, or by pre-stressing the tension face.

(2) In the context of the failure results, constructing sandwich slabs using similar techniques and two-way reinforcement will be relatively more efficient than the beams. Longitudinal strain concentration in the lower face is less likely to cause a horizontal shear failure in a slab due to the supports being in

two directions.

(3) Beams and slabs of different dimensions, loading and reinforcement need to be constructed and to be studied to give more data for dealing with such sandwich constructions commercially as loaded elements. Anchorage of the reinforcement of the tension face is recommended.

(4) Methods for measuring, precisely, the consistency of the polystyrene bead-concrete are needed.

(5) The mechanism of this type of face, particularly in tension, needs to be studied to establish an understanding of the effects of the diamond mesh, in particular its mesh size and strand width, on the elastic properties and ultimate behaviour of the face.

(6) Finally, data is required about the heat conductivity of such sandwich constructions, their performance as sound insulators, and their performance when exposed to fire hazards.

However, the work reported here shows that such structural elements may be produced, having predictable stiffness and strength characteristics, and very good strength-to-weight ratio.

REFERENCES

1. ALLEN, G.H. "Analysis and design of structural sandwich panels", Pergamon Press Ltd., London, 1969.

2. ANON, T. "Tentative methods of testing for determining strength properties for core materials for sandwich construction", Forst Products Laboratory report 1555 Dec. 1946, Oct., 1948.

3. BENJAMIN, B.S. "Structural design with plastic" Van Nostrand 1969.

4. BREBBIA, C.A. and CONNOR, J.J. "Fundamental of Finite element techniques", Butterworth & Co., (Publishers) Ltd., London, 1973.

5. BAUMANN, H.G. and SUSMAN, V. "Expanded, polystyrene beads lighten the load" SPE Journal March 1972, vol. 28, pp.18-21.

6. BRITISH STANDARD 3797 Part 2, 1976, Specification for lightweight aggregate for concrete.

7. BRITISH STANDARD 3681 Part 2, 1973, Method for sampling and testing of lightweight aggregates for concrete.

8. BRITISH STANDARD 1881 Part 1, 1970 Method of sampling and testing of lightweight aggregates for concrete.

   Part 3, 1970 Methods of making and curing test specimens.

   Part 4, 1970 Methods for testing concrete for strength.

9. BRITISH STANDARDS INSTITUTION. The structural use of concrete Part 1 : Design, materials and workmanship. London, CP 110 Part 1 : 1972.

10. CASE, J. and CHILVER, A.H. "Strength of materials and structures", Edward Arnold, London, 1971.

11. COLLINS, D.L. "An experimental and analytical study of hyperbolic paraboloid sandwich panels", Ph.D. thesis, University of Durham 1977.

12. DESAI, S.C. and ABEL, J.F. "Introduction to the finite element method", Van Nostrand 1972.

13. ELVERY, R.H. and SAMARAI, M.A. "The influence of fibres upon crack development in reinforced concrete subject to uniaxil tension", Magazine of concrete research : vol. 26, No. 89 : December, 1974.

14. ELVERY, R.H. and SAMARAI, M.A. "An examination of the behaviour of fibres in reinforced concrete" compo. July 1976, pp.180-184.

15. ELLIOTT, D.J. "The structural properties of flat sandwich panels" M.Sc. University of Durham, 1970.

16. EDLIND, O. "Some properties and practical aspects of hardened aerated concrete" Proc. 1st Int. Congress on lightweight concrete vol. 1, pp. 65-75 (London, cement and conc. Assoc. May 1968).

17. EXPAMET INDUSTRIAL PRODUCTS LIMITED "Expamet expanded steel and expanded aluminium" leaflet No. IP2, March 1976.

18. FOLIE, G.M. "The theory of sandwich panels subjected to transverse loads under various Edge conditions", Dept. of Civil Eng., University of Southampton.

19. HANSON, J.A. "American practice in proportioning lightweight aggregate concrete", Proc.1st Int.Congress on lightweight concrete vol.1 pp. 39-54 (London May, 1968).

20. HENAGER, C.H. and ASCE, M. "Analysis of reinforced fibrous concrete beams" J. of the structural division, pp.177-187 Jan. 1976.

21. HOFF, N.J. and MAUTNER, S.E. "Bending and buckling of sandwich beams" The J. of Aeronautical (or Aero space) Sci. vol. 15, pp.707-720, Dec. 1948.

22. HOLLAWAY, L. "Glass reinforced plastics in construction", p. 89-117 Surrey University 1978.

23. KLUGE, R.W. "Structural lightweight aggregate concrete" J. Amer Concrete Institution 53,pp.383-402, (Oct.1956).

24. KOMMERS, W.J. "Strength properties of plastic honeycomb core materials" Forst Products Laboratory U.S.A. Report 1805, Dec. 1949.

25. MARKWARDT, L.J. and WOOD, L.W. "Case study of sandwich panel construction in Forst Products Laboratory U.S.A. Report 2165, Oct.1959.

26. MAKOWSKI, Z.S. "A history of plastics used in structures throughout the world" plastic in building, January 1965.

27. MURDOCK, J.W. and KESLER, C.E. "Effect of length to diameter ratio of specimens on the apparent compressive strength of concrete" A.S.T.M. Bul., pp.68-73 (April 1957).

28. NEVILLE, A.M. "Properties of concrete" Pitman Publishing Limited, London, 1977.

29. ONG. K.H. "Silicate stabilization of soft granular materials for sandwich plate cores" M.Sc. University of Durham 1979.

30. PARTON, G.M. "The structural behaviour of polyhedral sandwich shells" Ph.D. thesis University of Durham, 1974.

31. PLANTEMA, J.F. "Sandwich construction" John Wiley and Sons Inc. U.S.A., 1966.

32. PRICE, W.H. "Factors influencing concrete strength" J. Amer. concrete Institution. 47. pp. 417-432 (Feb. 1951).

33. SAGLAM, B. "The properties of fibre reinforced cement based sandwich beams" M.Sc. thesis, University of Durham, 1976.

34. SHIDELER, J.J. "Lightweight aggregate concrete for structural use". J. Amer. concrete Inst. 54, pp.299-328 (Oct. 1957).

35. SHORT, A. and KINIBURGH, W. "The structural use of aerated concrete" The struct. E., 39 No.1 pp.1-16 (London, Jan. 1961).

36. STEVENS, G.H. and KUENZI, E.W. "Mechanical properties of several honeycomb cores" Forst Products Laboratory report 1805 (July, 1962).

37. SWAMY, R.N. "Testing and test methods of fibre cement composites" The construction Press Ltd., Lancaster, England, 1978.

38. SWAMY, R.N. "Arch action and bond in concrete shear failures" The Journal of the structural division pp. 1069-1089, June, 1970.

39. THOM, P.W. "Feasibility study of a sandwich material composed of glass-fibre reinforced and aerated concrete". Project, University of Durham, 1971.

40. TECHENNE, D.C. "Lightweight aggregate; their properties and use in the United Kingdom, proc. 1st Int. Congress on lightweight concrete vol. 1 pp.23-37 (London, cement and concrete Assoc. May, 1968).

41. VOSS, A.W. "Mechanical properties of some low density materials and sandwich cores" Forst Products Laboratory report 1826, March 1952.

42. WERNER, G. "The effect of type of capping materials on the compressive strength of concrete cylinders" proc. A.S.T.M., 24, 58 pp. 1166-1181 (1958).

43. WOOD, L.W. "Sandwich panels for building Construction", Forst Products Laboratory U.S.A. Report 2121, Oct. 1958.

44. WOLF, J. "Private letter" Ref. JW/JG The expanded metal manufacturing Company Ltd., Hartlepool, 3rd August, 1979.

45. WRIGHT, G.L. "The properties of expanded steel reinforced sandwich beams" project, University of Durham, 1977.

46. WILLIAM, B. "Polystyrene beads, expanding and processing". Statement, private delivery, ACI factory, Wideopen, Newcastle-on-Tyne.

APPENDICES

Appendix (I.a) : Determining bulk specific gravity of beads type (2) and volume of the voids between them

Weight of dry beads filling the flask till the filter (A) = 18.0 gm.

Volume of water filling the flask till the filter (W) = 1112.0 cm^2.

Volume of water was added to the beads with kerosene surrounding the beads (V) = 423.0 cm^3.

Bulk specific gravity = $\frac{A}{W-A} = \frac{18}{1112-423}$ = 0.0262 gm./cm^3.

$\simeq$ 26.2 kg./m^3.

Volume of the voids between beads

$= \frac{423}{1112} \times 100$ = 38%

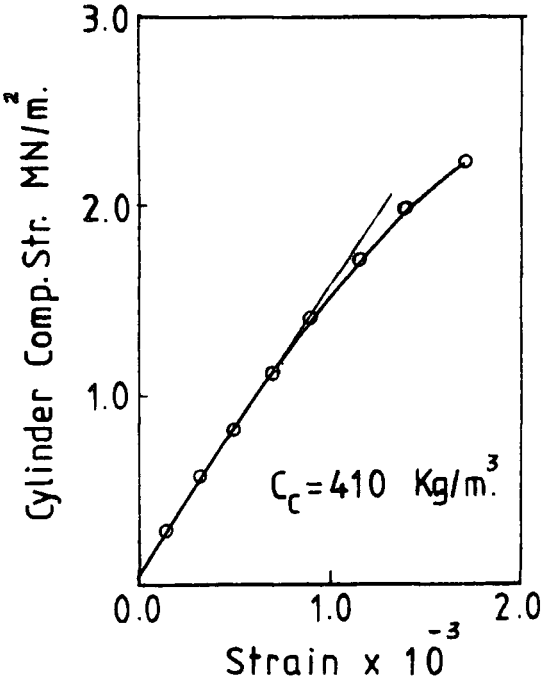

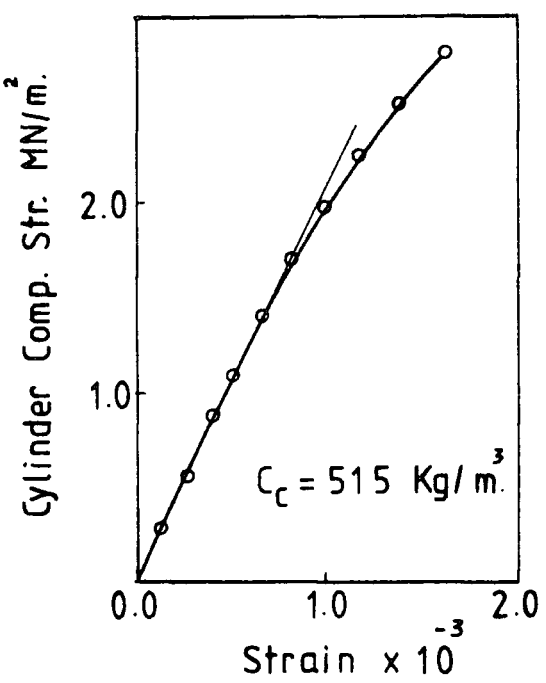

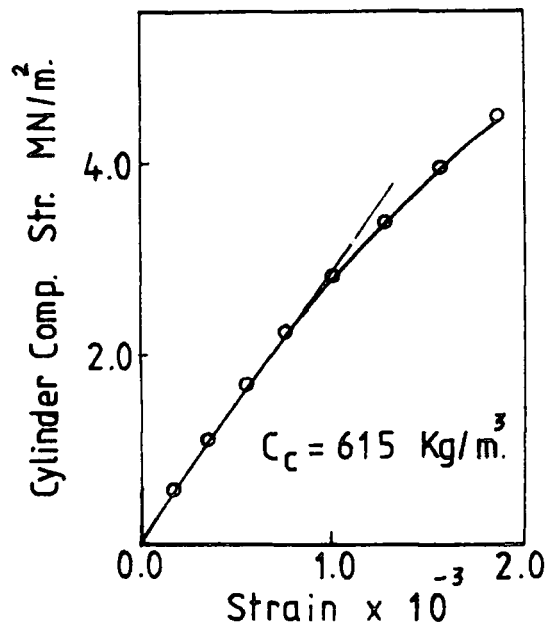

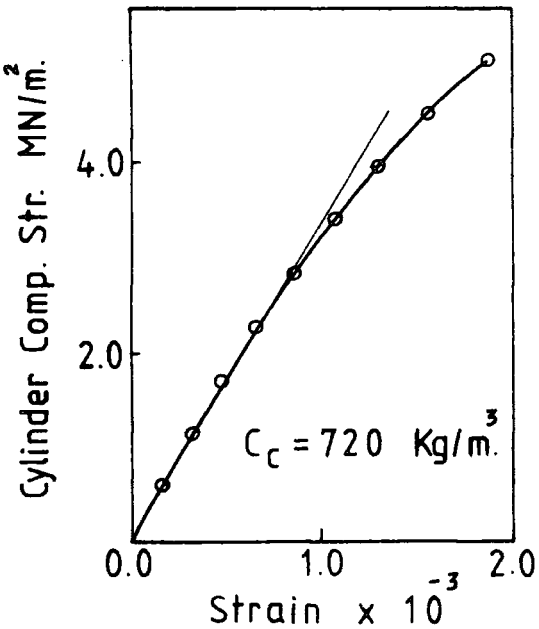

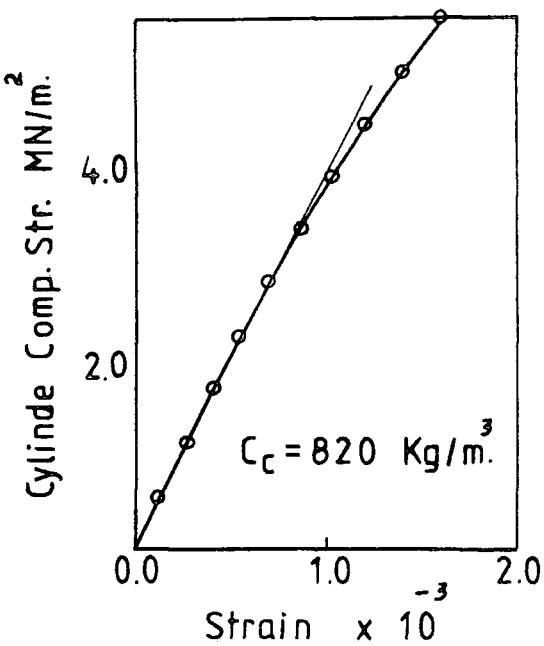

Appendix (I.b) Relationship between compression stress and strain for some samples of polystyrene concrete made from beads type 2 (group II) according to cement content (C_c) used.

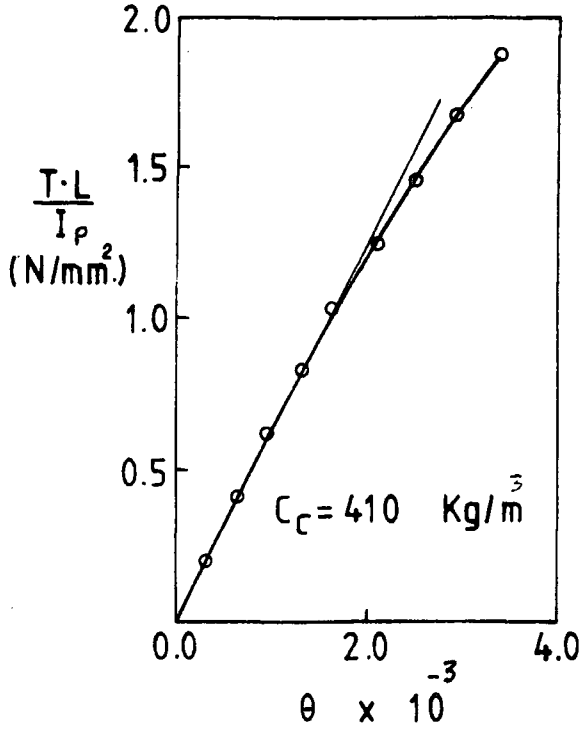

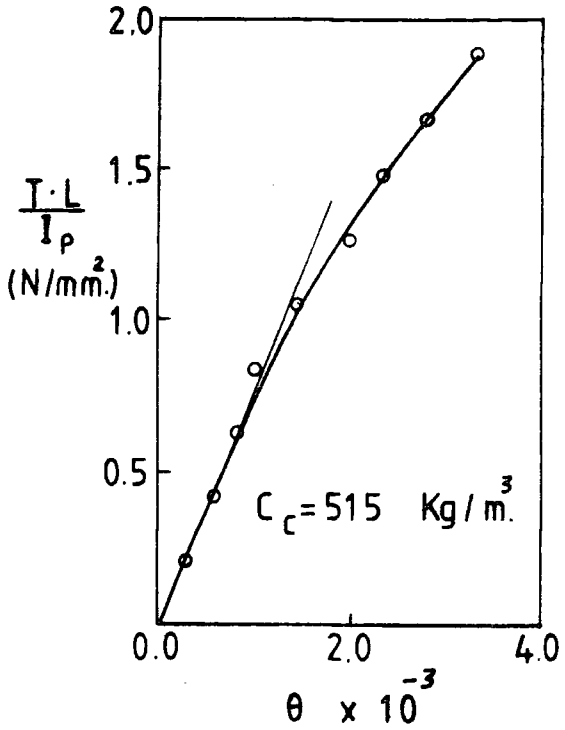

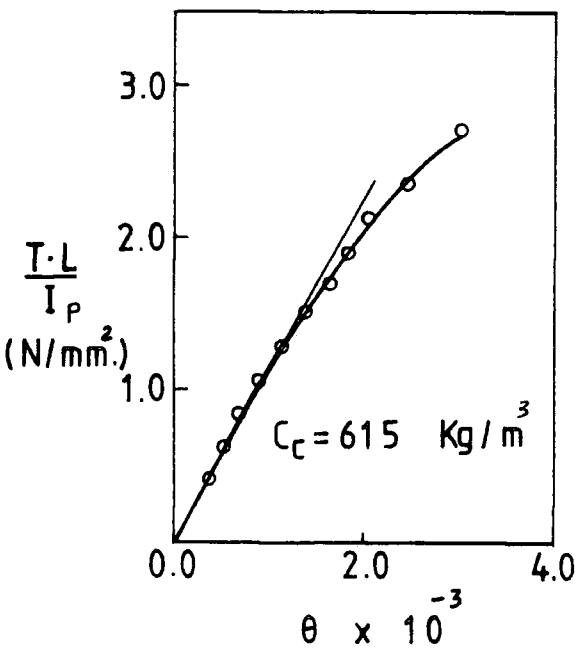

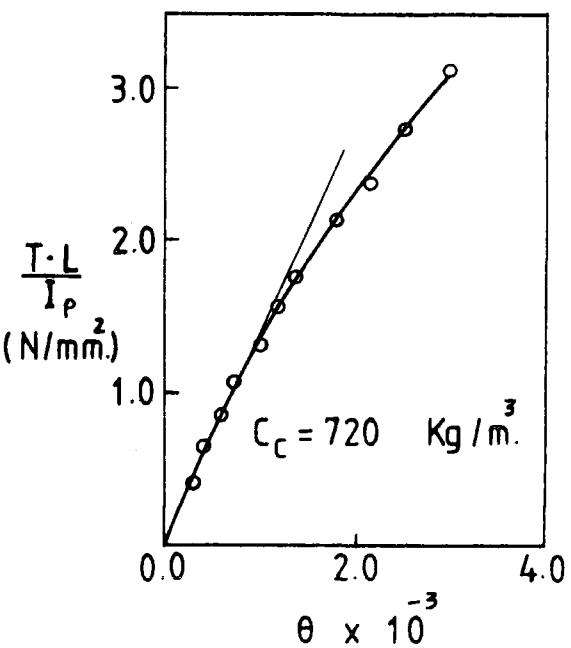

Appendix (I.c) Relationship between torque on cylinder and relative angle of rotation for samples made from beads type 2 (group II) typical to the cement content (C_c) used.

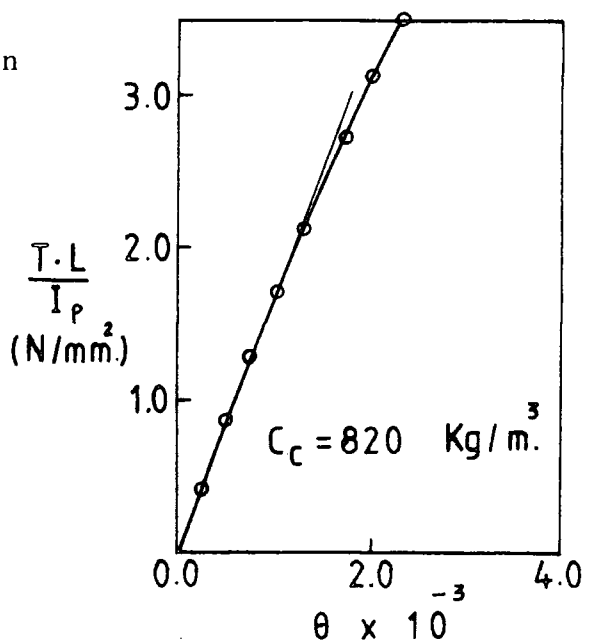

Mix of S/C = 1.0

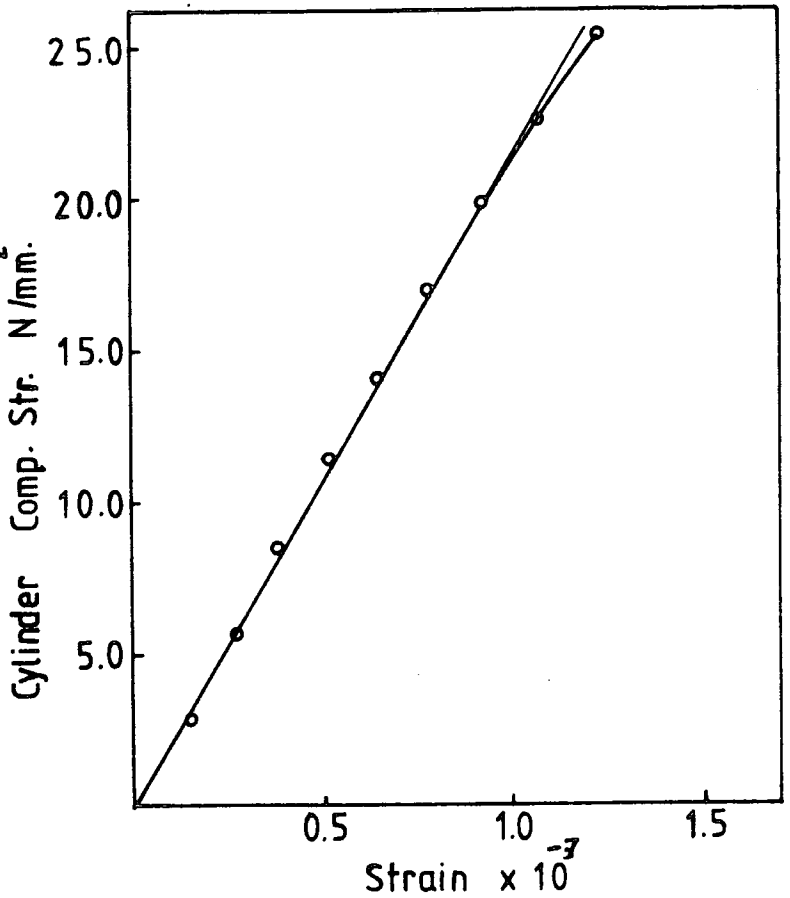

Mix of S/C = 2.0

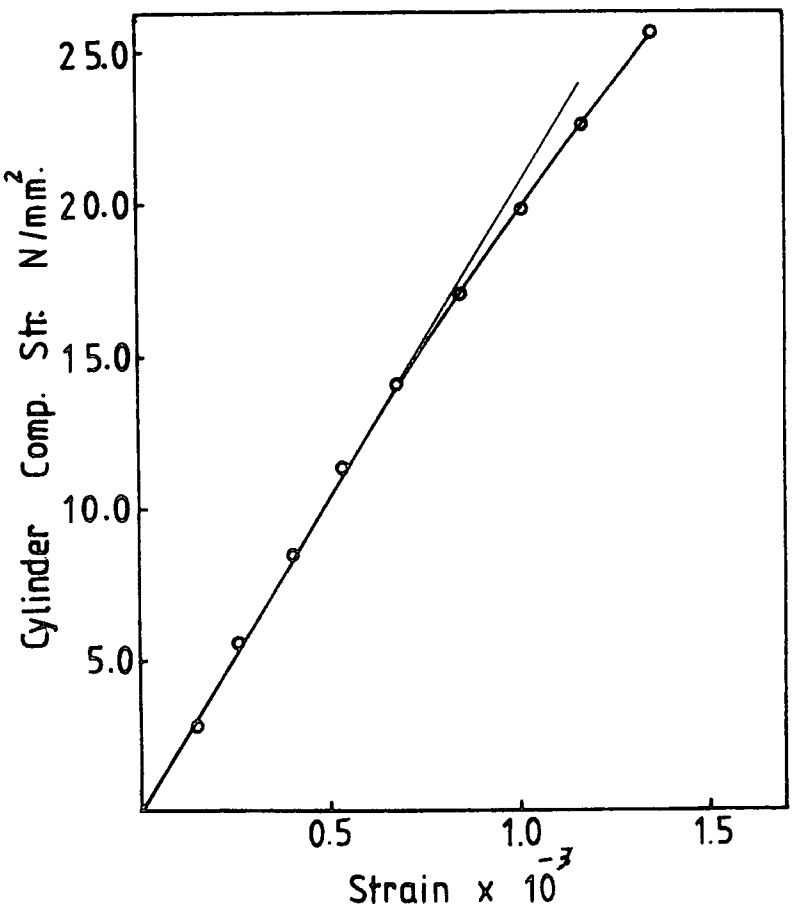

Appendix (II.a) Stress-strain relationship for some samples made from two of the concrete mixes made for faces according to the sand/cement (S/C) ratio.

Face : S_1

A_s = 41.0 mm^2.

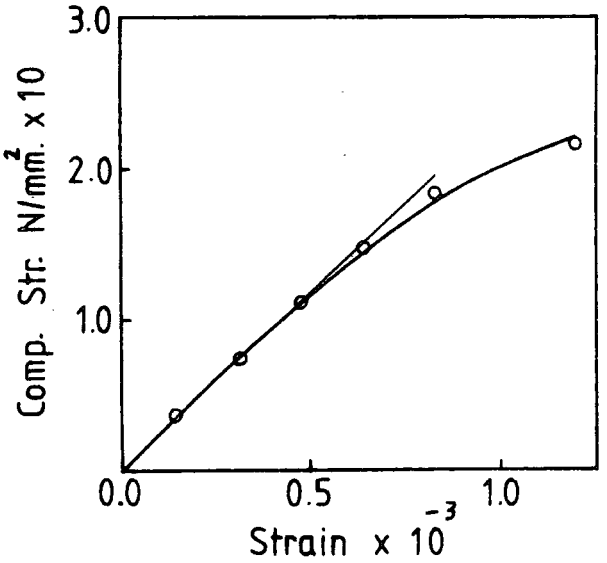

Face : S_2

A_s = 54.0 mm^2.

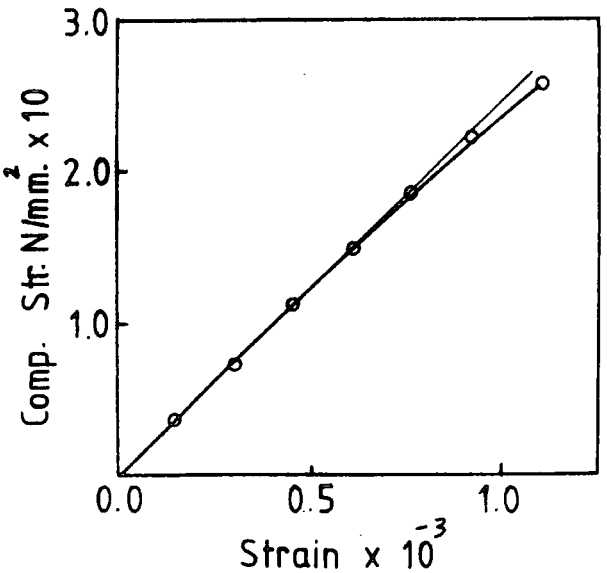

Face : S_3

A_s = 72.3 mm.

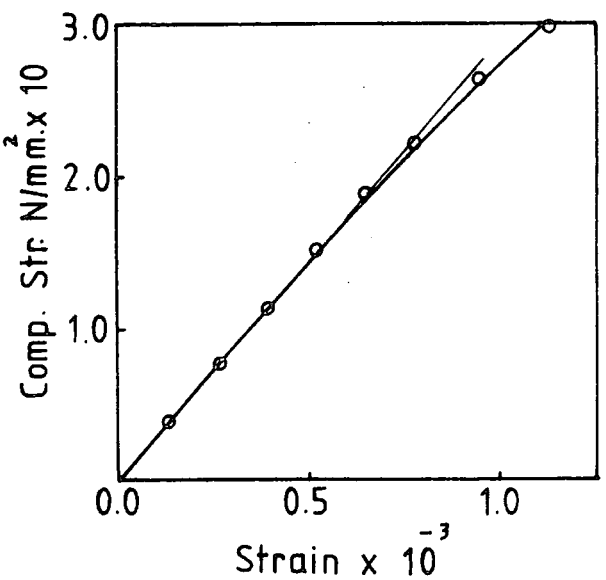

Appendix (II.b) Stress-strain relationship for compression samples from faces typical to the area of reinforcement (A_s) used and face symbol.

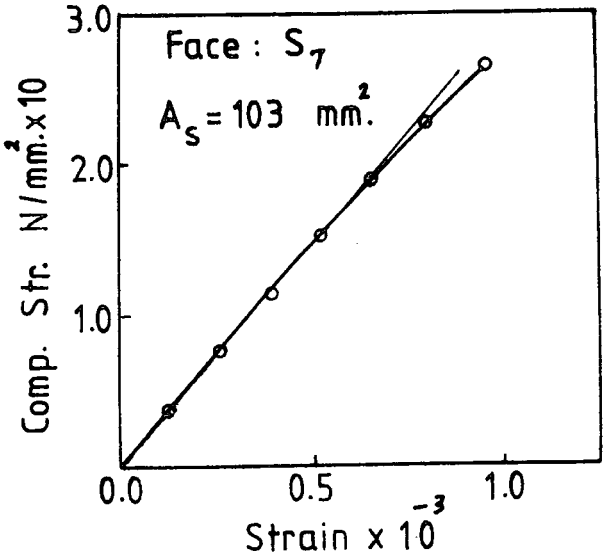

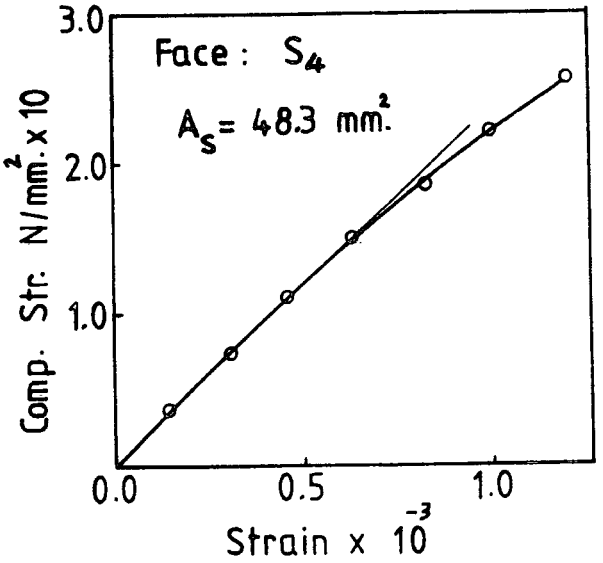

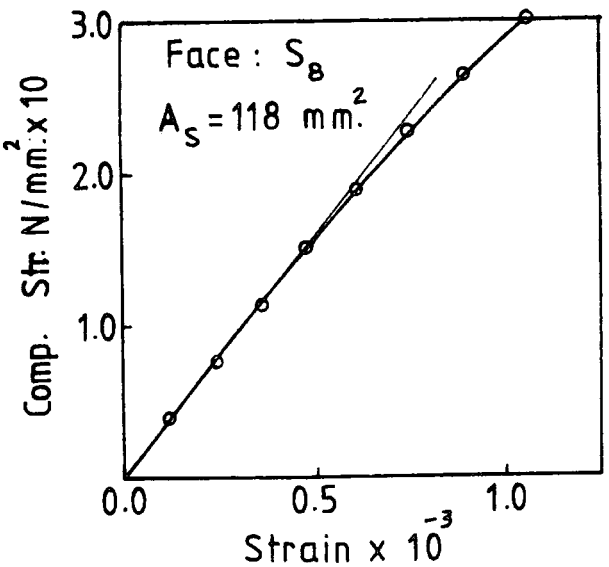

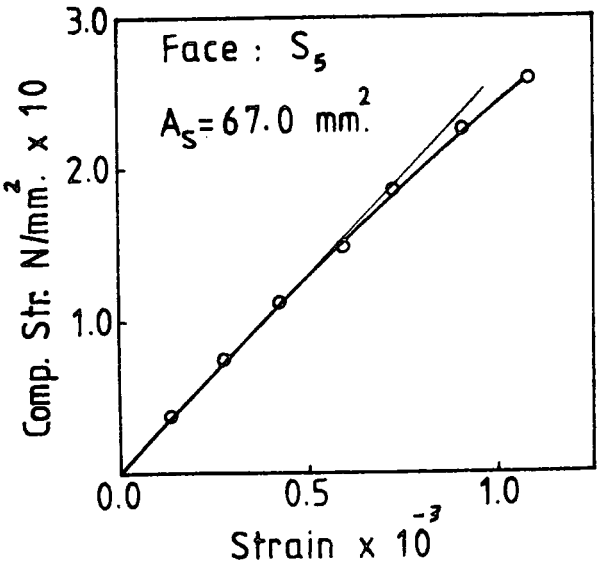

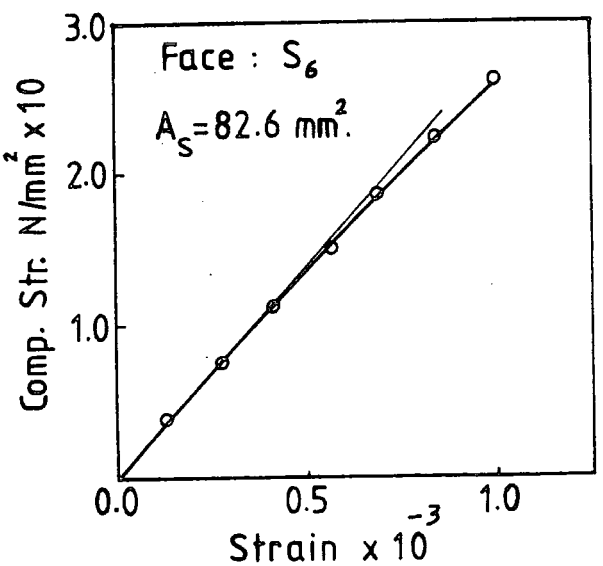

Appendix (II.b) continued.

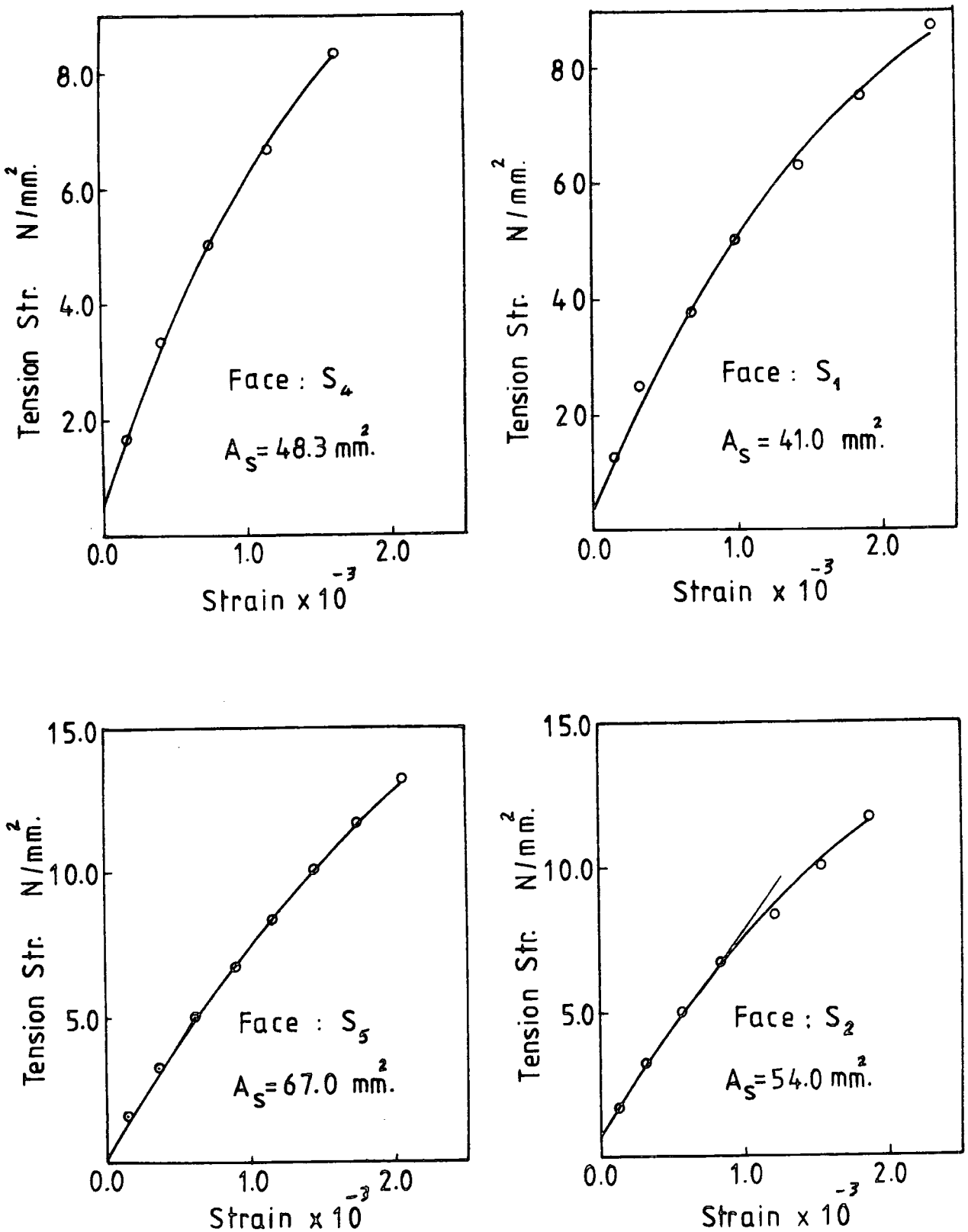

Appendix (II.c) Stress-strain relationship for tension samples from faces typical to the area of reinforcement (A_s) used and face symbol.

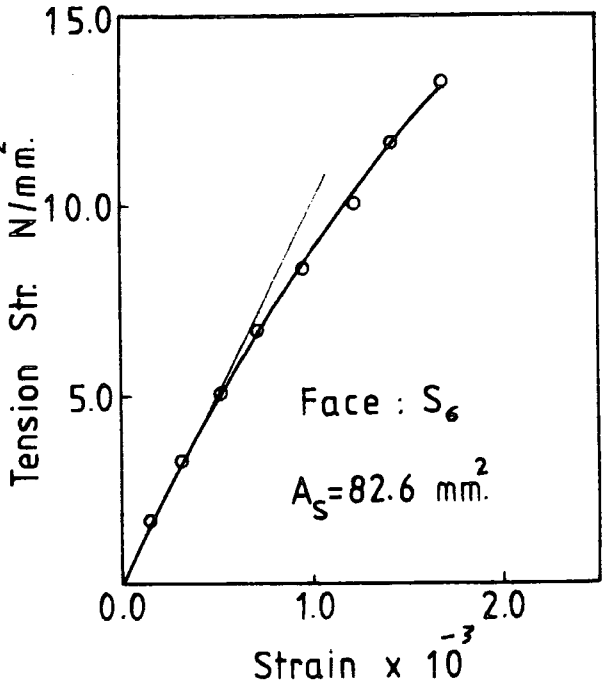

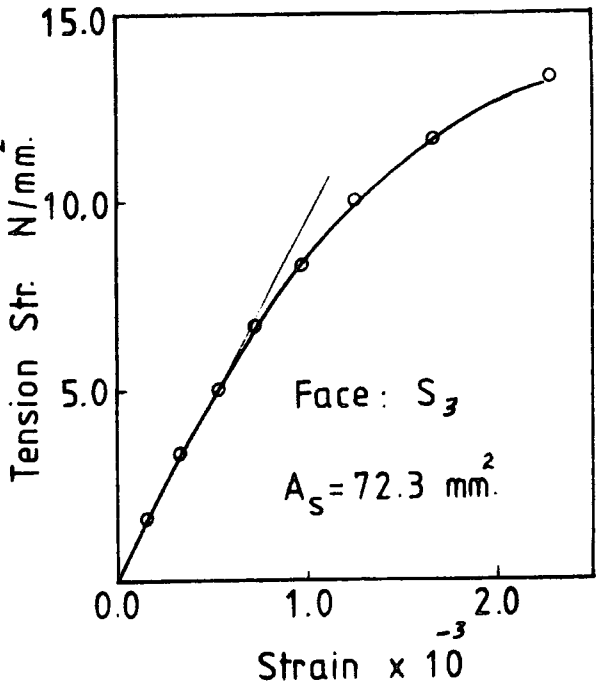

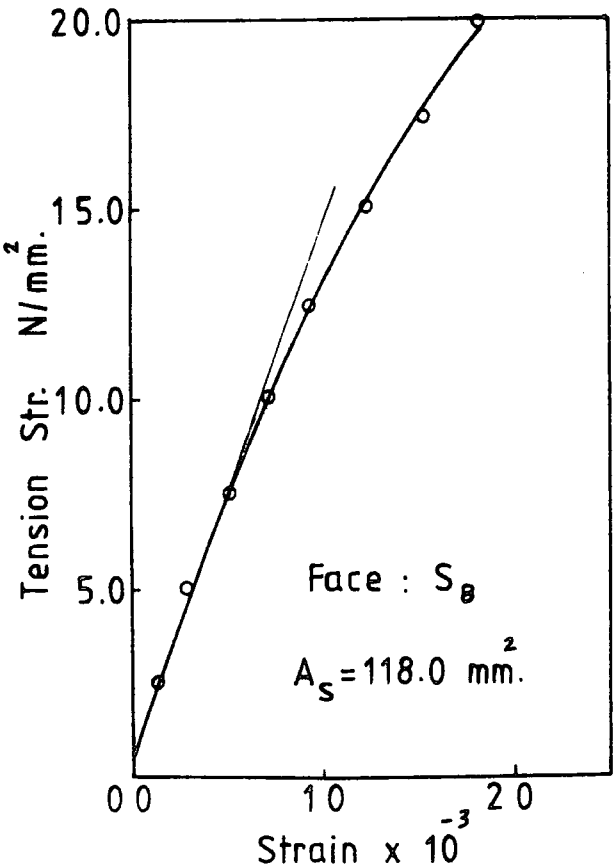

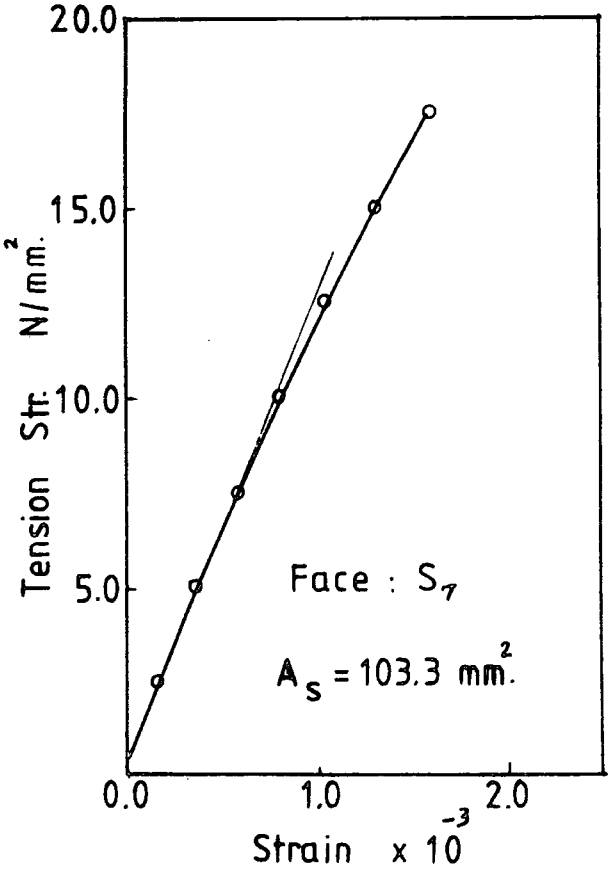

Appendix (II.c) continued.

Face S_1

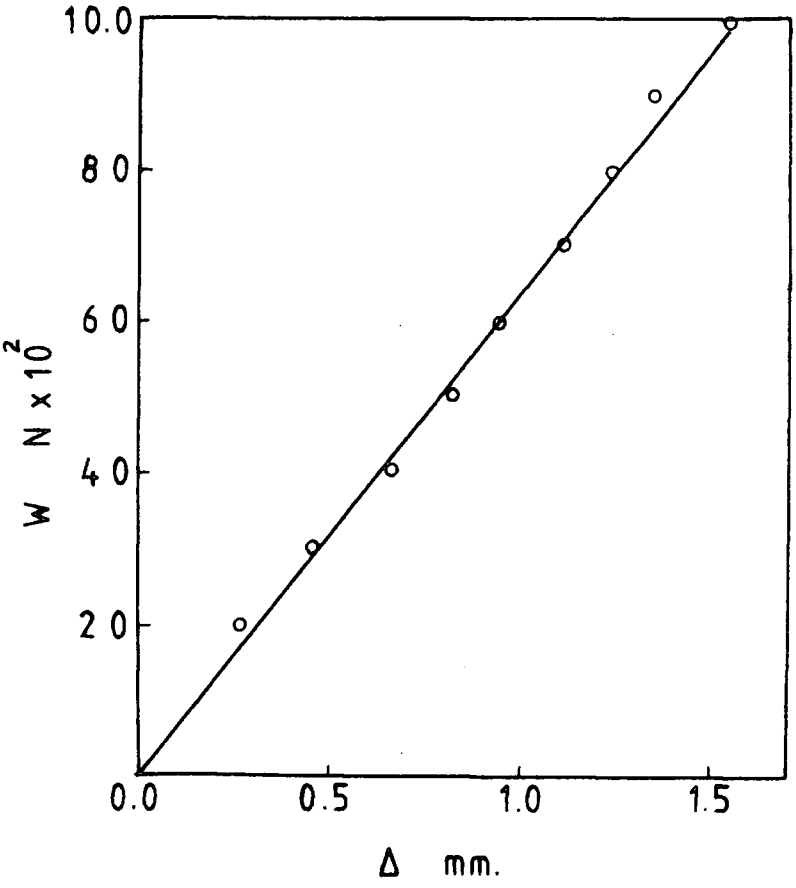

Appendix (II.d) Relationship between load and deflection for determining the flexural stiffness of the face.

Face S_3

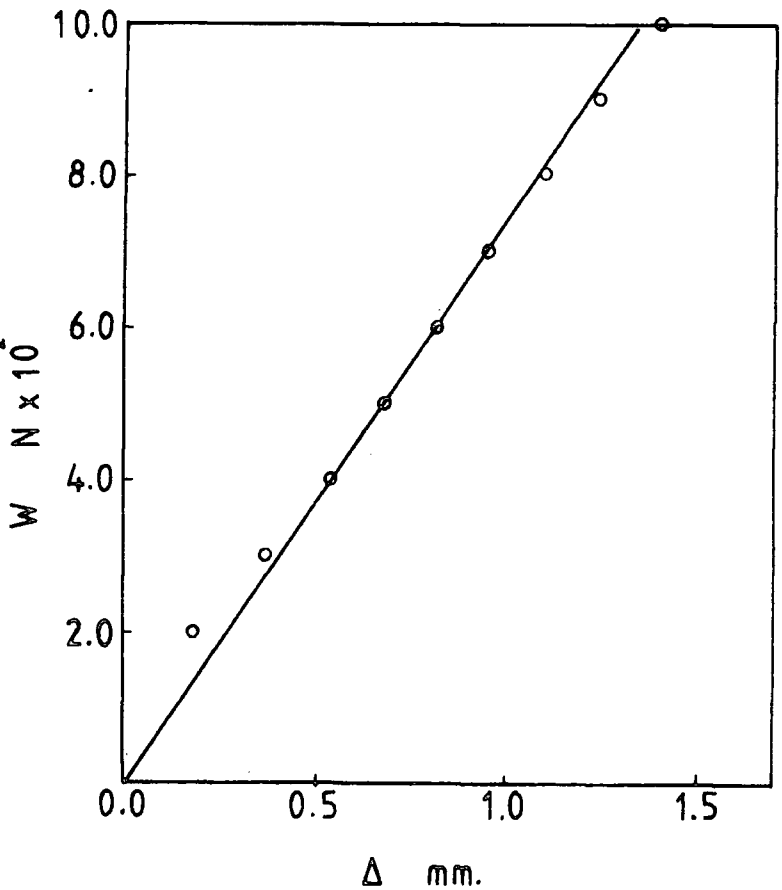

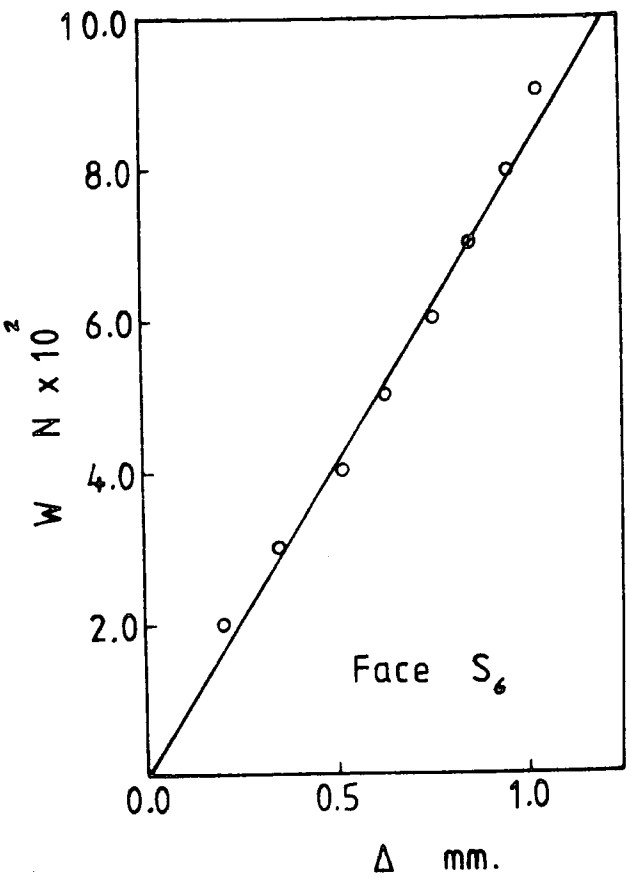

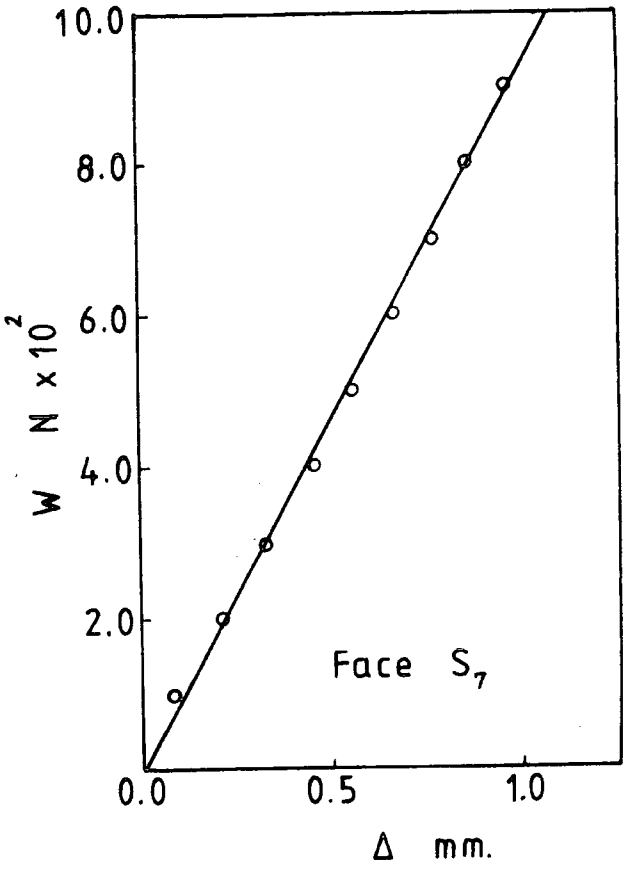

Appendix (II.d) continued.

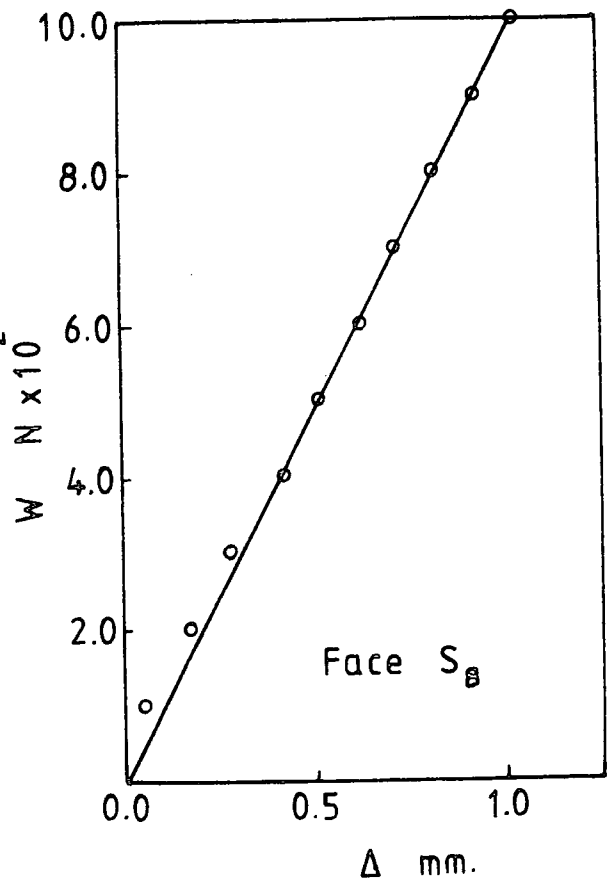

Appendix (II.e.1) Tension test results of sample from face S_3

(Mesh No. 1595 with A_s = 72.5 mm.^{2})

Tension load KN	Tension stress N/mm.^{2}	Tension Strain x 10^{-5}					Notes
		(1)	(2)	(3)	(4)	Average	
2.0	1.66	15	13	12	15	14	
4.0	3.33	36	34	32	33	34	
6.0	5.00	58	52	49	56	54	
8.0	6.66	78	70	67	78	73	
10.0	8.33	110	103	90	98	100	
12.0	10.00	138	128	119	125	128	
14.0	11.66	186	168	153	167	168	fine crack appeared at load 13 KN
16.0	13.33	261	225	210	230	231	
19.2	Failure load						

Appendix (II.e.2) : Tension test results of sample from face S_5

(Mesh No. 2091 with A_s = 67.0 mm.^{2})

Tension load KN	Tension stress N/mm.^{2}	Tension strain x 10^{-5}					Notes
		(1)	(2)	(3)	(4)	Average	
2.0	1.66	14	13	12.5	12	13	
4.0	3.33	41	38	31	29	35	
6.0	5.0	65	66	57	57	61	
8.0	6.66	95	92	87	86	89	
10.0	8.33	123	119	110	109	115	fine crack appeared at load 10 KN
12.0	10.00	148	147	138	136	142	
14.0	11.66	181	178	167	168	174	
16.0	13.33	217	210	199	201	207	
18.0	15.00	255	248	238	252	248	
18.75 Failure load							

Appendix (II.2.3) : Average of results from the tests carried out for determining faces' flexural stiffness

Load W N	Δ measurements according to the face designation x 10^{-2} mm.							
	S_1	S_2	S_3	S_4	S_5	S_6	S_7	S_8
100	6.8	15	5.2	11.8	4.5	8	8.6	6.0
200	27	30	18	29	21	20	21	17
300	46	44	37	46	38	35	33	28
400	67	57	54	61	53	52	46	43
500	83	70	68	81	68	64	56	52
600	95	82	82	94	85	77	67	63
700	112	94	96	111	103	87	78	72
800	125	109	111	128	117	98	87	82
900	135	119	125	142	133	114	97	94
1000	155	138	141	150	153	132	105	104

Appendix (III.1) : Shows the position of neutral axis of the beams according to area of reinforcement and core mix used

Area of reinforcement(A_s) in one face ($mm.^2$)	N.A from beam's top surface (mm.) according to the core mix used		
	Core mix G_1	Core mix G_2	Core mix G_3
41.0	33.5	38.2	42.5
48.3	31.3	35.4	38.5
56.0	35.7	37.3	38.4
67.0	34.5	35.3	37.3
72.5	35.5	39.0	41.3
82.6	39.7	40.8	42.0
103.3	39.7	40.4	40.8
118.0	40.0	40.3	40.9

Appendix (III.2) : Beams bending stiffness due to faces only and due to core in compression zone and relationship between them

A_s in one face (mm^2.)	Beams made using core G_1			Beams made using core G_2			Beams made using core G_3			face bending stiffness $D_f \times 10^7$ (N.mm)
	$D \times 10^{10}$ (N.mm.)	$D_c \times 10^{10}$ (N.mm.)	(D_c/D) per cent	$D \times 10^{10}$ (N.mm.)	$D_c \times 10^{10}$ (N.mm.)	(D_c/D) per cent	$D \times 10^{10}$ (N.mm.)	$D_c \times 10^{10}$ (N.mm.)	(D_c/D) per cent	
41.0	6.83	0.078	1.14	7.14	0.251	3.52	7.55	0.563	7.46	7.62
48.3	7.47	0.058	0.70	7.60	0.184	2.40	7.80	0.380	4.90	7.62
56.0	8.67	0.102	1.17	8.74	0.228	2.60	8.80	0.611	6.90	8.94
67.0	9.60	0.088	0.92	9.62	0.181	1.88	9.70	0.330	3.40	8.94
72.5	10.58	0.100	0.93	10.73	0.280	2.60	10.86	0.503	4.60	8.94
82.6	11.16	0.157	1.40	11.22	0.327	2.90	11.40	0.537	4.70	9.8
103.3	12.94	0.157	1.20	12.95	0.315	2.40	12.96	0.480	3.70	11.1
118.0	14.82	0.160	1.10	14.83	0.315	2.10	14.84	0.484	3.30	11.7

Appendix (III.3) : Axial force resisted by core and consequent B.M of core in percent of the total B.M according to A_s and core mix used

A_s in one face (mm^2)	Core mix G_1		Core mix G_2		Core mix G_3	
	N_c (N)	$(M_c/M)\%$	N_c (N)	$(M_c/M)\%$	N_c (N)	$(M_c/M)\%$
41.0	140	4.9	307	10.85	448	15.8
48.3	112	3.95	243	8.57	365	12.9
56.0	131	4.6	242	8.55	328	11.55
67.0	128	4.5	240	8.47	369	13.0
72.5	129	4.5	275	9.70	438	15.4
82.6	164	5.7	312	11.0	465	16.4
103.3	128	4.5	234	8.26	333	11.76
118.0	121.5	4.28	215	7.58	322	11.33

Appendix (IV.a1) : Typical wooden mould used for casting three cylinders of 2 x 3 inch dimensions in polystyrene concrete.

Appendix (IV.a2) : The clips and steel bases used for Torsion test.

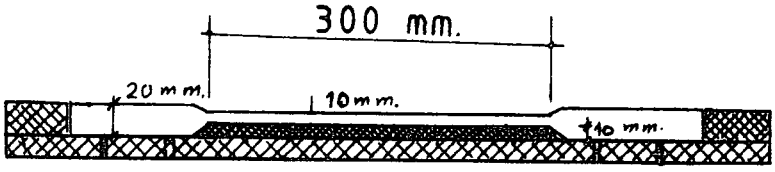

Section X — X

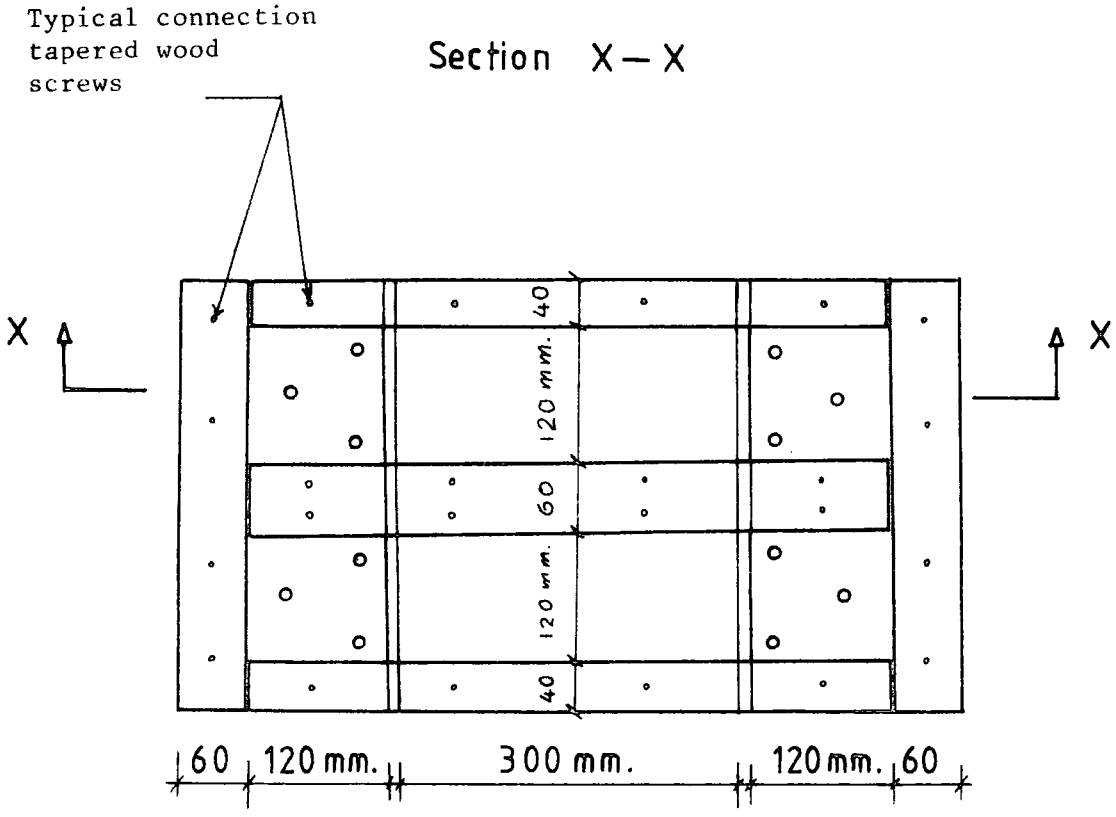

Plan

Appendix (IV.b) Details of the mould used for casting the tension samples of the faces.

Appendix (IV.c) Details of wooden moulds used for beams' casting